

**DNA Damage Response and  
Anti-apoptotic Proteins  
Expression in NPMc+ Mutated  
Cells in Acute Myeloid Leukaemia**

**Haitham Mohammed Habib Qutob, BSc, MSc.**

**Thesis submitted to the University of Nottingham for the  
degree of Doctor of Philosophy**

**July 2014**

## **Abstract**

Nucleophosmin 1 (NPM1) is a multi-functional phosphoprotein, which shuttles between the nucleolus and the cytoplasm. It participates in many cellular processes including ribosome biogenesis and transport, centrosome duplication, and also contributes to the control of genomic stability. NPM1 interacts with many proteins including those that participate in DNA damage repair processes. C-terminal mutations in NPM1 occur in 35% of patients with acute myeloid leukaemia and are associated with a good prognosis. They are characterised by delocalisation of NPM1 into the cytoplasm. This may have a role in the sensitivity of mutant cells to chemotherapy via inactivation of the DNA damage response processes.

Firstly, we aimed to identify potential differences in DNA repair in response to double-strand breaks (DSB) and alkylating inducers and then assess them through the comet assay in the wild-type and mutant NPM1 cell lines. The percentage and kinetics of DNA damage in both cell lines was identical, indicating that DNA lesions were repaired efficiently in both the wild-type and mutant cell lines. The  $\gamma$ -H2AX foci were also evaluated which increased to similar levels in mutant and wild-type cells lines after exposure to DNA damaging agents and decreased with similar rates when the cells were allowed 24 hours to repair the damage. Interestingly, following DNA damage, the amount of NPM1 increased significantly in NPMc+ cells, both in the nucleus and the cytoplasm, which was not seen in NPM1 wild-type cells.

Next, we determined the subcellular localisation of APE1, which is a DNA repair enzyme in the base excision repair pathway and a transcriptional co-activator. APE1 has

previously been shown to associate with NPM1. Using confocal microscopy, we found that the APE1 in both wild-type and NPMc+ mutant cell lines is predominately localised in the cytoplasm, while it is translocated into the nucleus after the cells were exposed to MMS, presumably to play a role in the DNA damage repair mechanism.

As we could find no apparent difference in DNA repair between NPM1 mutated and wild type cells we went on to look at proteins involved in cell survival - BCL-2 and MCL-1. The NPMc+ mutant cell line expressed the highest level of mRNA BCL-2 and MCL-1 when compared to the NPM1 wild-type cell lines. The NPMc+ mutated cells have previously been shown to be sensitive to the effect of all-trans retinoic acid (ATRA). We looked to see whether ATRA has an effect on the anti-apoptotic proteins. The results demonstrate that the BCL-2 and MCL-1 levels were down-regulated to a greater level in the NPM1 mutant cell line than in the NPM1 wild-type cells. In patient samples, the BCL-2 and MCL-1 mRNA down-regulation was seen in 3/5 and 5/5 NPMc+ samples, respectively. Thus, these findings indicate that BCL-2 and MCL-1 mRNA expression is down-regulated following ATRA in NPMc+ mutant cells.

Finally, siRNA was used to decrease levels of either total NPM1 or mutant NPM1 alone. Results showed that in the NPM1 mutant cells there was a down-regulation of BCL-2 mRNA, while in the NPM1 wild-type cells, no effect on the BCL-2 mRNA level was found. Furthermore, levels of P53 were up-regulated in the mutant NPM1 cells after knocking-down the total NPM1, whereas the wild-type cell line showed no change in the P53 level. These results provide evidence suggesting that down-regulation of NPM1 in the NPMc+ cell line increases total P53, possibly by interaction of ARF and HDM2, resulting

Qutob, H

in down-regulation of the BCL-2 in the mutated cells. In conclusion, perturbation of NPM1 subcellular localisation in NPMc+AML has no effect on the DNA repair mechanisms but we found differences in the anti-apoptotic proteins expression compared to NPM1 wild-type cells.

## **Acknowledgements**

All praise and thanks are to Allah (the lord of all worlds), who is the most gracious and the most merciful, for giving me the health, strength, and patience during my whole life.

I would like to thank my project supervisors Professor Nigel Russell, and Dr Claire Seedhouse for accept me in their department to study the PhD. In particular, deep thanks to Dr Claire Seedhouse for her assistance, support and advice. She has gone above and beyond to provide me with magnificent advice, both professionally and scientifically. She has also been an astonishing person to work for and with throughout my time here. I would also like to thank the other members of the Academic Haematology Department; Dr Monica Pallis, Dr Martin Grundy, and Ning Yu for their technical support and advices. I would also like to thank the members of respiratory medicine, Oncology departments, and Kai Linag (MSc student in University of Nottingham, 2011) for their technical assistance.

a huge thanks to my parents - (Father: Mohammed Habib, and Mother: Amrah) for their prayers, encouragement, advices and supporting me throughout all of my education, it has been a very long road! I would especially like to thank my sisters; Hanadi, Soha, Sammar, and Isra'a, and all my brothers and family in-law for all of their prayers and support throughout the years.

My wife (Amal) and sons (Hashim, and Ammar), words cannot explain or tell how much you mean to me and what you have done during my study but your are the part of this achievement and thanks for your love, encouragement, patience, and understanding.

Finally, I would like to thank King Abdullah Bin Abdulaziz, and the ministry of High education for funding all my post-graduate studies.

## List of Abbreviations

7-AAD	7-amino-actinomycin D
$\beta$ 2M	Beta 2 macroglobulin
$\gamma$ -H2AX	Phosphorylation of Ser139 of histone variant H2AX
ALCL	Anaplastic large cell lymphoma
ALK	Anaplastic lymphoma kinase
AML	Acute myeloid leukaemia
AP-1	Activator protein 1
Apaf-1	Apoptotic protease-activating factor
APE1	Apurinic/aprimidinic endonuclease-1
APL	Acute promyelocytic leukaemia
ARF	Alternate reading frame
ATM	Ataxia telangiectasia mutated
ATP	Adenosine trip
ATR	Ataxia- and Rad-related
ATRA	All trans-retinoic acid
ATRIP	ATR-interacting protein
BCL-2	B-cell leukaemia/lymphoma 2
BER	Base excision repair
BH	Bcl-2 homology
BRCA1	Breast cancer type 1 susceptibility protein
BRCA2	Breast cancer type 2 susceptibility protein
BSA	Bovine serum albumin
cDNA	Complementary DNA
CEBPA	CCAAT/enhancer binding protein $\alpha$
CO <sub>2</sub>	Carbon dioxide
CR	Complete remission
Csf2	Colony stimulating factor 2

C-terminus	Carboxyl-(COOH)-Terminus of a Protein
CY3	Cyanine fluorescent dyes 3
DAPI	4',6-diamidino-2-phenylindole
DDR	DNA damage response
del	Deletion
DEPC	Diethylpyrocarbonate
DMSO	Dimethyl sulfoxide
DNA	Deoxyribonucleic acid
DNA-PK	DNA-dependent protein kinase
DNase	Deoxyribonuclease
dNTPs	Deoxynucleotide triphosphates
DSB	Double-strand break
DTT	Dithiothreitol
EDTA	Ethylenediamine tetra-acetic acid
FAB	French-american-british
FACS	Fluorescence activated cell sorting
Fbw7 $\gamma$	F-box protein
FCS	Foetal calf serum
FITC	Fluorescein isothiocyanate
FLT3	Fms-like tyrosine kinase 3
FSC	Fixed stained cells
G-CSF	Granulocyte-colony stimulating factor
GEP	Gene expressions profiling
GFP	Green fluorescent protein
GM-CSF	Granulocyte-macrophage colony-stimulating factor
HEXIM1	Hexamethylene-bis-acetamide inducible protein 1
HOX	Homeobox
HR	Homologous recombination
HSC	Haematopoietic stem cell
IDH1	Isocitrate dehydrogenase 1

IgG	Immunoglobulin G
IgG-HRP	IgG-horseradish peroxidase
IL-3	Interleukin 3
IL-6	Interleukin 6
Inv	Inversion
IRIF	Irradiated-induced foci
ITD	Internal tandem duplications
LIC	Leukaemia-initiated
LSC	Leukaemia stem cells
MAP	Mitogen-activated protein
MCL-1	Myeloid cell leukaemia 1
MDC1	Mediator of DNA damage checkpoint 1
MDS	Myelodysplastic syndrome
MFI	Mean fluorescence index
MgCl <sub>2</sub>	Magnesium chloride
MMLV	Moloney murine leukemia virus
MMR	Mismatch repair
MMS	Methyl methanesulfonate
mRNA	Messenger RNA
NER	Nucleotide excision repair
NES	Nuclear-export signal
NF-κB	Nuclear factor kappa-light-chain- enhancer of activated B cells
NHEJ	Non-homologous end joining
NK-AML	Normal karyotype – AML
NLS	Nuclear localization signal
NPM1	Nucleophosmin 1
NPMc+AML	Cytoplasmic NPM1 mutations in AML
N-terminus	Amino-(NH <sub>2</sub> )-Terminus of a Protein
NΔ33APE1	33 N-terminal deletion of APE1

OS	Overall survival
PBS	Phosphate buffered saline
PBS-AA	Phosphate-buffered saline albumin azide
PCR	Polymerase chain reaction
PE	Phycoerythrin
pre-rRNA	Preribosomal RNA
p-STAT-5	Phosphorylated Signal Transducer and Activator of Transcription factor 5
PTD	Partial tandem duplication
PVDF	Polyvinylidene difluoride
qPCR	Quantitative polymerase chain reaction
RNA	Ribonucleic acid
RNase	Ribonuclease
rpm	Revolutions per minute
RPMI	Roswell Park memorial Institute Medium
rRNA	Ribosomal Ribonucleic acid
SCF	Stem cell factor
SCGE	Single gel electrophoresis assay
SD	Standard deviation
SDS-PAGE	Sodium dodecyl sulfate - Polyacrylamide gel electrophoresis
siRNA	Small-interfering ribonucleic acid
SSB	Single-strand break
ssDNA	Single-strand DNA
STAT-5	Signal Transducer and Activator of Transcription factor 5
STR	Short tandem repeat
TBE	Tris/borate/edta
TBST	Tris buffer saline tween20
TKD	Tyrosine kinase domain

Qutob, H

TNF	Tumor necrosis factor
UV	Ultraviole light
WHO	World Health Organization
wt	Wild-type
XRCC1	X-ray repair cross-complementing

## Table of Contents

<b>Abstract</b> .....	I
<b>Acknowledgments</b> .....	IV
<b>List of Abbreviations</b> .....	V
<b>Table of Contents</b> .....	X
<b>List of Tables</b> .....	XVI
<b>List of Figures</b> .....	XVII
<b>1. Introduction</b> .....	1
1.1 Acute myeloid leukaemia.....	2
1.1.1 AML heterogeneity.....	3
1.1.2 AML with cytogenetic abnormalities.....	3
1.1.3 AML with normal cytogenetic and molecular mutations.....	7
1.1.3.1 Internal tandem duplication of Fms- like tyrosine kinase-3 (FLT3-ITD) in AML.....	7
1.1.3.2 Frame-shift mutations of NPM1 in AML	9
1.1.3.3 Other mutations in cytogenetically normal AML.....	10
1.2 Nucleophosmin 1 (NPM1) gene and protein.....	11
1.2.1 NPM1 structure.....	11
1.2.2 NPM1 transport in wild-type NPM1.....	13
1.2.3 NPM1 functions.....	14
1.2.3.1 The role of NPM1 in ribosome biogenesis.....	14
1.2.3.2 The role of NPM1 in regulation of cell growth and proliferation.....	15
1.2.3.3 The role of NPM1 in regulation of tumour suppressor proteins.....	16
1.2.3.4 The role of NPM1 in maintenance of genomic stability.....	18

1.3 Mutations in NPM1 in haematological malignancies.	19
1.3.1 NPM1 gene translocations in leukaemia and lymphoma.....	19
1.3.2 NPM1 cytoplasmic mutations in AML (NPMc+AML).....	21
1.3.2.1 Mechanism of abnormal NPM1 subcellular localisation in NPMc+AML...	22
1.3.2.2 Role of NPMc+ in leukaemogenesis.....	23
1.3.2.3 Clinical features of patients with NPMc+AML.....	26
1.3.2.4 Gene expressions profiling (GEP) in NPMc+AML.....	28
1.3.2.5 Prognostic impact of NPMc+AML.....	29
1.3.2.6 All-trans retinoic acid (ATRA) treatment in AML.....	30
1.4 DNA damage response (DDR).....	32
1.4.1 Sensing of DNA damage.....	32
1.4.2 DNA repair mechanisms.....	33
1.4.2.1 Double strand breaks.....	35
1.4.2.2 Base excision repair.....	36
1.4.2.3 Other DNA repair mechanisms.....	37
1.4.2.4 DDR in resistance to therapy.....	37
1.4.3 Apoptosis.....	38
1.4.4 Interaction of NPM1 with proteins involved in DNA damage response.....	40
1.5 Aim of the study.....	41
<b>2. Materials and Methods.....</b>	<b>44</b>
2.1 Chemicals.....	45
2.2 Antibodies.....	45
2.3 Cell culture.....	46
2.4 Patient samples.....	47
2.5 Cell viability assays.....	48

2.5.1 Cell counting by haemocytometer.....	48
2.5.2 Alamar blue assay.....	48
2.5.3 7-AAD Cell viability assay.....	49
2.6 Molecular methods.....	49
2.6.1 RNA extraction.....	49
2.6.2 Polymerase chain reaction (PCR) optimisations.....	50
2.6.3 NPM1 and FLT3-ITD mutations analysis.....	51
2.6.4 Gene expression measurements.....	52
2.6.5 Sequencing.....	53
2.7 Assessing the interaction of NPM1 and APE1 in the leukaemic cell lines.....	54
2.7.1 Preparation of slides.....	54
2.7.1.1 LiquiPrep cytology system.....	54
2.7.1.2 Coverslip technique.....	54
2.7.1.3 Cytospin technique.....	54
2.7.1.4 Fibronectin coating technique.....	55
2.7.2 Indirect immunofluorescence method for detection of subcellular localisation by confocal microscopy.....	55
2.7.3 Cytoplasmic-nuclear extracts.....	56
2.7.3.1 Preparation of cytoplasmic-nuclear extracts.....	56
2.7.3.2 Determination of protein concentration.....	57
2.7.4 Western blot analysis.....	57
2.7.5 Co-immunoprecipitation.....	58
2.7.6 MMS Cytotoxicity assay.....	58
2.8 DNA damage response.....	59
2.8.1 Comet assay.....	59
2.8.1.1 Preparation of slides.....	59
2.8.1.2 Analysis of comet assay.....	61

2.8.2 $\gamma$ -H2AX immunocytochemistry assay.....	61
2.9 Anti-apoptotic protein levels in NPMc+AML cells and response to ATRA.....	62
2.9.1 ATRA and AC220 concentration optimisations.	62
2.9.2 Blood cell morphology.....	63
2.9.3 CD11b differentiation marker analysis.....	63
2.9.4 Apoptosis detection by Annexin-V.....	64
2.9.5 BCL-2 and MCL-1 protein levels detection.....	64
2.9.6 Total P53 protein measurement.....	65
2.9.7 RNA interference of NPM1.....	65
2.9.8 Preparation of lysate from cell culture.....	66
2.10 Statistical analysis.....	67
<b>3. DNA damage repair activity in NPMc+AML cells...</b>	<b>68</b>
3.1 Introduction.....	69
3.2 Results.....	71
3.2.1 NPM1 and FLT3-ITD mutations detection.....	71
3.2.2 DNA damage repair activity in response to a DSB-inducing agent.....	73
3.2.2.1 Assessment of DNA damage repair activity by the comet assay.....	73
3.2.2.2 Immunocytochemistry detection of $\gamma$ - H2AX.....	78
3.2.3 Assessment of DNA damage repair function in response to an alkylating agent.....	80
3.2.4 Expression of NPM1 in AML cell lines upon DNA damage inducing agent.....	83
3.3 Discussion.....	86
<b>4. The effect of NPMc+AML on APE1 subcellular localisation.....</b>	<b>91</b>
4.1 Introduction.....	92
4.2 Results.....	94

4.2.1 NPM1 and APE1 subcellular localization by immunofluorescence.....	94
4.2.2 NPM1 and APE1 subcellular localization by western blot.....	97
4.2.3 Detection of potential NPM1 and APE1 interaction by co-immunoprecipitation.....	99
4.2.4 Detection of possible APE1 alternative splicing variants.....	101
4.2.5 MMS cytotoxicity assay in wild-type and mutant NPM1 AML cell lines.....	102
4.3 Discussion.....	104
<b>5. The effect of down-regulation of NPM1 on BCL-2 and MCL-1 anti-apoptotic levels in NPMc+AML....</b>	<b>108</b>
5.1 Introduction.....	109
5.2 Results.....	111
5.2.1 Knock-down of total NPM1 or mutant NPM1 by siRNA in OCI-AML3 and M-07e cells.....	111
5.2.2 Basal anti-apoptotic levels in wild-type and mutant NPM1 cell lines.....	116
5.2.3 BCL-2 and MCL1 mRNA levels in wild-type and mutant NPM1 cell lines following down-regulation of NPM1 with siRNA.....	118
5.2.4 P53 levels in M-07e and OCI-AML3 after total NPM1 knock down.....	120
5.2.5 Measurement of the differentiation marker (CD11b) in M-07e and OCI-AML3 after total NPM1 knock down.....	121
5.3 Discussion.....	122
<b>6. The impact of ATRA on BCL-2 and MCL-1 levels on NPMc+AML.....</b>	<b>127</b>
6.1 Introduction.....	128
6.2 Results.....	130

6.2.1 Response of NPMc+AML and wild-type NPM1 cell lines to ATRA.....	130
6.2.2 ATRA induces differentiation and apoptosis in NPMc+AML cell line.....	131
6.2.3 The effect of ATRA on BCL-2 mRNA and protein levels.....	135
6.2.4 The effect of ATRA on MCL-1 mRNA and protein.....	137
6.2.5 The effect of ATRA in combination with the FLT3 inhibitor AC220.....	139
6.2.6 The effect of ATRA and AC220 on differentiation marker and apoptosis.....	141
6.2.7 The effect of ATRA and AC220 on BCL-2 and MCL-1 mRNA and protein levels.....	143
6.2.8 Response of primary AML cells to ATRA and/or AC220.....	146
6.3 Discussion.....	151
<b>7. General discussion.....</b>	<b>156</b>
<b>References.....</b>	<b>170</b>
<b>Appendix.....</b>	<b>193</b>
4.1 APE1 mRNA sequencing results in the leukaemic cell lines.....	193

## **List of Tables**

Table 1.1: WHO (2008) classifications.....	5
Table 1.2: Cytogenetics-risk group classifications in AML.	6
Table 1.3: DDR mechanisms.....	34
Table 2.1: The characterisations of Leukaemic cell lines...	47
Table 2.2: PCR optimisation conditions.....	51
Table 2.3: Primers used in real-time PCR.....	53
Table 5.1: The ratio of NPM1-A/wild-type NPM1.....	116
Table 6.1: BCL-2 and MCL-1 mRNA expressions in patient samples after exposed to ATRA and/or AC220..	150

## List of Figures

Figure 1.1: Impact of cytogenetic entities recognised in 2008 WHO classification on survival.....	6
Figure 1.2: NPM1 structure.....	13
Figure 1.3: Survival analysis of NPM1 and FLT3 mutations in AML patients.....	30
Figure 1.4: DNA damage repair mechanisms.....	34
Figure 2.1: Comet assay protocol steps.....	61
Figure 3.1: PCR optimisation for NPM1 primers.....	71
Figure 3.2: NPM1 and FLT3 length mutations in AML cell lines.....	73
Figure 3.3: Viability of AML cell lines in response to etoposide.....	76
Figure 3.4: Comet assay in response to DSB agent.....	77
Figure 3.5: Cell viability in parallel with comet assay upon etoposide treatment.....	78
Figure 3.6: $\gamma$ -H2AX Immunocytochemistry analysis.....	79
Figure 3.7: Viability of AML cell lines upon MMS treatment.....	81
Figure 3.8: Alkaline comet assay in response to MMS.....	82
Figure 3.9: Cell viability in parallel with comet assay upon MMS.....	82
Figure 3.10: Detection of NPM1 by Western Blot.....	84
Figure 3.11: The level of NPM1 mRNA upon DNA damage inducers.....	85
Figure 4.1: NPM1 subcellular localisation after cytospin centrifugation.....	94
Figure 4.2: Immunofluorescent subcellular detection of NPM1.....	95
Figure 4.3: Immunofluorescent subcellular detection of APE1.....	96

Figure 4.4: Immunofluorescent subcellular detection of NPM1 after MMS treatment.....	97
Figure 4.5: NPM1 and APE1 subcellular localization by western blot.....	100
Figure 4.6: Detection of NPM1 and APE1 interaction by co-immunoprecipitation.....	101
Figure 4.7: Detection of APE1 spliced variant in AML cell lines.....	102
Figure 4.8: The cytotoxic sensitivity assay on wild-type and mutated NPM1 cells in response to MMS.	103
Figure 5.1: Custom designed NPM1-A siRNA.....	111
Figure 5.2: NPM1 expression following siRNA designed to either total NPM1 or the mutant NPM1 only....	113
Figure 5.3: Total NPM1 and mutant NPM1 expressions after siRNA.....	115
Figure 5.4: Relative fluorescent quantification of NPM1-A and NPM1-wt alleles.....	115
Figure 5.5: Detection of BCL-2 and MCL-1 mRNA expression and protein levels in the different leukaemic cell lines.....	117
Figure 5.6: BCL-2 and MCL-1 mRNA level after siRNA total NPM1 or the mutant NPM1 only.....	119
Figure 5.7: The protein level of P53 in the leukaemic cell lines upon NPM1_7 siRNA.....	120
Figure 5.8: Expression of the differentiation marker CD11b after leukaemic cell lines were nucleofected with siRNA NPM1_7.....	121
Figure 5.9: Models of BCL-2 regulation in NPMc+AML cells.....	125
Figure 6.1: The growth inhibition of AML cell lines upon ATRA treatment.....	131

Figure 6.2: The effect of ATRA on differentiation in AML cell lines.....	132
Figure 6.3: The effect of ATRA on apoptosis in AML cell lines.....	134
Figure 6.4: Anti-apoptotic BCL-2 levels upon ATRA treatment.....	136
Figure 6.5: The effect of ATRA on MCL-1 mRNA and protein expression.....	138
Figure 6.6: The viability of AML cell lines upon AC220 treatment.....	140
Figure 6.7: The effect of AC220, alone or in combination with ATRA, on differentiation and apoptosis in AML cell lines.....	142
Figure 6.8: The effect of AC220 alone or combined with ATRA on BCL-2 and MCL-1 mRNA and protein levels in the AML cell lines.....	145
Figure 6.9: The viability of primary cells upon ATRA, AC220, or ATRA/AC220 treatment.....	148
Figure 6.10: Primary cell lines in response to FLT3 inhibitors at different concentrations.....	149

# **1. Introduction**

### **1.1 Acute myeloid leukaemia:**

Acute myeloid leukaemia (AML), also known as acute myelogenous leukaemia, is a haematological malignancy that arises from myeloid precursor cells. These cells fail to differentiate normally and to activate normal cell apoptosis signals leading to abnormal accumulation of immature myeloid cells and increase in cell proliferation. The incidence of AML varies with age, it is most common in older adults with a median age of approximately 68 years and accounts for 80-90% of acute leukaemia in adults (reviewed in (Konoplev and Bueso-Ramos 2006)). In addition, 10% of AML incidences affect younger children whose age are less than 10 years, while in patients aged between 10 and 15 years AML comprises 30% of cases (reviewed in (Konoplev and Bueso-Ramos 2006)). Males are more likely to suffer from AML than females and the incidence of AML is increased in patients who suffer with certain genetic disorders such as Fanconi anaemia, Kostmann syndrome, Down syndrome and Klinefelter (Konoplev and Bueso-Ramos 2006, Shipley and Butera 2009).

AML is diagnosed by the accumulation of 20% blast cells in the bone marrow, and these blasts express surface antigen associated with myeloid differentiation such as CD33 and CD13 (reviewed in (Estey and Doehner 2006)). AML treatment consists of an anthracycline, such as daunorubicin or idarubicin, combined with cytarabine and the therapy is based on two steps, which are attempt to produce complete remission by decreasing the blast cells to reach 5%, and then prolong the complete remission (reviewed in (Estey and Doehner 2006)).

### **1.1.1 AML heterogeneity:**

AML is an extremely heterogeneous disease and several systems have been used to divide AML cases into subgroups. AML has been classified into different categories according to cell morphological, immunological, cytochemical, and cytogenetic features (Konoplev and Bueso-Ramos 2006). The most commonly used is the World Health Organisation (WHO) classification, which has essentially taken over from the French-American-British classification (FAB). The FAB classification depends on cell morphology and cytochemical features, but a number of subtypes, which are identified by high technology methods, were not included in the FAB classification (Wakui, *et al* 2008). Thus, the demand for a more precise and comprehensive system was accomplished in the WHO classification, which relies on immunological, cytogenetical and clinical features, in addition to the FAB criteria, and has been cited as being more comprehensively useful than the FAB classification (Table 1.1) (Vardiman, *et al* 2009).

### **1.1.2 AML with cytogenetic abnormalities:**

Chromosomal rearrangements, which include balanced translocations, inversions, deletions, additions or trisomies, are seen in approximately 55% of AML cases (reviewed in (Mrozek, *et al* 2004)). Cytogenetic analysis contributes important information to prognosis in AML and divides cases into three groups: favourable, intermediate, and adverse (Doehner, *et al* 2010). The t(8;21), t(15;17) and inv(16) are associated with the favourable group, whilst patients with abnormalities of 3q, deletion of 5q, or complex karyotype, which have 4 or more chromosomal abnormalities other than

t(8;21), inv(16) or t(16;16), and t(15;17), are classified with the adverse group (Table 1.2) (Grimwade, *et al* 2010). For example, the overall-survival (OS) in a patient with t(8;21) and deletion (9q) or other chromosome abnormalities, is not significantly different from those patients with only t(8;21) (Grimwade, *et al* 2010). However, the presence of t(3;3)/inv(3), del(5q)/-5, and -7 cytogenetic abnormalities are predictors of a poor prognosis (Figure 1.1) (Grimwade, *et al* 2010). The distributions of cytogenetic abnormalities are correlated with the patient's age. In younger patients, for instance, the balanced rearrangements of t(8;21), t(15;17) and inv(16) are more common than in older patients, whilst the unbalanced rearrangements occur in older patients (Grimwade, *et al* 2010).

**Table 1.1: WHO (2008) classifications;** Classification of acute myeloid leukaemia and related precursor neoplasms, and acute leukaemias of ambiguous lineage (Doehner, *et al* 2010).

<b>Categories</b>
<p><b>Acute myeloid leukaemia with recurrent genetic abnormalities:</b></p> <ul style="list-style-type: none"> <li>• AML with t(8;21)(q22;q22); RUNX1-RUNX1T1</li> <li>• AML with inv(16)(p13.1q22) or t(16;16)(p13.1;q22); CBFβ-MYH11</li> <li>• APL with t(15;17)(q22;q12); PML-RARA</li> <li>• AML with t(9;11)(p22;q23); MLLT3-MLL</li> <li>• AML with t(6;9)(p23;q34); DEK-NUP214</li> <li>• AML with inv(3)(q21q26.2) or t(3;3)(q21;q26.2); RPN1-EVI1</li> <li>• AML (megakaryoblastic) with t(1;22)(p13;q13); RBM15-MKL1</li> <li>• Provisional entity: AML with mutated NPM1</li> <li>• Provisional entity: AML with mutated CEBPA</li> </ul>
<p><b>Acute myeloid leukaemia with Myelodysplasia-related changes</b></p>
<p><b>Therapy-related myeloid neoplasms</b></p>
<p><b>Acute myeloid leukaemia, not otherwise specified (NOS):</b></p> <ul style="list-style-type: none"> <li>• Acute myeloid leukaemia with minimal differentiation</li> <li>• Acute myeloid leukaemia without maturation</li> <li>• Acute myeloid leukaemia with maturation</li> <li>• Acute myelomonocytic leukaemia</li> <li>• Acute monoblastic/monocytic leukaemia</li> <li>• Acute erythroid leukaemia</li> <li>• Pure erythroid leukaemia</li> <li>• Erythroleukemia, erythroid/myeloid</li> <li>• Acute megakaryoblastic leukaemia</li> <li>• Acute basophilic leukaemia</li> <li>• Acute panmyelosis with myelofibrosis (acute myelofibrosis; acute myelosclerosis)</li> </ul>
<p><b>Myeloid sarcoma (extramedullary myeloid tumour; granulocytic sarcoma; chloroma)</b></p>
<p><b>Myeloid proliferations related to Down syndrome:</b></p> <ul style="list-style-type: none"> <li>• Transient abnormal myelopoiesis (transient myeloproliferative disorder)</li> <li>• Myeloid leukaemia associated with Down syndrome</li> </ul>
<p><b>Blastic plasmacytoid dendritic cell neoplasm</b></p>
<p><b>Acute leukaemia's of ambiguous lineage:</b></p> <ul style="list-style-type: none"> <li>• Acute undifferentiated leukaemia</li> <li>• Mixed phenotype acute leukaemia with t(9;22)(q34;q11.2); BCR-ABL1</li> <li>• Mixed phenotype acute leukaemia with t(v;11q23); MLL rearranged</li> <li>• Mixed phenotype acute leukaemia, B/myeloid, NOS</li> <li>• Mixed phenotype acute leukaemia, T/myeloid, NOS</li> <li>• Provisional entity: Natural killer (NK)-cell lymphoblastic leukaemia/lymphoma</li> </ul>

**Table 1.2: Cytogenetics-risk group classifications in AML**  
(Grimwade, *et al* 2010).

Cytogenetic abnormality	Comments
<b>Favourable</b> t(15;17)(q22;q21) t(8;21)(q22;q22) inv(16)(p13q22)/t(16;16)(p13;q22)	Irrespective of additional cytogenetic abnormalities
<b>Intermediate</b> Entities not classified as favourable or adverse	
<b>Adverse</b> Abnormal (3q) [excluding t(3;5)(q21_25;q31_35)], inv(3)(q21q26)/t(3;3)(q21;q26), add(5q), del(5q), _5, _7, add(7q)/del(7q), t(6;11)(q27;q23), t(10;11)(p11_13;q23), t(11q23) [excluding t(9;11)(p21_22;q23), and t(11;19)(q23;p13)] t(9;22)(q34;q11), _17/abnormal(17p), Complex ( $\geq 4$ unrelated abnormalities)	Excluding cases with favourable Karyotype

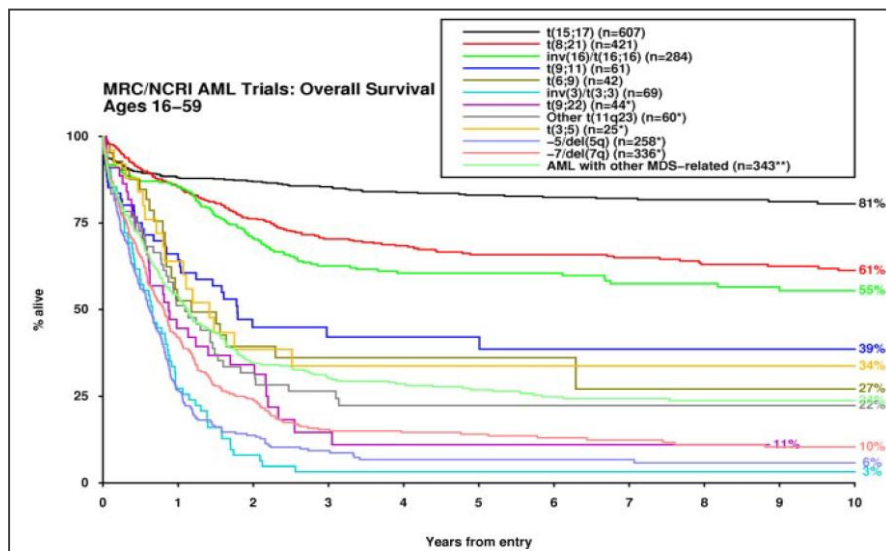


**Figure 1.1: Impact of cytogenetic entities recognised in 2008 WHO classification on survival** (Grimwade, *et al* 2010). \*Excluding patients with t(15;17), t(8;21), inv(16), t(9;11), t(6;9), inv(3)/t(3;3). \*\*Excluding patients with any other abnormalities.

### **1.1.3 AML with normal cytogenetic and molecular mutations:**

Despite the refinement of the cytogenetic classification by Grimwade 2010 (Grimwade, *et al* 2010), approximately 40 to 50% of AML cases have a normal karyotype and these cases are classified in the intermediate prognosis group based on cytogenetics even though some patients with a normal karyotype respond very well to treatment and some respond very badly (reviewed in (Estey and Dohner 2006)). Recently, many of these normal karyotype AML cases have been shown to harbour specific gene mutations, or deregulation of gene expression which may account for the heterogeneity within this group of patients (reviewed in (Dohner and Dohner 2008)). The type of mutations required to result in AML are categorised into two different groups: the first group, class I, involves the activation of signal transduction pathways causing hyper-proliferation and survival of the leukaemic cells, such as FLT3-ITD and RAS mutations (reviewed in (Dohner and Dohner 2008)). The second group, class II, leads to an impaired differentiation and/or irregular gaining of self renewal properties, such as CEBPA, MLL-PTD, where the mutations affect transcription factors, or its co-activation components (reviewed in (Dohner and Dohner 2008)).

#### **1.1.3.1 Internal tandem duplication of Fms-like tyrosine kinase-3 (FLT3-ITD) in AML:**

The most common mutations in normal karyotype AML are length mutations in fms-like tyrosine kinase-3 (FLT3) and nucleophosmin 1 (NPM1). FLT3 is a member of the class III receptor tyrosine kinase, and is normally expressed in haematopoietic stem cells but this expression is reduced as

these cells differentiate (Lyman, *et al* 1994). It plays a major role in cell survival and proliferation through increase in the expression of FLT3 in haematopoietic cells leading to activation of the tyrosine kinase activity and stimulate the growth of progenitor cells in the bone marrow (Kikushige, *et al* 2008).

FLT3 mutations are caused either by internal tandem duplication (ITD), which is described by an insertion of 3 to hundreds of amino acids into the FLT3 juxtamembrane domain, or by point mutation in the activation loop of the tyrosine kinase domain of FLT3, which are observed in approximately 5% of all patients with AML (Kusec, *et al* 2006, Ponziani, *et al* 2006, Reindl, *et al* 2006). FLT3 mutations lead to constitutive activation of the receptor and subsequent downstream activation of signal transducers and activators of transcription 5 (STAT-5), mitogen-activated protein (MAP) kinase, and phosphatidylinositol 3 (PI3) resulting in leukaemic cell survival and proliferation (Brandts, *et al* 2005, Mizuki, *et al* 2000). The signalling pathways have an effect on a large number of related proteins and genes (Seedhouse, *et al* 2006, Tickenbrock, *et al* 2005).

Internal tandem duplication (ITD) in the FLT3 gene is a common mutation in AML and accounts for 25% of AML and patients with an FLT3-ITD are classified as having an adverse prognosis because it is correlated with a high risk of disease relapse leading to the lowering of the overall survival (Grimwade, *et al* 2010, Kottaridis, *et al* 2001). One explanation for the inferior outcome is due to the resistance of the leukaemic cells to chemotherapy, possibly as a result of enhancing the DNA damage repair in the cells. Consequently, a possibility for this occurrence is due to the increase of phosphorylation of STAT-5 (p-STAT-5) and the homologous

recombination mechanism (Seedhouse, *et al* 2006). This causes an increase of the RAD51 expression, which has been noted to correlate with a poorer clinical outcome in many types of tumours and induces anti-apoptotic programmes (Helleday 2010).

In preclinical studies, abnormal over-expression of FLT3-ITD is considered to be a useful therapeutic target in AML. Small FLT3 tyrosine kinase inhibitors have been developed to block the aberrant signal transduction in FLT3-ITD patients and these molecules show an ability in inhibition to both the wild-type and FLT3-ITD auto-phosphorylation and an increase in cytotoxicity against the primary FLT3-ITD mutant blast cells (reviewed in (Kindler, *et al* 2010)). These agents were classified as high selective to target FLT3, such as AC220, intermediate (sunitinib), and less selective (lestaurtinib) and all are under investigation as single agents and in combination with conventional chemotherapy (Mollgard, *et al* 2008, Schittenhelm, *et al* 2009, Seedhouse, *et al* 2006).

#### **1.1.3.2 Frame-shift mutations of NPM1 in AML:**

On the other hand, the NPMc+AML mutations account for 35% of all adult AML and it is characterised by an aberrant delocalisation of NPM1 into the cytoplasm (Falini, *et al* 2005). NPMc+AML is associated with a favourable prognosis, however, the presence of FLT3-ITD with NPMc+ mutations has a negative influence on the prognosis and converts it into an intermediate prognosis (Dohner, *et al* 2005, Schnittger, *et al* 2005, Thiede, *et al* 2006, Verhaak, *et al* 2005). The precise mechanisms connecting the NPM1 mutation to the development of AML and the increased risk of patients

harbouring the NPM1 mutation and FLT3-ITD has not been clarified.

The subject of this thesis is on NPM1 and therefore the most recent insights into the molecular, biological, pathological features of NPM1 mutations in AML will be discussed in sections 1.2.

### **1.1.3.3 Other mutations in cytogenetically normal AML:**

There are other mutations that have been detected in normal-karyotype AML, such as CEBPA, MLL-PTD, NRAS, WT1, and RUNX1. Mutations in CCAAT/enhancer binding protein  $\alpha$  (CEBPA) are detected in 15% of patients with normal-karyotype in AML (Lin, *et al* 2005). CEBP protein encodes a master regulatory transcription factor in haematopoiesis and it up-regulates genes, which are involved in haematopoietic stem cell and granulocyte differentiation (Lin, *et al* 2005). CEBPA mutations include mutations in the N-terminal region leading to the production of a truncated isoform with negative effect, and in-frame mutations in the C-terminal resulting in CEBPA proteins with reduced DNA binding (Lin, *et al* 2005). CEBPA mutations in AML are associated with favourable prognosis and the overall survival rates are very comparable to those patients with NPMc+ without FLT3-ITD (reviewed in (Dohner and Dohner 2008)).

Furthermore, the MLL gene, which is located on chromosome 11q23, encodes the protein involved in the epigenetic regulation of gene expression in haematopoiesis (Whitman, *et al* 2005). MLL partial tandem duplications (MLL-PTD) are detected in 7% of AML patients with normal cytogenetics and have a short complete remission rate and relapsed-free

survival (Whitman, *et al* 2005). Approximately 25% of MLL-PTD cases are associated with FLT3-ITD and the prognoses are very poor (Zorko, *et al* 2012). NRAS mutations cause a constitutive activation of the RAS protein, which plays an important role in the modulation of signal transduction. They bind to different membrane receptors leading to the regulation of cell growth, differentiation and apoptosis. NRAS mutations are found in 14% of younger adult AML patients and the disease prognosis is controversial. Some studies found that patients with NRAS mutations have poor prognosis, while others assumed the prognosis impact is associated with a more favourable outcome (Neubauer, *et al* 1994, Paquette, *et al* 1993).

## **1.2 Nucleophosmin 1 (NPM1) gene and protein:**

NPM1, also called nucleolar protein B23, is a multifunctional phosphoprotein that resides mainly in the nucleolus. It shuttles rapidly between the nucleus and the cytoplasm, and transports proteins between the cellular compartments (reviewed in (Falini, *et al* 2007b)). Due to its shuttling role, NPM1 is involved in many cellular activities, including both cell proliferation and growth-suppressive roles (Grisendi, *et al* 2006). The gene mapping of NPM1 has located the gene to chromosome 5q35 and it contains 12 exons and encodes a protein of 294 amino acids (Chen, *et al* 2006, Falini, *et al* 2005).

### **1.2.1 NPM1 structure:**

The genetic structure of NPM1 encodes for three alternative nucleophosmin isoforms termed B23.1, B23.2 and B23.3, which share N-terminal residues, but, which differ in the last

amino acids of the C-terminal domain (Hingorani, *et al* 2000). B23.1 is localised in the nucleolus and is the predominant form in all tissues. The composition of NPM1 B23.1 is divided into three parts; N-terminal, acidic stretches, and C-terminal (Figure 1.2). The N-terminal residue, which is common to the NPM1 isoforms, is a hydrophobic region involved in oligomerisation and chaperon activity for proteins, nucleic acids and histones (Falini, *et al* 2007b, Hingorani, *et al* 2000). NPM1 is mainly present as an oligomer, a form which is adopted during both cell proliferation and resting, and accounts for 95% of NPM1 protein (Chan and Chan 1995). The N-terminal residues are followed by two acidic stretches that act to help in the histone binding activity of NPM1 and, which are also required for ribonuclease activity (Falini, *et al* 2007b, Hingorani, *et al* 2000). The third region of the B23.1 isoform is the C-terminal, which is involved in nucleic acid binding and ribonuclease activity (Hingorani, *et al* 2000). It is then followed by aromatic short stretches containing two tryptophan residues at positions 288 and 290, which assist in the localisation of the NPM1 in the nucleolus (Hingorani, *et al* 2000, Nishimura, *et al* 2002). Importantly, the NPM1 contains the nuclear-export signal (NES) motifs and bipartite nuclear localisation signal (NLS) motifs at the N-terminal domain and the acidic region, which are important for its shuttling activity (Wang, *et al* 2005). Moreover, the gene contains numerous phosphorylation sites, which are important for specific functions including, the regulation of centrosome duplication and nucleic acid binding during specific cell cycle stages (Hingorani, *et al* 2000).

B23.2, which is a truncated isoform, is composed of 257 amino acids, while the B23.3 consists of 259 amino acids (Dalenc, *et*

*al* 2002)). B23.2 is similar to B23.1, but lacks the last 35 C-terminal amino acid and is expressed in the nucleoplasm and found in all tissues, but at a lower level than B23.1 (Dalenc, *et al* 2002, Falini, *et al* 2007b).

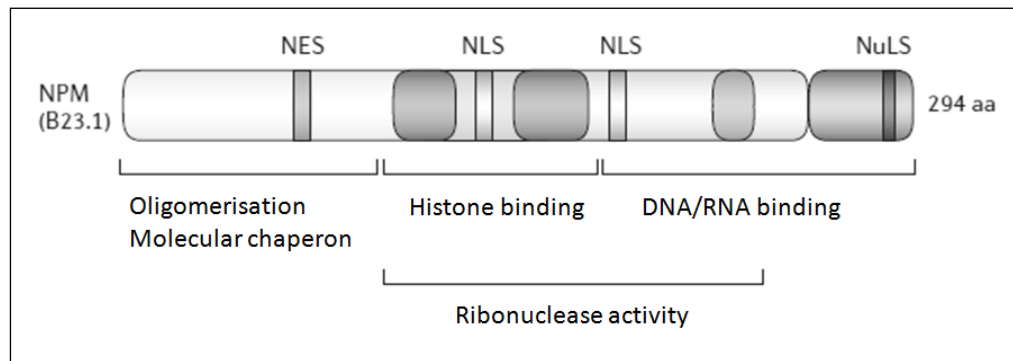


**Figure 1.2: NPM1 structure;** The N-terminal motif is involved in oligomerisation and chaperon activity, followed by the central portion which is important in ribonuclease activity and histone binding. The C-terminal domain is involved in nucleic acid binding and contains two tryptophan residues which are essential for nucleolar localisation of NPM1 (Grisendi, *et al* 2006).

### 1.2.2 NPM1 transport in wild-type NPM1:

NPM1 is a nucleocytoplasmic shuttling protein, which is predominantly localised in the nucleolus (Cordell, *et al* 1999). The two highly conserved nuclear export signal (NES) motifs in the wild-type NPM1 are located within residues 94 to 102 with the sequence I-xx-P-xx-L-x-L, and the other at the N-terminus within amino acid 42 to 49 with the sequence L-x-L-xx-V-x-L at the N-terminus. These motifs are essential in regulation the nuclear export of NPM1 through interaction of the conserved export receptor CRM1 with these motifs (Kau, *et al* 2004). Furthermore, the nuclear localisation signal (NLS), which is located between the two acidic regions in NPM1, drives the NPM1 into the nucleoplasm where it is translocated to the nucleolus through its nucleolar-binding domains; tryptophan 288 and 290 (Nishimura, *et al* 2002).

### **1.2.3 NPM1 functions:**

Through all of these descriptions of the NPM1 structure, it seems that NPM1 serves as an important protein in cellular activities (Rau and Brown 2009). It has an ability to bind to distinct cellular molecules such as nucleoli factors, transcription factors, histones, and other proteins, which are involved in cell proliferation (Falini, *et al* 2007b). NPM1 functions include involvement in ribosome biogenesis, cell proliferation and growth suppression, and it also has a role in controlling genetic stability. As a result, it can be considered as both an oncogene, and a tumour-suppressor protein, depending on the expression level of NPM1.

#### **1.2.3.1 The role of NPM1 in ribosome biogenesis:**

Ribosomal biogenesis is the process of making ribosomes. NPM1 is involved in this process, specifically in the subunit assembly and nuclear export of ribosomes. Transportation of the ribosome elements between the nucleus, and cytoplasm, is a function attributed to NPM1. NPM1 has two leucine residues at 42 and 44, which are important in the CRM1-dependent nuclear export process (Falini, *et al* 2006). Ribosomal L5 and 5S rRNA are transported into the cytoplasm by an interaction with NPM1, which therefore regulates the protein translation mechanism (Yu, *et al* 2006).

Furthermore, NPM1 is found to form complexes with the APE1 protein, which is a DNA repair enzyme and a transcriptional co-activator. Interaction of APE1 with NPM1 occurs via the N-terminal of both proteins and forms the NPM1-APE1 complex (Vascotto, *et al* 2009). This interaction is essential in the production of functional ribosome molecules through

regulation of endonuclease activity during the rRNA synthesis (Vascotto, *et al* 2009). NPM1 also prevents protein aggregation in the nucleolus during this process because of its shuttling function and intrinsic RNase activity. In contrast, inhibition of the ribosomal biogenesis machinery leads to a decrease in the protein shuttling and translation, which causes the cell cycle to arrest. It was shown by Itahana *et al.* that reduction of NPM1 mRNA, inactivated the pre-rRNA process and in murine cells, the ribosome profile changed as a result of the down regulation of the NPM1 gene (Itahana, *et al* 2003).

### **1.2.3.2 The role of NPM1 in regulation of cell growth and proliferation:**

NPM1 has been associated with the regulation of proliferation and cell growth because its over-expression is strongly correlated with proliferation rates in many cell types. NPM1 is involved in the proliferative response through various mechanisms. NPM1 enhances the proliferation of haematopoietic stem cell (HSC) and progenitor cells and over-expression of NPM1 leads to a reduction of protein levels of negative cell cycle regulators and induces entry of haematopoietic cells into the cell cycle (Li, *et al* 2006). NPM1 is involved in enhancing cell proliferation through functioning as an effector for numerous positive cell cycle regulators (Du, *et al* 2010). Phosphorylation of NPM1 at the Ser10 and Ser70 residues promotes the interaction between NPM1 and Cdc25c and prevents phosphorylation of Cdc25c at Ser216. Cdc25c is a key activator of Cdk1/cyclin-B, which regulates cell cycle transition to M phase, and Cdc25c activation is important in cell cycle progression, while inhibition of Cdc25c is associated with cell cycle checkpoint activation (Du, *et al* 2010). As a result, the interaction between Cdk1 and Cdc25c rises and

contributes to enhance the activity of Cdk1, which causes it to enhance cell cycle progression and proliferation (Du, *et al* 2010).

Furthermore, the transcription factor c-Myc, which is the most frequently activated oncogene, is important for cellular proliferation and a high expression of c-Myc enhances cell hyperproliferation and transformation (Li, *et al* 2008). c-Myc has a role in the ribosomal biogenesis process by regulation of the RNA polymerases during transcription (Boon, *et al* 2001). c-Myc induced proliferation and transformation is mediated by NPM1 through interaction with c-Myc target gene promoters which are involved in transcriptional activation and repression of c-Myc (Li, *et al* 2008). Moreover, c-Myc subcellular localisation in nucleoli is regulated by NPM1 which binds to c-Myc in the nucleoplasm and mobilises it into the nucleoli to induce rRNA synthesis (Boon, *et al* 2001, Li and Hann 2013). It has been shown that the over-expression of both NPM1 and c-Myc stimulates rRNA synthesis, whereas c-Myc fails to induce rRNA synthesis when NPM1 is down-regulated (Li and Hann 2013). Therefore, NPM1 is essential for c-Myc localisation in the nucleoli and has the ability to enhance its function in the ribosomal assembly and cell hyperproliferation (Li and Hann 2013, Li, *et al* 2008).

### **1.2.3.3 The role of NPM1 in regulation of tumour suppressor proteins:**

The interaction of NPM1 with P53, ARF and HDM2 provides NPM1 with a tumour-suppressor feature (Colombo, *et al* 2002, Kurki, *et al* 2004b). P53 is stabilised and enhanced via NPM1 binding to the negative P53 regulator - HDM2, which is a nucleoplasmic and nucleolar RING-finger protein (Colombo, *et*

*al* 2002, Kurki, *et al* 2004b). When the cell is damaged by UV, cytotoxic drugs, or DNA intercalating agents, NPM1 is translocated into the nucleoplasm and interacts with HDM2 leading to stabilisation of the P53 protein level and activation of its functions (Colombo, *et al* 2002, Kurki, *et al* 2004a). In contrast, other report found that over-expression of NPM1 can antagonise P53 by inhibiting the IR-induced P53 phosphorylation in normal haematopoietic cells and in cells treated with chemotherapeutic agents, this can lead to an increase in the resistance to apoptosis (Li, *et al* 2005). Moreover, up-regulation of NPM1 with a deletion of the C-terminal domain, the domain which interacts with P53, had no effect on the cellular resistance to apoptosis, whereas suppression of NPM1 increased stress-induced apoptosis (Li, *et al* 2005).

ARF is another tumour-suppressor protein associated with NPM1 and plays an essential role in cell cycle arrest and proliferation (reviewed in (Grisendi, *et al* 2006). It acts as a positive regulator of P53 by binding to HDM2 and in turn resulting in P53 stabilisation and enhancement of its transcriptional targets (Gjerset 2006, Khan, *et al* 2004). NPM1 insulates ARF in the nucleoli and hampers its function in the activation of the P53-dependant pathway (Korgaonkar, *et al* 2005). In stressed cells, however, a modest decrease in NPM1 protein level translocates ARF into the nucleoplasm and bind to the P53 negative regulator protein – HDM2 and activate P53-dependent process, whilst in unstressed cells, NPM1 prevent ARF from localising in the nucleoplasm and blocks the ARF-mediated P53 activation pathway (Korgaonkar, *et al* 2005). In NPM1 knock-down cells, the interaction of ARF with HDM2 increases, but the expression of ARF is reduced,

which reflects the importance of NPM1 in the stabilisation of ARF (Korgaonkar, *et al* 2005).

#### **1.2.3.4 The role of NPM1 in maintenance of genomic stability:**

NPM1 participates in the control of chromosomal ploidy and DNA repair. NPM1 regulates centrosome duplication through inhibition of the process by binding to unduplicated centrosome (Okuda, *et al* 2000). In the mitosis process, CDK2-Cyclin-E, which is a family of serine/threonine kinases and important for centrosome duplication initiation, phosphorylate NPM1 leading to a dissociation of the centrosome and trigger of the initiation of the centrosome duplication process (Okuda, *et al* 2000). Aberrant multiple centrosomes are detected in NPM1<sup>-/-</sup> cells, and blocking the phosphorylation sites in NPM1 caused repression of centrosome duplication (Grisendi, *et al* 2005). Furthermore, NPM1 is a BRCA2-associated protein and required for maintaining the numerical integrity of the centrosomes (Wang, *et al* 2011). Detail on the exact mechanism has not been identified, but the inhibition of the interaction of NPM1 with BRCA2 showed an abnormal amplification of centrosome numbers (Wang, *et al* 2011).

NPM1 is implicated in DNA damage repair through modulation of the function of proliferating cellular nuclear antigen (PCNA). This is a necessary component in the nucleotide excision repair mechanism (Wu, *et al* 2002). In a UV-treated cell, the up-regulation of NPM1 was correlated with a higher level of PCNA leading to an increase in cell growth and inhibition of apoptosis by increases the activity of NER (Wu, *et al* 2002). In addition, NPM1 is required for normal DNA damage repair by binding to

other proteins at the site of DNA damage (Koike, *et al* 2010). In response to irradiation treatment, the formation of irradiated-induced foci (IRIF) is initiated and followed by phosphorylation of H2AX ( $\gamma$ -H2AX) and the mediator of DNA damage checkpoint 1 (MDC1). Subsequently, the lysine (K63)-linked polyubiquitin is catalysed by E3 ubiquitin ligase, which is recruited by MDC1, at the site of DSBs. It has been shown that phosphorylated NPM1 foci are formed and recruited to the DSB sites, where it interacts with K63-linked polyubiquitin conjugates and participates in the DSB-induced RNF8-dependent pathway (Koike, *et al* 2010). Furthermore, cells with mutant NPM1 lacking the phosphorylated domain (T199A-NPM1) demonstrated an increase in DNA fragments after 12 and 24 hours of irradiation treatment, whereas in wild-type NPM1 the fragments were repaired efficiently (Koike, *et al* 2010). In addition, the RAD51-IRIF foci, which are a marker of the homologous recombination (HR) pathway, reached a peak after 6 hours in wild-type and T199A mutant NPM1. Thereafter, the foci was reduced in NPM1 wild-type cells, whilst in the mutant cells, the foci continued to increase until 18 hours after the treatment (Koike, *et al* 2010). Therefore, the role of NPM1 in regulation of centrosome duplication and DNA damage repair is critical in the maintenance of genomic stability.

### **1.3 Mutations in NPM1 in haematological malignancies:**

#### **1.3.1 NPM1 gene translocations in leukaemia and lymphoma:**

The NPM1 gene is involved in the pathogenesis of several types of cancer. Over-expression of NPM1 has been seen in many solid tumours such as gastric, colon, ovarian, and

prostate carcinoma (reviewed in (Grisendi, *et al* 2006)). In haematological malignancies, the NPM1 locus is implicated in chromosomal translocations, deletions and mutations. An oncogenic fusion protein is formed due to locus translocation leading to the induction of an oncogenesis process. The most recognised haematological translocation, due to chromosomal abnormalities of the NPM1 gene are: lymphoma (NPM1-ALK), NPM1-RAR- $\alpha$  and NPM1-MLF1, which are all characterised by the formation of oncogenic fusion and a decrease in wild-type NPM1 (reviewed in (Naoe, *et al* 2006)).

Anaplastic large cell lymphoma (ALCL) accounts for 3% of adult non-Hodgkin lymphoma due to a chromosomal translocation of the 5q35 locus of NPM1 gene with the 2q23 of anaplastic lymphoma kinase (ALK) gene t(2;5) (reviewed in (Falini, *et al* 2007a)). As a result, the N-terminal of NPM1 is fused to the catalytic domain of ALK causing a constitutive activation of the ALK kinase fusion protein (reviewed in (Naoe, *et al* 2006)). The subcellular localisation of the NPM1-ALK chimeric kinase is distributed in the cytoplasm and nucleus, whereas wild-type NPM1 is localised in the nucleus. In leukaemia, a translocation of the NPM1 protein to the RAR- $\alpha$  protein, which is a result of the integration of the NPM1 gene to a retinoic-acid receptor- $\alpha$  gene, causes the translocation to form a rare type of acute promyelocytic leukaemia (APL) with an NPM1-RAR- $\alpha$  fusion product (reviewed in (Falini, *et al* 2007a)). NPM1-RAR- $\alpha$  t(5;17) suppresses the retinoid-responsive transcription, which is restored by ATRA treatment, similar to the more common t(15;17) APL disease (reviewed in (Naoe, *et al* 2006)). Another form of NPM1 translocation in leukaemia is NPM1-MLF1, where the t(3;5) translocation creates the NPM1-MLF1 chimeric protein and, occurs in less

than 1% of myelodysplastic syndrome and AML cases (reviewed in (Falini, *et al* 2007a)). Myelodysplasia/myeloid leukaemia factor-1 (MLF1) is localised in the cytoplasm and plays a negative role in the regulation of MLF11P in erythropoietin-induced differentiation (reviewed in (Naoe, *et al* 2006)). The MLF1 in the NPM1-MLF1 chimeric protein has been shown to be localised in the nucleolus and interrupts the function of MLF1 in erythroid differentiation (reviewed in (Naoe, *et al* 2006)).

### **1.3.2 NPM1 cytoplasmic mutations in AML (NPMc+AML):**

Nucleotide insertions in NPM1 mutations (NPMc+) were discovered in 2005 and they are now considered to be one of the genes most commonly mutated in AML (Falini, *et al* 2005). These NPM1 mutations are characterised by the abnormal subcellular localisation of the NPM1 protein in the cytoplasm (hence the designation NPMc+) and occur in approximately 60% of adult AML cases with a normal karyotype (Falini, *et al* 2005). NPM1 mutations usually occur at exon 12 (Falini, *et al* 2005), but mutations in exon 9 and 11 have been reported in rare cases (Albiero, *et al* 2007, Mariano, *et al* 2006). There are 55 NPM1 mutations in exon 12 that have identified, but an addition of a TCTG tetra-nucleotide at 956 to 959 is the most common NPM1 mutation (Falini, *et al* 2006). This mutation is called mutation A and accounts for 75-80% of the NPMc+ cases (reviewed in (Falini, *et al* 2007b, Rau and Brown 2009)). NPM1 mutations B and D account for 10% and 5% of cases, respectively, whereas other mutations are rare (Chen, *et al* 2006, Falini, *et al* 2007b). All of the NPMc+ mutations cause a frame shift in the C-terminus resulting in a replacement of the last 7 amino acids with 11 different residues, while the N-terminal is conserved (Chen, *et al* 2006, Verhaak, *et al* 2005).

Although the NPMc+ mutations are heterozygous and retain a wild-type allele, the wild-type NPM1 is delocalised from the nucleoli into the cytoplasm through the N-terminal dimerisation domain, which is conserved in all NPM1 mutants. The mutant NPM1 therefore forms heterodimers with wild-type NPM1 which disrupts the function of NPM1 (Falini, *et al* 2006, Verhaak, *et al* 2005).

### **1.3.2.1 Mechanism of abnormal NPM1 subcellular localisation in NPMc+AML:**

The abnormal distribution of NPM1 in NPMc+AML is caused by two major changes at the C-terminus and the last 9 amino acids are crucial for mutant function because they determine the subcellular localisation of the protein (Verhaak, *et al* 2005). These are an insertion of an NES motif and the loss of tryptophan 288 and 290, or the loss of tryptophan 290 alone (Falini, *et al* 2006). The loss of tryptophan 288 and 290, or tryptophan 290 alone, causes delocalisation of the mutant NPM1 in the nucleoplasm, where the additional NES motif at COOH terminus of NPM1 reinforces the protein to be exported into the cytoplasm (Bolli, *et al* 2007, Falini, *et al* 2006). A loss of tryptophan 290 is observed in all NPMc+AML but the highest translocation of mutant NPM1 to the nucleoplasm occurs when both tryptophan (288 and 290) are lost; around 90% of NPMc+AML cases have lost both tryptophan residues (Falini, *et al* 2006). NPM1 is retained in the nucleolus after reinsertion of tryptophan 280 and 290 indicating that the presence of these residues are essential for nuclear export of NPM1 (Falini, *et al* 2006). The loss of both tryptophan 288, and 290 are frequently correlated with the most common NES motif in NPMc+ (L-xxx-V-xx-V-x-L). The loss of tryptophan 290 only shows the same NES motif (L-xxx-V-xx-V-x-L), but

the valine in the second position is replaced with leucine, phenylalanine, cysteine or methionine leading to an increase in the NES export activity (Bolli, *et al* 2007, Falini, *et al* 2006). Bolli *et al.* found that the two NES motif in wild-type NPM1 cannot counterbalance the force of nuclear localisation signal (NLS) and tryptophans, which are responsible for NPM1 subcellular localisation in the nucleolus. However, an insertion of NES motif in NPMc+ and a loss of tryptophan 290 showed an increase in the nuclear export activity more than the NES motif (L-xxx-V-xx-V-x-L) with mutations of both tryptophans (Bolli, *et al* 2007). Furthermore, by combining the NES motif (L-xxx-V-xx-V-x-L), which is found in NPM1 mutations (type-A), with tryptophan 288 only or NES motif (L-xxx-L-xx-V-x-L), which is seen in NPM1 mutation (type-E), with a loss of both tryptophans, these were not efficient enough to export NPM1 into the cytoplasm, which indicates that the NPM1 mutants are naturally selected to enforce the protein exportation into the cytoplasm (Bolli, *et al* 2007).

#### **1.3.2.2 Role of NPMc+ in leukaemogenesis:**

The mechanism of leukaemogenesis in NPMc+AML has not been elucidated, but there are many suggestions that should be considered, particularly in terms of the main characterisation of the mutated cells – that is delocalisation of NPM1 into the cytoplasm which also displaces the protein partners thereby interfering with a range of functions. At the level of tumour suppressor protein regulation, it is known that P53 stability and activity is mediated by ARF and NPM1 through binding to HDM2 (Colombo, *et al* 2002). In NPMc+AML, mutant NPM1 binds to ARF and delocalises into the cytoplasm leading to the inhibition of P53 dependent and independent pathways (Colombo, *et al* 2006, Korgaonkar, *et al*

2005). The work of Bonetti *et al.* (2008) agrees with this and demonstrates the role of another factor, which may contribute to the development of leukemogenesis in NPMc+AML (Bonetti, *et al* 2008). Specifically, they found that the stability of c-Myc is regulated by NPM1 through the interaction with the F-box protein (Fbw7 $\gamma$ ), which is a component involved in the ubiquitination and proteasome degradation of c-Myc (Bonetti, *et al* 2008). In NPMc+AML, the Fbw7 $\gamma$  is delocalised in the cytoplasm by mutant NPM1, which leads to an increase in the stability of c-MYC and an increase in the cell proliferation (Bonetti, *et al* 2008). As a result, the hyperproliferation of the cells as a result of the increase in the c-MYC activation, perturbs ARF and P53 activity and this may result in tumorigenesis (Li and Hann 2009).

Another possible factor which may play a role in NPMc+ leukaemogenesis is the impairment of HEXIM1 protein subcellular localisation. The NPM1 was found to regulate RNA polymerase II transcription through the interaction of hexamethylene-bis-acetamide inducible protein 1 (HEXIM1), which has an inhibitory effect on RNA polymerase II transcription (Gurumurthy, *et al* 2008). The interaction of NPM1 with HEXIM1 results in NPM1 inactivation of HEXIM1 and enhances the RNA polymerase II transcription (Gurumurthy, *et al* 2008). In NPMc+AML, the HEXM1 protein has been reported to delocalise in the cytoplasm causing an increase in the transcription of RNA polymerase II and enhancement of the expression of genes that may be related to the leukaemic phenotype such as MCL-1 and cyclin D1 (Glaser, *et al* 2012, Gurumurthy, *et al* 2008). Therefore, it seems that aberrant localisation of NPM1 in the cytoplasm effects many proteins, which may contribute to leukaemogenesis.

In vivo, complete abrogation of NPM1 gene expression (NPM1<sup>-/-</sup>) in mouse result in embryonic lethality (Grisendi, *et al* 2005). Although the mutant embryos were smaller in size than in wild-type and heterozygote NPM1, the heart, neural tube, brachial arches and limb buds were comparatively well-developed (Grisendi, *et al* 2005). However, the number of haematopoietic precursor in the blood islands of the NPM1<sup>-/-</sup> yolk sacs was decreased and their ability to differentiate into various lineages was impaired and the blood cells contain large multi-nucleated cells with 4 nuclei and copious centrosomes due to supernumerary centrosome amplification (Grisendi, *et al* 2005). The apoptosis level was up-regulated in NPM1<sup>-/-</sup> embryos and the level and the activity of P53 was increased (Grisendi, *et al* 2005). Thereafter, the haematopoiesis analysis of heterozygous NPM1 (NPM1<sup>+/-</sup>) demonstrated myelodysplastic syndrome (MDS) features and bone marrow of NPM1<sup>+/-</sup> showed dyserythropoiesis and megakaryocyte dyspoiesis (Grisendi, *et al* 2005). As a result, it seems that NPM1 is in embryogenesis and the development of haematopoiesis, while impairment in NPM1 function by loss its function leads to develop tumorigenesis (Grisendi, *et al* 2005).

Furthermore, the expression of NPMc+ in transgenic mice and in a zebrafish embryonic model, demonstrated myeloid proliferation. In the transgenic mice, the mutant NPM1 localised in the cytoplasm and the mice exhibited features of myeloproliferation and an accumulation of myeloid cells in the spleen. In addition, it has demonstrated that the NPM1 mutant blocked megakaryocytic differentiation leading to an increase in the mean platelet number and the number of megakaryocyte cells in bone marrow and the spleen (Cheng, *et al* 2010, Sportoletti, *et al* 2013, Vassiliou, *et al* 2011).

Moreover, The zebrafish model showed the same results as the transgenic mice with an increase in the numbers of erythro-myeloid progenitors and haematopoietic stem cells (Bolli, *et al* 2010). However, in both models, there was no evidence of disease development and this concludes that the NPM1 mutant alone itself is insufficient to trigger all the characteristics necessary for AML. Vassiliou *et al.* agreed with this and they used human-NPMc+ knock-in mice and combined it with insertional mutagenesis in other genes such as the *Csf2* gene, which encodes GM-CSF and is activated in 48% of leukaemia, or in the *FLT3* gene (*FLT3*-ITDs are common in NPMc+AML) (Vassiliou, *et al* 2011). They found that the presence of mutations in other genes are important in the growth of leukaemic cells through the activation of proliferating molecules and pathways (Vassiliou, *et al* 2011).

### **1.3.2.3 Clinical features of patients with NPMc+AML:**

Several clinical characterisations have been shown to significantly correlate with NPMc+AML. In many studies, NPM1 mutations cooperate with other gene mutations such as *FLT3*-TKD, *CEBPA*, *NRAS* and *IDH1* mutations (Dohner, *et al* 2005, Schnittger, *et al* 2005, Thiede, *et al* 2006, Verhaak, *et al* 2005). However, the most common mutation co-expressed with NPMc+ is an internal tandem duplication of *FLT3* (*FLT3*-ITD): *FLT3*-ITDs occur in about 40% of NPMc+ mutated AMLs (Boissel, *et al* 2005, Falini, *et al* 2005). Chromosomal abnormalities in NPMc+AML are uncommon and account for only 19% and 4% of NPMc+ cases in adults and children, respectively (Rau and Brown 2009). Karyotype abnormalities are considered secondary to NPM1 mutations because; a) the chromosome abnormalities arise at relapse in the NK-AML patient; b) the cells show a mixture of leukaemic cells

harbouring cytogenetic abnormalities and subclones of normal karyotype, and c) the feature of NPMc+AML patients with chromosomal abnormalities, in terms of type and frequency, are similar to secondary chromosomal changes developed in AML patients harbouring recurrent karyotype abnormalities (Falini, *et al* 2005).

The incidence of NPMc+ mutations in AML is higher in adults than in paediatric cases, and the risk of NPMc+ mutations is more frequent in adult female than in adult male (Chou, *et al* 2006, Shimada, *et al* 2007). Moreover, the frequency of the NPMc+ mutations is increased in American and European populations compared with Asian populations (Gale, *et al* 2008, Shimada, *et al* 2007). NPMc+ mutations are found in all FAB subtypes in adult patients except M3 and M7, whereas M4 and M5 have the highest frequency of NPMc+. The blast cells and platelet counts are elevated in NPMc+ (Dohner, *et al* 2005, Falini, *et al* 2005, Schnittger, *et al* 2005).

Although a minor population of CD34 positive cells were identified, the NPMc+AML cells are generally CD34 negative (Nomdedeu, *et al* 2011). The minor population of CD34 positive were transplanted into mice to test their ability to initiate leukaemia. CD34 positive cells, which are bearing NPM1 wild-type in NPMc+AML, gave rise to normal multilineage haematopoiesis after transplantation into mice, whilst cells with NPMc+ mutations either CD34 negative or CD34 positive initiated leukaemia. Interestingly, the CD34 expression was lost after re-transplantation of the AML cells into the secondary recipients (Taussig, *et al* 2010). Moreover, Martelli *et al.* found that CD34 positive cells carrying NPMc+ mutations generated a leukaemia with the same features as seen in the NPMc+AML patients, but they found that CD34

negative cells gave rise to different patterns to those observed in NPMc+AML (Martelli, *et al* 2010). Therefore, CD34 positive and CD34 negative cells are considered as being leukaemia-initiated (LIC) cells in NPMc+ AML, but the origin of the leukaemia stem cells (LSC) in NPMc+AML still remains to be clarified and the question of whether the disease has arisen from early progenitors or long-term repopulating cells is still not clear (Martelli, *et al* 2010, Taussig, *et al* 2010).

#### **1.3.2.4 Gene expressions profiling (GEP) in NPMc+AML:**

Gene expression profiling (GEP) assists in identifying the pathogenesis of AML through understanding which genes are up or down regulated (Bacher, *et al* 2009). The Homeodomain genes (HOX-A and HOX-B), TALE, PBX3, and MEIS1 are the genes whose aberrant regulation is most correlated with NPM1 mutations; these genes are over-expressed (Andreeff, *et al* 2008, Bacher, *et al* 2009). The HOX genes encode transcription factors and regulate the early stages of haematopoiesis, including self renewal and haematopoietic stem cell, differentiation as well as the proliferation of cells (Andreeff, *et al* 2008). In normal cells, up-regulated HOX genes are associated with haematopoietic stem cells and CD34 positivity, whilst expression is reduced during normal differentiation (Alcalay, *et al* 2005, Bacher, *et al* 2009). NPMc+ causes the activation of many members of the HOX family and TALE possibly leading to leukaemogenesis (Bacher, *et al* 2009). NPMc+/FLT3-ITD cells have a higher level of HOX than NPMc+/FLT3-wt cells and NPM-wt/FLT3-ITD (Andreeff, *et al* 2008). The reason for this appears to be because the FLT3-ITD affects a small number of non-clustered HOX genes, particularly HOX-B5, which is expressed abnormally (Andreeff, *et al* 2008). Alterations in HOX gene expression have been

associated with disease prognosis and responsiveness to chemotherapy and it has been noted that decreasing levels of HOX-A9 and CD34 are associated with a favourable prognosis, as seen in NPMc+AML cases (Bacher, *et al* 2009, Verhaak, *et al* 2005).

#### **1.3.2.5 Prognostic impact of NPMc+AML:**

In normal karyotype AML, the prognostic impact of NPMc+ varies amongst patients with different AML-associated mutations. FLT3-ITD, for example, is associated with an adverse outcome after conventional chemotherapy, whereas patients carrying CEBPA mutations have been associated with a favourable outcome (Shipley and Butera 2009). NPM1 mutations have been associated with favourable prognosis and many studies have found that the complete remission rate is higher amongst these patients compared to patients with wild-type NPM1 (Dohner, *et al* 2005, Schnittger, *et al* 2005, Thiede, *et al* 2006, Verhaak, *et al* 2005). Furthermore, in patients with NPMc+/FLT3-ITD, the complete remission rate was lower than in the presence of NPMc+ mutations only (Boissel, *et al* 2005). In addition, the event-free survival, overall survival and relapse-free survival rates, were noted to be better in NPMc+/FLT3-wild-type than other normal karyotype AML patients (Figure 1.3) (Dohner, *et al* 2005, Gale, *et al* 2008, Thiede, *et al* 2006, Verhaak, *et al* 2005).

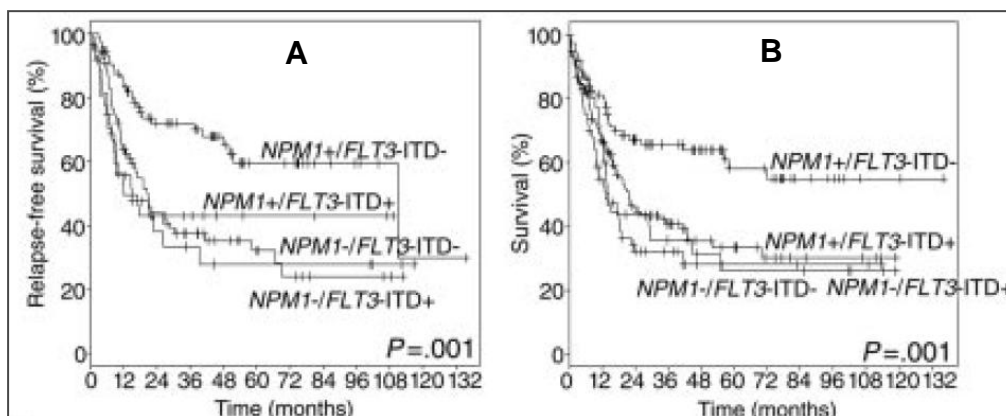


**Figure 1.3: Survival analysis of NPM1 and FLT3 mutations in AML patients; (A)** Relapsed-free survival, and **(B)** Overall Survival according to the combined NPMc+ and FLT3-ITD mutations status in AML patients younger than 60 years old (Dohner, *et al* 2005).

### 1.3.2.6 All-trans retinoic acid (ATRA) treatment in AML:

All-trans retinoic acid (ATRA), vitamin-A derivative, is used in the treatment of acute promyelocytic leukaemia (APL) (Seiter, *et al* 2000). APL is an AML type characterised by chromosomal translocation that results in a chimeric fusion gene of RAR $\alpha$  to a second gene, most commonly PML in t(15;17), but also NPM1 in t(5;17) and PLZF in t(11;17) (reviewed in (Zhang, *et al* 2000)).

The action of ATRA in the treatment of APL has been investigated. In PML-RAR $\alpha$  positive APL, ATRA degrades the oncogenic PML-RAR $\alpha$  fusion protein and restores the normal structure of PML oncogenic domains (reviewed in (Zhang, *et al* 2000)). Furthermore, ATRA modulates receptors that are involved in cell differentiation by affecting the co-repressor (CoR) and co-activator (CoA) complexes (reviewed in (Zhang, *et al* 2000)). CoR binds to the chimeric fusion PML-RAR $\alpha$ , or NPM1-RAR $\alpha$ , causing it to block cell differentiation. However, in ATRA treatment, CoR is released from the complex and recruited to CoA for transcriptional activation and a reverse of

the differentiation block (reviewed in (Zhang, *et al* 2000)). At the gene expression level, many signalling pathways have been induced upon ATRA treatment in APL cells. A high expression of genes participating in the signal transduction pathway such as, cAMP dependent protein kinase A (cAMP/PKA), and protein kinase C (PKC) have been reported, whereas genes involved in Mitogen-activated protein (MAP) kinases particularly P38, ERK3 and JNK are down-regulated (Yang, *et al* 2003b, Zhang, *et al* 2000).

Administration of ATRA with chemotherapy to non-APL AML patients did not improve clinical outcome (Burnett, *et al* 2010, Milligan, *et al* 2006). Conversely, other researchers found that patients with NPMc+ mutations without FLT3-ITD did benefit from adding ATRA to chemotherapy and demonstrated a significantly higher complete remission rate and overall survival (Schlenk, *et al* 2011, Schlenk, *et al* 2009). In vitro, treatment of the HL-60 AML cell line with ATRA showed an inhibition of cell proliferation and an increase in cell differentiation (Jian, *et al* 2011, Wang, *et al* 2009). In NPMc+AML, the effect of ATRA on the OCI-AML3 (NPMc+) cell line was studied and these NPMc+ cells were found to be more susceptible to differentiation upon ATRA exposure at a low concentration when compared to the HL-60 (NPM1-wt) cell line (Kutny, *et al* 2010). Furthermore, ATRA treatment resulted in a reduction in the NPM1 mutant level, causing an activation of components involved in apoptosis such as caspase-8, caspase-3, and BAX, which indicated that the cell death pathway in NPMc+AML is affected by ATRA treatment (Martelli, *et al* 2007). However, during clinical trials, the administration of ATRA to NPMc+AML patients demonstrated variable results. In a United Kingdom Medical Research Council (MRC) trial,

younger patients with NPM1 mutations had no significant increase in complete remission (CR) rate, or overall survival (OS) when treated with ATRA (Burnett, *et al* 2010). On the other hand, an Austrian-German study found that patients harbouring NPMc+ mutants had a high CR and a better overall survival and relapse-free survival when treated with ATRA, compared to those patients harbouring other prognostically important mutations - FLT3-ITD, FLT3-TKD, and MLL-PTD (Schlenk, *et al* 2011, Schlenk, *et al* 2009). The conflict between the two studies was proposed to be because of differences in the treatment protocols; ATRA was administered on the third day of chemotherapy in the Austrian-German study, whereas in the MRC study ATRA was started on day one (Burnett, *et al* 2010, Schlenk, *et al* 2009).

#### **1.4 DNA damage response (DDR):**

DDR mechanisms are activated because our genome is introduced to many different types of DNA damage, both endogenous and exogenous, leading to the production of thousands of DNA lesions. Genome integrity is maintained by many DNA damage response (DDR) mechanisms involving cell cycle arrest, DNA repair, and apoptosis (reviewed in (Jackson and Bartek 2009)). Failure in the activation of the DDR process can result in the proliferation of cells harbouring damaged DNA leading to develop tumorigenesis (reviewed in (Polo and Jackson 2011)).

##### **1.4.1 Sensing of DNA damage:**

Genomic DNA is packaged into highly condensed chromatin structures with histone and non-histone proteins. The DNA repair process begins with the re-modulation of the chromatin

structure, which facilitates DNA repair enzymes accession to chromatin (Wong, *et al* 2006). The chromatin structure alteration can occur either by adjustment of the histone composition or by chromatin remodelers, which use the energy from ATP hydrolysis to weaken the interactions between histones and the surrounding DNA (Fyodorov and Kadonaga 2001, Jenuwein and Allis 2001). In response to DNA damage, phosphorylation the variant histone H2AX ( $\gamma$ -H2AX) at the DNA damage site, is required for formation of irradiated-induced foci (IRIF), which contain several factors involved in the DNA repair process (Burma, *et al* 2001, Huang, *et al* 2004). The  $\gamma$ -H2AX formation is dependent on the phosphatidylinositol 3-kinase-like kinases (PI3-KK) family proteins - Ataxia telangiectasia mutated (ATM), which is mainly activated by DSB, and Ataxia- and Rad-related (ATR), which is activated by the formation of RPA-coated ssDNA complexes (Burma, *et al* 2001, Ward and Chen 2001). ATM and ATR are phosphorylated and recruited to the site of damage by Mre11, RAD50, and NBS1 (MRN) complex, and ATR-interacting protein (ATRIP), respectively (reviewed in (Yang, *et al* 2003a)). Furthermore, activation and accumulation of PI3-KK family at the site of the DNA damage leads to the enhancement of the phosphorylation of other proteins that are targeted by ATM, such as BRCA1, MDC1, Chk2, and P53, and by ATR, such as Rad17, Chk1, ATRIP, and P53 (reviewed in (Shimada and Nakanishi 2006)).

#### **1.4.2 DNA repair mechanisms:**

DNA is repaired by pathways involving many different steps in order to eliminate DNA damage that may threaten genome integrity. Different mechanisms are involved in DNA repair, and each DNA repair pathway is activated depending upon the

specific type of DNA lesion (Table 1.3) (Figure 1.4) (Jackson and Bartek 2009).

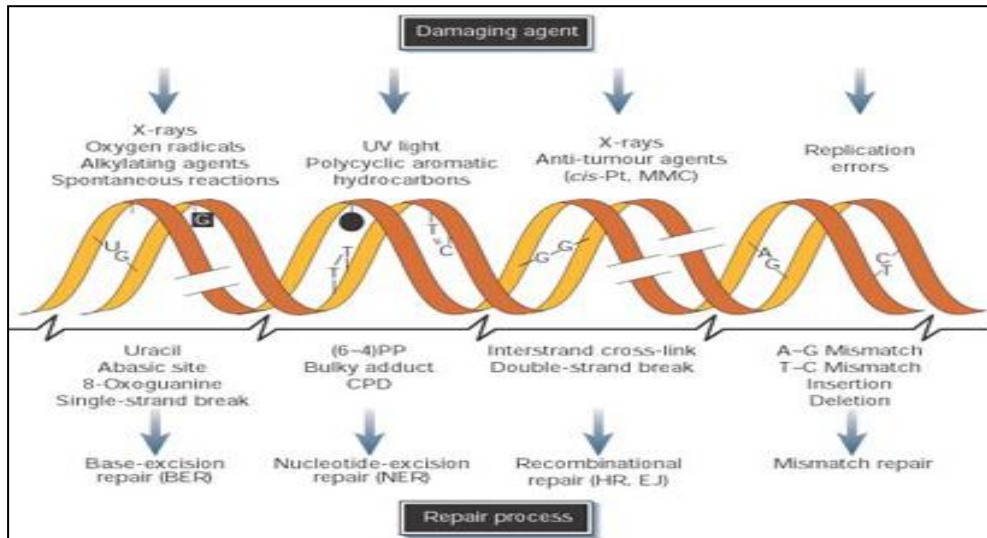


**Figure 1.4: DNA damage repair mechanisms;** The four different pathways that are implicated in response to damaging agent and the type of DNA lesions (Hoeijmakers 2001).

**Table 1.3: DDR mechanisms;** Different DDR pathways are available, use depends on the DNA lesions type (Jackson and Bartek 2009)

DDR mechanisms	Prime lesion acted upon
Mismatch repair	DNA mismatches and insertion/deletion loops arising from DNA replication
Base excision repair and SSB repair	Abnormal DNA bases, simple base adducts, SSBs generated as base-excision repair intermediates by oxidative damage or by abortive topoisomerase I activity
Nucleotide excision repair (NER)	Lesions that disrupt the DNA double helix, such as bulky base adducts and ultraviolet photo-products
Trans-lesion bypass mechanisms	Base damage blocking replication-fork progression
Non-homologous end-joining (NHEJ)	Radiation or chemically-induced SBs plus V(D)J and class-switch recombination intermediates
Homologous recombination (HR)	DSBs, stalled replication forks, inter-strand DNA crosslinks and sites of meiotic recombination and abortive topoisomerase II action
Fanconi anaemia (FANC) pathway	Inter-strand DNA crosslinks
ATM-mediated DDR signalling	DSBs
ATR-mediated DDR signalling	ssDNA, resected DSBs

#### **1.4.2.1 Double strand breaks:**

DSBs are repaired by either non-homologous end-joining (NHEJ), which repairs the DSB without the need for a template, or homologous recombination (HR), which use a sister chromatid as a homologous template (Jackson and Bartek 2009, Wong, *et al* 2006). NHEJ begins by recognising the DSBs through the Ku70 and Ku80 proteins, which binds and activates the protein kinase DNA-PK. Thereafter, the DNA-PK recruits other repair proteins, such as ligase-IV/Xrcc4 complex, Artemis, PNK and Polymerase X to allow the NHEJ repair to proceed (reviewed in (Jackson and Bartek 2009, Polo and Jackson 2011)).

On the other hand, HR uses sister chromatid sequences for the repair process, which is instigated through the MRN complex (reviewed in (Polo and Jackson 2011)). The first step in the HR pathway to repair the DSB is the production of 3' ssDNA overhang through resection of 5' end by the MRN complex. Subsequently, a nucleoprotein filament is formed after RAD51 recruitment, which is the central protein in HR that binds to the exposed single-strand tail (reviewed in (Rastogi, *et al* 2010)). This step is enhanced by a Rad55/Rad57 protein heterodimer, which inactivates the inhibitory effect of ssDNA-binding complex protein (RPA) coating the ssDNA overhang, and  $\gamma$ -H2AX, which recruits more RAD51 to the site of damage (Sonoda, *et al* 2007, Wolner, *et al* 2003). Thereafter, the filament, together with RAD51, and other HR factors explore for an intact copy of the broken DNA from the sister chromatid template (reviewed in (Rastogi, *et al* 2010)). After the insertion of the strand into the homologous template, the extension and ligation process occur via the DNA polymerase and ligase I, respectively (Mazon, *et al* 2010). Finally, the

cleavage and resolution of HR intermediates are mediated by DNA helicase and resolvase enzymes to form intact and repaired DNA molecules (Mazon, *et al* 2010).

#### **1.4.2.2 Base excision repair:**

Another mechanism that is involved in DNA repair is the base excision repair pathway (BER). BER functions on base lesions that are generated from oxidative stress, alkylating agents such as MMS and other sources (reviewed in (Jackson and Bartek 2009)). The process begins when a specific DNA glycosylase recognises and removes a damaged base. Next, the apurinic/aprimidinic endonuclease (APE1), which is an essential enzyme in BER, hydrolyses the phosphodiester backbone at the 5' position (reviewed in (Fishel and Kelley 2007)). Subsequently, a normal 3'-hydroxy group is generated and DNA polymerase fills the gap. DNA ligase can then re-join the strands (reviewed in (Fishel and Kelley 2007)). The BER pathway has two repair sub-pathways, which are short-patch and long-patch BER, and are initiated after APE1 action. Short-patch BER, which is activated in the presence of one nucleotide lesion, involves recruitments of poly (ADP-ribose) polymerase-1 (PARP-1) (Fortini and Dogliotti 2007). Then, the damaged nucleotide is replaced by scaffold protein X-ray repair cross-complementing (XRCC1) and  $\beta$ -polymerase followed by the action of DNA ligase III to seal the nick and restore the integrity of DNA (Fortini and Dogliotti 2007). On the other hand, long-patch BER, which is implied on DNA have two or more nucleotide lesions, recruits proliferating cell nuclear antigen (PCNA) with  $\beta$ -polymerase or  $\epsilon/\delta$ -polymerase to extend and fill the gap by inserting 2-13 nucleotide (Fortini, *et al* 1998). Thereafter, the ensuing DNA flap is displaced by

the flap endonuclease (FEN-1) protein and then the nick is ligated by DNA ligase I (Fortini and Dogliotti 2007).

#### **1.4.2.3 Other DNA repair mechanisms:**

Nucleotide excision repair (NER) is an essential process in the removal of DNA lesions, which are produced by ultraviolet light (reviewed in (Rastogi, *et al* 2010)). NER recognises helix-distorting base lesions and operates through two different sub-pathways, which are global genome (GG-NER) and transcription-coupled NER (TC-NER) (Costa, *et al* 2003)). GG-NER is activated in lesions produced in a transcriptionally silent area. Whereas, TC-NER targets a transcription blocking lesion, which is encountered by the transcription mechanism RNA polymerase II (Costa, *et al* 2003). In a mis-match repair (MMR) pathway, an incision of single-strand is introduced to the damaged DNA which is produced by insertion, deletion, and mismatch bases during DNA replication (reviewed in (Jackson and Bartek 2009)). Then, the MMR process is achieved by the actions of polymerase and ligase enzymes to restores the intact DNA (Jiricny 2006)).

#### **1.4.2.4 DDR in resistance to therapy:**

In cancer therapy, enhanced DDR can have a negative impact on the clinical response to chemotherapies and radiotherapy because aggressive activation of DDR may cause an increased repair of genotoxic lesions resulting in the resistance of tumour cells to the therapy (reviewed in (Helleday, *et al* 2008)). In ovarian cancer, for instance, positive expression of XRCC1, a protein involved in BER, showed to be correlated with aggressive outcome and resistance to platinum therapy, whereas cases that showed negative XRCC1 were associated

with favourable prognostic impact (Abdel-Fatah, *et al* 2013). In addition, ovarian and gastro-oesophageal cancer cases with positive expression of APE1 is predicted to have a negative impact in the response to chemotherapy compared to those cases with negative APE1 expression (Al-Attar, *et al* 2010). Homologous recombination dysfunction in tumour cells confers susceptibility to anti-cancer drugs, while glioma stem cells, where the HR is activated, are less sensitive to therapy (Helleday 2010). Furthermore, RAD51, which is a protein involved in the homologous recombination process, is seen in high levels in FLT3-ITD AML samples, a mutation associated with an adverse prognosis (Seedhouse, *et al* 2006). Therefore, understanding the DDR mechanism is crucial in therapy resistance tumour development and there are potential benefits in cancer treatment by developing effective inhibitors that inhibit the DNA repair function and increase the sensitivity of tumour cells to radiation or chemotherapies (Helleday, *et al* 2008, Madhusudan, *et al* 2005).

#### **1.4.3 Apoptosis:**

Apoptosis or programmed cell death is an essential process to remove infected, unwanted or damaged cells. There are two distinct principle pathways which are the extrinsic and intrinsic cell death pathways (reviewed in (Gustafsson and Gottlieb 2007)). The extrinsic pathway is induced by ligands binding to a death receptor on the cell surface, these ligands are members of the tumour necrosis factors (TNF) family (reviewed in (Adams and Cory 2007)). Subsequently, the Fas-associated death domain (FADD) protein activates and recruits caspase-8 into a death-inducing signalling complex, then downstream caspases are activated (reviewed in (Adams and Cory 2007)). The intrinsic pathway is enhanced when

cytochrome-c is released from the mitochondria causing it to activate caspase-9 through an apoptotic protease-activating factor (Apaf-1). This leads to the activation of the effector caspases (reviewed in (Adams and Cory 2007)). The intrinsic pathway is regulated by the BCL-2 family, which is composed of pro- and anti-apoptotic proteins which share up to four conserved domains called BCL-2 homology (BH) domains (reviewed in (Tzifi, *et al* 2012)).

The anti-apoptotic proteins, BCL-2, MCL-1, contain four BH domains, named BH1, BH2, BH3, and BH4, whilst the pro-apoptotic proteins are divided into two groups: the multi-domain proteins (BAX and BAK), which have the first three domains as present in the anti-apoptotic proteins. The other group are the BH3-only proteins such as BAD, NOXA, and PUMA (reviewed in (Adams and Cory 2007)). BH3-only proteins are the sensors of cell death signals and two of these proteins – Noxa, and Puma – are essential in the regulation of apoptosis induced by the tumour suppressor protein P53 in response to DNA damage, while BID and BIM are the activators of BAX and BAK (reviewed in (Gustafsson and Gottlieb 2007, Letai 2008)). In normal cells, BAX and BAK are maintained in an inactive state by binding to the anti-apoptotic proteins – BCL-2, MCL-1 and BCL-xL. In response to cell death, the BH3-only proteins bind to the anti-apoptotic proteins BCL-2, MCL-1 and BCL-xL leading to release BAX and BAK and initiate intrinsic apoptosis pathway (reviewed in (Gustafsson and Gottlieb 2007)).

In cancer development, there is evidence that the expression of anti-apoptotic BCL-2 proteins is perturbed and the resistance of tumour cells to cytotoxic drugs is elevated (Bradbury, *et al* 1996, Glaser, *et al* 2012). In t(14;18)

lymphoma cells, which is distinguished by translocation of the BCL-2 from 18q21 to the 14q32 locus an increase in BCL-2 levels are seen which promotes cell survival (Graninger, *et al* 1987). Moreover, in FLT3-ITD AML, MCL-1, which is an anti-apoptotic protein and is critical for AML cell survival, has been shown to be up-regulated to a greater extent than in normal hematopoietic stem cells (Yoshimoto, *et al* 2009). Therefore, developing drugs to target the anti-apoptotic proteins are under investigation for effective treatment of tumour cells (Adams and Cory 2007, Glaser, *et al* 2012, Shore and Viallet 2005).

#### **1.4.4 Interaction of NPM1 with proteins involved in DNA damage response:**

The main function of NPM1 is shuttling between the nucleus and the cytoplasm, but NPM1 interacts with many proteins, particularly those involved in the DNA damage response mechanisms such as ARF, P53, HDM2, and APE1. NPM1-ARF complex is formed by binding of the C-terminal of NPM1 to the N-terminal of ARF in the nucleus. The C-terminal region of NPM1 is essential for a complex formation, as well as nucleic acid binding properties (Korgaonkar, *et al* 2005). The NPM1-ARF complex disappears after the cell has been exposed to a DNA damage response, such as UV. ARF is then translocated to the nucleoplasm where it binds to HDM2, resulting in the stabilisation and activation of P53 (Lee, *et al* 2005). In addition, NPM1 binds to HDM2 using the same domains as ARF, which leads to the formation of the NPM1-HDM2 complex (Korgaonkar, *et al* 2005, Kurki, *et al* 2004b). The NPM1-HDM2 complex is usually formed during the later stages of the DNA damage response, which indicates that NPM1 interacts with newly synthesised HDM2, or when it is released from P53

(Colombo, *et al* 2002, Korgaonkar, *et al* 2005). ARF-HDM2 and NPM1-HDM2 disappear after the DNA is repaired and, the ARF-NPM1 complex is reformed and relocated in the nucleus. This process suggests that NPM1 contributes in controlling DNA damage response mechanisms through interaction with the tumour-suppressor proteins (Colombo, *et al* 2005, Colombo, *et al* 2002, Kurki, *et al* 2004a). Moreover, the APE1 protein is an essential enzyme in the DNA base-excision repair pathway and functions as a redox factor modulating many transcription factors such as, AP-1, NF- $\kappa$ B, and P53 (Fishel and Kelley 2007). NPM1 interacts with the N-terminal residues of APE1 in the nucleus and translocates it into the nucleolus. This interaction is essential in controlling the APE1 endonuclease activity, and results in an increase in the enzyme activity (Vascotto, *et al* 2009). The importance of NPM1 in regulation of proteins, which are involved in DNA repair pathway, gave an attention to the DNA damage response mechanisms in NPMc+AML.

### **1.5 Aim of the study:**

AML harbouring NPMc+ mutations is a disease with distinct clinical features and diagnosis. Patients with NPMc+ mutations have a favourable prognosis and the complete remission rate is higher than those patients with wild-type NPM1. The exact role of NPMc+ in tumorigenesis and the reasons behind the favourable prognosis of patients with NPMc+ mutations have not yet been precisely determined. However, it is assumed that the role of NPM1 in the regulation of tumour-suppressor proteins including P53, ARF, and HDM2, is significant (Colombo, *et al* 2005, Kurki, *et al* 2004b). In NPMc+AML, the NPMc+ mutations cause delocalisation of ARF to the cytoplasm with NPM1, which could lead to a disturbance of the DDR

functions and increase the sensitivity of tumour cells to chemotherapies (Colombo, *et al* 2006). In addition, NPM1 is required for APE1 subcellular localisation in nucleoli and the modulation of the APE1 endonuclease activity during rRNA synthesis. Thus, we aimed to investigate the effect of delocalisation of NPM1 into the cytoplasm on DNA damage repair function and on APE1 subcellular localisation in an NPMc+AML cell line and to compare with AML cell lines bearing wild-type NPM1.

Clinically, the benefits of ATRA administration in NPMc+AML patients are controversial. An MRC trial failed to show the benefit of adding ATRA to standard chemotherapy in patients with NPMc+AML and non-APL AML cases, whilst the Austrian-German AML study group demonstrated an improvement in overall survival in NPMc+ patients receiving ATRA in combination with chemotherapy (Burnett, *et al* 2010, Schlenk, *et al* 2011, Schlenk, *et al* 2009). In vitro, the treatment of an NPMc+ cell line with ATRA showed down-regulation of NPM1 mutant protein, and activation of the apoptosis process (Martelli, *et al* 2007). Previously, the anti-apoptotic protein BCL-2 has been demonstrated to be more sensitive to cells that do not express CD34, which is the main feature of NPMc+ cells, than to CD34 positive cells (Bradbury, *et al* 1996). Therefore, the status of the anti-apoptotic proteins BCL-2 and MCL-1 in NPMc+AML cell line will be undertaken alongside the evaluation of the influence of ATRA on BCL-2 and MCL-1 levels in NPMc+AML and wild-type NPM1.

An extra level of complexity is the relationship between FLT3 and NPM1 mutations. Many patients have both mutations and the co-expression of the FLT3-ITD mutation with NPMc+ effects patient outcome by converting the prognosis from

favourable to intermediate. The risk stratification of NPM1-wt/FLT3-ITD is classified into the adverse prognostic group (Dohner, *et al* 2005, Gale, *et al* 2008, Thiede, *et al* 2006, Verhaak, *et al* 2005). Whilst the presence of FLT3 mutations on clinical outcomes are well documented, little is known about the biological mechanisms and more effort is required in understanding the pathology of these mutations. Hence, we aimed to target NPMc+ and FLT3-ITD mutations by adding FLT3 inhibitor (AC220) and ATRA, and then assess the effect of these drugs on the levels of anti-apoptotic BCL-2 and MCL-1 in NPMc+/FLT3-ITD cells.

## **2. Materials and Methods**

## 2.1 Chemicals:

Reagents were purchased from Sigma-Aldrich unless otherwise stated. Glycine, Tris-Base, Sodium azide and paraformaldehyde were provided by Fisher Scientific Ltd (Loughborough, UK). AC220 - FLT3 inhibitor - was obtained from Selleck Chemicals (Munich, Germany). All trans-retinoic acid (ATRA), Etoposide and AC220 were dissolved in 100% DMSO (dimethyl sulfoxide) to a stock concentration of 100mM and then aliquoted and frozen at -20°C. Further dilution was made in cell culture medium.

## 2.2 Antibodies:

Negative control mouse IgG1 (X093101), negative mouse IgG1-FITC (x0927), monoclonal mouse anti-human NPM1 clone 376 (M7305), monoclonal mouse anti-human BCL-2 oncoprotein clone 124 (F7053), polyclonal goat anti-mouse IgG-FITC (F0479), and rabbit polyclonal anti-mouse IgG-FITC (F0313) were obtained from Dako. Rabbit polyclonal anti-APE1-N-Terminal (ab82859), mouse monoclonal anti-MCL-1 (ab31948), mouse monoclonal  $\beta$ -actin antibody (ab6276), and goat polyclonal CY-3 secondary antibody to rabbit IgG (ab6939) were from Abcam. PE mouse anti-STAT5 (pY694) (612567) and PE mouse IgG1- $\kappa$  isotype control (555749) were purchased from BD biosciences. Secondary goat anti-mouse IgG-HRP (SC-2005), secondary goat anti-rabbit IgG-HRP (SC-2054) and mouse monoclonal anti-IgG<sub>2b</sub> Lamin A/C antibody (SC-7292) were obtained from Santa Cruz Biotechnology. Rabbit polyclonal anti-APE1 (NB100-101), and mouse monoclonal anti-phospho-histone H2AX (ser139) antibody clone JBW301 (05-636) were purchased from Novus biological and Upstate-Millipore, respectively.

### **2.3 Cell culture:**

Five different AML cell lines were used in the project (Table 2.1). OCI-AML3, MOLM-13 and M-07e were obtained from the German Collection of Microorganisms and Cell Cultures (DSMZ, Germany), whilst the MV4-11 cell line was obtained from the American Type Culture Collection (ATCC; USA) and HL-60 were from European Collection of Animal Cell Cultures (ECACC; Health Protection Agency Culture Collections, UK). OCI-AML3, MOLM-13, MV4-11, and HL-60 were maintained in RPMI-1640 medium supplemented with 10% foetal calf serum (FCS; First Link, UK), 2mM L-glutamine, 100U/ml penicillin and 10µg/ml streptomycin. 10ng/ml of GM-CSF (A gift from Novartis, Switzerland) was added to M-07e cell line because it is dependent on this cytokine for growth. All cell lines were grown in a humidified 5% CO<sub>2</sub> incubator at 37°C, and refreshed every two or three days by feeding and diluting them to prevent an overgrowth of the cells. All experiments were performed with cell lines in log phase, and used for a specific number of passages to minimise the chances of any genetic drift. In addition, these cell lines were regularly analysed with short tandem repeat (STR) to verify that the experiment results belong to the selected cell line with a specific genotype.

**Table 2.1: The characterisations of Leukaemic cell lines;** List of Leukaemic cell lines which are used in the experiments.

Cell Line	Origin	P53/NPM/FLT3 Genotype
<b>M-07e</b>	Established from the peripheral blood of a 6-month old girl with acute megakaryoblast leukaemia	Wild-Type FLT3 Wild-Type NPM Wild-Type P53
<b>OCI-AML3</b>	Established from the peripheral blood of a 57-year old man with acute myeloid leukaemia	Wild-Type FLT3 Mutant NPM Type A Wild-Type P53
<b>MOLM-13</b>	Established from the peripheral blood of 20-year old man with acute myeloid leukaemia	Heterozygous FLT3-ITD Wild-Type NPM Wild-Type P53
<b>MV4-11</b>	Established from the blast cells of a 10-year old man with biphenotypic B-myelomonocytic leukemia	Homozygous FLT3-ITD Wild-Type NPM Wild-Type P53
<b>HL-60</b>	Established from a 36-year old Caucasian woman with acute promyelocytic leukaemia	Wild-Type FLT3 Wild-Type NPM Mutant P53

## 2.4 Patient samples:

Peripheral blood (PB) or bone marrow (BM) samples were obtained from AML patients presenting to Nottingham City Hospital. Samples were obtained after written informed consent from AML patients. Use of these samples was approved by the Nottingham 1 Ethics Committee (reference 06/Q2403/16) and the Nottingham University Hospitals NHS Trust. Mononuclear cells were isolated from PB or BM by standard density gradient techniques using Histopaque and were either frozen in RPMI-1640 medium with 20% foetal calf serum, and 10% of DMSO in liquid nitrogen or used directly in an experiment. The frozen sample were thawed at 37°C and then added to RPMI-1640 supplemented with 10% FCS, and 1% heparin. After pelleting the thawed cells, the supernatant was removed and cells were resuspended in rest medium which comprised 40% FCS, and 2mM L-glutamine for 90 minutes in a humidified 5% CO<sub>2</sub> incubator at 37°C. The cell

viability was assessed by 7-AAD (7-amino-actinomycin D) (see section 2.5.3). During experiments, the patient samples were incubated in RPMI-1640 supplemented with 10% FCS, 2mM L-glutamine, 100U/ml penicillin, 10µg/ml streptomycin, 10ng/ml GM-CSF (Novartis, Switzerland), 25ng/ml G-CSF (NEUPOGEN, Amgen Inc), 20ng/ml IL-6 (PeproTech EC Ltd, UK), 20ng/ml IL-3 (a gift from Novartis, Switzerland), 20ng/ml SCF (255-SC, R&D system, USA), and 0.07µl/ml β-mercaptoethanol in a 5% CO<sub>2</sub> incubator at 37°C.

## **2.5 Cell viability assays:**

### **2.5.1 Cell counting by haemocytometer:**

The cells were resuspended in a known volume of medium were mixed thoroughly and then 10µl was transferred into an eppendorf tube. 10µl of sterile Trypan-Blue (1:1 volume) was mixed with the cells. Thereafter, 10µl was introduced into the V-shaped well of a haemocytometer to totally cover the whole area with the cell suspension. The counting chamber was then placed under a microscope. The viable cells in the four corner squares in the chamber were counted. Finally, the number of cells/ml was calculated by multiplying the average count per square by the dilution factor and 10<sup>4</sup>.

### **2.5.2 Alamar blue assay:**

5×10<sup>5</sup>/ml OCI-AML3, MV4-11, M-07e and HL-60 cells were prepared in medium and then 100µl was transferred into 96 well plates. Thereafter, the cells were treated with etoposide or methyl methanesulfonate MMS at different concentrations and incubated at 37°C in a humidified 5% CO<sub>2</sub> incubator for 24 hours. After 20 hours, 10µl of Alamar Blue reagent was added to the wells and the plate incubated for another 4 hours. The

resulting fluorescence was then read at 560/590nm using a plate reader (FluoStar-Optima, BMG Lab Technology, German). The percentage of viable cells was calculated by dividing the treated cells by the untreated cells. In addition, cells were treated with DMSO at the highest concentration in which it had been used as a drug diluent in the experiment to ensure that the cell viability was not affected by DMSO.

### **2.5.3 7-AAD cell viability assay:**

The patient cells, or the cell lines, were mixed with fixed stained cells (FSC), which were collected from a normal donor, in 1:1 volume. Subsequently, 50µl of 25µg/ml of 7-AAD was added and incubated for 15 minutes on ice, and then the cells were analysed by flow cytometry, and BD FACSCanto software was used (FACS; BD FACSCanto II). The number of viable cells was quantified by excluding dead cells and multiplying by the number of FSC, which is added with the patient cells or cell lines and counted by the haemocytometer (Pallis, *et al* 1999).

## **2.6 Molecular methods:**

### **2.6.1 RNA extraction:**

RNA extraction was performed using a QIAamp blood RNA isolation kit (cat# 52304; Qiagen, Crawley, UK). However, a DNase digestion (cat#79254, Qiagen) was added to the standard procedure. The concentration of RNA was measured by a Thermo Scientific nanodrop 2000 (Labtech International Ltd, UK). Thereafter, cDNA was prepared from 2µg RNA which was heated to 65<sup>0</sup>C to denature it and then placed on ice for 5 minutes. Subsequently, it was mixed with 21.5µl of reverse transcription master mix, containing 200µl of 5x first strand buffer (Y02321; Invitrogen, Life Technologies Ltd, UK), 40µl of

25mM dNTPs (10297-018; Invitrogen), 100µl of 0.1M DTT (Y00147; Invitrogen), 33µl of random primer concentration 3µg/µl (12097-018; Invitrogen), and 65µl of DEPC-treated water, 1µl of 40u/µl RNasin (N251B; Promega, UK) and 1.5µl of MMLV reverse transcriptase concentration 200u/µl (28025-013; Invitrogen). The cycles were run in two stages at 37<sup>0</sup>C for 60 minutes, then 95<sup>0</sup>C for 10 minutes and then put on hold at 4<sup>0</sup>C. Finally, the cDNAs were stored at -20<sup>0</sup>C.

### **2.6.2 Polymerase chain reaction (PCR) optimisations:**

Genomic DNA was extracted from the above cell lines using QIAamp blood DNA isolation kit (cat# 51104; Qiagen) according to the manufacturer's protocol. Thereafter, the optimal condition for the amplification of NPM1 or APE1, which was done on cDNA, was determined by assessing different annealing temperatures and MgCl<sub>2</sub> concentrations. The annealing temperature was set between 54<sup>0</sup>C and 65<sup>0</sup>C; 54.9<sup>0</sup>C, 55.2<sup>0</sup>C, 55.9<sup>0</sup>C, 57.0<sup>0</sup>C, 58.2<sup>0</sup>C, 59.4<sup>0</sup>C, 60.5<sup>0</sup>C, 61.7<sup>0</sup>C, 62.9<sup>0</sup>C, 64.0<sup>0</sup>C, 64.7<sup>0</sup>C, and 65.0<sup>0</sup>C and the MgCl<sub>2</sub> concentrations tested were 1.0, 1.5, 2.0 and 2.5mM, Other PCR components are shown in Table 2.2. The primer sequences were: NPM1 [F-CTTAACCACATTTCTTTTTTTTTTTTTTCCA, R-GGACAACATTTATCAAACACGGTAG] (Invitrogen)(Gale, *et al* 2008) and APE1 [F-ATATTGCTTCGGTGGGTGAC, R-CTTGGAACGGATCTTGCTGT] primers (Invitrogen). The APE1 primers were designed by using primer3 input version 4.0 (<http://primer3.sourceforge.net>) (Rozen and Skaletsky 2000). Thereafter, the PCR products were loaded on an agarose gel (1x TBE, 2% (weight by volume) of agarose, and 0.5µg/100ml ethidium bromide and run for 1 hour at 200 volts following

which products were visualised under UV light and compared to a DNA ladder of known sizes (Invitrogen)

**Table 2.2: PCR optimisation conditions;** The four different conditions of MgCl<sub>2</sub> used in the PCR optimisation.

Content	A	B	C	D
DNA	1µl	1µl	1µl	1µl
Taq polymerase (Amplitaq Gold)	0.2µl	0.2µl	0.2µl	0.2µl
10x PCR Buffer	2.5µl	2.5µl	2.5µl	2.5µl
MgCl <sub>2</sub> (25mM)	1µl	1.5µl	2µl	2.5µl
Forward primer (20pmol)	1.25µl	1.25µl	1.25µl	1.25µl
Reverse primer (20pmol)	1.25µl	1.25µl	1.25µl	1.25µl
dNTPs (200µM)	1µl	1µl	1µl	1µl
H <sub>2</sub> O	16.8µl	16.3µl	15.8µl	15.3µl
Total Volume	25µl	25µl	25µl	25µl

### 2.6.3 NPM1 and FLT3-ITD mutations analysis:

The genomic PCR amplification of NPM1 and FLT3-ITD to assess length mutations was performed as follows: 1x buffer PCR (Applied Biosystems, Warrington, UK), 2mM, and 1.5mM MgCl<sub>2</sub> (Applied Biosystems), for NPM1 and FLT3-ITD correspondingly, 2 units of Taq-polymerase (Amplitaq Gold, Applied Biosystems), 200µM dNTPs (Amersham Pharmacia Biotech), 1.25µl of 20pmol/µl NPM1 forward and reverse primers or FLT3-ITD forward (F-GCAATTTAGGTATGAAAGCCAGC) and reverse (R-CTTTCAGCATTTTGACGGCAACC-3) primers (Invitrogen) (Kiyoi, *et al* 1999, Seedhouse, *et al* 2009b), 1µl of DNA, with the volume being made up to 25µl with water. The NPM1 and FLT3 reverse primers were labelled with Carboxyfluorescein (FAM). The fluorescent-PCR cycles started with a Taq activation stage at 95°C for 10 minutes, then, 30 cycles of 95°C for 1 minute, 63°C or 52°C for 1 minute for NPM1 or FLT3, correspondingly, and 72°C for 1 minute. The 30 cycles were followed by a final

extension step at 72<sup>0</sup>C for 10 minutes (Biometra, T-Gradient, Germany). The products were subsequently loaded onto a 3130 Genetic analyser (Applied Biosystems) for size separation and analyzed by GeneMapper ID software V3.2 (Applied Biosystems).

#### **2.6.4 Gene expression measurements:**

NPM1, BCL-2, and MCL-1 expressions were measured using quantitative real-time PCR. Quantitative PCR was completed on an ABI prism 7500-Fast machine (Applied Biosystems) using real-time mastermix with SYBR Green (Applied Biosystems). The PCR master-mix contained 0.8 $\mu$ l of diluted cDNA (1:15), 5 $\mu$ l sybr green PCR master-mix (4309159; Applied Biosystems), and 1pmol of the specific primers for the relevant gene (Table 2.3);  $\beta_2$ -Microglobulin ( $\beta_2$ M) (Pallisgaard, *et al* 1999), BCL-2 (Pattyn, *et al* 2003), NPM1, and MCL-1 (Qiagen; Table 2.3). The volume was then made up to 10 $\mu$ l with molecular grade water. cDNA from the KG1a cell line was used to make up a standard curve with doubling dilutions giving concentrations 125ng to 1.9ng. The cycle conditions were 50<sup>0</sup>C for 2 minutes, 95<sup>0</sup>C for 10 minutes, then, 40 times at 95<sup>0</sup>C for 15 seconds, 60<sup>0</sup>C for 1 minute, and 75<sup>0</sup>C for 10 seconds. Consequently, the products were heated from 60<sup>0</sup>C to 95<sup>0</sup>C over 20 minutes to allow melting curve analysis to be performed to assess the product specificity and ensure the absence of primer-dimers. Template-free reactions were included in each experiment as a negative control and all reactions were done in triplicate. The standard curve was used to assign values to the samples and the housekeeping gene  $\beta_2$ M was used to calculate the relative expression levels of the selected genes.

**Table 2.3: Primers used in real-time PCR.**

Gene	Primer Sequences	Code	Source
<b>β2M</b>	F-GAGTATGCCTGCCGTGTG R-AATCCAAATGCGGCATCT	-----	Invitrogen
<b>BCL-2</b>	F-ATGTGTGTGGAGAGCGTCAACC R-TGAGCACAGTCTTCAGAGACAGCC	-----	Invitrogen
<b>NPM1</b>	Custom primers	QT00091875	Qiagen
<b>MCL-1</b>	Custom primers	QT00094122	Qiagen

### 2.6.5 Sequencing:

PCR products from OCI-AML3, HL-60, and M-07e were purified using QIAquick PCR Purification kit (Qiagen). Thereafter, each sample has two reactions; one for the forward primer and the second for the reverse. 1µl of the PCR product was mixed with 3.2pmol of forward or reverse primers, 3µl of sequence mix (BigDye Terminator V3.1–Cycle Sequencing Kit, cat# 4337455, AB Applied Biosystems), 5µl 2.5x buffer with the volume being made up to 20µl by H<sub>2</sub>O. The sequencing cycles were repeated 25 times as follows; 96<sup>0</sup>C for 1 minutes, 96<sup>0</sup>C for 10 seconds, 50<sup>0</sup>C for 5 seconds, and 60<sup>0</sup>C for 4 min by using T-Gradient Thermocycler (Whatman Biometra). Thereafter, 20µl of the sequenced products were purified using 2µl of sodium acetate (3M at pH5.2) and 50µl 100% ethanol, and then incubated on ice for 20 minutes. After centrifugation for 20 minutes at 14000 rpm, the liquid was discarded and 150µl 70% ethanol was added to wash the pellet. The tubes were spun again, 5 minutes 14000 rpm and the supernatant was removed. Thereafter, the pellets were left to air dry for 5 minutes and stored at -20<sup>0</sup>C until ready for analysis. The sequencing products were resuspended in HiDye (Applied Biosystems) and run on ABI Prism 3130 Genetic Analyser (Applied Biosystems). Sequencing analysis was performed using Applied Biosystems Sequencing Analysis software 5.2.

## **2.7 Assessing the interaction of NPM1 and APE1 in the leukaemic cell lines:**

### **2.7.1 Preparation of slides:**

#### **2.7.1.1 LiquiPrep cytology system:**

$5 \times 10^5$  cells were mixed with 5ml cell preservative solution (Vector Labs, UK) and incubated for 30 minutes with occasional mixing. The cells were pelleted by centrifugation for 5 minutes at 200g, and then the supernatant was removed and the cell pellet resuspended by adding 50 $\mu$ l of cellular base solution (Vector Labs). After mixing the cells, one drop of cell preparation was applied onto the centre of a labelled slide and left to dry for approximately 1 hour. The cells were fixed by 4% paraformaldehyde for 15 minutes.

#### **2.7.1.2 Coverslip technique:**

$5 \times 10^5$  cells were transferred to a cover slip and incubated for 24 hours in a humidified 5% CO<sub>2</sub> incubator at 37°C. On the next day, the medium was aspirated carefully from the cover slip and the cells were fixed in 4% paraformaldehyde (Colombo, *et al* 2002).

#### **2.7.1.3 Cytospin technique:**

$5 \times 10^5$  cell suspension was dispensed into a cytospin tube and then centrifuged at 1000 rpm for 5 minutes. Thereafter, the slides were left to air dry for 30 minutes and the cells fixed with 4% paraformaldehyde (Gruszka, *et al* 2010).

#### **2.7.1.4 Fibronectin coating technique:**

Fibronectin solution was prepared at 20µg/ml in PBS. 400µl of the solution was added to a slide and incubated overnight at 4°C. On the next day, the slides were washed twice with filtered PBS and then incubated for 2 hours at 37°C in a closed box. Thereafter, the slides were left to air dry for one hour in a safety hood to prevent contamination. Subsequently,  $5 \times 10^5$  cells were added to the slides and incubated for one hour at room temperature in the safety hood and then were fixed with 4% paraformaldehyde.

#### **2.7.2 Indirect immunofluorescence method for detection of subcellular localisation by confocal microscopy:**

NPM1 and APE1 localizations were observed using an immunofluorescence technique. After the cells were fixed by 4% paraformaldehyde for 15 minutes at room temperature, they were permeabilized for 5 minutes in PBS containing 0.2% (wt/vol) Triton X-100 and 2% normal goat serum albumin and then incubated for 30 minutes in 2% normal goat serum in PBS at room temperature to block non-specific binding of the antibodies. Cells were incubated with rabbit polyclonal anti-APE1 diluted 1:150 in blocking solution overnight at 4°C. After washing, cells were incubated for 1 hour with goat polyclonal secondary antibody to rabbit IgG (CY-3 labelled, pre-adsorbed) (1:250). For NPM1 subcellular localization detection, the permeabilized cells were incubated with monoclonal mouse anti-NPM1 1:80 overnight at 4°C. Thereafter, the slides were washed twice with PBS and then incubated with polyclonal rabbit anti-mouse IgG FITC 1:100 for 1 hour in the dark.

The slides were then washed in PBS and the nuclei were stained by 4,6-diamidino-2-phenylindole dihydrochloride (DAPI) (VectaShield Mounting Medium with DAPI, Cat# H-1200, Vector Laboratories, USA). The slides were visualized through 100× oil objective using a NIKON C2 confocal microscope system and captured by NIS-elements imaging software.

### **2.7.3 Cytoplasmic-nuclear extracts:**

#### **2.7.3.1 Preparation of cytoplasmic-nuclear extracts:**

The cytoplasmic and nuclear extraction was performed using a nuclear extract kit (Active Motif, cat# 40010, Belgium).  $8.8 \times 10^6$  cell line cells (treated with/without drugs) were washed with cold PBS/phosphatase inhibitors and then centrifuged at 500 rpm for 5 minutes at 4<sup>0</sup>C. Supernatant was removed and the pellet was resuspended in 1x hypotonic buffer, which was supplied in the kit, then incubated on ice for 15 minutes, thereafter, 25µl of the detergent supplied by the kit was added and vortexed for 10 seconds. Consequently, the suspensions were centrifuged at high speed for 30 seconds and the resulting cytoplasmic fraction was transferred into a clean 1.5ml tube. The nuclei were collected by resuspending the nuclear pellet in complete lysis buffer, which is supplied in the kit (Active Motif), and vortexing at high speed for 10 seconds. After 30 minutes of incubation on ice, the suspension was centrifuged at 10000 rpm for 10 minutes at 4<sup>0</sup>C. Finally, the supernatant was collected as a nuclear protein extract and used for western blot and co-immunoprecipitation or stored at -80<sup>0</sup>C.

### **2.7.3.2 Determination of protein concentration:**

Protein concentration was determined using BioRad dye reagent (Bio-Rad protein assay, cat# 500-0006, Bio-Rad Lab GMBH, German). 1ml of the BioRad protein buffer was diluted in 4ml distilled water, and then 100 $\mu$ l was transferred into wells of a 96 well plate. Bovine Serum Albumin (BSA) was used to establish a standard curve at 4, 2, 1, 0.5, 0.2, 0.1mg/ml in lysis buffer. 2 $\mu$ l of BSA standard or sample was added to the plate. The absorbance was measured at 590nm. The protein concentrations of samples were calculated from the BSA standard curve by the software provided with the plate reader (FluoStar-Optima, BMG Lab Technology, German).

### **2.7.4 Western blot analysis:**

10 $\mu$ l of molecular weight marker (Amersham High-Range Rainbow Molecular Markers, code# RPN756E, GE Healthcare Life Sciences) and 40 $\mu$ l of the protein solutions, which were mixed with an electrophoresis sample buffer in a 1:1 ratio (2x Laemmli buffer: 4% SDS, 10% 2-mercaptoethanol, 20% glycerol, 0.004% bromophenol blue, 0.125M Tris HCl, pH:6.8), and added to 10% SDS-PAGE for separation in migration buffer (25mM Tris base, 190mM Glycine, 0.1% SDS, pH:8.3) at 200V for 1 hour. The resolved proteins were transferred from the gel to a PVDF membrane for 45 minutes at 100V in transfer buffer (25mM Tris base, 190mM Glycine, 20% methanol). The membranes were blocked by 5% non-fat free milk (Blotting Grade Blocker, cat# 170-6404, USA) for 1 hour at room temperature. After three washing steps with 1x TBST buffer (10x TBST buffer: 24.2g Tris base, 87.6g NaCl, 1000ml dH<sub>2</sub>O, 10mls Tween 20, pH 7.4 – 7.6), 1:1000 of rabbit anti-

APE1, 1:4000 of mouse anti-NPM1 were incubated overnight at 4<sup>0</sup>C, while the loading control of 1:10000 of mouse anti- $\beta$ -actin or 1:700 of mouse anti-Lamin A/C was incubated for 1 hour at room temperature or overnight at 4<sup>0</sup>C, respectively. After three washes with 1x TBST, goat anti-rabbit-HRP (1:2500) or anti-mouse-HRP (1:3000) secondary antibodies were applied. The binding of antibodies was detected using enhanced chemiluminescence (ECL Western Blotting Detection Reagents; code#RPN2209, GE Healthcare Life Sciences) and the densitometry of the bands was performed by using Image-J analysis software (NIH) (Schneider, *et al* 2012).

### **2.7.5 Co-immunoprecipitation:**

100 $\mu$ g of cellular protein was mixed with 2 $\mu$ g of primary antibody (NPM1 or APE1); and incubated for 1 hour at 4<sup>0</sup>C; these were the same antibodies as had been previously used in subcellular localisation detection and in western blotting. 20 $\mu$ l of well mixed protein A/G plus-agarose (cat# sc-2003, santa cruz biotechnology) was then added and incubated at 4<sup>0</sup>C on a rocker platform overnight. The immunoprecipitate was collected by centrifugation at 2500 rpm for 5 minutes at 4<sup>0</sup>C, and then the supernatant was discarded. The pellet was washed 4 times with PBS. Finally, the pellet was resuspended in 40 $\mu$ l of 1x electrophoresis sample buffer, and the proteins were separated as described previously (section 2.7.4).

### **2.7.6 MMS cytotoxicity assay:**

Methyl methanesulfonate (MMS) sensitivity was investigated using wild-type and mutated NPM1 cell lines.  $5 \times 10^5$  cells were treated with different concentrations of MMS (0.8 $\mu$ M, 1 $\mu$ M, 2 $\mu$ M, 3 $\mu$ M, 4 $\mu$ M, 5 $\mu$ M, 10 $\mu$ M, 15 $\mu$ M, 20 $\mu$ M and 25 $\mu$ M) for 1

hour. Then, the cells were washed 3 times with RPMI medium and incubated for 72 hours in drug-free medium. The growing medium was replenished every 24 hours. Cell viability was tested by flow cytometry using the 7-AAD assays (section 2.5.3).

## **2.8 DNA damage response:**

### **2.8.1 Comet assay:**

#### **2.8.1.1 Preparation of slides:**

Neutral and alkaline comet assays were performed on the selected leukaemic cell lines OCI-AML3, M-07e, and MV4-11 using commercially available comet assay slides (Trevigen, USA). Both basal levels of DNA damage and drug-induced damage were assessed. In the neutral comet assay,  $1 \times 10^5$  cells were suspended in PBS then mixed with cooled molten low-melting-point agarose (Trevigen) at a ratio of 1:10 (v/v). 75 $\mu$ l of the mixture was added to the comet slides (Trevigen) which were then placed in the dark at 4<sup>0</sup>C for 10 minutes to improve the adherence of samples in agarose in a high humidity environment.

The slides were immersed overnight in pre-chilled lysis solution (Trevigen) at 4<sup>0</sup>C. After removing the excess buffer from the slides, they were gently washed twice by placing in neutral buffer (1x TBE; 89mM Tris-base, 89mM boric acid, 2mM EDTA, pH 8.0) for 30 min at room temperature to remove the lysis solution and to enable DNA to unwind.

The slides were then placed in a horizontal electrophoresis tank which contained a neutral buffer, and electrophoresis was conducted for 15 min at 22V (1 V/cm, 400mA). After removing

excess electrophoresis buffer from the slide, they were rinsed briefly in distilled water, and then the cells were fixed through immersion in 70% ethanol for 5 minutes and air dried at room temperature in the dark overnight. The sample slides were stained for approximately 5 minutes with the green fluorescent DNA-binding dye, SYBR Green I (Sigma). The migrated DNA (comet) was observed under an epifluorescence microscope at 20x magnification (BX61, Olympus Tokyo, Japan) and analysed as described in section 2.8.1.2. The steps of the comet assay are summarised in Figure 2.1.

The alkaline comet assay used the same protocol except for the unwinding and electrophoresis steps, where the neutral buffer was replaced by an alkaline buffer (300mM NaOH, 1mM EDTA, pH >13.0) – unwinding proceeded for 10 minutes and electrophoreses for 20 minutes. Thereafter, the slides were washed gently three times with a neutralisation buffer to remove excess alkali. 70% ethanol was used to fix the cells, which were then left to air dry at room temperature in the dark overnight. Finally, SYBR Green I was added to the slides and DNA migration was observed under an epifluorescence microscope.

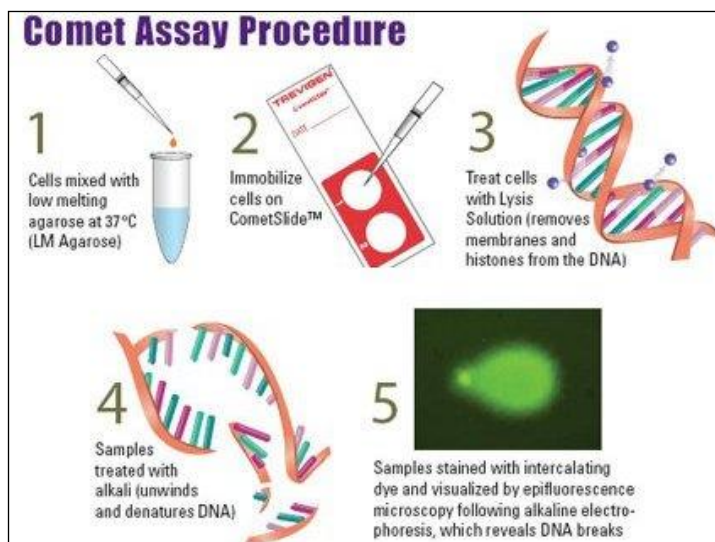


**Figure 2.1: Comet assay protocol steps;**  
(<http://www.amsbio.com/Comet-Assays.aspx>)

### 2.8.1.2 Analysis of comet assay:

DNA damage was assessed using an automatic image analysis system (CometAssay IV software, Perceptive Instruments, UK) to measure the olive tail moment (Sigurdson, *et al* 2005). This is defined as the amount of DNA in the tail and the displacement between the centre of mass of the comet head and the centre of mass of the tail (tail length) (Kumaravel, *et al* 2009). Duplicate agarose spots were prepared for each experimental condition, and 50 cells in each spot were randomly selected and analysed.

### 2.8.2 $\gamma$ -H2AX immunocytochemistry assay:

$\gamma$ -H2AX foci in OCI-AML-3 and MV4-11 cell lines were evaluated by immunofluorescence.  $3 \times 10^5$  cells were fixed with 20  $\mu$ l of reagent-A (ABD Serotec, Bio-Rad) for 15 minutes at room temperature in the dark. Subsequently, 2ml of 100% methanol was added and the cells incubated for 10 minutes on ice. The cells were then washed twice in phosphate buffered

saline with sodium azide (1% bovine serum albumin/0.5% sodium azide in PBS) (PBS-AA) and 20 $\mu$ l of reagent B (ABD Serotec) was added for permeabilisation. The cells were incubated with 200 $\mu$ l of primary antibody anti- $\gamma$ -H2AX (1:500) at room temperature in the dark for 2 hours, while in the control tube 200 $\mu$ l of negative control mouse-IgG (1:50) was added. After two washing steps with PBS-AA, the cells were incubated with 3 $\mu$ l of appropriate secondary antibodies, anti-mouse IgG-FITC, for an hour in the dark at room temperature, before being washed. Thereafter, cells were resuspended in 20 $\mu$ l PBS-AA and mounted in mounting medium with 4',6'-diamidino-2-phenylindole (DAPI) (cat# H-1200, Vectashield Mounting Medium with DAPI, Vector Laboratories, USA). Foci were visualized in 100 cells by using fluorescence microscope at 100x magnification. As the number of foci varied per cell, these were quantified using an H score system (Katz, *et al* 1990, Seedhouse, *et al* 2009a). According to the number of foci in each cell, the results are divided into five groups: N (no foci), L (1-6 foci), M (7-12 foci), H ( $\geq$ 13), C (completely damaged). The H score was calculated as follows: N + 2L + 3M + 4H + 5C.

## **2.9 Anti-apoptotic protein levels in NPMc+AML cells and response to ATRA:**

### **2.9.1 ATRA and AC220 concentration optimisations:**

2 $\times$ 10<sup>5</sup> cells/ml of the cell lines were treated with different concentrations of ATRA (5nM, 10nM, 50nM, 100nM, 250nM, 500nM, 1000nM) and the highest concentration of DMSO, which was used in ATRA dilution, was used in a control condition to test for the effect on cell survival. After 72 hours,

the viable cells were counted by the haemocytometer method (section 2.5.1).

For AC220, the same procedure was followed but the drug concentrations ranged between 0.5nM-15nM for MV4-11 and MOLM-13 cell line, and 0.5nM-1000nM for the OCI-AML3 and M-07e cell lines.

### **2.9.2 Blood cell morphology:**

The different cell lines were incubated for three days with ATRA at 500nM. Then,  $1 \times 10^5$  cells were prepared by the cytopspin method at 400rpm for 5 minutes and left to air dry for 30 minutes. After this, the slides were placed in methanol for 30 seconds, and then immersed in Wright-Giemsa stain for 1 minute. Subsequently, the slides were removed from the stain and placed in de-ionized water for 10 minutes and then rinsed briefly in running de-ionized water and left to air dry. Cellular morphology was observed by light microscopy and signs of differentiation were evaluated.

### **2.9.3 CD11b differentiation marker analysis:**

$2 \times 10^5$  cells were washed twice with PBS-AA and incubated with 2.5 $\mu$ l of normal mouse serum for 30 minutes. Thereafter, 2.5 $\mu$ l of anti-CD11b was added and incubated for another 30 minutes. After two washing steps with PBS-AA, the cells were resuspended in 300 $\mu$ l of PBS-AA and analysed by flow cytometry.

#### **2.9.4 Apoptosis detection by Annexin-V:**

Evaluation of apoptosis in the cell lines treated with ATRA, or AC220 was carried out by annexin-V FITC assay (cat#4830-01-K, TACS Annexin-V kit, Trevigen). After 72 hours ATRA treatment,  $2 \times 10^5$  of cells were washed twice with cold PBS. Then, 100 $\mu$ l of mixed annexin-V (84.5 $\mu$ l dH<sub>2</sub>O, 0.5 $\mu$ l Annexin-V, 5 $\mu$ l Propidium Iodide, 10 $\mu$ l 10X binding buffer) was added and incubated for 1 hour at room temperature in the dark. Thereafter, 400 $\mu$ l of 1x binding buffer (TACS Annexin-V kit, Trevigen) was added to the tubes and they were processed by flow cytometry.

#### **2.9.5 BCL-2 and MCL-1 protein levels detection:**

$1 \times 10^6$  of untreated and ATRA treated OCI-AML3, M-07e, MOLM-13, and MV4-11 cell lines were fixed with 4% paraformaldehyde for 15 minute at room temperature. After two rinsing steps with PBS-AA, the cells were resuspended in fresh saponin buffer (0.1% saponin, 0.5% BSA in PBS) and 200 $\mu$ l was transferred to a tube. For MCL-1, 10 $\mu$ l of negative mouse IgG and anti-MCL-1 (1:10; diluted in saponin buffer) was added in different tubes. They were incubated for one hour at room temperature in the dark and then washed twice in PBS-AA. Thereafter, the tubes, which have primary antibodies in, were incubated with 80 $\mu$ l of normal rabbit serum for 30 minutes and then 5 $\mu$ l of rabbit anti-mouse FITC was added and incubated for 30 minutes at room temperature in the dark. Consequently, the cells were washed two times with PBS-AA and resuspended in 300 $\mu$ l of the saponin buffer. For BCL-2, 5 $\mu$ l of negative mouse IgG1-FITC and anti-BCL-2 (1:10; diluted in saponin buffer) was added to the prospective tube and incubated at room temperature for an hour in the

dark. Subsequently, the cells were washed in PBS-AA and resuspended in saponin buffer. Finally, the proteins levels were measured by Flow cytometry (FACS; BD FACSCanto II).

### **2.9.6 Total P53 protein measurement:**

$1 \times 10^6$  cells were fixed with 4% paraformaldehyde for 15 minutes at room temperature. After two washing steps with PBS-AA, the cells were resuspended in fresh saponin buffer.  $2 \times 10^5$  of the cells were incubated with  $2 \mu\text{l}$  of negative mouse IgG and  $2 \mu\text{l}$  ( $2 \mu\text{g}$ ) of anti-P53 in different tubes for one hour at room temperature in the dark and followed by two rinsing steps with PBS-AA. Thereafter, the tubes were incubated with  $80 \mu\text{l}$  of normal rabbit serum for 30 minutes and then  $5 \mu\text{l}$  of rabbit anti-mouse FITC was added and incubated for another 30 minutes at room temperature in the dark. Consequently, the cells were washed two times with PBS-AA, resuspended in  $300 \mu\text{l}$  of saponin buffer and analyzed by flow cytometry.

### **2.9.7 RNA Interference of NPM1:**

NPMc+AML and NPM1 wild-type cell lines were nucleofected with 15nM siRNAs targeting both the wild-type and mutant NPM1 (AAAGGTGGTTCTCTCCCAA) (Hs\_NPM1\_7, SI02654960, Qiagen). siRNA NPM1\_7 was found to be more effective in knocking-down NPM1 than Hs\_NPM1\_1 (SI00300979). Moreover, a siRNA species was designed to knockdown only the mutated NPM1 allele [NPM1-A (sense strand 5'-UCAAGAUCUCUGUCUGGCAtt-3')] (cat# S444412, Applied Biosystems) via Cell Line Nucleofector Kit-T (cat# VCA-1002, Lonza, Switzerland) with the programme X-001 in a Nucleofector-2b device (Lonza). The nucleofection programme was selected and a lot of work went into

optimising the nucleofection conditions for the cell lines (unpublished work by Shili Shang).  $1 \times 10^6$  cells were nucleofected according to the manufacture's protocol. Thereafter, the cells were maintained in RPMI-1640 with the required supplements and incubated for 48 hours.  $2 \mu\text{g}$  of pmaxGFP vector (Lonza) was used as a positive transfection control and cells nucleofected with  $15 \text{ nM}$  of AllStars negative control siRNA (cat# 1027281, Qiagen) was also included in the experiment. The transfection efficiency and the cell viability were assessed by flow cytometry via mixing  $2 \times 10^5$  of the cells with  $12.5 \mu\text{g/ml}$  of 7-AAD. RNA from the negative control, and the cells with the total NPM1 or the mutant NPM1 knocked-down, were extracted as previously described (section 2.6.3). The cDNA was used in real time PCR to measure the expression of NPM1, BCL-2, and MCL-1. In addition, the differentiation marker (CD11b) and P53 protein levels (see sections 2.9.3 and 2.9.6, respectively) were also evaluated in the OCI-AML3 and M-07e after knocking-down the total NPM1.

### **2.9.8 Preparation of lysate from cell culture:**

Protein was extracted from different cell lines following different conditions according to nuclear extract kit (Active Motif). Approximately  $3.2 \times 10^6$  OCI-AML3 cells were washed two times with ice-cold PBS containing 1:20 of phosphatase inhibitors. The cells were pelleted, and resuspended in complete lysis buffer, which is supplied in the kit (Active Motif), and vortexed for 10 second. The suspensions were incubated on ice for 30 minutes and then sonicated for 10 seconds at 30% power setting (Bandelin Sonopuls ultrasonic homogenizer HD2070) and left on the shaker in the cold room for another 30 minutes. The sonicates were centrifuged at  $4^{\circ}\text{C}$  at high speed for 10 minutes, then the supernatants were

transferred into a new pre-cooled eppendorf and assessed by western blot (section 2.7.4) or stored at  $-80^{\circ}\text{C}$ .

### **2.10 Statistical analysis:**

Statistical analysis was performed using SPSS version 21 (SPSS Inc., USA). All experiments were repeated at least three times and the data are presented as mean  $\pm$  standard deviation (SD). A p-value  $\leq 0.05$  was considered statistically significant.

# **3. DNA Damage Repair Activity in NPMc+AML Cells**

### **3.1 Introduction:**

DNA damage response is essential for the maintenance of genomic stability through the repair of DNA damage or the initiation of programmed cell death. A reduction in DNA repair activity could lead to an accumulation of mutations and DNA breaks, whilst an elevation of the DNA activity may inhibit cell apoptosis and enable highly damaged cells to attempt repair and survival with mis-repaired DNA damage (reviewed in (Seedhouse and Russell 2007)). Therefore, aberrant activity of DNA repair mechanisms is susceptible to the development of genetic instability that causes tumorigenesis. In clinical trials, extreme activation of DNA damage repair has been documented and associated with poor phenotype tumours. Moreover, the reduction, or absence of DDR and its factors, correlate with a favourable outcome (reviewed in (Helleday 2010, Madhusudan and Middleton 2005)). For instance, a positive expression of APE1 corresponds with a poor prognosis because the resistance to chemotherapy and radiation is increased, meanwhile the reduction in APE1 expression enhances the cytotoxicity of the cells in response to the therapy (Al-Attar, *et al* 2010, Fishel and Kelley 2007, Zhang, *et al* 2009). Thus, inhibition of DNA repair function plays an essential role in the response of the tumour cells to chemotherapy.

There are several types of DNA lesion and each group of DNA damage is repaired by a distinct DNA repair mechanism. For example, double-strand breaks are repaired by either homologous recombination (HR) or non-homologous end joining (NHEJ) mechanisms, whereas single-strand breaks, or abnormal DNA bases, are repaired by the base excision repair mechanism (reviewed in (Jackson and Bartek 2009)).

Numerous kinds of tumours have developed due to mutations in genes that are involved in DNA damage repair, such as mutations in ATM lead to Ataxia-telangiectasia in which individuals are predisposed to cancer, and mutations in the BRCA1 or BRCA2 genes significantly increase the risk in women of developing breast or ovarian cancer (reviewed in (Kastan 2008)).

In NPMc+ cells, disruption of NPM1 subcellular localisation from the nucleus into the cytoplasm causes the delocalisation of some of the proteins that are involved in the activation of the P53-mediated response to DNA damage, such as ARF (Colombo, *et al* 2006, den Besten, *et al* 2005). In addition, it has been reported that interaction of NPM1 with apurinic/aprimidinic endonuclease-1 (APE1), which is an essential protein in the base excision repair (BER) pathway, is important for APE1 subcellular localisation and for regulating the rRNA process ((Vascotto, *et al* 2009)).

It is well known that NPMc+ AML on its own has a favourable prognosis (Dohner, *et al* 2005, Schnittger, *et al* 2005, Thiede, *et al* 2006). We proposed that the delocalisation of NPM1 into the cytoplasm in NPMc+ mutated AML cells may result in a reduction in DNA damage repair mechanisms leading to an increase in the sensitivity of such cells to chemotherapy. Hence, we aimed to evaluate the DNA damage repair function within NPMc+AML cells.

## 3.2 Results:

### 3.2.1 NPM1 and FLT3-ITD mutations detection:

The status of NPM1 and FLT3-ITD mutations in haematological cell lines was determined by fluorescent PCR with detection of products on the 3130 genetic analyser. Firstly, the reaction containing the NPM1 primers, which had previously been used by Gale *et al.* (Gale, *et al* 2008), was optimised for use in our laboratory by using different MgCl<sub>2</sub> concentrations and annealing temperatures and 30 cycles of amplification were performed. As shown in figure 3.1, the PCR products at 2mM of MgCl<sub>2</sub> and the annealing temperature is at 63<sup>0</sup>C were chosen due to the presence of a single, tight, and bright band.

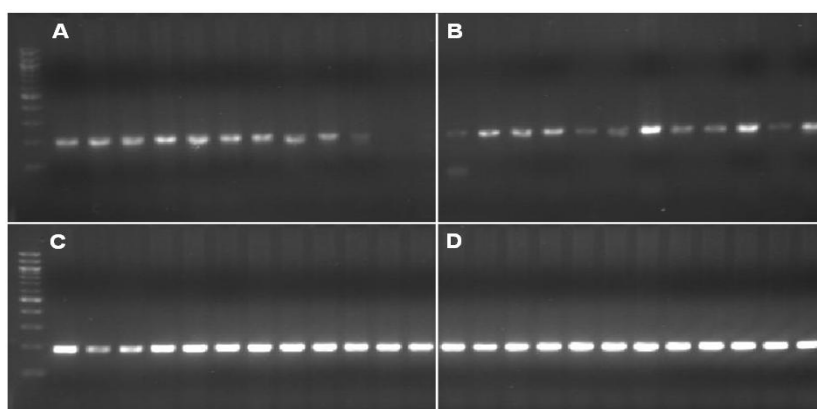


**Figure 3.1: PCR optimisation for NPM1 primers;** The NPM1 primers were optimised at 4 different MgCl<sub>2</sub> concentrations, which are **(A)** 1mM, **(B)** 1.5mM, **(C)** 2mM, and **(D)** 2.5mM, and at different annealing temperatures: 54.9°C, 55.2°C, 55.9°C, 57.0°C, 58.2°C, 59.4°C, 60.5°C, 61.7°C, 62.9°C, 64.0°C, 64.7°C, and 65.0°C. A 1000bp-loading marker was used in the 2% agarose gel. A negative template control was included in the experiments.

Thereafter, we assessed the genetics status in M-07e, OCI-AML3, MV4-11, and MOLM-13 cell lines for NPM1 mutation, using the conditions determined above, and FLT3-ITD which was already being routinely used to screen samples in the

laboratory (Seedhouse, *et al* 2006). Figure 3.2A, shows the mutation status of NPM1 in MOLM-13 and OCI-AML3 cell lines, a single peak at 198 base pairs in the MOLM-13 cell line was detected indicating wild-type NPM1, whereas in the OCI-AML3 cell line there were two peaks, which indicate a wild-type allele and a product with a 4 base pair addition. This is the result of a heterozygous NPMc+ mutation in the OCI-AML3 cell line (Quentmeier, *et al* 2005). The presence of FLT3 internal tandem duplication mutations was also detected in these cell lines and results showed that the MV4-11 cell line harbours a 356bp of FLT3-ITD, with no wild-type peak compared to the MOLM-13 cell line, which has a wild-type FLT3 peak and a 347bp of FLT3-ITD (Figure 3.2B). In contrast, the wild-type FLT3 was detected in the OCI-AML3 and M-07e cell lines. These findings are consistent with the published findings on FLT3-ITD status among cell lines (Quentmeier, *et al* 2005, Quentmeier, *et al* 2003). Minor peaks, which are stutter bands, were seen before the main allele. The stutter bands are characterised by the presence of fewer repeat units compared to the main allele band which is caused by strand slippage during the extension step of the PCR.

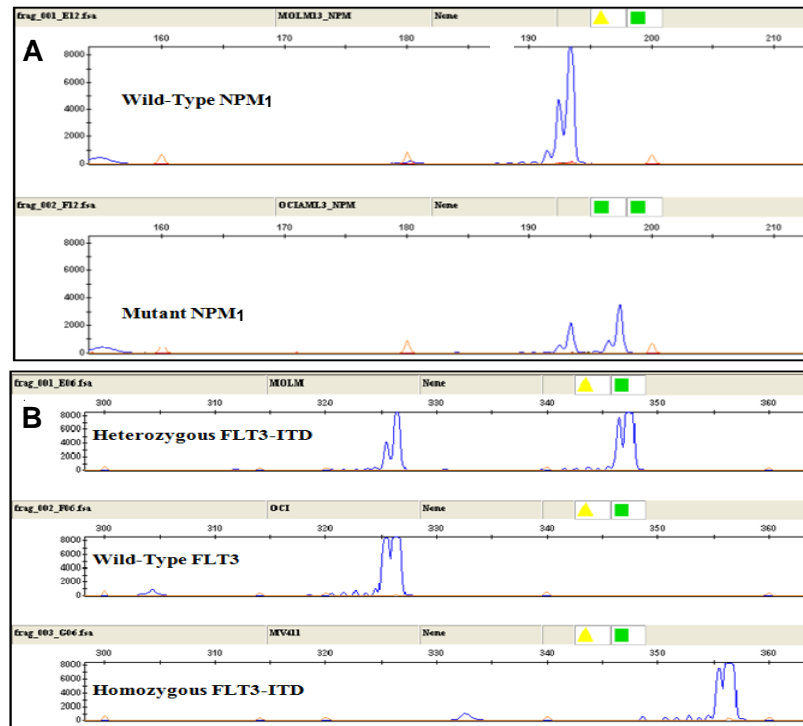


**Figure 3.2: NPM1 and FLT3 length mutations in AML cell lines; NPM1 and FLT3-ITD mutations were detected by PCR using fluorescence primers. (A)** A homozygous peak at 193bp in MOLM-13 indicates wild-type NPM1, while two peaks in OCI-AML3 one at 193bp for wild-type NPM1 and the second at 197bp for the mutated NPM1 indicates the heterozygosity of OCI-AML3 for the NPMc+ mutation. **(B)** Wild-type FLT3 at 326bp and FLT3-ITD at 347bp were detected in MOLM-13, whereas in OCI-AML3 was only one peak is seen at the wild type position (326bp). In the MV4-11 cell line one peak was detected at 356bp which indicates homozygosity of this cell line for FLT3-ITD. All the samples were run twice.

### 3.2.2 DNA damage repair activity in response to a DSB-inducing agent:

#### 3.2.2.1 Assessment of DNA damage repair activity by the comet assay:

In this chapter we aimed to evaluate DNA damage repair in the OCI-AML3 cell line, which harbour NPM1 mutations and wild-type P53, and compare it with other leukaemic cell lines that bear both wild-type NPM1 and P53. The comet assay or single cell gel electrophoresis assay (SCGE) is used to detect

the DNA damage at the level of the individual cell (reviewed in (Kumaravel, *et al* 2009). It is based on the ability of negatively charged DNA to migrate to the anode in the presence of an electric field after unwinding the DNA through agarose gel in either a neutral or alkaline buffer. Neutral comet assay detects primarily double-strand breaks, whereas alkaline comet detects DNA single-strand breaks (SSB), double-strand breaks (DSB), and alkali labile sites (reviewed in (Collins 2004)).

It is known that NPM1 plays a critical role in P53 activation through binding to ARF and HDM2 (Colombo, *et al* 2002, Gjerset 2006); thus, the delocalization of NPM1 in the mutated NPM1 cell line was suggested to impair the DSB repair pathway. Therefore, neutral and alkaline comet assays were used for assessing the DNA repair as loss of damage over time in M-07e, OCI-AML3 and MV4-11 cell lines. The cell lines were treated with etoposide at different concentrations for 24 hours to choose the optimal drug concentration, which caused 30% of cell death to ensure the cells had been damaged but not reach the point where all cells were undergoing to apoptosis (Figure 3.3A,B). Thereafter, M-07e, OCI-AML3 and MV4-11 cell lines were exposed to etoposide at 6 $\mu$ M, 4 $\mu$ M, and 0.4 $\mu$ M, respectively, for 24 hours. Following incubation with etoposide, the cells were incubated in drug-free medium and aliquots of cells were removed at different time points over 2 days to investigate the DNA damage/repair process.

In neutral comet analysis, the tail moment increased after 24 hours of treatment in all cell lines. During recovery process, the tail moment reduced by 20% after 24 hours in OCI-AML3 cell lines and followed by a further reduction to reach about 60% after 48 hours (p-value: 0.010), as the same percentage

as detected in MV4-11 and M-07e cell lines (p-values, which represent the difference in tail moment between 24 hours treated condition and after 48 hours of recovery process, in OCI-AML3, MV4-11 and M-07e cells are: 0.01, 0.068, and 0.092, respectively) (Figure 3.4A). On the other hand, the alkaline comet analysis demonstrated that the level of damage after 24 hours of recovery had reached the basal level in all three cell lines but the OCI-AML3 cells has a significant reduction when we compared with the 24 hours treated condition (p-value in OCI-AML3: 0.021, while in M-07e and MV4-11 p-value is around 0.346) (Figure 3.4B).

The percentage of cell survival during the comet assays was evaluated in all cell lines during the 48 hour repair phase and showed that cell survival was reduced to approximately 25% during recovery indicating that the majority of cells were lost via apoptosis and the damaged cells had died, while the undamaged cells had survived (Figure 3.5).

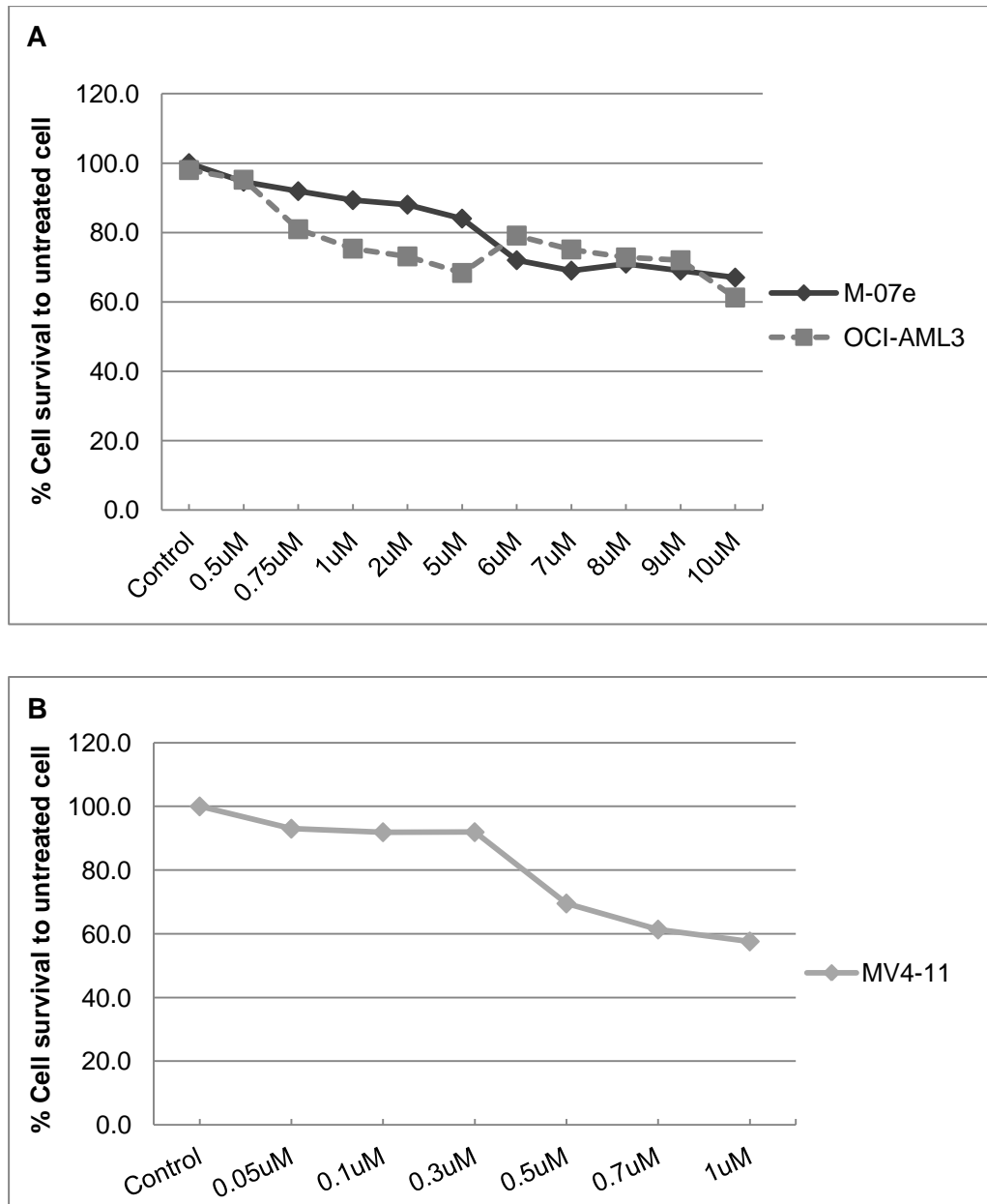


**Figure 3.3: Viability of AML cell lines in response to etoposide;** Cell lines were treated with etoposide at different concentrations for 24 hours. **(A)** M-07e and OCI-AML3 were treated with etoposide with concentrations range between (0.5 $\mu$ M to 10 $\mu$ M), while **(B)** MV4-11 cell line was between (0.05 $\mu$ M to 1 $\mu$ M). The cell viability was measured by Alamar Blue assay and the percentage of cell survival was calculated by dividing treated cells by the untreated cells. The experiment was performed once.

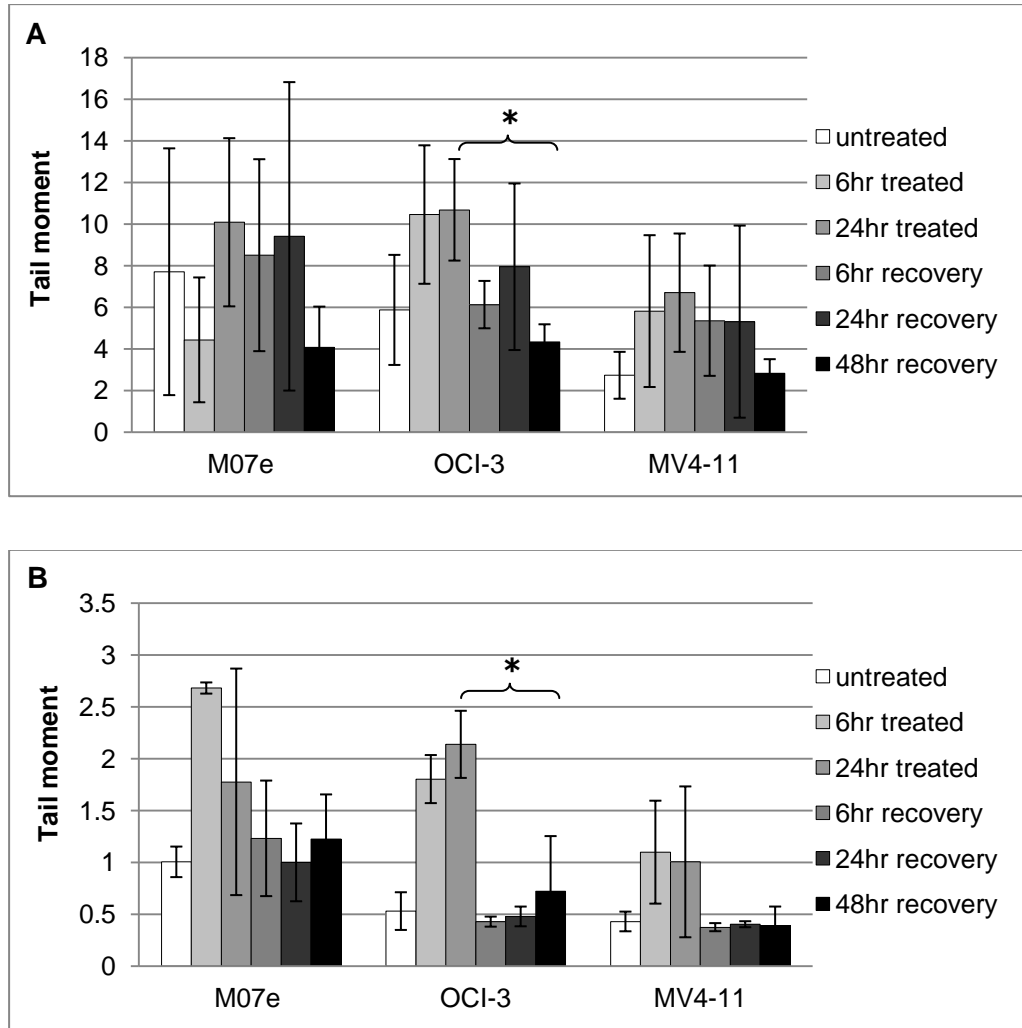


**Figure 3.4: Comet Assay in response to DSB agent;** Cell lines were treated with etoposide at concentrations of 6 $\mu$ M, 4 $\mu$ M, and 400nM for OCI-AML3, M-07e and MV4-11, respectively. The tail moment was measured as described in the materials and method section. The data shown represents the mean and standard deviation of triplicate experiments: **(A)** tail moment of the neutral comet assay, **(B)** tail moment for the alkaline comet assay. (\* indicates p-value <0.05 when the tail moment after 48 hours of recovery compared with 24 hours of treated condition)

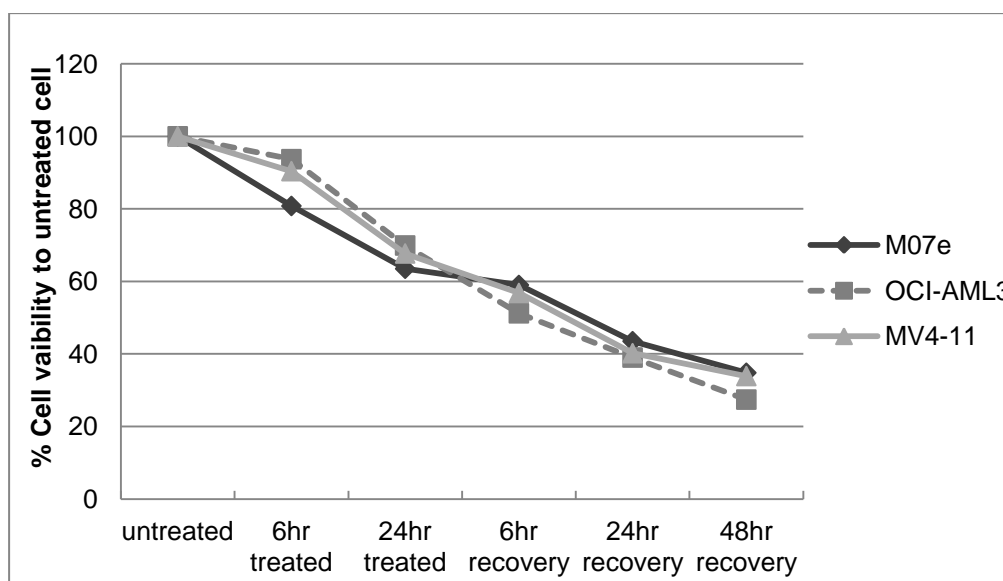


**Figure 3.5: Cell viability in parallel with comet assay upon etoposide treatment;** The viability of M-07e, OCI-AML3, and MV4-11 cell lines were evaluated after 6 hours and 24 hours of etoposide treatment at the respective concentration, then the drug was washed out and the cell viability was tested during the recovery process. An aliquot of cells were mixed with 7-AAD and the cell viability was measured using the flow cytometry method. The experiment was performed once.

### 3.2.2.2 Immunocytochemistry detection of $\gamma$ H2AX:

Phosphorylation of H2AX ( $\gamma$ -H2AX) in the response to DNA damage is essential in the response of a cell to double strand breaks (DSB) (Huang, *et al* 2004). Phosphorylation of H2AX is considered to be an early step in response to DSBs and is therefore considered to be a biomarker of the initiation of DNA-DSB repair process (Burma, *et al* 2001, Rothkamm, *et al* 2003). Measurements of  $\gamma$ -H2AX foci were evaluated by use of the H-score system which was originally developed to determine oestrogen receptor status in breast carcinomas (Katz, *et al* 1990). A total of 100 cells per condition was assessed and the number of foci present in each cell was counted and divided into the following groups; N (no foci), L (1-6 foci), M (7-12 foci), H ( $\geq 13$  foci), and C (completely damaged – uncountable foci). Thereafter, the H-score

calculated as follows:  $N+2L+3M+4H+5C$ , and the differences of H-score between the untreated cells and treated cells were calculated (Katz, *et al* 1990, Seedhouse, *et al* 2009a).

The  $\gamma$ -H2AX immunocytochemistry assay indicated that the percentage of H score in OCI-AML3 and MV4-11 cell lines reached around 40% after 24 hours of treatment with etoposide compared with untreated cells (Figure 3.6). In the OCI-AML3 cell line, the percentage of H score persisted after 1 hour of recovery in drug-free medium, but then decreased significantly over 24 hours, to reach 15% of the baseline (p-value: 0.03). In contrast, after 1 hour of recovery in the MV4-11 cell line, the H score reduced to 20% and remained stable at that level even after 24 hours of recovery (Figure 3.6). These results indicate that loss of  $\gamma$ -H2AX was delayed in the OCI-AML3 cell line during the first hour of DNA recovery compared to MV4-11 cells (p-value: 0.061), but after 24 hours it was hugely reduced to reach a same level to that seen in MV4-11 cells.

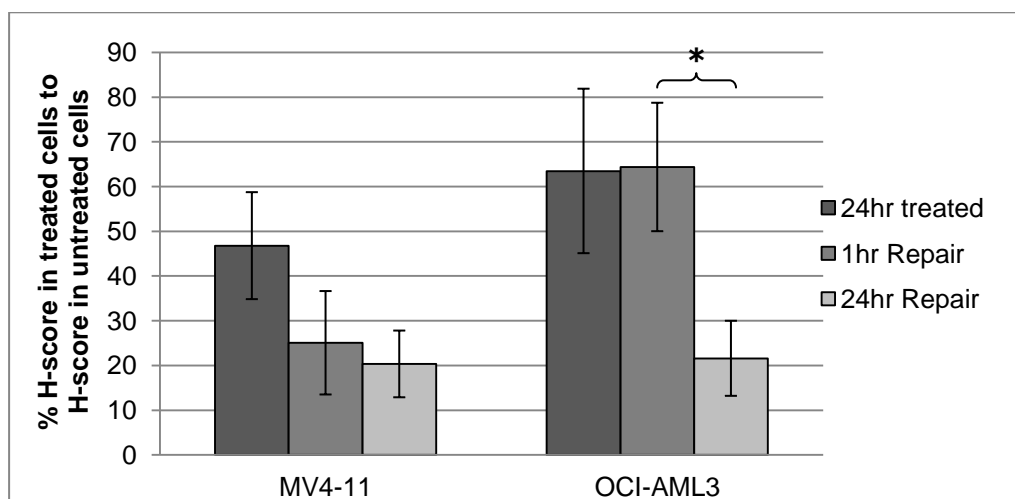


**Figure 3.6:  $\gamma$ -H2AX Immunocytochemistry analysis;**  $\gamma$ -H2AX was examined in MV4-11 and OCI-AML3 upon etoposide treatment and followed by 1hour, and 24 hours drug-free incubation to allow recovery. The percentage of  $\gamma$ -H2AX cells was calculated after dividing H score in a specific cell condition by the H score in untreated cells value. The results presented are the means of two experiments and the error bars are SD. (\* indicates p-value <0.05 when compared with 1 hour of repair condition)

### **3.2.3 Assessment of DNA damage repair function in response to an alkylating agent:**

Methyl methanesulfonate (MMS) is a DNA alkylating agent which is known to generate DNA damage, particularly in the form of base adducts which are predominantly repaired by the base excision repair pathway. Following MMS treatment DNA damage was assessed by the alkaline comet assay which facilitates the detection of alkali label sites, single strand and double strand breaks via unwinding the DNA at pH greater than 12 after cell lysis at a high salt concentration. In order to assess the DNA repair function in response to MMS in wild-type and mutated NPM1 cell lines, M-07e, OCI-AML3 and MV4-11 cell lines were treated with MMS at a concentration of 700nM, 700nM and 400nM, respectively, which caused around 30% of cell death after 24 hours (Figure 3.7A,B). Thereafter, the drug was washed out and the cells were incubated in drug-free medium to investigate the repair process at different times over 48 hours. The results showed that the tail moment among these cell lines increased during the drug treatment, whereas during recovery the tail moment reduced by approximately 30% after 6 hours in M-07e and OCI-AML3 cell lines, but additional reductions in tail moment did not occur after 24 hours of recovery (p-value: 0.123, and 0.131, respectively) (Figure 3.8). After 48 hours of recovery process, M-07e and OCI-AML3 cell lines showed a further reduction in the tail moment (Figure 3.8). In two these cell lines the percentage of cell survival was reduced from 60% after 24 hours of MMS treatment to 40% after 48 hours of cell recovery which indicates that the damaged M-07e and OCI-AML3 cells underwent apoptosis (Figure 3.9). In the MV4-11 cell line, the tail moment showed a steady decrease during the 48 hours of

incubation in a drug-free media, and reached around the same value as seen in untreated cells (Figure 3.8). In addition, the percentage of cell survival in MV4-11 cells was 80% after 24 hours of drug treatment and viability remained high during the recovery process suggesting that the DNA damage was repaired efficiently and the cells survived (Figure 3.9).

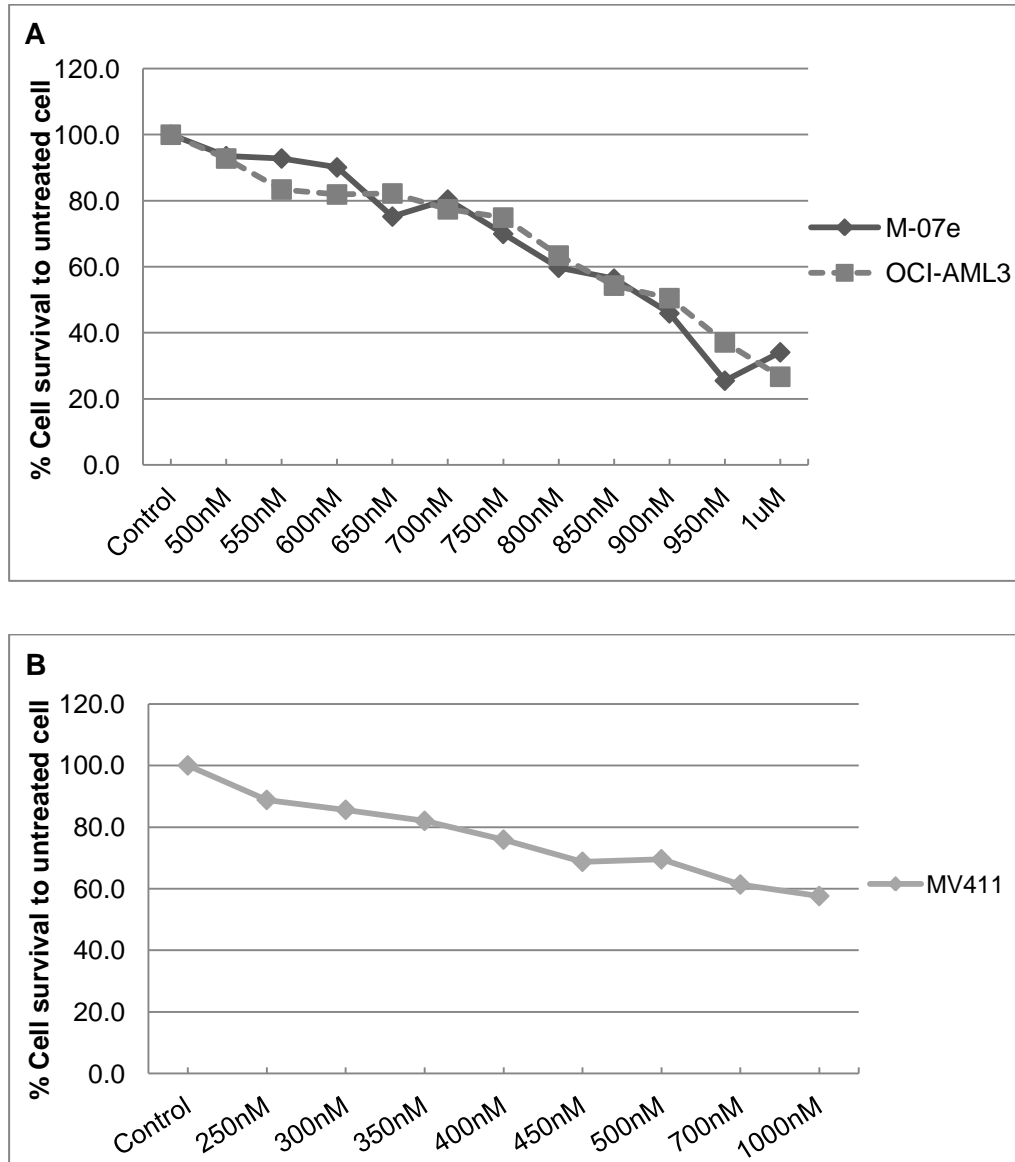


**Figure 3.7: Viability of AML cell lines upon MMS treatment;** (A) M-07e and OCI-AML3 cell lines were treated with etoposide with concentrations range between (0.5µM to 1µM) for 24 hours, while (B) MV4-11 cell line was between (250nM to 450nM) for 24 hours. The cell viability was measured by the Alamar Blue assay and the percentage of cell survival was calculated by dividing the treated cells by the untreated. The experiment was performed one time.

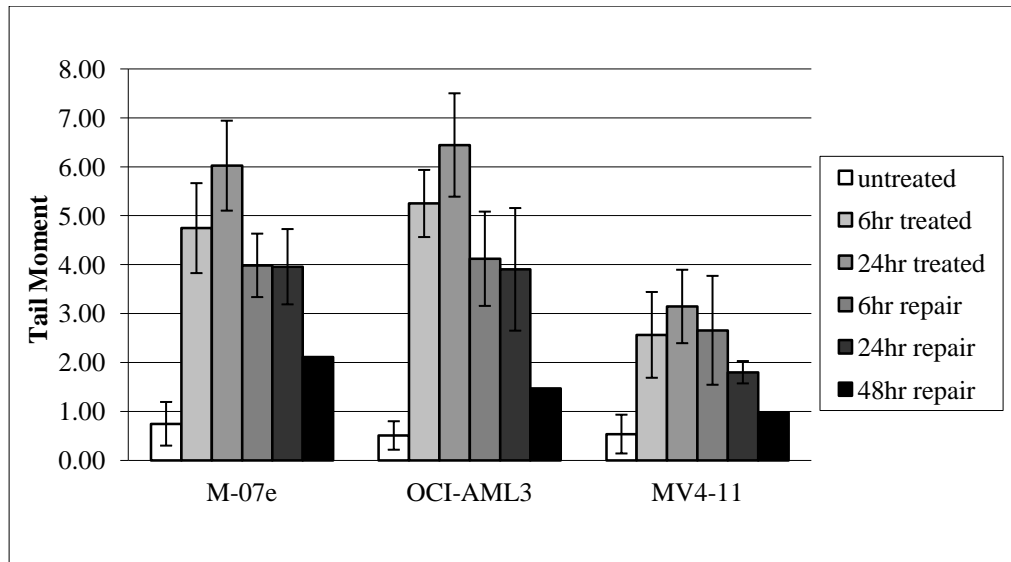


**Figure 3.8: Alkaline comet assay in response to MMS;** Measuring repair of MMS was assessed by the alkaline comet assay in OCI-AML3, M-07e and MV4-11. The tail moment was measured in untreated cells at 6 hours and 24 hours of MMS treatment, followed by 6 hours, 24 hours and 48 hours in drug-free medium to evaluate DNA repair. The mean and standard deviation of three independent experiments are shown. However, the 48 hour timepoint was performed only once.

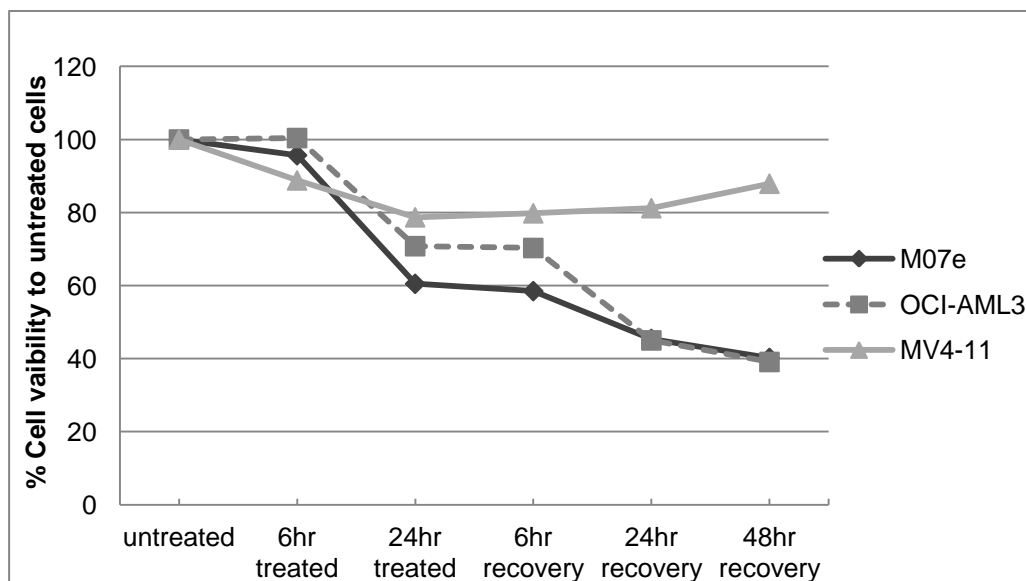


**Figure 3.9: Cell viability in parallel with comet assay upon MMS;** Viability of cells used in the comet assay was tested at different time during the drug exposure and through 48 hours of recovery. M-07e, OCI-AML3, and MV4-11 were treated with the respective concentration of MMS. An aliquot of cells were mixed with 7-AAD and then the cell viability was measured using the flow cytometry method. The experiment was performed once.

### **3.2.4 Expression of NPM1 in AML cell lines upon DNA damage inducing agent:**

We investigated the mRNA and protein levels of NPM1 in OCI-AML3 and M-07e cell lines before and after the cell lines were treated with MMS or etoposide. OCI-AML3 and M-07e cell lines were treated with 4 $\mu$ M, and 12 $\mu$ M etoposide, respectively, or 2 $\mu$ M MMS for both cell lines for 4 hours. As NPM1 shuttles between the nucleus and cytoplasm and there are differences in the subcellular localisation between cells expressing wild-type or mutated NPM1 protein detection of NPM1 by western blot was done on cytoplasmic and nuclear lysates.

In OCI-AML3, as expected for a cell line expressing mutant NPM1, the western blot showed that NPM1 was mainly observed in the cytoplasmic lysate fraction in untreated cells. However, after exposure to MMS or etoposide, NPM1 levels increased in the nuclear lysates relative to the loading control (p-value: 0.046 and 0.089, respectively) (Figure 3.10A). In contrast, the NPM1 localisation in the untreated M-07e cells was mainly in the nucleus and this reduced after the cells were treated with MMS or etoposide (p-value: 0.020 and 0.018) (Figure 3.10B).

NPM1 mRNA levels were also assessed in these cell lines, using the same conditions, to verify whether NPM1 transcript expression could be altered in response to the DNA damage inducer. Figure 3.11, shows that there was no significant difference in the expression of NPM1 mRNA in the OCI-AML3 NPMc+ cell line following treatment with MMS or etoposide (p-value: 0.244). NPM1 mRNA expression was also not altered among the three different conditions in the NPM1 wild-type cell line M-07e (p-value: 0.200).

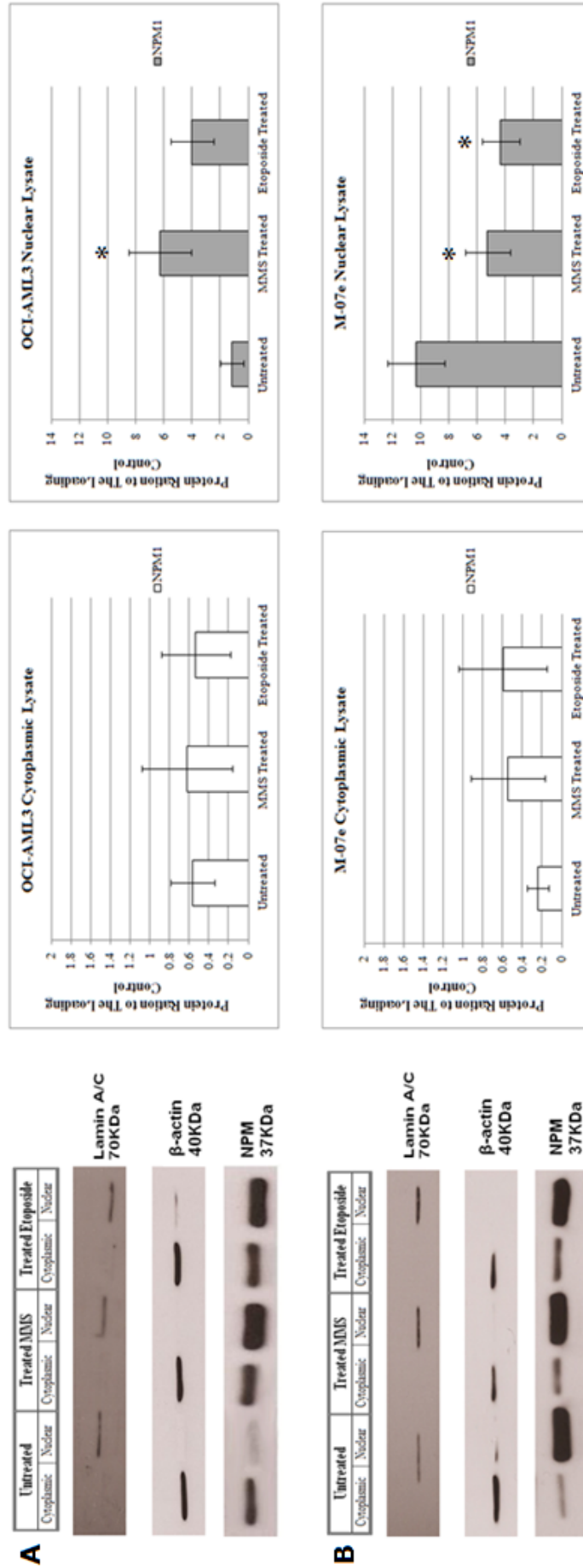


**Figure 3.10: Detection of NPM1 by Western Blot;** NPM1 protein level was detected by western blot. **(A)** OCI-AML3 and **(B)** M-07e cell lines were treated with MMS and etoposide for 4 hours and then the cytoplasmic and nuclear fractions were extracted as described previously in the materials and methods chapter. 10 $\mu$ g of lysate was added to SDS-PAGE gel for the detection of NPM1 (37KDa), and loading controls for cytoplasmic and nuclear extractions, Anti- $\beta$ -actin (40KDa) and anti-lamin A/C (70KDa/65KDa), respectively. Densitometry of the bands was performed by using Image-J analysis software (NIH). The western blot experiment was performed 3 times and the charts represent the calculated mean, while the bars represent the SD. (\* indicates p-value <0.05 compared with untreated cells)

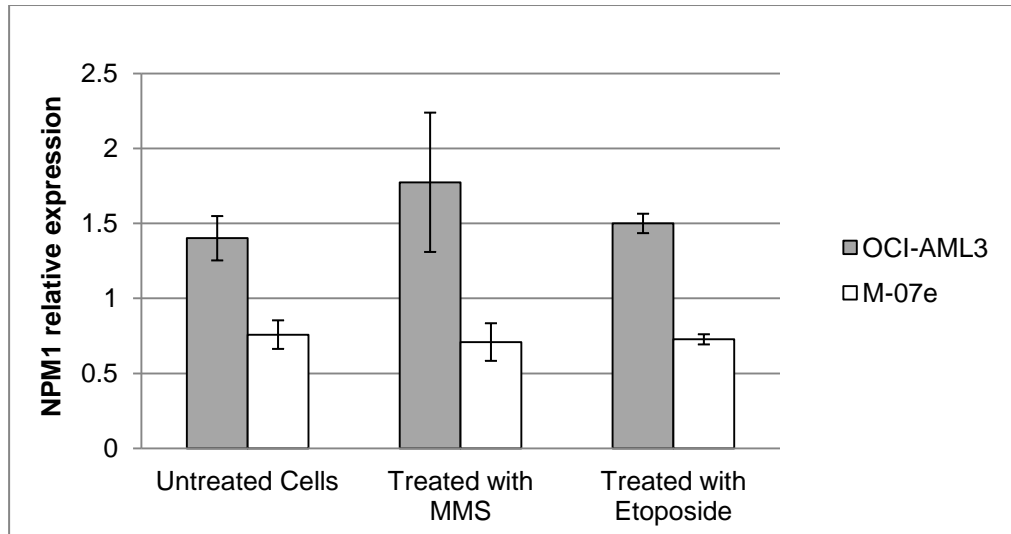


**Figure 3.11: The level of NPM1 mRNA upon DNA damage inducers;** The NPM1 mRNA expression was measured by real-time PCR after RNA was extracted from the cell lines treated with MMS or etoposide for 4 hours.  $\beta$ 2M, which is a housekeeping gene, was used to normalise the gene expression. The mean of 3 experiments was calculated and the error bars represent the SD.

### 3.3 Discussion:

This chapter focuses on the DNA damage response in a NPMc+ mutated AML cell line with comparisons made to haematological cell lines with wild-type NPM1. The genotyping of the haematological cell lines demonstrated a PCR product with an additional 4 bases pairs, in addition to a product of the expected size, in the NPM1 mutated OCI-AML3 cell line, this is characteristic of the heterozygous duplication of TCTG tetra-nucleotide position 956 to 959 in this cell line as demonstrated by Quentmeier *et al.* (Quentmeier, *et al* 2005).

One of the earliest events in the response to DSBs is the phosphorylation of ATM at the site of DNA damage which leads to the phosphorylation of H2AX, another early step in the cellular response to DSB (Burma, *et al* 2001, Rothkamm, *et al* 2003). This is subsequently followed by a rapid induction of numerous proteins and signalling pathways in response to the damage, eventually leading to the repair of the DNA damage or apoptosis. One important signalling pathway in the cellular response to DNA damage is the P53 pathway, which promotes cell cycle arrest and repair or apoptosis. It has been established that NPM1 plays a vital role in P53 stabilization by re-locating the tumour suppressor protein ARF to the nucleoplasm which result in the inactivation of HDM2, the negative regulator of P53 (Colombo, *et al* 2002, Gjerset 2006, Kurki, *et al* 2004b). In response to UV-damage or DNA intercalating agents such as daunorubicin, the NPM1 protein is translocated from nucleoli into the nucleoplasm where it binds to HDM2 which releases P53 leading to an increase in P53 stability and activity (Kurki, *et al* 2004a). In NPMc+AML mutations, we proposed that delocalisation of NPM1 into the cytoplasm leads to inactivate ARF function by altering its

subcellular localisation from the nucleus into the cytoplasm. As a result, the activity of P53 is reduced causing to perturb DNA repair functions and increase in sensitivity of NPMc+ cells to chemotherapy.

In the experiments reported in this chapter, the results suggest that the delocalisation of NPM1 into the cytoplasm in the NPM1 mutated cell line OCI-AML3, has not impaired the DNA damage response when compared to two cell lines harbouring wild type NPM1. The reason for this is because the comet assays showed that the tail moment was reduced efficiently after the cells were exposed to a DNA damage inducer – etoposide - and the percentage of cell survival decreased during the recovery process. This indicates that some of the cells were undergoing apoptosis. Moreover, we confirmed our findings by measuring  $\gamma$ -H2AX foci following etoposide treatment; a reduction in the foci, after 24 hours of drug-free cell recovery in the OCI-AML3 and MV4-11 cell lines, suggests that the DSBs are being repaired efficiently.

With respect to DNA damage repair, it has been shown that APE1 proteins interact with NPM1 and this complex is responsible for the subcellular localization of APE1 in HeLa cell line (Vascotto, *et al* 2009). APE1 is considered to be a vital enzyme in the BER pathway, where it functions to remove AP sites and cleaves the DNA strand 5' to the AP site producing a DNA primer with a 3'-hydroxyl end (Fishel and Kelley 2007). Due to the association of NPM1 with APE1 we proposed to look at the repair of damage caused by the alkylating agent MMS; this agent induces damage in the form of base adducts which are primarily removed by the BER pathway (Fishel and Kelley 2007). When comparing the NPMc+AML cell line to the wild type cell line, the loss of damage over time was no different

between the two cell lines indicating that the NPM1 aberrant cytoplasmic localisation in NPMc+AML did not affect the response of the cell to methylation damage. As a result, we have not looked at the pathways in more detail in patient samples, because the results did not show a difference in the DDR between the wild-type NPM1 and NPMc+ cell lines.

A number of papers have reported that the subcellular localisation of NPM1 is affected in response to DNA intercalating agents and UV damage when it translocates from nucleoli into the nucleoplasm to participate in DDR via activation of the P53-dependent pathway (Colombo, *et al* 2002, Kurki, *et al* 2004a, Kurki, *et al* 2004b). In our work, albeit in cells damaged by drugs which induce different types of damage to that induced by UV, damage did not alter the mRNA expression of NPM1 in the wild-type or mutant NPM1 cells. Conversely, NPM1 protein level was significantly increased in the mutant OCI-AML3 cell line in the nuclear fraction, but in the wild-type NPM1 cell line NPM1 decreased upon drug exposure.

It is known that NPM1 targets ARF to nucleoli in a dose-dependent manner; hence moderate to low NPM1 levels induces ARF activity by relocation of ARF into the nucleoplasm, whereas normal to slight elevation of NPM1 expression represses ARF to bind to HDM2 by locating it in the nucleoli (Korgaonkar, *et al* 2005). In western blot densitometry, strikingly, we showed a reduction trend in the protein level of NPM1 in the wild-type NPM1 cell line, whereas the level of NPM1 protein in the OCI-AML3 was raised approximately to the same level as detected in the M-07e cells. It seems that in the presence of DNA damage, the increased level of NPM1 protein in the nuclear compartment in OCI-AML3 cells reaches

the same levels seen in wild-type NPM1 cells and this contributes to the activation and stabilisation of P53 by increasing the NPM1 production and relocating the NPM1 in the nucleus. Once there it binds to ARF and HDM2. Moreover, the amount of NPM1 protein, which is present in the nucleus of OCI-AML3, could be enough to initiate the DDR processes. Consistent with this, Koike *et al.* found that a small fraction of NPM1 and phosphorylation at Threonin-199 is employed to DSB sites alongside the  $\gamma$ -H2AX and BRCA1 foci to participate in the DSB-induced repair process (Koike, *et al* 2010). Therefore, it seems that the NPMc+AML cells do not appear to affect the DDR during the DNA damage repair because our comet assay results and other repair assays demonstrated no difference between NPMc+ and wild-type NPM cells.

There are some aspects, which should be considered in our results. The experiments were performed on one cell line bearing NPMc+AML and compared to cell lines with wild-type NPM1 and P53. In addition, the western blot and the expression of NPM1 mRNA were tested after treatment with the cell lines by DNA inducer agent for 4 hours. While, in the comet and  $\gamma$ -H2AX assays, the cells were treated for 24 hours at a specific concentration of DNA inducer agent to produce 30% loss of cell viability. In order to produce consistency in the results, the cells in western blot and NPM1 expression should be maintained in the same condition as the comet assays cells were treated.

To summarise the findings in this chapter, we proposed that DDR in NPMc+ cells is impaired due to the delocalisation of NPM1 from the nucleus into the cytoplasm leading to perturb the function of some proteins involved in the activation DNA damage response (DDR). Our results suggest that

delocalisation of NPM1 into the cytoplasm in NPMc+AML cells does not impair the function of DDR in response to DNA damage drugs. In addition, the NPM1 protein level in NPMc+ cells increased in the nucleus upon the DNA damage inducers which is suggested that it may contributes in the regulation of the proteins involved in the DDR pathways. However, providing confirmation of these finding are required to be investigated particularly at the protein and mRNA levels of NPM1 during the DNA repair mechanisms and the importance of NPM1 in the DNA repair process in NPMc+AML cells.

# **4. The Effect of NPMc+AML on APE1 Subcellular Localisation**

#### 4.1 Introduction:

APE1 (Apurinic/aprimidinic endonuclease-1) is a multi-functional protein that plays a vital role in the repair of damaged and mismatched bases and therefore is integral to the cellular response to oxidative and alkylation responses. It is involved in the base excision repair (BER) pathway and also in the transcriptional regulation of gene expression by acting as a redox co-activator of transcription factors such as NF- $\kappa$ B and P53 (Fishel and Kelley 2007).

APE1 consist of two distinct functional domains, which are the N-terminal and C-terminal regions (Xanthoudakis, *et al* 1994). The N-terminal domain, which contains a nuclear localisation signal sequence, is responsible for redox activity and interacts with other proteins such as NPM1, whereas the C-terminal is employed to release its enzymatic activity on the abasic sites of DNA in the BER pathway (Fantini, *et al* 2010, Xanthoudakis, *et al* 1994). The subcellular localization of APE1 distribution is variable and depends on the cell type. In most cell types, APE1 is predominantly found within the nucleus, the location where it performs its DNA repair and co-transcriptional functions (Tell, *et al* 2005). However, in some cells, for example fibroblasts, lymphocytes and hepatocytes, APE1 is predominantly found in the cytoplasm (Tell, *et al* 2009).

With respect to the focus of this thesis, a paper was published showing that APE1 interacts with NPM1 in the nucleus with a subsequent translocation into the nucleolus (Vascotto, *et al* 2009). We therefore hypothesised that in NPMc+AML the delocalisation of NPM1 to the cytoplasm may also affect the subcellular localisation of APE1, this in turn might inhibit the APE1 DNA repair activity leading to increased sensitivity of

NPMc+ cells to chemotherapy agents which produce DNA adducts that rely on BER for repair. Thus, the aim of the work in this chapter was to examine the effect of cytoplasmic NPM1 on APE1 subcellular distribution and DNA repair following alkylating damage.

## 4.2 Results:

### 4.2.1 NPM1 and APE1 subcellular localization by immunofluorescence:

In order to perform the immunofluorescence staining, the cells were adhered on to slides by different methods. The LiquiPrep cytology and coverslip techniques (described in section 2.7.1) did not effectively coat the cells on the slides, whereas the cytopsin procedure caused damage to intracellular organelles resulting in an artifactual NPM1 staining pattern in the OCI-AML3 cells – specifically nucleolar staining appeared unaffected but cytoplasmic staining disappeared (Figure 4.1). However, the use of fibronectin-coated slides was successful in maintaining the cells on the slides without affecting the subcellular localisation of the proteins.

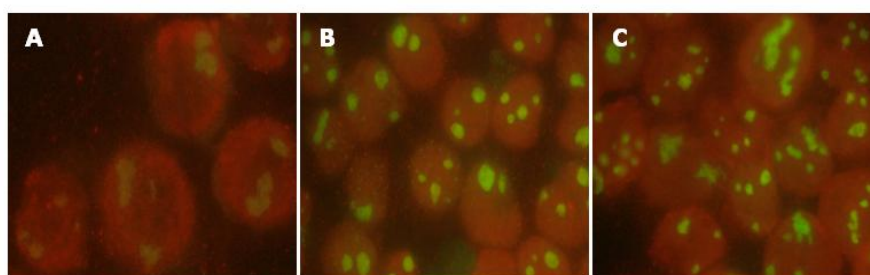


**Figure 4.1: NPM1 Subcellular localisation after cytopsin centrifugation;** the subcellular localisation of NPM1 was detected in **(A)** OCI-AML3, **(B)** HL-60, and **(C)** M07e cell lines. The cells were prepared by cytopsin and the NPM1 was detected by indirect immunofluorescence using FITC. The nuclei are stained in red with propidium iodide. The arrows indicate the localisation of NPM1 in the cell lines.

Anti-NPM1 antibodies were used to detect NPM1 for the purpose of investigating the subcellular localization of NPM1 protein in OCI-AML3, HL-60 and M-07e cell lines. Immunostaining revealed the aberrant expression of NPM1 in the cytoplasm of the OCI-AML3 cell line, while the HL-60 and M-07e AML cell lines, bearing wild-type NPM1, demonstrated staining restricted to the nucleoli (Figure 4.2). Therefore,

these results confirmed the cytoplasmic delocalisation effect of the mutation in NPM1 in the OCI-AML3 cell line (the presence of mutation had previously been confirmed by PCR (see section 3). As can be seen in Figure 4.2a, in OCI-AML3 cells NPM1 staining is predominantly seen in the cytoplasm.

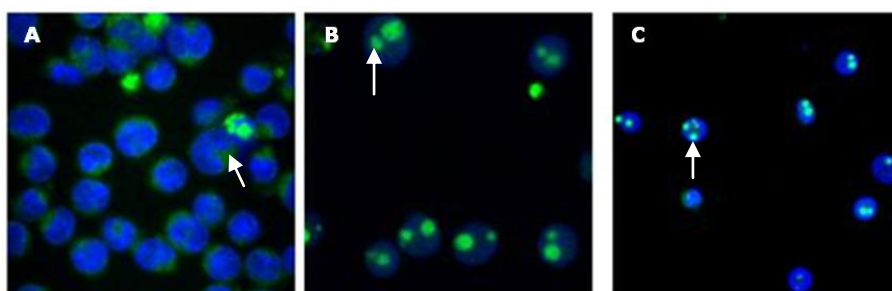


**Figure 4.2: Immunofluorescent subcellular detection of NPM1;** Subcellular localization of NPM1 was detected in **(A)** OCI-AML3, **(B)** HL-60, and **(C)** M07e cell lines. The cells were fixed and stained with anti-NPM1 antibody. NPM1 was visualised by indirect immunofluorescence using FITC whilst the nucleus was stained with DAPI, images were captured using a confocal laser microscope. The green fluorescence, where the arrows are, indicates the localisation of NPM1 in the cells.

When APE1 localisation was studied, immunofluorescence analysis showed a predominantly cytoplasmic localisation of the protein both in wild-type NPM1 and NPMc+ cell lines (Figure 4.3). Differences in APE1 subcellular localization were examined after induction of DNA damage by an alkylation agent to establish whether NPM1 affected the localisation of APE1 under these conditions. When the cells were treated with MMS, APE1 was found to accumulate in the nucleus in the wild-type and mutant NPM1 cell lines (Figure 4.3). In addition, OCI-AML3 showed a translocation of NPM1 from cytoplasm into the nucleus (Figure 4.3) and the results were confirmed by western blot as described in chapter 3 (section 3.2.4 – Figure 3.10A). As a result, NPM1 and APE1 proteins are restricted in the cytoplasm of the NPMc+ cell line, but in response to DNA damage they are re-localised in the nucleolus.

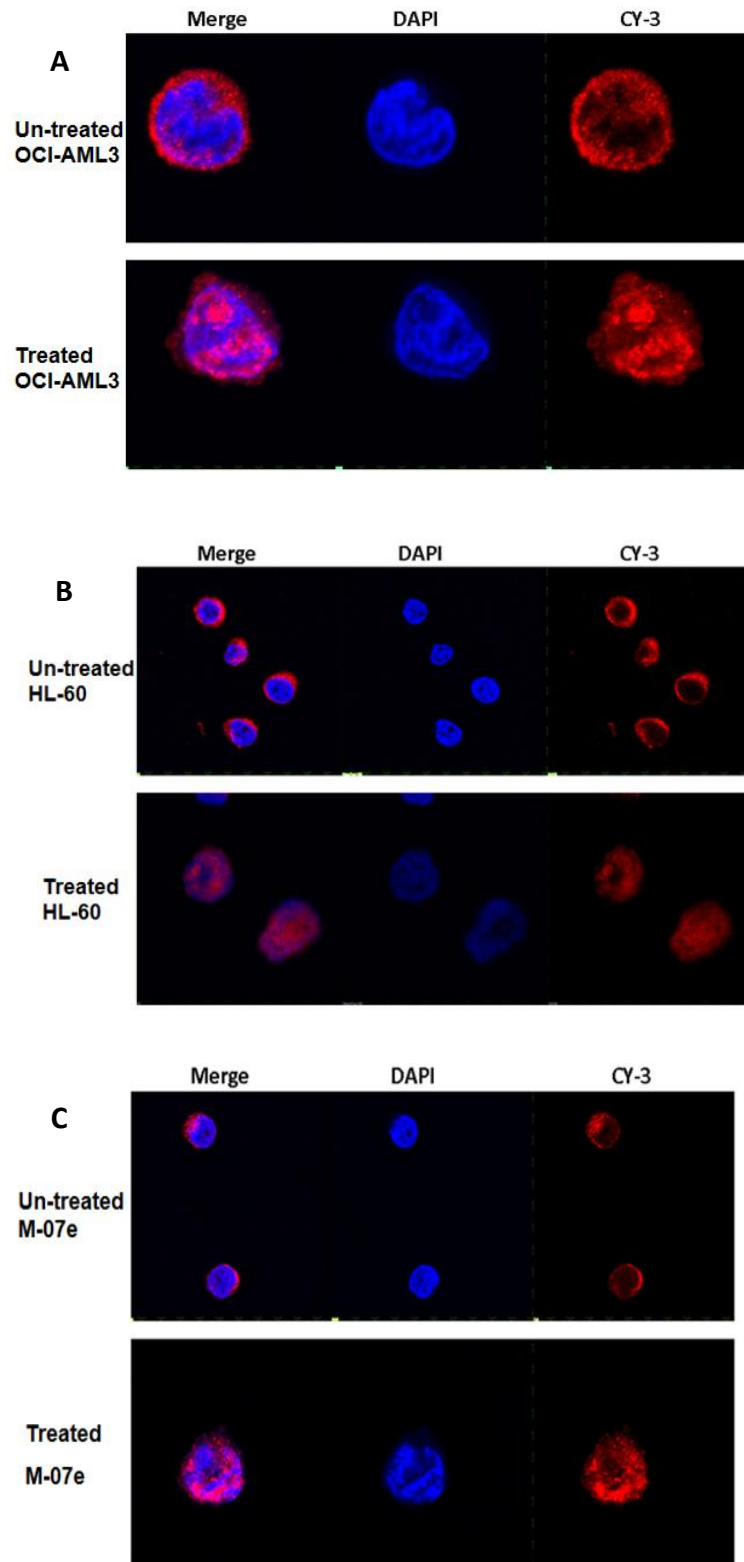


**Figure 4.3: Immunofluorescent subcellular detection of APE1,** Subcellular localization of APE1 was detected in **(A)** OCI-AML3, **(B)** HL-60 and **(C)** M-07e cell lines. The APE1 protein was examined under two different conditions: untreated or treated with MMS at  $2\mu\text{M}$  for 4 hours. The cells were fixed and stained with anti-APE1 antibodies and visualized by indirect immunofluorescence using CY-3 with a confocal laser microscope. The red colour indicates the APE1 localization, while the blue is the DAPI nucleus stain.

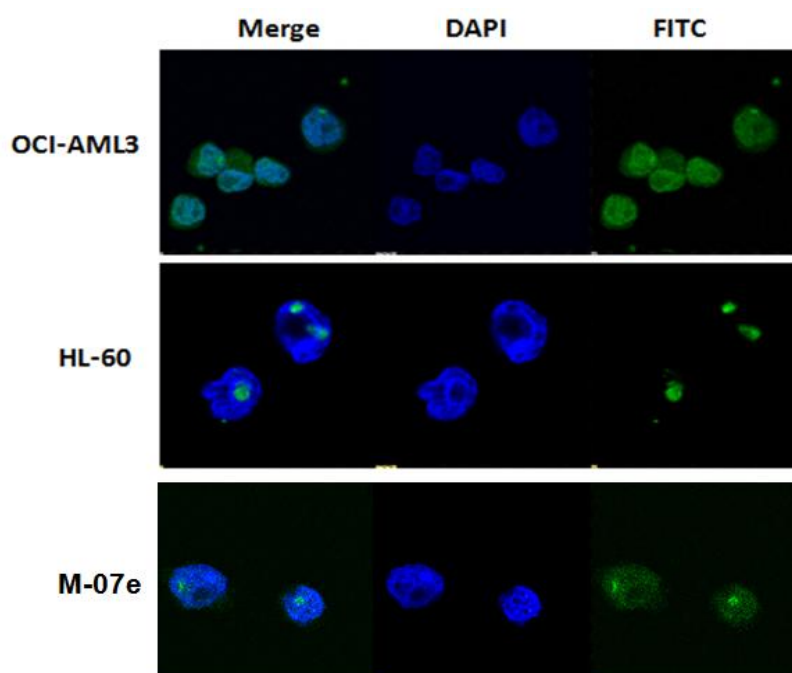


**Figure 4.4: Immunofluorescent subcellular detection of NPM1 after MMS treatment;** Subcellular localization of NPM1 was detected in MMS-treated OCI-AML3, HL-60, and M07e cell lines. The antigen-antibody interactions were observed by a confocal laser microscope using secondary FITC-antibodies.

#### **4.2.2 NPM1 and APE1 subcellular localization by western blot:**

The subcellular localization of both proteins was also analysed using western blotting. The cytoplasmic and nuclear extracts for OCI-AML3, HL-60 and M-07e cell lines were subjected to SDS-PAGE. As shown in Chapter 3, in OCI-AML3 cell line, larger amounts of NPM1 protein were present in the cytoplasmic fraction than in nuclei, but after cell treatment with MMS, the protein was visualised equally in both fractions with more in the nuclei extract following MMS treatment compared to the nuclear fraction from untreated OCI-AML3s (Figure 4.5A). In contrast and also as shown in Chapter 3, the NPM1 protein was mainly present in the nuclei fraction of M-07e cell line in both conditions (Figure 4.5B). In the HL-60 cell

line, it was present in the cytoplasmic fraction and in the nuclei of untreated and MMS-treated HL-60 cells (Figure 4.5C). The OCI-AML3 and Mo7e NPM1 protein expression results are shown here, in addition to Chapter 3, for easy comparisons to be made with the APE1 results.

Following western blotting of the APE1 protein, the OCI-AML3 cell line showed a band at 37KDa, which is the expected size of APE1, was present in the cytoplasmic and nuclear fractions of both untreated and treated cells, whilst in the cytoplasmic fraction a lower band was also present in both the untreated and treated cells (Figure 4.5A). However, in the HL-60 and M-07e cell lines, APE1 was observed as a single band at 37KDa in both the nuclear and cytoplasmic fractions of untreated and treated cells (Figure 4.5B,C).

A detailed literature search was undertaken to try and find out what the lower band may be. The APE1 antibody (NB100-101) recognises the C-terminus domain of APE1 and two proteins may be detected with 37-KDa and 34-KDa molecular masses. Later, the 34-KDa band was identified as a truncated form of APE1 lacking the N-terminal 33 amino acids (Yoshida, *et al* 2003). As a consequence, in an attempt to identify the lower band present only in the OCI-AML3 cells, the blot was incubated with an APE1 antibody which only binds to the N-terminal domain of APE1, which should therefore not detect an N-terminally truncated protein. In OCI-AML3, the lower band remained when the N-terminal APE1 antibody was used (Figure 4.5A). In the other cell lines, the N-terminal APE1 antibody detected the band at the same molecular weight as seen previously with APE1 antibody (Figure 4.5B,C). The lysates were checked for purity by using specific antibodies for

detecting  $\beta$ -actin that can only be found in cytoplasm and Lamin A/C which is only found in the nucleus (Figure 4.5).

#### **4.2.3 Detection of potential NPM1 and APE1 interaction by co-immunoprecipitation:**

The possible interaction between NPM1 and APE1 proteins was investigated by immunoprecipitation assays. Cytoplasmic extracts were isolated from OCI-AML3 and HL-60 cell lines, and then the cellular lysates were incubated with anti-NPM1 or anti-APE1, and immunoprecipitated with protein A/G-agarose beads. As shown in Figure 4.6, in OCI-AML3 and HL-60 cell lines, the NPM1 protein was present in the immunocomplexes precipitated by the anti-NPM1 and blotted by anti-NPM1, while it was absent in the immunocomplexes precipitated by anti-APE1 (Figure 4.6A). The results were confirmed when the immunocomplexes were immunoprecipitated and blotted by APE1 antibodies (Figure 4.6B). Whilst, in the HL-60 cell lines, there was a band in the complex precipitated by anti-NPM1 and detected by APE1 antibody, this is most likely non-specific since it was not observed when the complexes were precipitated by anti-APE1 and detected by anti-NPM1 (Figure 4.6B).

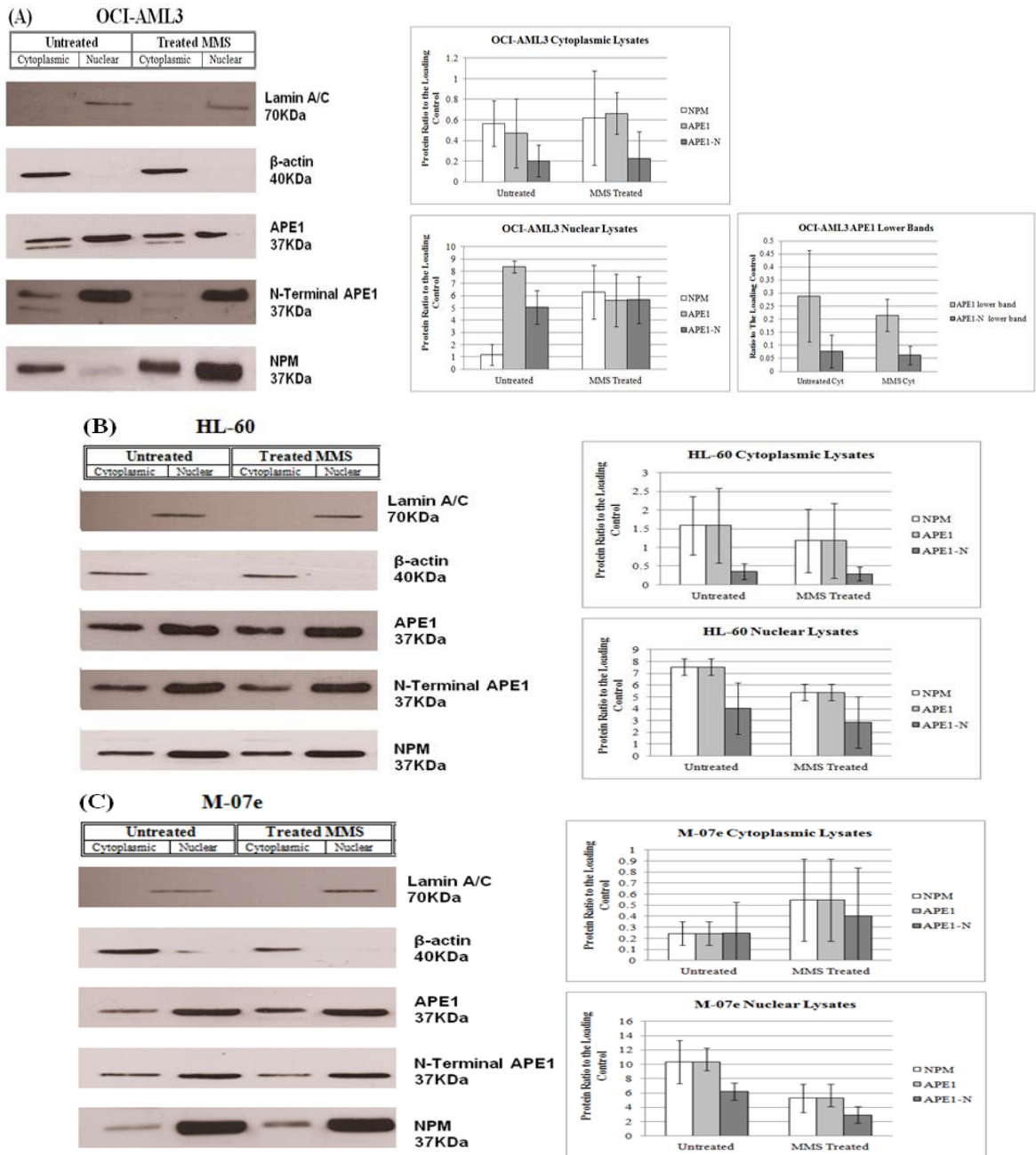


**Figure 4.5: NPM1 and APE1 subcellular localization by Western Blot;** Western blotting was used to investigate the subcellular localization of NPM1 and APE1 in **(A)** OCI-AML3, **(B)** HL-60, and **(C)** M-07e cell lines. The cytoplasmic and nuclear extracts of cell lines, untreated and treated with MMS, were extracted as described in the materials and method section (see section 2.7.3). 10µg was added to SDS-PAGE gel for the detection of NPM1 (37 KDa), APE1 (34kDa/37KDa). Anti-β-actin (40 KDa), and anti-lamin A/C (70KDa) were used as loading controls for cytoplasmic and nuclear extraction. The bands were quantified by densitometry using Image J analysis software (NIH). The ratio was calculated by dividing density of the test band by the density of the loading control. The experiment was performed three times independently, and the error bars represent the SD.

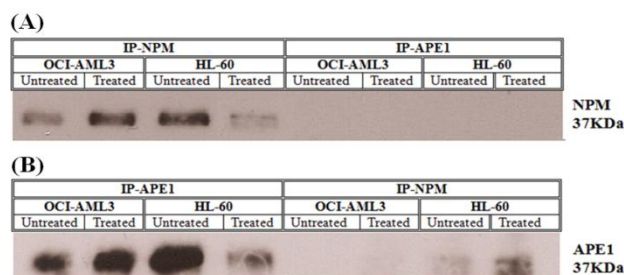


**Figure 4.6: Detection of NPM1 and APE1 interaction by co-immunoprecipitation;** The cytoplasmic protein was prepared from OCI-AML3 and HL-60 cell lines and immunoprecipitated with anti-NPM1 or anti-APE1 (section 2.7.5). The immunocomplexes were analysed using the Western Blot technique (section 2.7.4). **(A)** The immunocomplexes were detected by anti-NPM1, while **(B)** used anti-APE1.

#### 4.2.4 Detection of possible APE1 alternative splicing variants:

In an attempt to identify the lower molecular weight product detected with the anti-APE1 antibodies we looked to see if we could detect alternatively spliced variants of APE1. Forward and reverse PCR primers were designed using Primer3 programme against APE1 mRNA to detect aberrantly sized transcription products. The PCR was optimized using different annealing temperatures and four different  $MgCl_2$  concentrations. As shown in Figure 4.7A, the best PCR reaction, as determined by a single bright band, was in condition B, where the concentration of  $MgCl_2$  was 1.5mM, and the annealing temperature was at  $62.9^{\circ}C$ . Using these conditions, cDNA from OCI-AML3, M-07e and HL-60 cell lines were amplified and loaded to 1.7% agarose gel. The results showed that all the cell lines have one product at 963bp (Figure 4.7B), this was confirmed by sequencing the PCR products (Appendix 3.1) which demonstrated full length APE1 and suggests that the lower band is not likely to be a result of splicing variant of APE1.

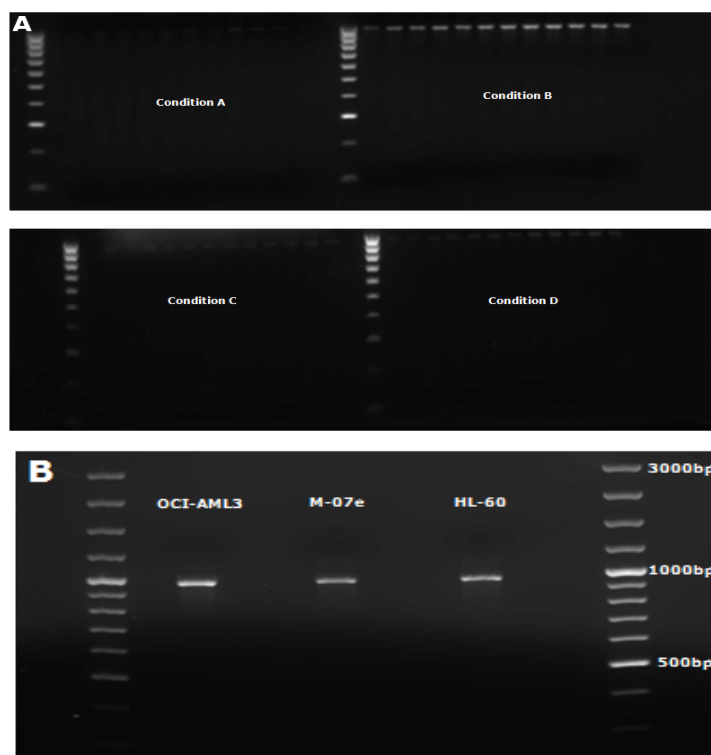


**Figure 4.7: Detection of APE1 spliced variant in AML cell lines;** APE1 mRNA was converted into cDNA and then amplified by PCR. **(A)** The APE1 primers were optimized at different annealing temperatures: 54.9°C, 55.2°C, 55.9°C, 57.0°C, 58.2°C, 59.4°C, 60.5°C, 61.7°C, 62.9°C, 64.0°C, 64.7°C, and 65.0°C and four different concentration of MgCl<sub>2</sub> were used. The Gene-Ruler 100bp DNA ladder which range between 100bp-1000bp, was used in the 1.7% agarose gel. **(B)** The PCR products from OCI-AML3, M-07e and HL-60 cell lines and the Gene-Ruler 100bp plus DNA ladder which range between 100bp to 3000bp, were loaded onto the 1.7% agarose gel. A negative no template control was included in the experiments.

#### 4.2.5 MMS cytotoxicity assay in wild-type and mutant NPM1 AML cell lines:

It has been demonstrated that knocking-down APE1 or inhibiting APE1 DNA repair activity causes an increase in sensitivity of tumour cells to chemotherapy (McNeill and Wilson 2007, Wang, *et al* 2004). Thus, we investigated the sensitivity of NPMc+ and wild-type NPM1 cell lines to MMS and looked for possible differences in the sensitivity of the cells harbouring the NPM1 mutation by comparing the OCI-AML3 cell line to two different wild-type NPM1 cell lines (both with wild type P53). MMS cytotoxicity was determined after the

cells treated with MMS at different concentrations for 1 hour and then the cells were incubated for 72 hours in drug-free medium. In figure 4.8, the MMS sensitivity test showed that survival of the OCI-AML3 cell line at 4 $\mu$ M was around 7% compared to untreated cells. It then decreased further at 10 $\mu$ M and there were no viable cells at higher concentrations. In the same way, the M-07e cell line showed a similar pattern to the OCI-AML3 cells, whereas MV4-11 cell line showed that the cells did not survive at a concentration higher than 4 $\mu$ M. At the statistical level, there was no significant difference between OCI-AML3 and wild-type NPM1 cell lines (MV4-11, and M-07e) at 4 $\mu$ M (p-value: 0.295, and 0.114, respectively) and at 2 $\mu$ M (p-value: 0.333, and 0.230, respectively). In conclusion, the differences in the sensitivity to MMS among these cell lines indicates that the NPM1 mutated cell line does not have a different sensitivity to MMS compared to cell lines containing wild-type NPM1.

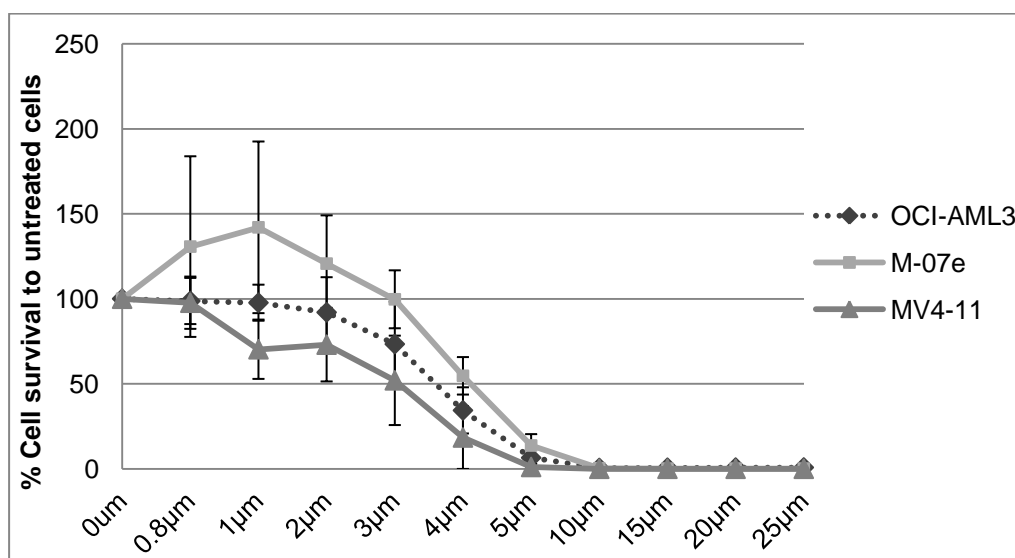


**Figure 4.8: The cytotoxic sensitivity assay on wild-type and mutated NPM1 cells in response to MMS;** The cells were treated with MMS at different concentrations for an hour, then washed and incubated for 72 hours in a drug-free medium. The cell viability was assessed by flow cytometry as described in section 2.5.3. The percentage of cell survival was calculated by dividing the number of cells in the treated condition by those counted in the untreated control. The mean and standard deviation of three independent experiments are shown.

### 4.3 Discussion:

APE1, which is a critical protein in the BER pathway, has been shown to associate with NPM1 in the nucleus which modulates its activity and function (Vascotto, *et al* 2009). A physical interaction between APE1 and NPM1 through the N-terminal was observed leading to a translocation of APE1 into the nucleolus in order to contribute in the rRNA processes (Vascotto, *et al* 2009). To date, any effect that the NPMc+ mutation may have upon the NPM1-APE1 interaction has not been studied and so this was the aim of the work in this chapter.

Firstly, we determined the subcellular localisation of NPM1 in OCI-AML3, M-07e and HL-60. As expected, the NPM1 subcellular localisation in NPMc+ cells was delocated in the cytoplasm, whilst in the wild-type NPM1 cell lines NPM1 was localised in nucleoli. Confirmatory experiments using the western blotting technique demonstrated the same findings which are consistent with previous findings (Falini, *et al* 2005). The APE1 subcellular localisation in haematological cell lines is predominantly located in the cytoplasm as identified in our results and as has been previously shown in HL-60 and U937 cell lines (Yoshida and Ueda 2003, Yoshida, *et al* 2003). It has been suggested that APE1 cytoplasmic localisation is associated with high proliferative rates and the function of APE1 as a redox may be required to keep newly synthesised transcription factors in a reduced state during their translocation to the nucleus (Duguid, *et al* 1995, Fung, *et al* 2001, Tell, *et al* 2009).

Previous work has demonstrated that APE1 is relocated in the nucleus after wild-type NPM1 haematological cell lines, HL-60

and U937, were exposed to an oxidative agent (Yoshida and Ueda 2003, Yoshida, *et al* 2003). In NPMc+AML cells, the APE1 translocation into the nucleus was not perturbed by the presence of mutant and wild-type NPM1 in the cytoplasm and we were unable to show an interaction between APE1 and NPM1 in the cytoplasmic fractions. In addition, the sensitivity of the mutated NPM1 cell line to MMS, an alkylating agent which causes the production of AP sites, was not perturbed by the delocalisation of NPM1 into the cytoplasm. These results suggest that APE1 subcellular localisation has not been affected by the mutant NPM1 in NPMc+AML and it seems that APE1 is translocated into the nucleus, where it may participate in the DNA repair process, in response to the DNA damage inducer.

The APE1 protein consists of two domains, which are the N-terminal and C-terminal domains (Xanthoudakis, *et al* 1994). APE1 has its own nuclear localisation signal in the N-terminal of the protein (Fantini, *et al* 2010, Vascotto, *et al* 2009), which is responsible for localising the protein in the nucleus, which could be a suggested reason for APE1 not being affected by delocalisation of NPM1 to cytoplasm – that is, its own nuclear localisation signal is stronger than any effects of an interaction with cytoplasmic NPM1.

In our study, certain technical issues had to be considered during the preparation of the coated slides with cells. Four different techniques were used to coat the cells on the slides in order to preserve their morphology and subcellular components. In the literature some groups have used a coverslip technique to grow cell lines overnight (Colombo, *et al* 2002), while researchers, who have studied NPM1 subcellular localisation in the OCI-AML3 cell line, performed

the immunofluorescence on paraffin sections, which is the optimal method in the detection of NPMc+AML in patient samples (Falini, *et al* 2011, Falini, *et al* 2005). In addition, it has been demonstrated that blood smears, or air-drying methods, are not suitable for the detection of NPMc+AML by immunohistochemistry or immunofluorescence, due to artefact diffusion leading to false positive or negative results (Mattsson, *et al* 2010). Moreover, we showed that the cytocentrifugation preparation method causes a false negative of NPMc+AML detection due to the re-localisation of NPM1 into the nucleus in the OCI-AML3 cell line. Vascotto *et al.* found a physical interaction between NPM1 and APE1, while our results did not show any evidence of interaction. However, in their experiments, Vascotto's group have used a Hela cell line, where APE1 is localised in the nucleus. Furthermore, the interaction between APE1 and NPM1 was detected by co-localisation analysis using an immunofluorescence confocal microscope and confirmed by mapping the domain of NPM1, which is involved in the interaction with APE1 by using Glutathione-S-transferases (GST) pull-down method. On the other hand, our work was performed on haematological cell lines, where APE1 is predominantly found in the cytoplasm, and APE1 and NPM1 interaction was performed using co-immunoprecipitation methods on the cytoplasmic lysates.

In the western blot, we identified a lower band that ran beneath the 37KDa APE1 in the cytoplasmic fraction of the OCI-AML3 cell line, whereas in the wild-type NPM1 cell lines this was not observed. Subcellular localisation of an N-terminal truncated form of APE1 (N $\Delta$ 33APE1) has previously been detected in the cytoplasm and in mitochondria (Chattopadhyay, *et al* 2006, Fantini, *et al* 2010). In

heamatological cell lines, this truncated form of APE1 was detected in HL-60 after being exposed to 50 $\mu$ M etoposide (Yoshida, *et al* 2003). Therefore, we blotted the membrane with an APE1 antibody that binds to the APE1 protein at the N-terminal region, to elucidate whether the lower band is a N $\Delta$ 33APE1 (if the N-terminal is missing then we would not expect a band with this antibody). However, the lower band was also detected with the N-terminal APE1 antibody suggesting that that the smaller product is not N $\Delta$ 33APE1. Thereafter, reverse-transcription PCR was used to examine whether the lower band protein resulted from alternative splicing of APE1 mRNA. However, we did not detect any splicing variants in the OCI-AML3 cell line and the sequence of the cDNA was the same as in the wild-type NPM1 cell lines. The next step would be to purify the lower band and subject it to peptide sequence analysis and compare this to the full APE1 amino acid sequence.

In summary, we confirmed the cytoplasmic localisation of NPM1 in OCI-AML3, whereas in the wild-type cell lines this was found in the nucleus, specifically in the nucleoli. Thereafter, we reported the subcellular localisation of APE1 in the cytoplasm in the heamatological cell lines tested. In response to an alkylating agent, the sensitivity of mutant NPM1 cell line to MMS was similar to the wild-type NPM1 cell lines indicating that APE1 is likely not interpreted by the cytoplasmic NPM1 by its translocation into the nucleus in order to participate in DNA repair. However, a lower band which was detected by APE1 antibody still needs to be identified.

# **5. The Effect of Down-regulation of NPM1 on BCL-2 and MCL-1 Anti- apoptotic Levels in NPMc+AML**

## 5.1 Introduction:

Programmed cell death (apoptosis) is an essential process for removal of unwanted or damaged cells and it is regulated by several genes including the BCL-2 family of genes. The members of BCL-2 are considered to be vital in the cell survival pathway of normal and tumour cells. They have been classified into two groups according to their function: pro-apoptotic (such as BAX, and BAK) and anti-apoptotic proteins (such as BCL-2, BCL-xL, MCL-1) (reviewed in (Tzifi, *et al* 2012)). The anti-apoptotic BCL-2 is expressed in normal and malignant cells (Andreeff, *et al* 1999), whereas MCL-1 is expressed in haematopoietic stem cells (HSCs) and is necessary for maintenance of cell survival (Glaser, *et al* 2012). In AML, expression of both MCL-1 and BCL-2 is extremely variable but 90% of AML samples taken at diagnosis have a high expression of BCL-2, whereas high levels of MCL-1 have been reported in human lymphoid leukaemia and FLT3-ITD cell lines (Kaufmann, *et al* 1998, Tothova, *et al* 2002, Yoshimoto, *et al* 2009). Moreover, MCL-1 expression correlates with mutant NPM1 in primary AML samples (unpublished results from Amina's work - MSc student in University of Nottingham 2011).

In NPMc+AML, activation of RNA polymerase II transcription by delocalisation of HEXIM1 into the cytoplasm by the mutant NPM1, leads to an enhancement of gene expression, which may be associated with an increase in cell growth and proliferation (Gurumurthy, *et al* 2008). Therefore, The aim of this study was to examine the level of BCL-2 and MCL-1 in wild-type NPM1 and NPMc+ cell lines and examine the consequences of NPM1 down-regulation by siRNA, targeting either total or just mutant NPM1, on BCL-2 and MCL-1 levels in

these cell lines. Parts of this work were performed by an MSc student who I co-supervised both at the bench level and with respect to the directions the research project took; these parts are acknowledged in the text.

## 5.2 Results:

### 5.2.1 Knock-down of total NPM1 or mutant NPM1 by siRNA in OCI-AML3 and M-07e:

We aimed to knock-down total NPM1 in both OCI-AML3, which harbour a type A mutation in NPM1, and M-07e, which is a wild-type NPM1, cell lines and to knock-down just the mutated NPM1 allele in OCI-AML3. Cells were nucleofected with siRNAs designed to either total NPM1 or mutant NPM1 state and compared to cells transfected with the AllStars negative control, which detects potential non-specific effects of siRNA transfection. The antisense strand of NPM1-A siRNA was complimentary with NPM1-A allele, whilst with NPM1 wild-type allele there were five mismatches found (Figure 5.1).

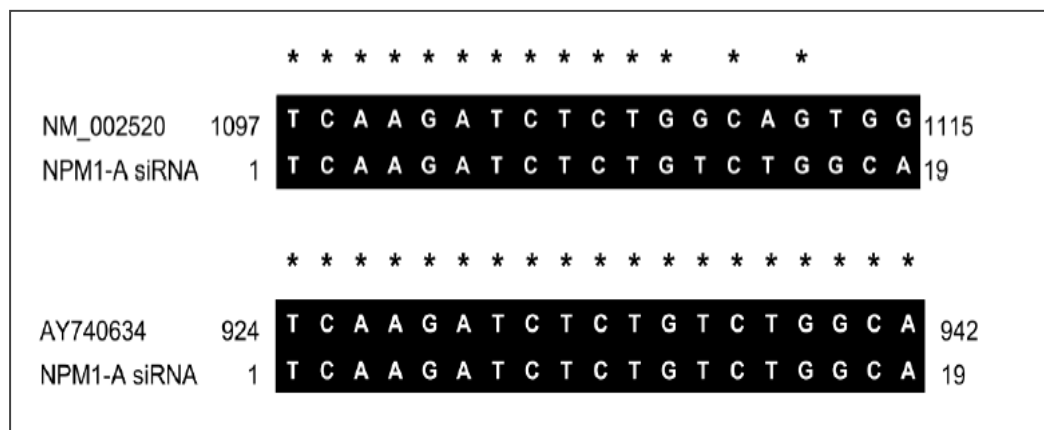


**Figure 5.1: Custom designed NPM1-A siRNA;** NPM1-A has identical sequence matches with NPM1-A allele (AY740634) but not with NPM1 wild-type allele (NM\_002520). \* denotes a sequence match. (K Liang, MSc dissertation, University of Nottingham 2011)

Transfection efficiency, cell viability, and NPM1 expression were measured to confirm the success of the nucleofection technique and the effect of the siRNAs. Several different total NPM1 siRNAs were tested and the one which consistently gave the most knock-down, NPM1\_7, was taken on to further

experiments. In OCI-AML3, the transfection efficiency and the cell viability were achieved 50% and 75%, respectively at 48 hours post-transfection. Moreover, in M-07e, the transfection efficiency was approximately 95% and the cell viability reached to 70% after 48 hours post-transfection. The NPM1 expression in OCI-AML3 and M-07e cell lines after 48 hours of knocking-down NPM1 reached a level of approximately 15% of the control level (OCI-AML3 p-value: <0.05, M-07e p-value: <0.05), whereas after knocking-down the mutant NPM1 in the OCI-AML3 cell line the level of total NPM1 was 60% of the control (p-value: 0.015) (Figure 5.2A). Furthermore, the western blot, which was performed during an MSc project (K Liang, MSc dissertation, University of Nottingham 2011), showed that NPM1 protein was also knocked-down after siRNA NPM1 (Figure 5.2B).

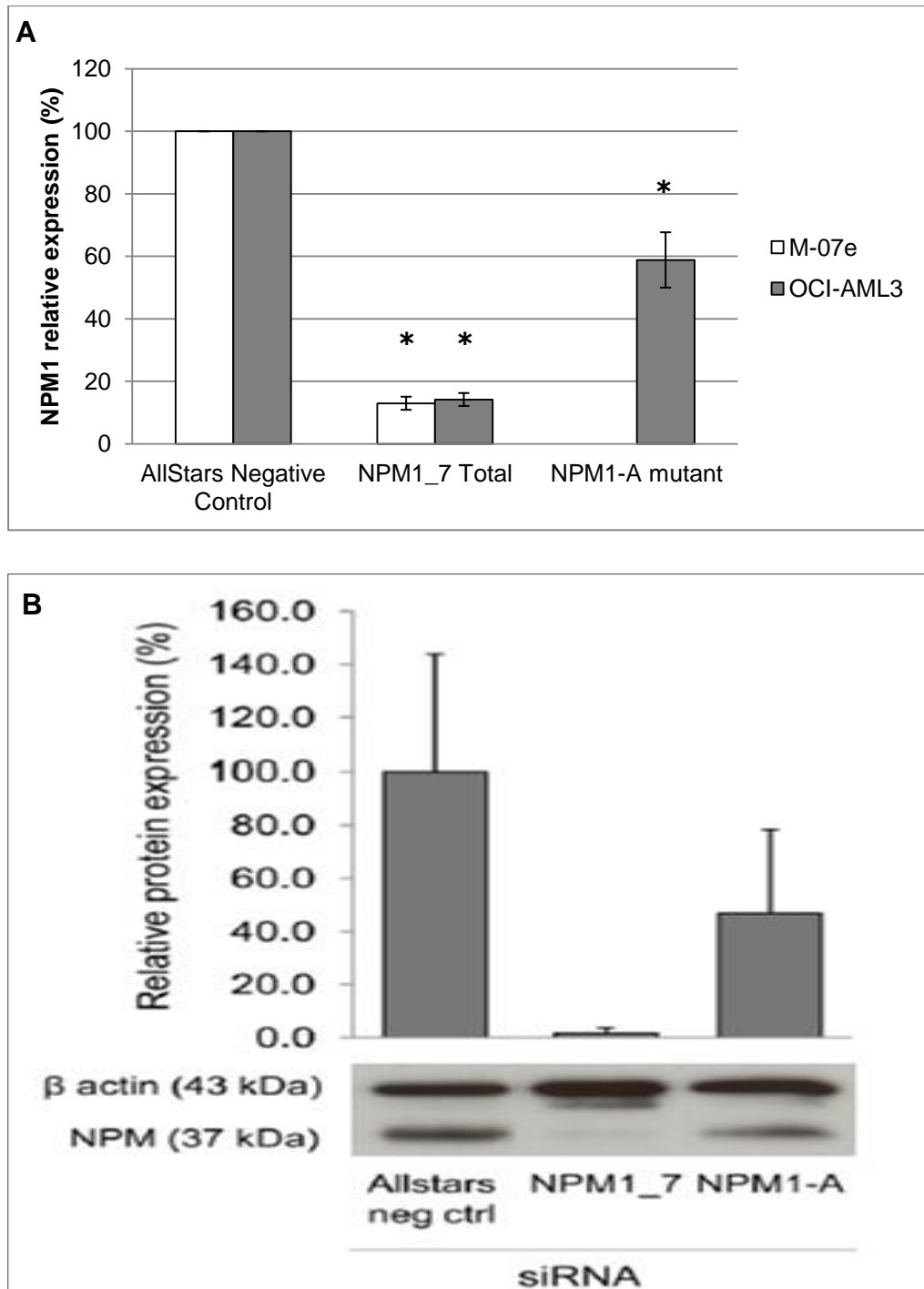


**Figure 5.2: NPM1 expression following siRNA designed to either total NPM1 or the mutant NPM1 only;** Total NPM1 in OCI-AML3 and M-07e were knocked-down by siRNA NPM1\_7, whereas the mutant NPM1 was down-regulated in OCI-AML3 by siRNA NPM1-A. After 48 hours, **(A)** the NPM1 mRNA was studied by real-time PCR. The gene expression was normalized by the  $\beta$ 2M house keeping gene and then the percentage of the NPM1 siRNA expression compared to AllStars negative control cells was calculated. **(B)** The protein was extracted from OCI-AML3 cell line and then western blot was used to confirm the protein reduction after siRNA (the picture was taken from Liang, K. dissertation, 2011). The experiment was performed 3 times for the NPM1 expression by real-time PCR, while the western blot was done 2 times, and the bars represent the SD. (\* indicates p-value <0.05 when compared with AllStars negative control)

In the previous work, measurements of NPM1 transcripts had been determined using primers designed to exons 9, 10, and 11 which amplified both wild-type and mutant transcripts. We wanted to quantify the mutant allele alone and therefore primers were purchased, one of which binds to the NPM1-A mutation site resulting in specific amplification of mutant transcripts. These primers had been designed by Gorello's group (Gorello, *et al* 2006). Total and mutant levels were consequently measured in the OCI-AML3 cell line.

Figure 5.3 shows the expression of total NPM1 was approximately 15% after 48 hours exposed to NPM1\_7 siRNA in OCI-AML3. In contrast, the expression of NPM1 in OCI-AML3 cell line nucleofected with the mutant NPM1 siRNA was around 60%, while the expression of mutant NPM1 declined to 40% indicating that NPM1-A siRNA induced silencing of the mutant NPM1 allele. We also looked at the distribution of the wild-type and mutated NPM1 alleles in OCI-AML3 cells by relative fluorescent quantitation on capillary electrophoresis system (Figure 5.4). As shown in table 5.1, the ratio of NPM1-A/wild-type NPM1 in cells transfected with either AllStars negative control or NPM1\_7, which down-regulates total NPM1, was close to one indicating that both wild-type and mutant transcripts had been similarly decreased, while the mutant specific siRNA reduced the mutant transcripts.

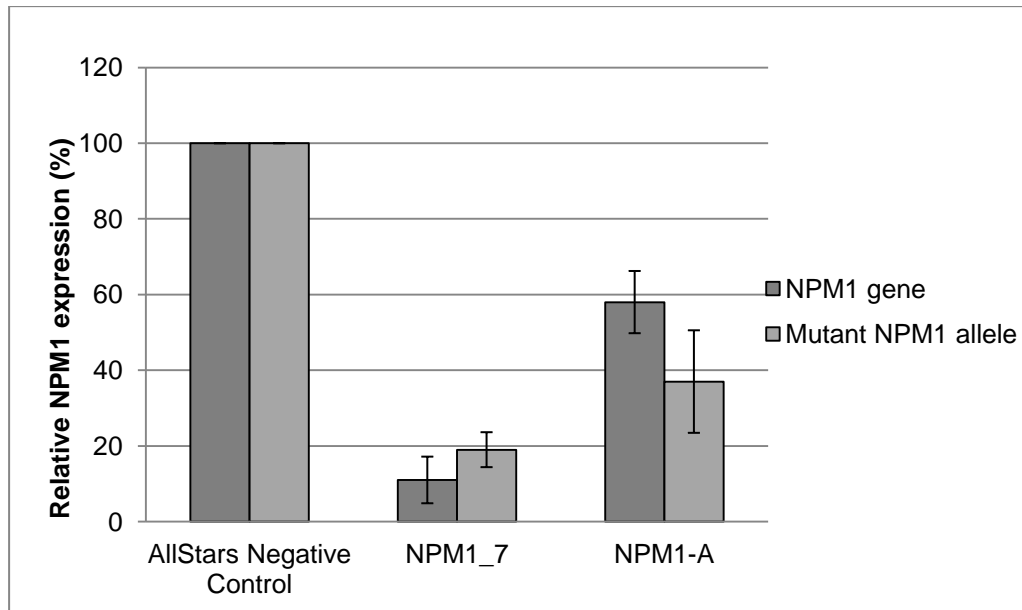


**Figure 5.3: Total NPM1 and mutant NPM1 expressions after siRNA;** Total NPM1 expression or mutant NPM1 expression only was measured in OCI-AML3 cell line. The cells were nucleofected with NPM1\_7 or NPM1-A siRNA to knock-down total NPM1 or mutant NPM1, respectively. After 48hrs, the RNA was extracted and converted into cDNA. The total NPM1 or mutant NPM1 only levels were measured by real-time PCR. The gene expression was normalized by the house keeping gene and then the percentage of the expression to control siRNA treated cells was calculated. The Columns represent the mean of 3 independent experiments and the bars are the SD.

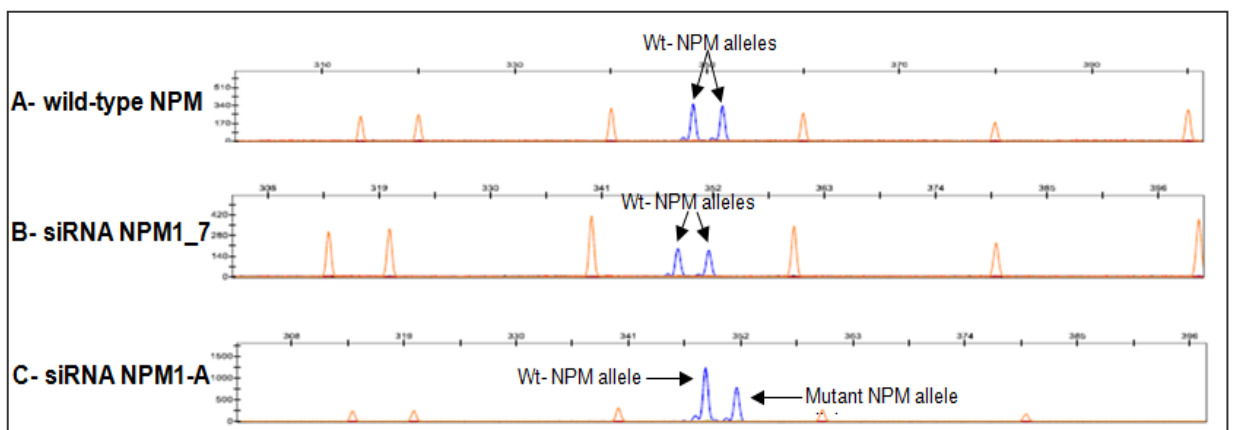


**Figure 5.4: Relative fluorescent quantification of NPM1-A and NPM1-wt alleles;** It was performed by capillary electrophoresis-based analysis of an NPM1 fluorescently labelled RT-PCR product. The experiment was done once (K. Liang, MSc dissertation). **(A)** The RNA was extracted from non-nucleofected OCI-AML3 cell lines. **(B)** The OCI-AML3 was nucleofected with siRNA targeting total NPM1, whereas **(C)** nucleofected with NPM1-A which down-regulates mutant NPM1 only.

**Table 5.1: The ratio of NPM1-A/ wild-type NPM1;** The peak height, which was detected by GeneMapper ID software v3.2, was calculated to compare the reduction in wild type and mutant NPM allele expression in the OCI-AML3 cell line after siRNA nucleofection.

siRNA	Peak Height		Peak Height Ratio (NPM1-A/wt-NPM1)
	NPM1-A	Wt-NPM	
AllStars Negative Control	195	217	0.90
NPM1_7	179	191	0.94
NPM1-A	785	1245	0.63

### 5.2.2 Basal anti-apoptotic levels in wild-type and mutant NPM1 cell lines:

Members of the anti-apoptotic BCL-2 family are over-expressed in AML and appear to play an essential role in leukaemogenesis (reviewed in (Tzifi, *et al* 2012)). The basal levels of BCL-2 and MCL-1 mRNA in the leukaemic cell lines were analyzed by real-time PCR. The level of BCL-2 and MCL-1 mRNA were significantly higher in OCI-AML3, which harbour mutant NPM1, specifically when compared to M-07e levels both MCL-1 and BCL-2 were increased approximately 3 fold in the OCI-AML3 cell line (p-value: <0.005). When comparing the OCI-AML3 cell line to the other wild-type NPM1 cell lines that co-express FLT3-ITD (MV4-11, and MOLM-13), BCL-2 mRNA was increased by 1.5 fold which is also statistically significant (p-value: 0.014 and 0.003, respectively) and MCL-1 mRNA in OCI-AML3 cells was 1.5 fold higher than in MV4-11 and MOLM-13 cells (p-value: 0.003 and <0.005, respectively) (Figure 5.5A). However, there was no significant difference in the BCL-2 protein at the basal level between the four different cell lines (p-value: >0.05). Similar to the mRNA results, MCL-1 protein level was highest in OCI-AML3, however this was only significant when compared to M-07e and MOLM-13 cell lines (p-value: 0.001 and 0.013, respectively) (Figure 5.5B). These

results indicate that the expressions of BCL-2 and MCL-1 transcripts in OCI-AML3 are significantly higher than in the other selected haematological cell lines.

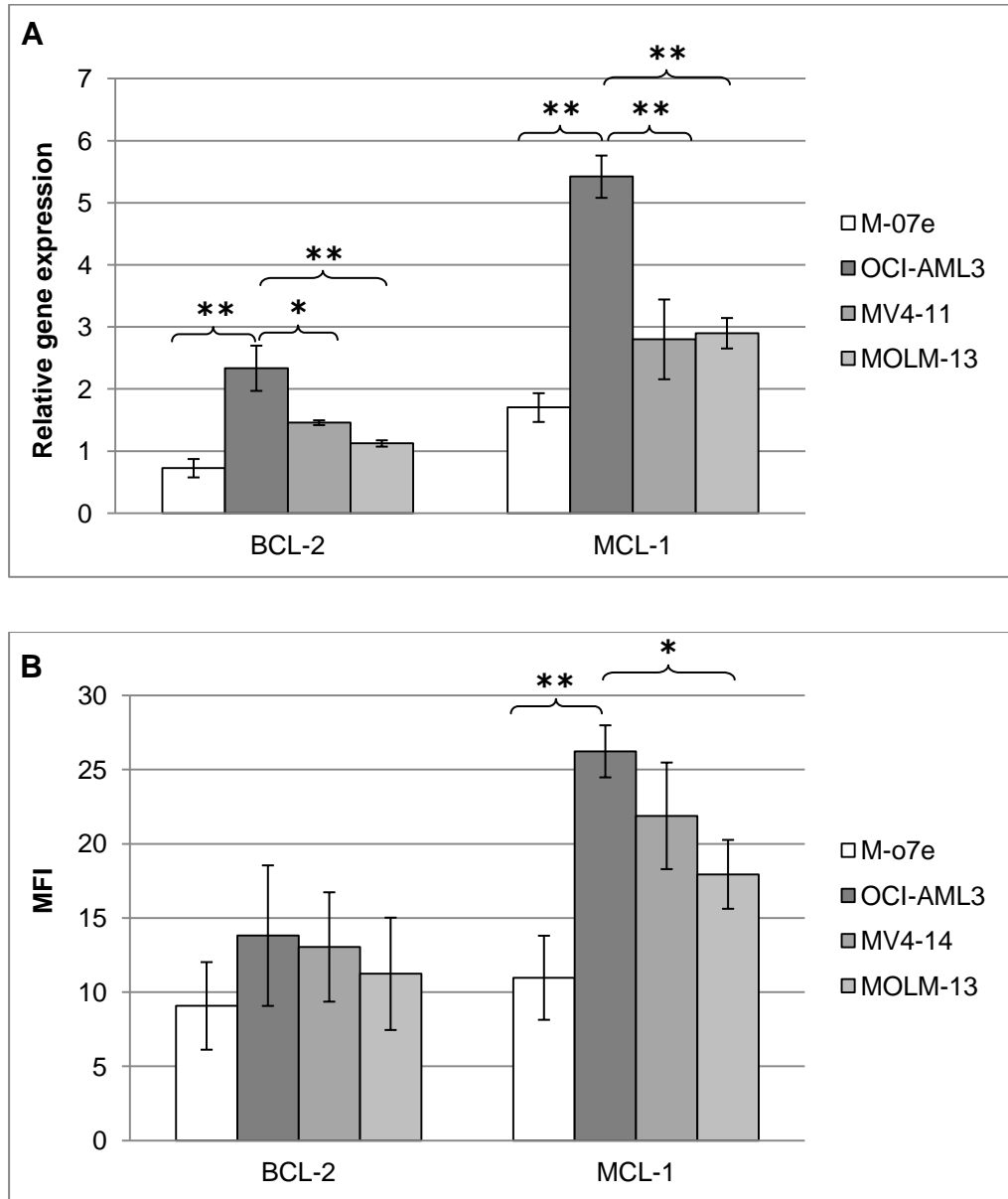


**Figure 5.5: Detection of BCL-2 and MCL-1 mRNA expression and protein levels in the different leukaemic cell lines. (A)** RNA was extracted from M-07e, OCI-AML3, MV4-11 and MOLM-13 and cDNA was prepared. Quantitative real-time PCR was performed with primer sets specific to BCL-2 or MCL-1. **(B)** The cells were fixed and incubated with the respective antibodies, and were analysed by flow cytometry for BCL-2 and MCL-1 protein levels. The mean fluorescence index (MFI) was calculated by dividing the mean of positive fluorescence to the negative control. Columns represent the mean of 3 independent experiments and the bars are the SD. (\* indicates p-value <0.05, while \*\* represent p-value <0.005)

### **5.2.3 BCL-2 and MCL-1 mRNA levels in wild-type and mutant NPM1 cell lines following down-regulation of NPM1 with siRNA:**

The transcript expression levels of BCL-2 and MCL-1 were evaluated in OCI-AML3 and M-07e after down-regulation of NPM1 with siRNA. Figure 5.6 shows that following transfection of OCI-AML3 with total NPM1 siRNA a down-regulation of BCL-2 and MCL-1 levels of around 60% and 40%, respectively, occurs (p-value: 0.025 and 0.034). However, after the mutant NPM1 was knocked-down, the level of BCL-2 and MCL-1 was 75% and 90%, respectively, when compared to the control cells (p-value: 0.049 and 0.096). The reduction of BCL-2 and MCL-1 upon NPM1 mutant siRNA was less than seen in cells nucleofected with NPM1 total siRNA. Interestingly, knockdown of NPM1 in the wild-type cell line (M-07e) showed no difference in the level of BCL-2 (p-value: 0.901) or MCL-1 expressions (p-value: 0.113) after NPM1 siRNA transfection. These results suggest that NPM1 may play a role in the regulation of BCL-2 and MCL-1 levels in OCI-AML3 cells.

However, knocking-down the mutant NPM1 was not used in detecting the level of BCL-2 and MCL-1 because after a while the mutant NPM1 allele was not targeted and it seems that the NPM1-A siRNA had degraded. Furthermore, the detection of P53 and CD11b levels in OCI-AML3 and M-07e cell lines after silencing the mutant NPM1 allele was not performed for the same reason.

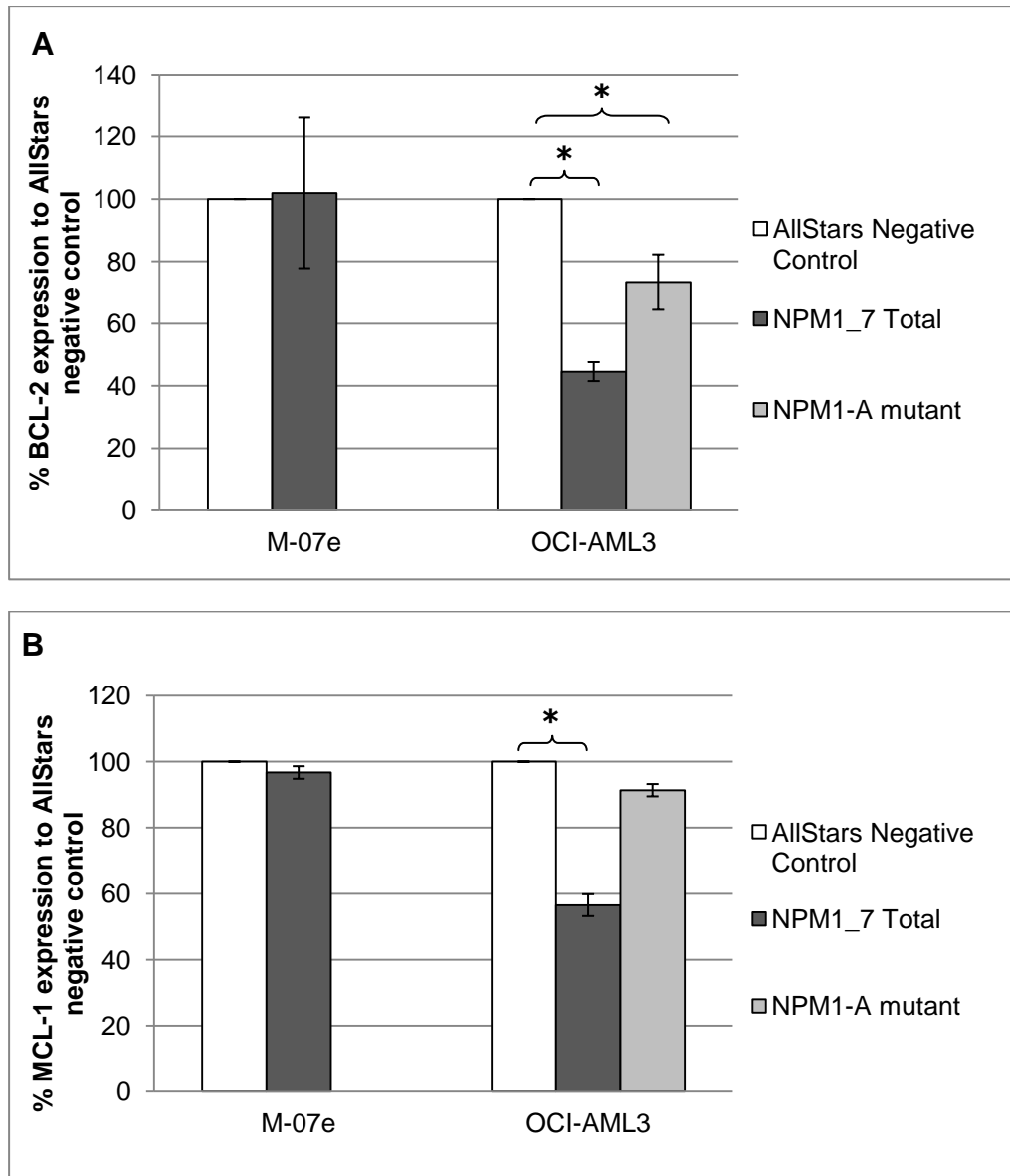


**Figure 5.6: BCL-2 and MCL-1 mRNA level after siRNA total NPM1 or the mutant NPM1 only.** (A) The BCL-2 and (B) MCL-1 mRNA level in OCI-AML3 and M-07e were measured by real-time PCR after total NPM1 knocked-down. The relative transcript level was determined by dividing the gene level to the house keeping gene, then the percentage to control cells was calculated. The experiment was performed 3 times and the bars represent the SD. (\* indicates p-value <0.05 when compared with AllStars Negative Control)

### 5.2.4 P53 levels in M-07e and OCI-AML3 after total NPM1 knock down:

It is known that NPM1 is involved in the stabilization and activation of P53 (Wu, *et al* 2001). Therefore, P53 protein levels were measured in the cell lines after NPM1\_7 siRNA transfection. Interestingly, a decrease in levels of total NPM1 was associated with an increase in total P53 in OCI-AML3 of approximately 50% (p-value: 0.035) (Figure 5.7), whereas in M-07e the level of P53 showed no evidence of change (p-value: 0.651).

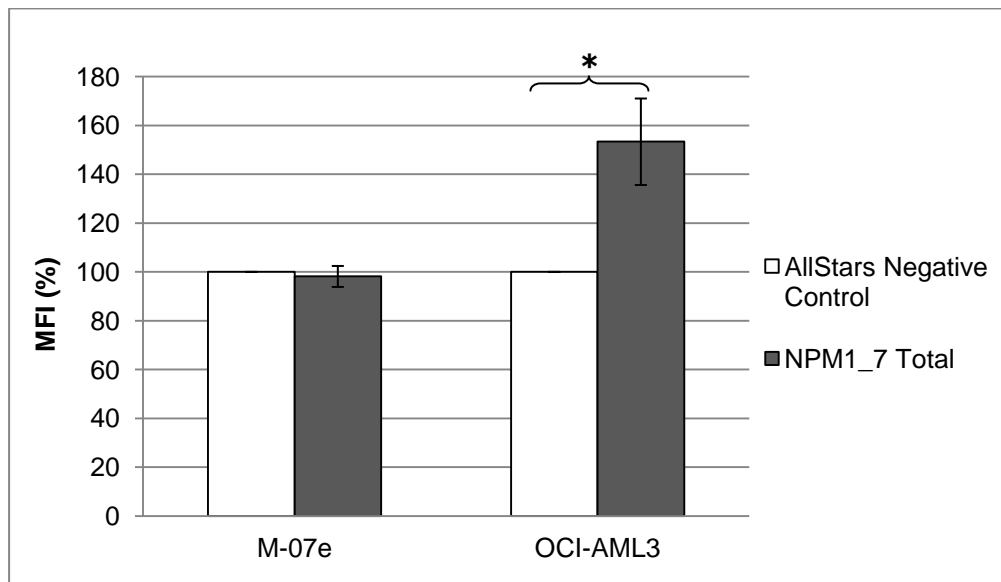


**Figure 5.7: The protein level of P53 in the leukaemic cell lines upon NPM1\_7 siRNA;** Flow cytometry were used to detect the total level of P53 in OCI-AML3 and M-07e following treatment with siRNA to total NPM1. After 48 hours of nucleofection with NPM1 siRNA, the total P53 was analysed using flow cytometry. The MFI was used to calculate the level of protein and then the percentage of P53 was calculated by comparing to the AllStars negative control. The experiment was performed 3 times and the bars represent the SD. (\* indicates p-value < 0.05 when compared with AllStars Negative Control)

### 5.2.5 Measurement of the differentiation marker (CD11b) in M-07e and OCI-AML3 after total NPM1 knock down:

We next determined the effects of NPM1 down-regulation on a differentiation marker of AML cells. As shown in figure 5.8, CD11b was slightly elevated in OCI-AML3 but it is not statistically significant (p-value: 0.19). In contrast, the level of CD11b in M-07e nucleofected with total NPM1\_7 siRNA was the same level as measured in cells transfected with AllStars negative control (p-value: 0.491) (Figure 5.8).

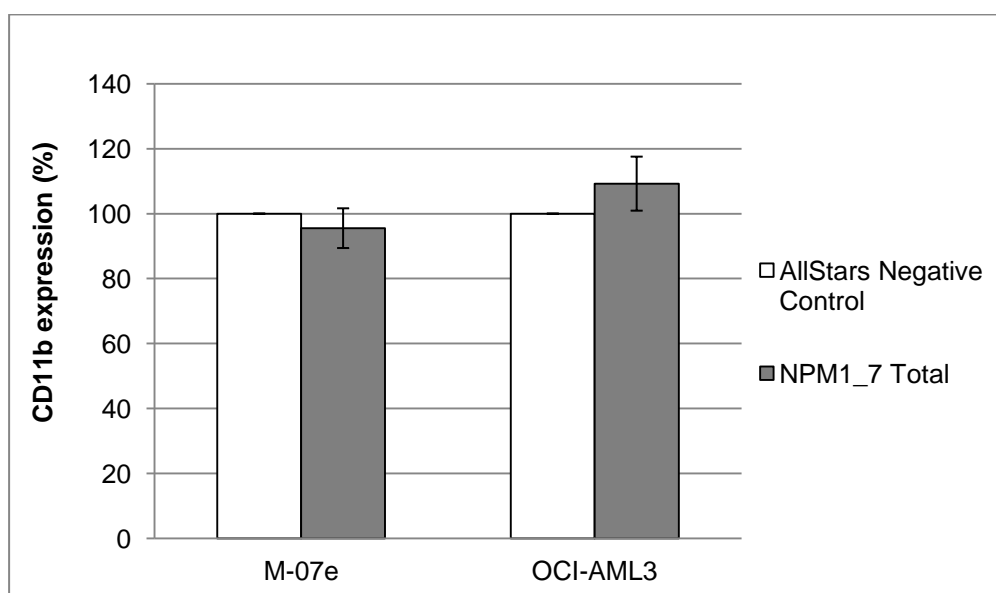


**Figure 5.8: Expression of the differentiation marker CD11b after leukaemic cell lines were nucleofected with siRNA NPM1\_7;** Flow cytometry was used to detect CD11b in OCI-AML3 and M-07e following treatment with siRNA to total NPM1. After 48 hours of nucleofection with NPM1 siRNA, The CD11b differentiation marker was detected using an anti-CD11b PE-labelled antibody. The percentage of expression was calculated by comparing to the AllStars negative control. The experiment was performed 3 times and the bars represent the SD.

### 5.3 Discussion:

Impairment in regulation of the cell death process is associated with cancer development and resistance to chemotherapy. In this chapter we have analysed and described the expression of BCL-2 and MCL-1 in different human leukaemic cell lines and have then investigated the effect of the down-regulation of NPM1 on the levels of BCL-2 and MCL-1 in wild-type and mutant NPM1 cell lines. The OCI-AML3 cell line is the only one to represent a model of NPMc+AML among the haematological cell lines, however it is important to note that whilst it differs in NPM1 mutation status it will also differ with respect to many other genetic and phenotypic abnormalities. However, as our interests were in DNA repair and apoptosis we did, at least, choose only those cell lines that are P53 wild-type. Ideally a series of isogenetic cells would be used in this work but were unfortunately not available.

It has previously been reported that in AML cell lines, the BCL-2 and MCL-1 anti-apoptotic proteins were found to be over-expressed in HL-60, KG1a, and ML-1 cell lines (Kaufmann, *et al* 1998). In addition, MCL-1 was highly expressed in the MV4-11 cell line, which harbours a homozygous FLT3-ITD mutation (Yoshimoto, *et al* 2009). However, in this study, we found that the BCL-2 and MCL-1 mRNA levels were highest in the NPMc+ cell line when compared to the other three cell lines studied. The protein level of MCL-1 was also higher in OCI-AML3 than in NPM wild-type cells, however, there were no significant differences in the levels of BCL-2 protein amongst the four cell lines, contradictory to the mRNA levels. This contradictory has been previously seen in lymphoid tissue and is suggested to be a result of suppression of the post-transcriptional process

of BCL-2 gene (Kondo, *et al* 1992). In addition, BCL-2 and MCL-1 protein levels were only measured by flow cytometry and it would be useful to measure levels by western blotting to check these results correlate.

Delocalisation of NPM1 in the cytoplasm may participate in the up-regulation of anti-apoptotic gene expression. This observation was confirmed when the total NPM1, or the mutant NPM1, was knocked-down in OCI-AML3. The levels of BCL-2 and MCL-1 mRNA were reduced in OCI-AML3 upon the nucleofection, whereas in M-07e the levels of BCL-2 and MCL-1 did not change. These findings suggests that mutant NPM1 plays a role in NPMc+AML cells leading to an increase in the level of BCL-2 and MCL-1.

Previously, Balusu *et al.* found that the P53 level increased in OCI-AML3, but not in HL-60 cell lines after down-regulation of total NPM1 (Balusu, *et al* 2011). Furthermore, the differentiation marker levels (CEBP- $\alpha$ , P53, P21, and CD11b) were also elevated in OCI-AML3 (Balusu, *et al* 2011). Consistent with this, the results presented here demonstrate that the level of P53 has increased in the NPMc+ cell line only following knockdown of total NPM1, but the differentiation marker (CD11b) illustrated a non-significant increase. However, the work in this chapter measured parameters 48 hours after NPM1 knock-down, while Balusu's group performed experiments after 96 hours of siRNA NPM1 introduction. During this work, we attempted to knock-down NPM1 for 72 hours but levels of NPM1 started to increase and so this time point was not continued with.

In NPMc+AML, the mutant NPM1 delocalises into the cytoplasm leading to a perturbation in other NPM1 protein

partners, such as ARF (Gjerset 2006, Lee, *et al* 2005). ARF is a positive regulator of P53 through an interaction with HDM2 allowing an increase in P53 stability and activity (Kurki, *et al* 2004b). The activity of ARF is regulated by NPM1 through targeting the protein into the nucleoli in a dose-dependent manner. For instance, high expression of NPM1 leads to inactivation of ARF by translocation of the protein into the nucleolus and thereby blocking ARF-mediated P53 activity, while modest reductions in NPM1 levels would cause some ARF fraction to relocate in the nucleoplasm and bind to HDM2 with subsequent activation of the P53-dependent pathway (Korgaonkar, *et al* 2005). Furthermore, P53 is a negative regulator of BCL-2 and it has previously been observed that a lack of P53 function leads to an up-regulation of BCL-2 (summarised in Figure 5.9A) (Wu, *et al* 2001). The precise mechanism by which the BCL-2 is up-regulated in OCI-AML3 was not elucidated, but it is possible that delocalisation of ARF by the mutant NPM1 in NPMc+ cells leads to a decrease in P53 stability and prevents the P53-mediated suppression of BCL-2 activity (Figure 5.9B). However, down-regulation of wild-type and mutant NPM1 in OCI-AML3 cells results in ARF being translocated into the nucleoplasm and enables its binding to HDM2. As a result, the stability and activity of P53 is increased which leads to inhibit BCL-2 activity (Figure 5.9C). In this respect, it has been shown that a slight reduction in NPM1 expression causes a partial localisation of ARF into the nucleoplasm and binds to HDM2 which acts to stabilise P53 (Korgaonkar, *et al* 2005).

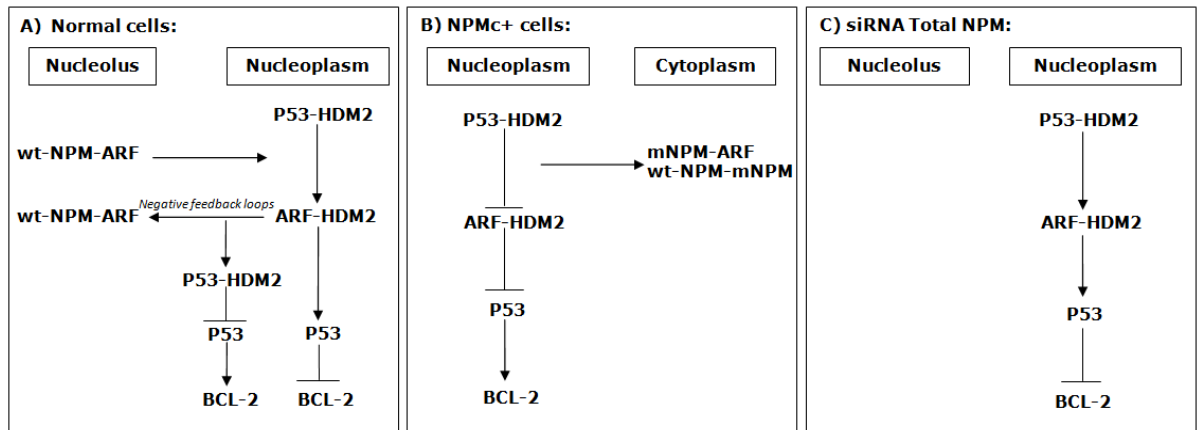


**Figure 5.9: Models of BCL-2 regulation in NPMc+AML cells; (A)** ARF localises with NPM1 in nucleolus, but in a stress response, it translocates into nucleoplasm where it binds to HDM2 and which allows stabilisation of P53, whereas over-activation of P53 leads to activate the negative feedback loop by promoting NPM1 to relocate ARF in the nucleolus. **(B)** In NPMc+ cells, ARF is delocalised in the cytoplasm with NPM1 leading to inhibition of P53 and an increase in BCL-2 levels. **(C)** down-regulation of total NPM1 leads to translocation of ARF in the nucleoplasm and continuously activates P53 resulting in BCL-2 inhibition.

Apoptosis is regulated by two different pathways, which are the intrinsic and extrinsic pathways. The intrinsic pathway is mediated by BCL-2 family proteins which are composed of pro- and anti-apoptotic proteins (Andreeff, *et al* 1998). The BCL-2 anti-apoptotic proteins interact with the pro-apoptotic proteins (BAX, BAK) and inactivate their function. In response to death stimulation, BH3-only proteins bind to BCL-2, BCL-xL, and MCL-1 and activate BAX and BAK (Shore and Viallet 2005). In addition, it has been noted that the up-regulation of BCL-2 and MCL-1 prevents translocation and activation of BAX and BAK, respectively (Letai 2008). This suggests that in NPMc+ cells delocalisation of NPM1 in the cytoplasm could lead to anti-apoptotic proteins binding to BH3-only domain pro-apoptotic proteins and prevention of the activation of BAX and BAK. In contrast, the extrinsic pathway is initiated by recruitment of pro-caspase-8 and other specific adaptor proteins into a death-inducing signalling complex. It has been demonstrated that NPM1 acts as a caspase inhibitor through direct interaction with caspase-6 and caspase-8 (Leong, *et al*

2010). In OCI-AML3, the impairment of caspase-6 and -8 signals would be by the aberrant localisation of NPM1 in the cytoplasm which further leads to suppression of cell death signalling (Leong, *et al* 2010).

In summary, the expression of the anti-apoptotic proteins BCL-2 and MCL-1 were up-regulated in the OCI-AML3 cell line compared to M-07e cell line. It seems that NPMc+ plays a crucial role in the regulation of these proteins by modulating other proteins through their interactions. However, further studies are required to understand the function of cytoplasmic NPM which will be discussed later in chapter 7.

# **6. The Impact of ATRA on BCL-2 and MCL-1 Levels in NPMc+AML Cells**

## 6.1 Introduction:

All-trans-retinoic acid (ATRA) is used in the treatment of acute promyelocytic leukaemia (APL) which is characterised by a chromosomal translocation resulting in rearrangement of retinoic acid (RA) receptor, most commonly with PML t(15;17) (Redner, *et al* 1996). As a result, the myeloid differentiation process is arrested at the promyelocytic stage due to disruption of the RA signalling pathway (Zhang, *et al* 2000). However, addition of ATRA to APL cells restores the wild-type RA receptor pathway and enhances the transcriptional expression of downstream genes (see section 1.5) (Zhang, *et al* 2000).

Many clinical trials have studied the addition of ATRA in combination with chemotherapy in non-APL AML but the results were variable (Burnett, *et al* 2010, Schlenk, *et al* 2011, Schlenk, *et al* 2009). However, the OCI-AML3 cell line, which harbours the NPMc+ mutation, exerts growth inhibition upon ATRA treatment suggesting that mutant NPM1 may confer sensitivity to ATRA (Martelli, *et al* 2007). The response of the NPMc+ cell line to ATRA was more sensitive than the wild-type NPM1 cell lines (Kutny, *et al* 2010). At low doses of ATRA, the percentage of cell viability in OCI-AML3 cells was approximately 50% and there were signs of differentiation, in contrast, in the HL-60 cell line, which harbours wild-type NPM1 (and also, conversely to OCI-AML3 bears a P53 mutation), approximately 90% of cells were viable following treatment with ATRA and there was no evidence of differentiation (Kutny, *et al* 2010).

FLT3-ITD mutations are one the most common genetic alterations in AML and are caused either by an internal tandem duplication in the juxtamembrane domain or, by a point mutation in the activation loop of the tyrosine kinase domain (Kusec, *et al* 2006, Ponziani, *et al* 2006, Reindl, *et al* 2006). It accounts for 25% of AML cases and patients with FLT3-ITD mutations have a significantly higher relapse rate and a poorer overall survival rate than AML patients lacking FLT3-ITD (Grimwade, *et al* 2010, Kottaridis, *et al* 2001). It has been demonstrated that FLT3-ITD express high levels of MCL-1, which is the most essential anti-apoptotic molecule for haematopoietic stem cell survival, and induces the survival of leukaemic cells (Glaser, *et al* 2012, Yoshimoto, *et al* 2009). FLT3 inhibitors have been introduced in preclinical studies through targeting the aberrant signal transduction that contributes to tumour cell development. AC220 is one of the FLT3 inhibitors for the treatment of FLT3-ITD AML. AC220 has shown to inhibit FLT3 activity and induce terminal differentiation of FLT3-ITD AML cells (Sexauer, *et al* 2012, Zarrinkar, *et al* 2009).

The aim of this chapter was to examine the effect of ATRA on the OCI-AML3 cell line, which harbours mutant NPM1, and other cell lines which are wild-type for NPM1. Further studies focused on extending the work in Chapter 5 and studying the anti-apoptotic proteins following ATRA treatment.

## **6.2 Results:**

### **6.2.1 Response of NPMc+AML and wild-type NPM1 cell lines to ATRA:**

The down-regulation of BCL-2 expression by ATRA has previously been associated with CD34 negative cells (Bradbury, *et al* 1996). More recently, it has been revealed that NPMc+AML cells are characterised by low expression of CD34 (Falini, *et al* 2005), however there is no evidence linking these two studies – that is ATRA down-regulates BCL-2 preferentially in NPMc+ cells. Hence, the sensitivity of NPMc+ and wild-type NPM1 cell lines to ATRA were evaluated by treating cells to different concentrations of ATRA for 72 hours. Loss of 50% viable cells in the NPMc+ cell line was achieved at 10nM of ATRA, while in the MV4-11 cell line, which harbours wild-type NPM1 and FLT3-ITD, the concentration required to achieve a 50% loss in viability was much higher at 500nM (see Figure 6.1). In the MOLM-13 and M-07e cell lines, which are wild-type NPM1, 50% loss of viability was not achieved with the percentage of viable cells at the highest concentration, 1 $\mu$ M, being approximately 70%.

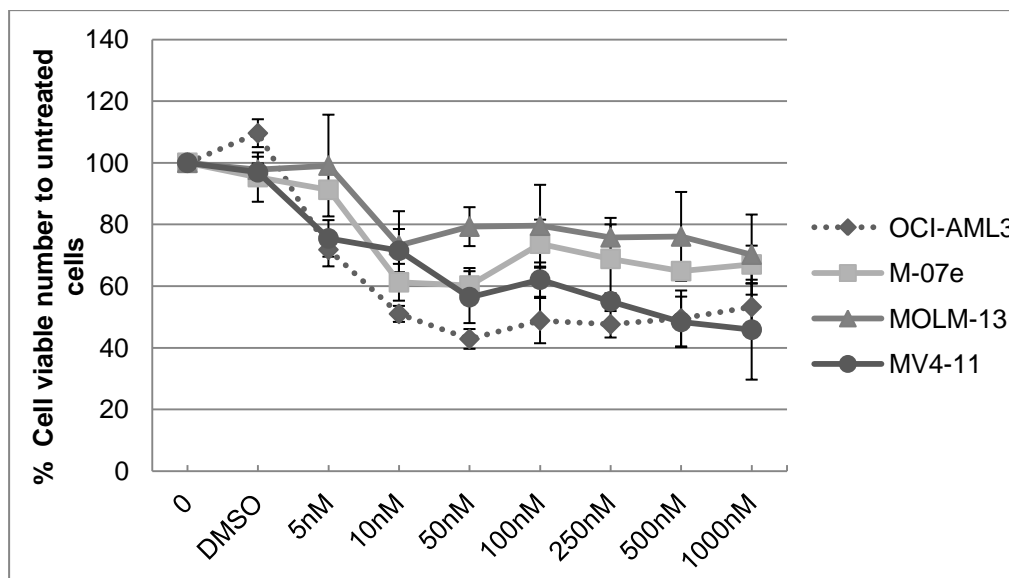


**Figure 6.1: The growth inhibition of AML cell lines upon ATRA treatment;** The different cell lines were treated with ATRA at different concentration. After 72 hours, the cell viability was assessed by using haemocytometer and the percentage of cell viable number was calculated from the untreated cells. The experiment was repeated 3 times and the error bars represent SD.

### 6.2.2 ATRA induces differentiation and apoptosis in NPMc+AML cell line:

A decrease in viable cell number could be due to growth inhibition, to apoptosis or to both. The effect of ATRA on the induction of differentiation and apoptosis in NPM1 mutant and wild-type NPM1 cells was examined by treating the cells with ATRA at 500nM and incubating for 72 hours. The cells were then stained with wright-giemsa and examined for signs of myeloid differentiation. Markers of differentiation included a decrease in nuclear/cytoplasmic ratio, nuclear segmentation, and cytoplasmic granules. As shown in figure 6.2A, the NPMc+ cells showed a more lobed nucleus and the ratio of nuclear/cytoplasmic ratio could be seen to have decreased after the addition of ATRA. In contrast, in M-07e cells, there were no signs of differentiation observed (Figure 6.2B). In order to confirm these results CD11b, which is a marker of myeloid

cell differentiation, was evaluated by flow cytometry and the percentage of CD11b expression was reported compared to untreated cells. The percentage of CD11b-positive cells increased in OCI-AML3 to nearly 17% (p-value: 0.025) following ATRA compared to MOLM-13 which increased only to 7% (p-value: 0.014) (Figure 6.2C). In contrast, the CD11b in M-07e did not change (p-value: 0.1), and a reduction in MV4-11 in the CD11b-positive cells was measured following ATRA treatment (p-value: 0.026) (Figure 6.2C).

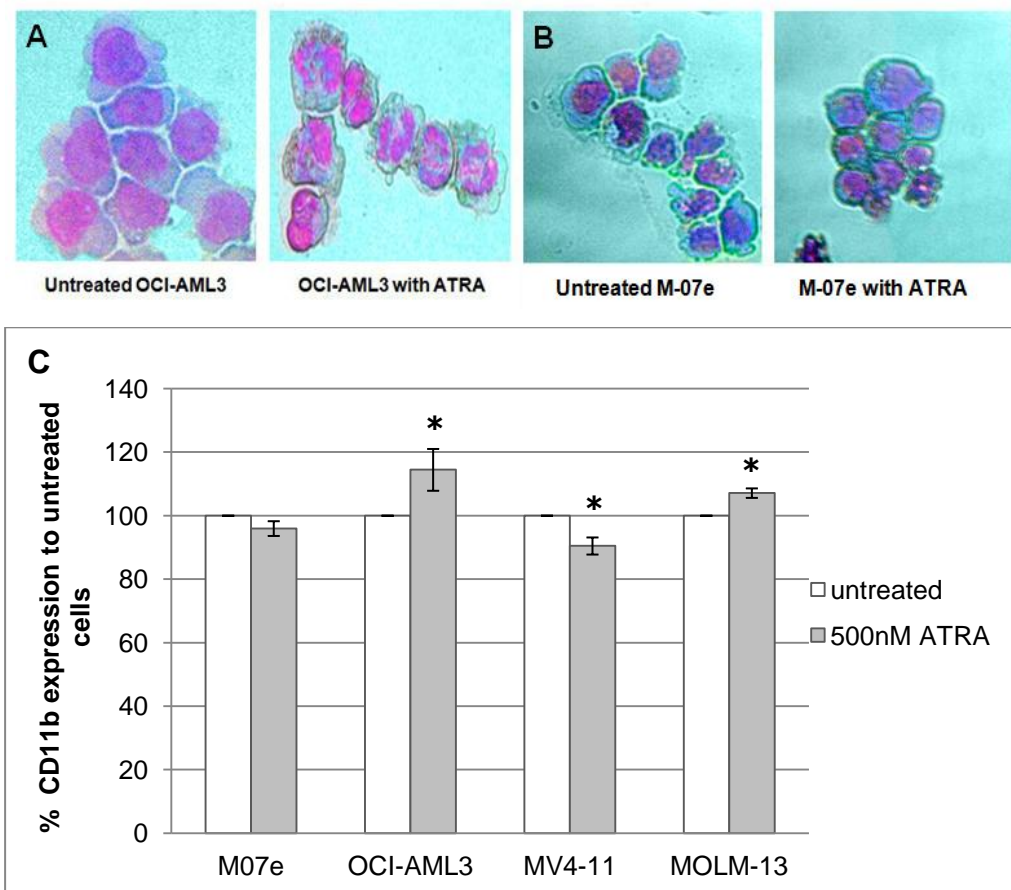


**Figure 6.2: The effect of ATRA on differentiation in AML cell lines;** Cell morphology and the CD11b differentiation marker were examined in **(A)** OCI-AML3 and **(B)** M-07e. The cell lines were treated with 500nM ATRA and incubated for 72 hours. **(A)** Wright-Giemsa stain was used and observed by light microscope in OCI-AML3 and M-07e cell lines. **(C)** CD11b, a differentiation marker, was used to confirm the morphology finding in the OCI-AML3 and M-07e cell lines. In addition, MV4-11 and MOLM-13 cell lines were also examined for CD11b expression. Analysis was by flow cytometry and the percentage of expression was calculated by comparing to the untreated cells. The experiments were performed 3 times and the bars represent the SD. (\* represent p-value<0.05 when compared with the untreated conditions)

Apoptosis was also determined by annexin-V staining followed by flow cytometry. The annexin-V experiment is more sensitive than the cell counting protocol because the annexin-V identifies changes in the cell membrane during the apoptosis process, whereas trypan blue can be excluded from cells in early apoptosis stages. Treatment with ATRA was shown to induce apoptosis to a significantly greater extent in the NPM1 mutant cell line by around 5 fold versus the untreated cells (p-value:0.004) (Figure 6.3B). In addition, the MV4-11 and MOLM-13 cell lines showed a 3 and 1.5 fold increase in the apoptotic cells, respectively (MV4-11 p-value:0.005, MOLM-13 p-value: 0.036) (Figure 6.3B). However, the other NPM1 wild-type cell lines showed a trend for significant increase in the apoptotic cells upon ATRA treatment (M-07e p-value: 0.063) (Figure 6.3B). The results suggest that following treatment of the NPMc+AML cell line with ATRA the cells are more likely to undergo differentiation and apoptosis than the other leukaemic wild-type NPM1 cell lines.

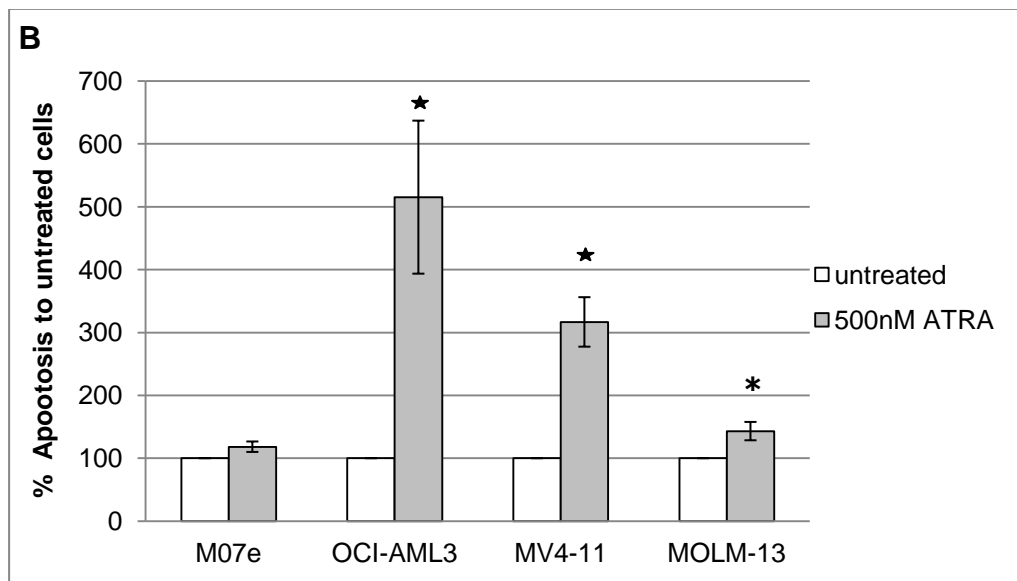
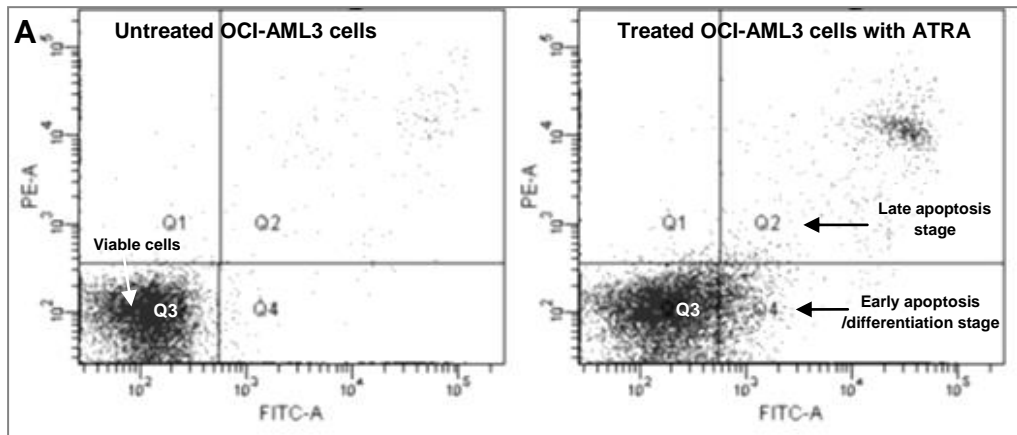


**Figure 6.3: The effect of ATRA on apoptosis in AML cell lines;** The apoptosis level was determined by staining M-07e, OCI-AML3, MV4-11 and MOLM-13 cell lines with annexin-V FITC with and without the cell lines had been treated with 500nM ATRA for 72 hours. **(A)** FACS plots showed the cell population in untreated cells is located in the lower left quadrant of dot plot (Q3) indicating that the cells are negative for the early or late apoptosis process; cells in the lower right quadrant (Q4) and upper right quadrant of dot plots (Q2) depict cells in early and late apoptosis stages, respectively. **(B)** The apoptosis level is shown as percentage of the treated cells to untreated. The experiments were performed 3 times and the error bars represent the SD. (\* indicates p-value <0.05, while ★ represents p-value<0.005 when compared with the untreated conditions)

### **6.2.3 The effect of ATRA on BCL-2 mRNA and protein levels:**

According to these results, which showed a much greater induction of differentiation and apoptosis in the mutant NPM1 cell line compared to the wild-type NPM1 cell lines, and also the work by Bradbury *et al.* which demonstrates the down-regulation of BCL-2 protein levels in CD34 negative AML cells treated with ATRA (Bradbury, *et al* 1996), the transcript and protein levels of BCL-2 after the dose of ATRA were assessed. Interestingly, the BCL-2 mRNA expression was reduced to 1% of its basal level following ATRA treatment of OCI-AML3 cells (p-value: <0.00005). In addition, the MV4-11 and MOLM-13 cell lines, which harbour homozygous or heterozygous FLT3-ITD, respectively, showed an 80% reduction in BCL-2 transcripts (p-value for MV4-11 and MOLM-13 cells: 0.001) (Figure 6.4A). However, M-07e showed a non-significant reduction in the level of BCL-2 mRNA (p-value: 0.114) (Figure 6.4A). The protein level of BCL-2 in OCI-AML3, MV4-11 and MOLM-13 cell lines were also decreased to around 35% compared to the basal level (p-value: <0.005 in OCI-AML3, MV4-11, and MOLM-13 cell lines), while the M-07e cell line was not significantly altered (p-value: 0.151) (Figure 6.4B).

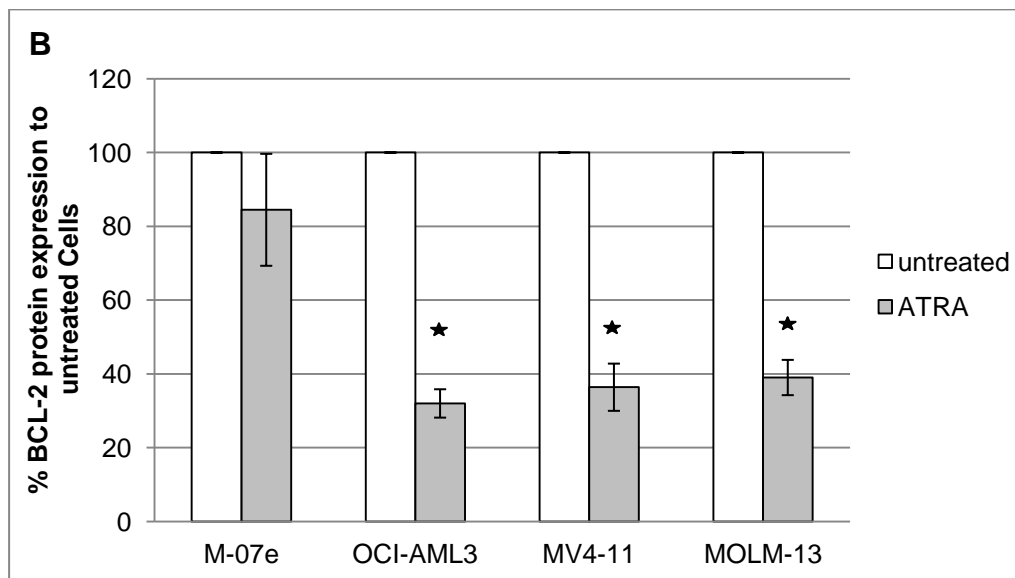
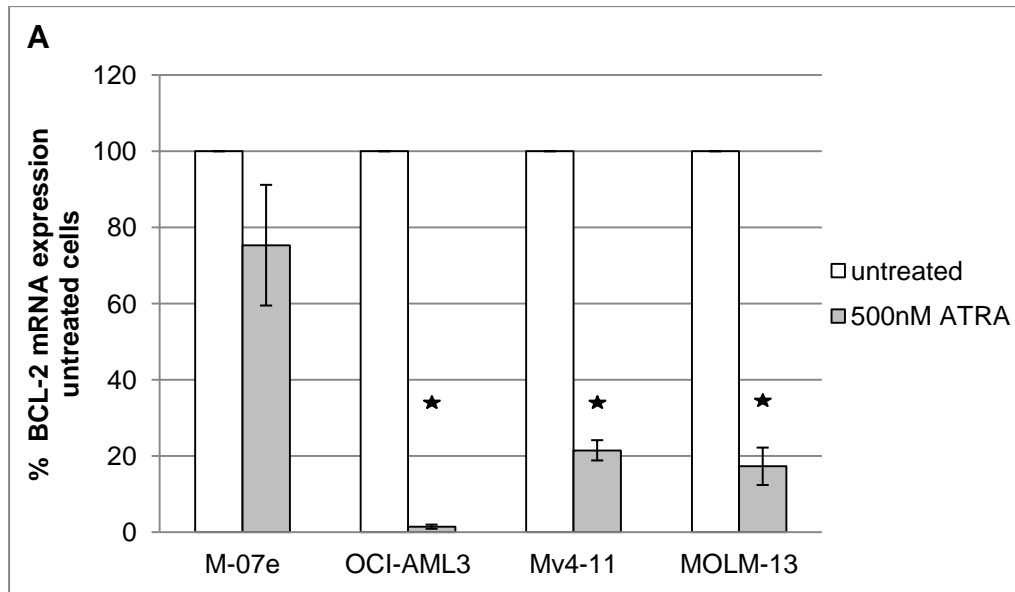


**Figure 6.4: Anti-apoptotic BCL-2 levels upon ATRA treatment; (A)** the BCL-2 mRNA levels were measured by real-time PCR after the cell lines were treated with 500nM ATRA for 72 hours. BCL-2 transcript levels were normalised to  $\beta$ 2M housekeeping gene and then the percentage of the expression was calculated by comparing to the control cells. **(B)** The BCL-2 protein level was analysed by flow cytometry. The MFI was calculated as described previously in the material and methods chapter. The chart represents the percentage of the protein levels to untreated cells. The mean of 3 experiments was calculated and the bars represent the SD. (★ represents  $p$ -value < 0.005 when compared with the relevant untreated conditions)

#### **6.2.4 The effect of ATRA on MCL-1 mRNA and protein:**

Myeloid cell leukaemia-1 (MCL-1), which is highly expressed in OCI-AML3 cells - as shown in Figure 5.5, is one of the BCL-2 anti-apoptotic family molecules. It has previously been reported that the transcripts and protein level of MCL-1 were up-regulated in FLT3-ITD AML cells (Yoshimoto, *et al* 2009). Therefore, the level of MCL-1 following ATRA treatment was evaluated in the selected cell lines. The result showed that MCL-1 mRNA levels were reduced in all cell lines following incubation with ATRA, but the MCL-1 mRNA expression in ATRA-treated OCI-AML3 decreased to 40% of the untreated cells ( $p < 0.005$ ), in comparison the three wild-type NPM cell lines reached a level of approximately 75% of untreated cells ( $p$ -value: 0.023, 0.043 and 0.018 in M-07e, MV4-11 and MOLM-13 cell lines, respectively) (Figure 6.5A). In contrast, 20% of the protein level was depressed in OCI-AML3 ( $p$ -value: 0.073), whereas MV4-11 cells showed 40% reduction in MCL-1 protein level ( $p$ -value: 0.039) (Figure 6.5B). on the other hand, M-07e showed no decrease in levels of MCL-1, while MOLM-13 had a trend of increase (Figure 6.5B).

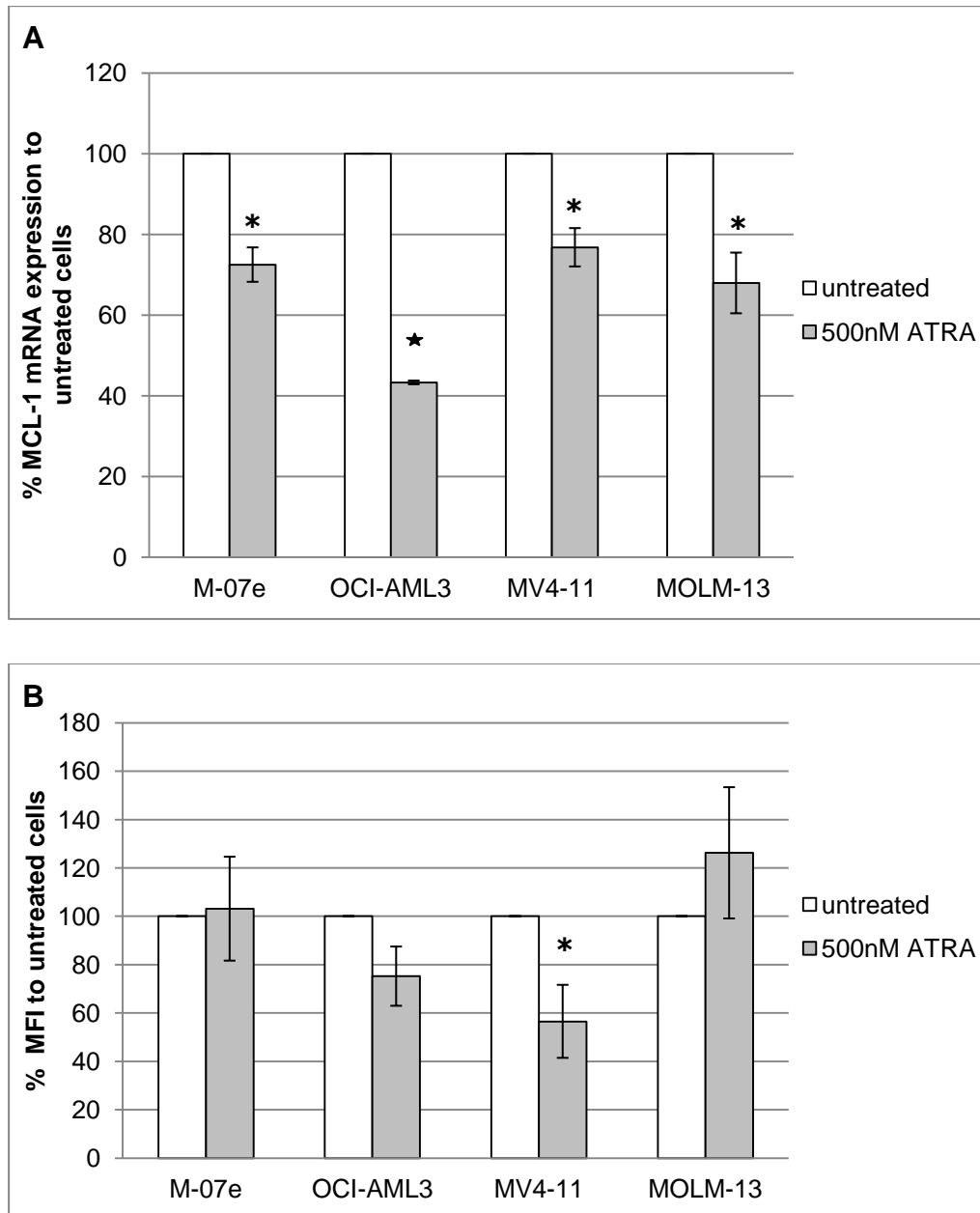


**Figure 6.5: The effect of ATRA on MCL-1 mRNA and protein expression; (A)** MCL-1 mRNA level was measured by qPCR after the cell lines were treated with 500nM ATRA. The  $\beta$ 2M housekeeping gene was used to normalise the gene expression and then the percentage of expression was calculated using the untreated cell value **(B)** MCL-1 protein level was analysed by flow cytometry. The MFI was calculated as described previously in the material and methods chapter. The chart represents the percentage of the protein levels compared to untreated cells. The mean of 3 experiments was calculated and the bars represent the SD. (\* indicates p-value < 0.05, while ★ represent p-value < 0.005 when compared with the untreated conditions)

### **6.2.5 The effect of ATRA in combination with the FLT3 inhibitor AC220:**

Due to the effects of ATRA on BCL-2 and MCL-1 levels and also taking into account previous work that has shown FLT3-ITD mutations to drive MCL-1 (Yoshimoto, *et al* 2009), we chose look at the effect of a FLT3 inhibitor on the cell lines. The FLT3-ITD inhibitor chosen for the study was AC220 which is a second-generation FLT3 inhibitor with high potency and selectivity (Zarrinkar, *et al* 2009). Therefore, the viability of the different cell lines was assessed after exposure to different concentrations of AC220. In the FLT3-ITD cell lines, the IC<sub>50</sub> was 1nM and 5nM in MV4-11 and MOLM-13 cells, respectively (Figure 6.6A), whereas in wild-type FLT3 cell lines 25% cell death was achieved at a much higher concentration 1000nM (Figure 6.6B), but the IC<sub>50</sub> was not achieved. Therefore, the MOLM-13 IC<sub>25</sub> was used in the following experiments in the wild-type FLT3 cell lines.

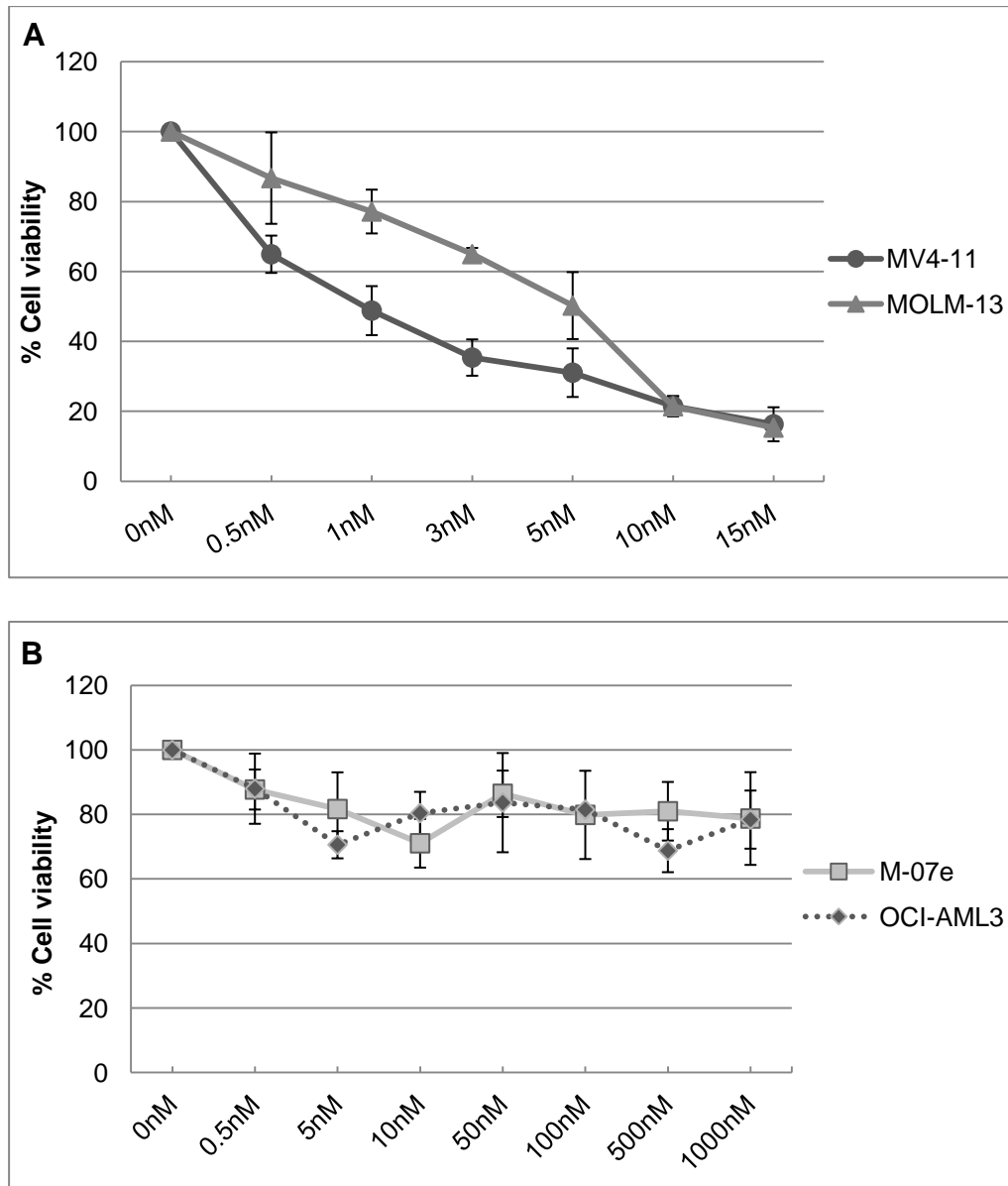


**Figure 6.6: The viability of AML cell lines upon AC220 treatment;** The four different cell lines were treated with AC220 at different concentration and incubated for 72 hours. **(A)** The concentration of AC220 in MV4-11 and MOLM-13 ranged from 0.5nM and 15nM, **(B)** While for OCI-AML3 and M-07e cell lines were between 0.5nM to 1000nM. The cell viability was assessed by cell counting using a haemocytometer, and the percentage viability was calculated by calculating the viability of the treated cells and comparing to the untreated cells. The experiments were repeated 3 times and the bars represent the SD.

### **6.2.6 The effect of ATRA and AC220 on differentiation marker and apoptosis:**

FLT3 inhibitors block the abnormal signal transduction pathways that contribute to malignancy in cells harbouring the FLT3-ITD mutation. AC220 has been shown to prevent the constitutive FLT3 phosphorylation present in FLT3-ITD cells; this results in an inhibition of cell proliferation in the MV4-11 cell line and induced differentiation and apoptosis in the MOLM-13 cell lines (Sexauer, *et al* 2012, Zarrinkar, *et al* 2009). Hence, M-07e, OCI-AML3, and MOLM-13 cell lines were treated with AC220 at 2nM and/or with ATRA at 500nM, while due to the sensitivity of the MV4-11 cell line to AC220, these cells were treated with 0.5nM AC220 and 500nM ATRA. Following treatment, differentiation and apoptosis were evaluated. As shown in figure 6.7, there was no significant difference between untreated and AC220 treated cell lines with respect to either the level of CD11b expression or induction of apoptosis. When AC220 was added to ATRA-treated cells, there was no significant difference in when compared to ATRA-treatment alone. These results suggest that only ATRA has activity against the studied cell lines and the addition of AC220 has no effect either alone or when used in combination with ATRA.

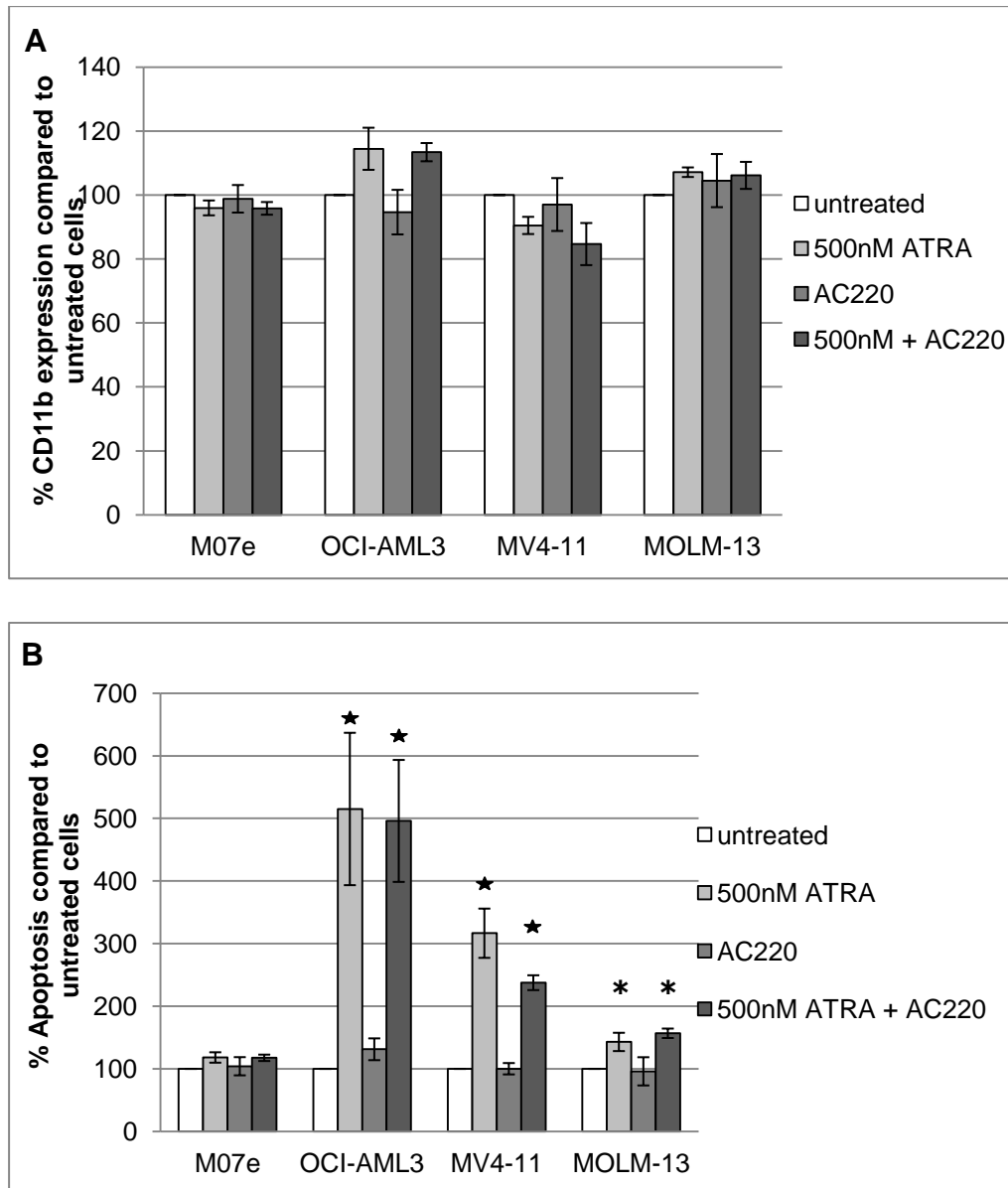
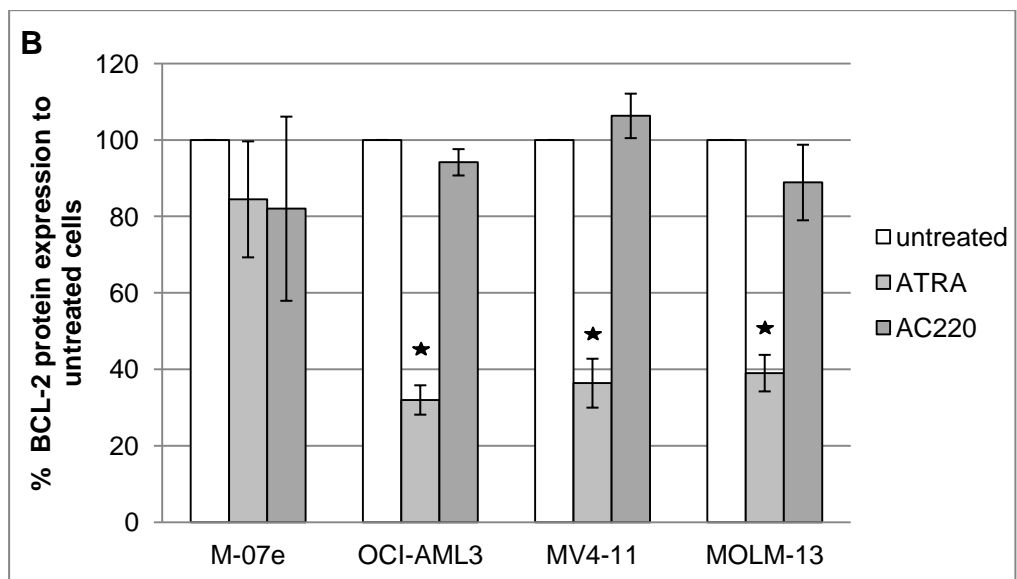
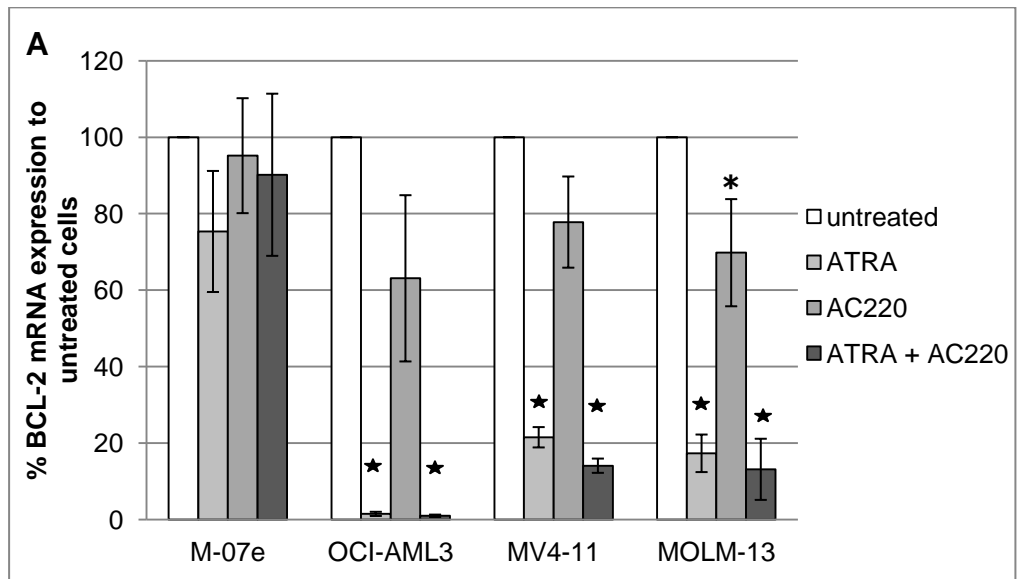


**Figure 6.7: The effect of AC220, alone or in combination with ATRA, on differentiation and apoptosis in AML cell lines;** The differentiation marker CD11b and apoptosis were examined in the cell lines which were treated with AC220 at 2nM for M-07e, OCI-AML3, and MOLM-13 cell lines, whereas MV4-11 cell line was at 0.5nM. In addition, the cells were treated with 500nM ATRA combined with the aforementioned concentration of AC220. **(A)** CD11b was used to evaluate differentiation of the cells. It was analysed by flow cytometry and the percentage of expression was compared to untreated cells. **(B)** The apoptosis level was determined by staining the cells with annexin-V FITC and represented as a percentage change by comparing treated and untreated cells. The experiments were performed 3 times and the bars represent the SD. (\* indicates p-value <0.05, while ★ indicates p-value <0.005 when compared with the untreated condition)

### **6.2.7 The effect of ATRA and AC220 on BCL-2 and MCL-1 mRNA and protein levels:**

Subsequently, the cells were examined for BCL-2 and MCL-1 levels after treatment with AC220 alone or in combination with ATRA. The BCL-2 mRNA level in the NPMc+/FLT3-wt cell line and in the NPM1-wt/FLT3-ITD cell lines were decreased, although the decrease is not statistically significant upon AC220 treatment in OCI-AML3 (p-value: 0.092) and MV4-11 (p-value: 0.081), while in MOLM-13 is statistically significant (p-value: 0.034). In contrast, the NPM1-wt/FLT3-wt cell line showed no change in BCL-2 mRNA levels after AC220 treatment (p-value: 0.633) (Figure 6.8A). When AC220 was combined with ATRA, however, the BCL-2 mRNA expression was reduced to the same level seen as when treated with ATRA alone in the OCI-AML3, MV4-11 and MOLM-13 cell lines (see section 6.2.3) (p-value in OCI-AML3, MV4-11, and MOLM-13 cell lines: <0.005), whilst there was no effect of combining AC220 and ATRA on the level of BCL-2 mRNA in M-07e cell line (p-value: 0.506) (Figure 6.8A). The MCL-1 mRNA level was reduced in MV4-11 and MOLM-13 upon AC220 treatment by around 25% and 50%, respectively (p-value: 0.048, and 0.021), whereas in OCI-AML3 and M-07e cell lines no significant decrease was shown in MCL-1 mRNA levels with AC220 alone (p-values: (OCI-AML3) 0.114, and (M-07e) 0.166) (Figure 6.8C). Combining AC220 and ATRA showed no additional significant reductions in MCL-1 levels when compared to ATRA alone (OCI-AML3) (p-value: 0.001), or AC220 alone (MV4-11 (p-value: 0.058), and MOLM-13 (p-value: 0.01)) (p-value: 0.001, 0.058, 0.01, and 0.078) and the p-values are the reduction in MCL-1 mRNA levels following ATRA and AC220 treatment compared to the untreated cells

(Figure 6.8B). When looking at the level of BCL-2 and MCL-1 protein in the AML cell lines treated with AC220 alone there was no significant difference to the level seen in untreated cells (p-values of BCL-2 protein levels: OCI-AML3 (0.099), MV4-11 (0.201), MOML-13 (0.158), and M-07e (0.157), while the p-values of MCL-1 protein levels: OCI-AML3 (0.835), MV4-11 (0.678), MOML-13 (0.489), and M-07e (0.567)) (Figure 6.8B,D).



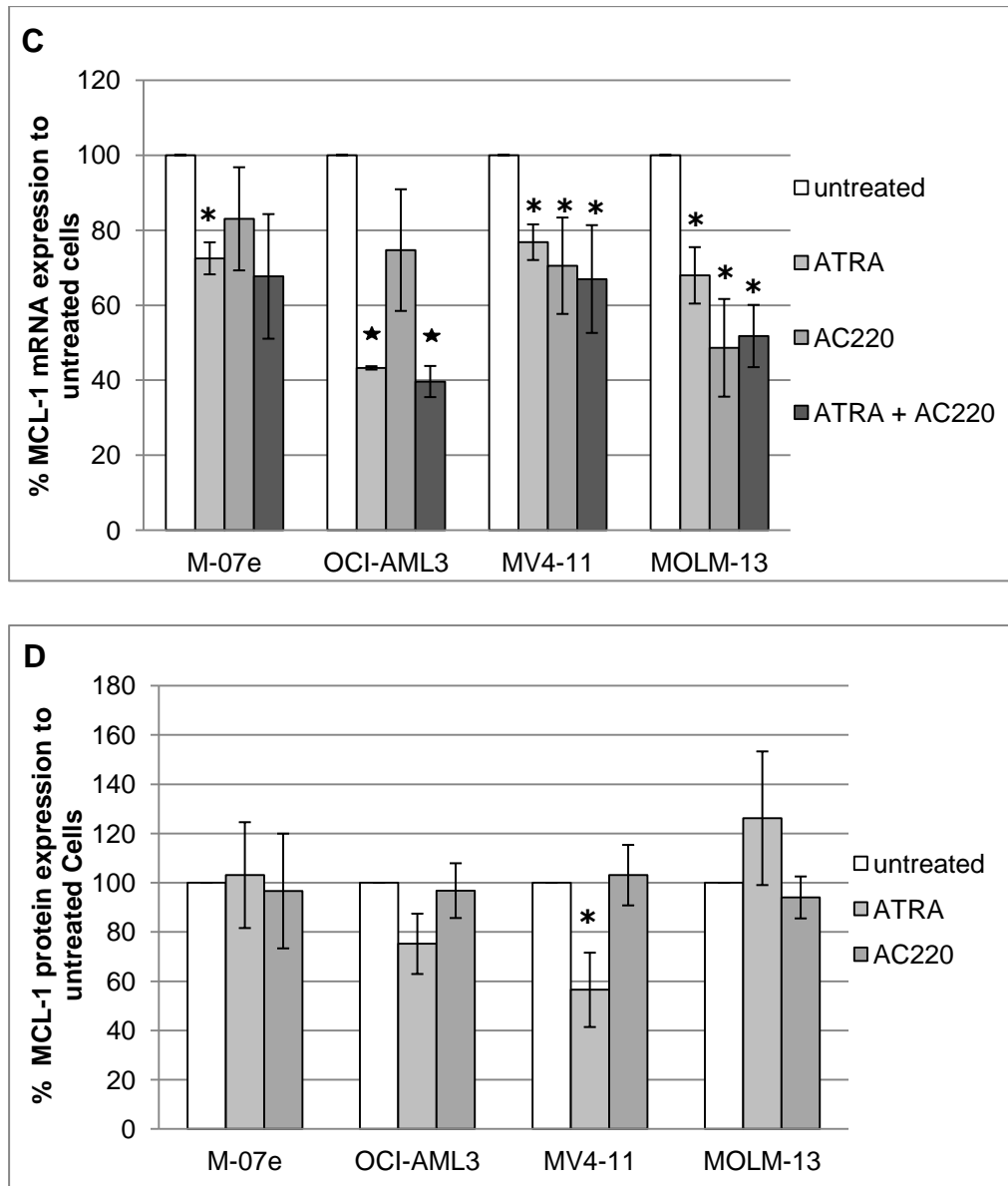


**Figure 6.8: The effect of AC220 alone or combined with ATRA on BCL-2 and MCL-1 mRNA and protein levels in the AML cell lines; (A) BCL-2 mRNA and (B) BCL-2 protein levels were measured by real-time PCR and by flow cytometry, respectively, after the cell lines were treated with 500nM ATRA, 2nM AC220 for M-07e, OCI-AML3 and MOLM-13, 0.5nM AC220 for MV4-11, or 500nM ATRA and 2nM or 0.5nM AC220. (C) MCL-1 mRNA and (D) MCL-1 protein levels were analysed by real-time PCR and by flow cytometry, respectively. The  $\beta$ 2M housekeeping gene was used to normalise the gene expression and then the percentage of the expression was divided and the control cells were calculated. The MFI was calculated as described previously in the material and methods chapter. The charts represent the percentage of the proteins level to untreated cells. The mean of 3 experiments was calculated and the bars represent the SD. (\* indicates p-value <0.05, while ★ represent p-value <0.005 when compared with the untreated conditions)**

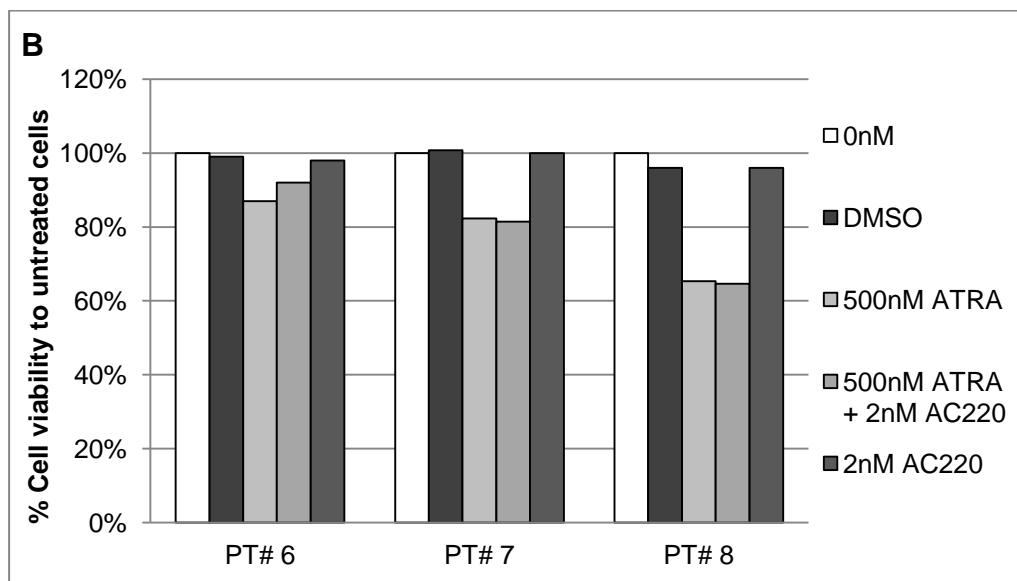
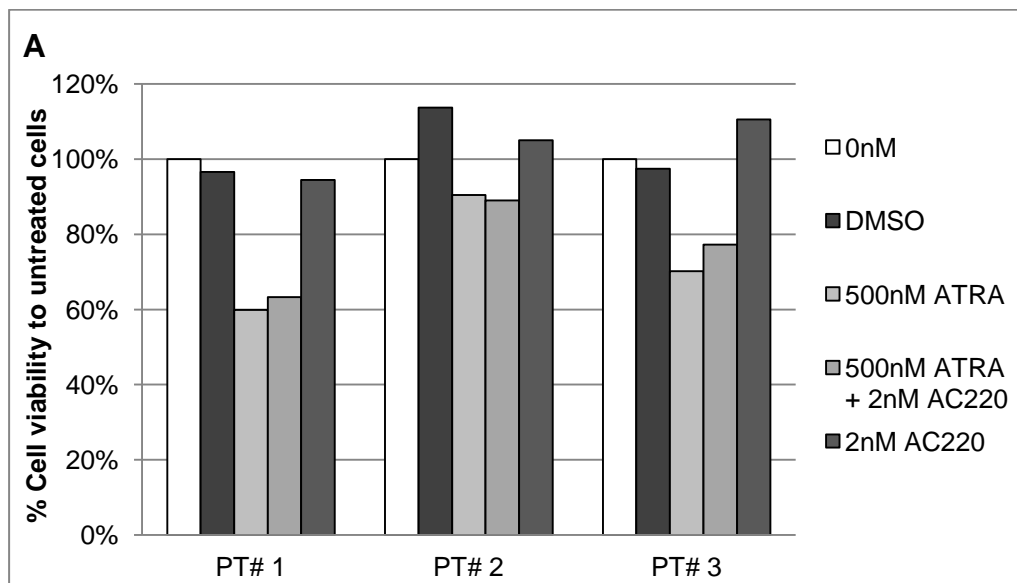
### **6.2.8 Response of primary AML cells to ATRA and/or AC220:**

It is known that around 40% of AML patients with the NPMc+ mutation co-express a FLT3-ITD mutation, this results in a poorer clinical prognosis than for those patients harbouring NPM mutant only (Falini, *et al* 2005). The anti-apoptotic protein MCL-1 has been shown to be up-regulated in FLT3-ITD cell lines (Yoshimoto, *et al* 2009), thus, targeting BCL-2 and MCL-1 anti-apoptotic proteins by ATRA, and AC220, respectively, lead to down-regulate these two major apoptotic proteins which would prime the NPMc+/FLT3-ITD cells for apoptosis. Therefore, we examine the effect of adding a FLT3 inhibitor to ATRA in AML patients that have the NPM1 and FLT3-ITD mutations and the work on the samples was done blind without knowing the mutation status of the samples until the experiments have completed.

Cells from a total of 8 patients were analysed for the effect of ATRA and AC220 on cell viability and BCL-2 and MCL-1 mRNA expression (there was not enough material to also look at the protein level). 10 further patient samples were thawed but these had to be excluded from the analyses because the post-rest viability was less than 80% or the cell viability was affected by DMSO, this was primarily due to the length of time the samples had been stored in liquid nitrogen (>10 years).

The cell viability in samples with wild-type NPM1 and wild-type FLT3 showed a reduction after being treated with 500nM ATRA of approximately 40%, 15% and 30%, in patient samples number 1, 2, and 3 respectively (Figure 6.9A). NPMc+ cells showed only a 15%-20% reduction in cell viability in 4 out of 5 samples and the fifth sample demonstrated a 40% reduction

(Figure 6.9B,C). In addition, the combination treatment of patient cells with ATRA and AC220 showed a decrease in the cell viability to a similar level as detected after treatment with ATRA only (Figure 6.9B,C). In the absence of a co-expressed FLT3-ITD mutation, neither wild-type or mutant NPM1 patient cells were sensitive to the FLT3 inhibitor (AC220) alone. However, FLT3-ITD/NPMc+ cells demonstrated a decrease in the cell viability of around 20% in one sample out of two (Figure 6.9C).



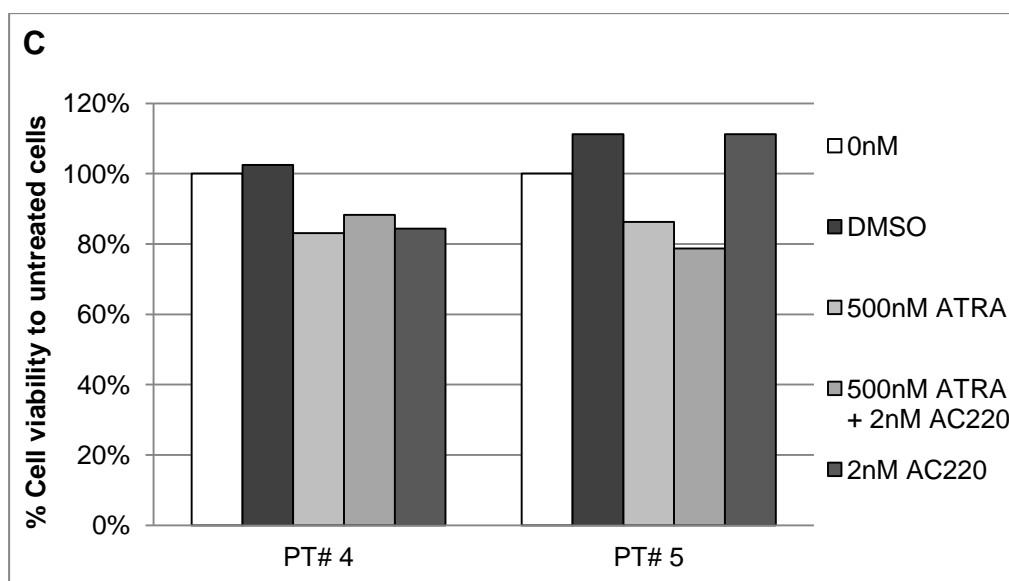


**Figure 6.9: The viability of primary cells upon ATRA, AC220, or ATRA/AC220 treatment;** Primary cells were treated with 500nM ATRA, 2nM AC220 or a combination of the two drugs. The cell viability was evaluated by flow cytometry as described in the material and methods chapter (2.5.3). **(A)** Represents the NPM1-wt/FLT3-wt samples, **(B)** NPMc+/FLT3-wt, and **(C)** NPMc+/FLT3-ITD samples.

Because only one patient sample showed a reduction in cell viability upon AC220, FLT3-ITD patient samples were further examined and treated with different concentrations of AC220 and, in addition, a second FLT3 inhibitor CEP-701 to evaluate the protocol and the activity of the inhibitors. The FLT3-ITD cell lines were run in parallel to test that the drug activity had not deteriorated during storage. The concentration of CEP-701 was chosen dependent on previous work which used a broad range (10–100nM) of CEP-701 concentrations on primary cells (Levis, *et al* 2002). The cells, which were treated with CEP-701, showed an 80% cell death at 100nM, whereas with AC220, cell viability was reduced by approximately 20% at 1000nM, a concentration 50x greater than that required to kill more than 80% of cells within the MV4-11 and MOLM-13 cell lines (Figure 6.10). These results show that the AC220 drug is active in the cell lines, but not effective on the patient sample

at the level of cell viability. However, the real-time patient results showed differences in the levels of BCL-2 and MCL-1, which indicate that AC220 was active in the patient cells. In addition, AC220 was used because of the evidence that it may also induce differentiation of FLT3-ITD cells (Sexauer, *et al* 2012).

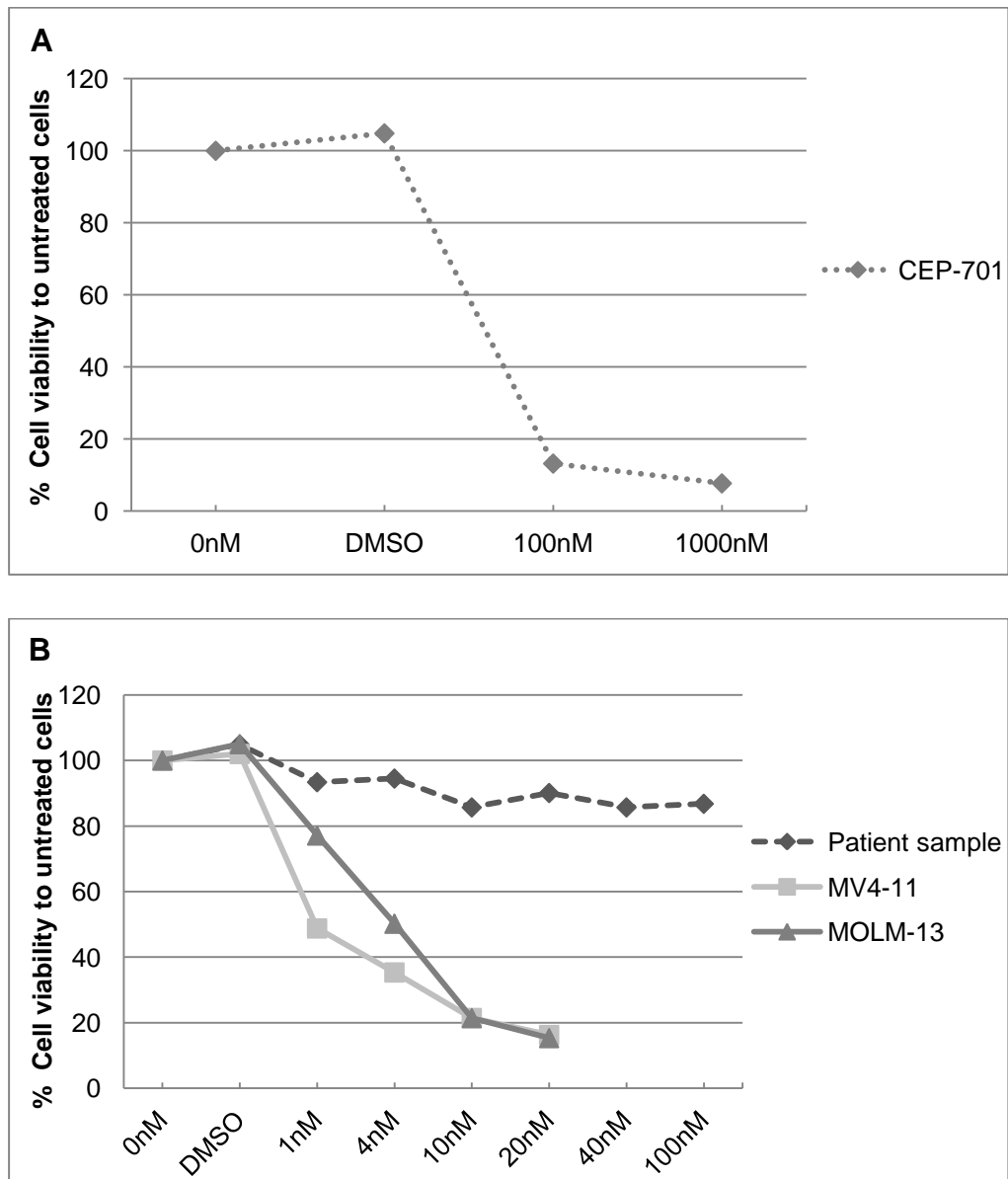


**Figure 6.10: Primary cell lines in response to FLT3 inhibitors at different concentrations;** Primary cells harbouring a FLT3/ITD were treated with two different FLT3 inhibitors, while the FLT3-ITD cell lines were only treated with AC220. The cells were treated with **(A)** CEP-701 at low (100nM) and high (1000nM) for 72 hours, or **(B)** with AC220 at different concentration (1nM – 100nM). The viability was determined by flow cytometry.

With regards to the anti-apoptotic mRNA expression levels, 3 out of 5 NPMc+AML cells (60%) showed a decrease more than 25% in BCL-2 mRNA upon ATRA treatment and one of these samples also had a FLT3-ITD mutation. BCL-2 mRNA level was reduced in 1 out of 3 NPM1-wt/FLT3-wt samples (33%). In contrast, the MCL-1 mRNA expression decreased in 2 out of 3 samples that are NPM1-wt/FLT3-wt, whereas if an NPMc+ mutation was present a decrease in MCL-1 was seen in each sample (5/5) (Table 5.1).

The BCL-2 and MCL-1 mRNA levels, upon adding AC220 in these patient samples, showed down-regulation of BCL-2 mRNA in 3/5 samples with an NPMc+ mutation and 1 sample with NPM1-wt/FLT3-wt, whereas the MCL-1 mRNA level decreased in 5/5 samples with mutant NPM1 and 2/3 samples with wild-type NPM1 (Table 5.1). This data indicates that ATRA down-regulates BCL-2 and MCL-1 mRNA levels in AML cells, harbouring NPM1 mutations more than in NPM1-wt/FLT3-wt cells. In addition, in combination with AC220, a reduction was observed in NPMc+ cells. However, because of the difficulty in the culture of primary cells and the majority of these cells did not survive, the number of patient samples was not sufficient. Therefore, further work in the department is going on and more samples are being recruited.

**Table 6.1: BCL-2 and MCL-1 mRNA expressions in patient samples after exposed to ATRA and/or AC220 treatment**

Patient	Genotype	Relative BCL-2 mRNA Expression			Relative MCL-1 mRNA Expression		
		500nM ATRA	500nM ATRA + 2nM AC220	2nM AC220	500nM ATRA	500nM ATRA + 2nM AC220	2nM AC220
1	FLT3 + NPM1 WT	234	296	160	85	55	87
2	FLT3 + NPM1 WT	51	61	109	98	107	105
3	FLT3 + NPM1 WT	166	151	80	94	70	71
4	FLT3-ITD + NPMc+	96	81	88	71	32	42
5	FLT3-ITD + NPMc+	45	56	133	87	107	93
6	FLT3 WT + NPMc+	64	54	91	95	85	113
7	FLT3 WT + NPMc+	124	177	111	78	116	89
8	FLT3 WT + NPMc+	74	76	83	63	64	97

### 6.3 Discussion:

The NPMc+AML cells are characterised by low expression of CD34, and down-regulation of BCL-2 by ATRA was shown to be more frequent in CD34 negative cells than CD34 positive (Bradbury, *et al* 1996). In addition, NPMc+AML cell line showed high expression of anti-apoptotic mRNA which could be a result of delocalization of mutant and wild-type NPM1 to the cytoplasm (chapter 5). For that reason, in this chapter the effect of ATRA on the levels of BCL-2 and MCL-1 in the mutant NPM1 cell line were evaluated and compared to levels in wild-type NPM1 cell lines, in addition primary AML samples were also studied.

Previously ATRA was found to down-regulate BCL-2 levels in the HL-60 cell line and AML samples, particularly in the CD34 negative patient cells which showed decline in the protein level upon ATRA treatment (Bradbury, *et al* 1996, Pisani, *et al* 1997). Treatment of the OCI-AML3 cell line with ATRA has previously been shown to result in an increase in cell differentiation and apoptosis (Balusu, *et al* 2009, Kutny, *et al* 2010). In keeping with this, our results confirmed the increase in CD11b positive cells and increase in apoptosis in the OCI-AML3 NPMc+ cell line treated with ATRA compared with the NPM1 wild-type cell lines. This indicates that the OCI-AML3 cell line, which harbours an NPM1 mutation, is more sensitive to ATRA-induced differentiation and apoptosis than the other AML cell lines studied. We next examined the effect of ATRA on BCL-2 levels in NPM1 mutant and wild-type cell lines. It was found that the level of BCL-2 mRNA decreased in the MV4-11 and MOLM-13 cells following ATRA treatment, but the reduction in the OCI-AML3 cells was greater, whereas in M-07e cell line did not shown a change. Thus, down-regulation of

BCL-2 mRNA level in OCI-AML3, which harbours NPMc+, is more likely to be achieved by ATRA. Although the huge reduction in the expression of BCL-2 mRNA was demonstrated, the BCL-2 protein level in OCI-AML3 cells decreased to approximately the same levels as the MV4-11 and MOLM-13 cell lines. The reasons behind this finding have not been elucidated but it seems that the long half-life of BCL-2 protein and other post-translational factors may affect the protein level (Gao and Dou 2000). However, the protein levels are going to be evaluated by western blot to confirm the flow cytometry results. In primary AML cells, 60% of the NPMc+AML cells with wild-type FLT3 showed a reduction in BCL-2 mRNA level in response to ATRA, and 50% of NPMc+/FLT3-ITD cells also responded to the drug. When considering MCL-1 mRNA and protein levels, these were decreased in OCI-AML3 upon ATRA treatment, and in 66% of NPMc+AML patient samples. The exact molecular mechanism through which ATRA has an effect on NPMc+AML cells is not completely clear. However, it was noted that NPMc+AML cells, when treated with ATRA, showed a down-regulation of the NPM1 mutant protein. As a result, the NPM1 wild-type is re-located in the nucleus and this leads the cell to initiate cell cycle arrest and apoptosis (Martelli, *et al* 2007).

Internal tandem duplication in the FLT3 juxtamembrane region cause constitutive kinase activation and signal for hematopoietic growth (Dohner and Dohner 2008). 40% of NPMc+ mutated AML samples also have a FLT3-ITD and the presence of the two mutations converts the good prognosis associated with NPMc+ into an intermediate prognosis (Falini, *et al* 2007b). FLT3-ITD cells show up-regulation of MCL-1 protein and transcript levels (Yoshimoto, *et al* 2009), thus we

evaluated the effect of adding AC220, which is a highly selective inhibitor of FLT3, to down-regulate MCL-1 levels in FLT3-ITD cell lines. Treating the MV4-11 and MOLM-13 cell lines with AC220 only showed a decrease in MCL-1 mRNA level, while the protein level did not change. In addition, the MCL-1 protein level in MOLM-13 cell line did not correspond to the MCL-1 mRNA expression level which was suppressed after treatment with ATRA. This conflict could be a result of other biological factors which cooperate in MCL-1 levels, particularly it is known that MCL-1 protein has a short turnover and there are other pathways that fine-tune MCL-1 expression (Gores and Kaufmann 2012). At the N-terminal domain of MCL-1, there are 2 sequences called PEST (proline, glutamic acid, serine, and threonine) sequences which are targeted by E3 ubiquitin ligases for rapid proteasomal degradation (Gores and Kaufmann 2012) Thus, deubiquitination or inactivation of E3 ligases molecules are expected to increase MCL-1 protein stabilisation (Schwickart, *et al* 2010, Wertz, *et al* 2011).

At the level of cell survival, none of the primary AML samples responded to AC220, even at high concentrations except one sample bearing NPMc+AML/FLT-ITD. Therefore, a FLT3-ITD sample was tested using two different FLT3 inhibitors. We followed the same protocol which was used by the Zarrinkar's group and the AC220 (IC<sub>50</sub>) in their patient samples varied between 0.8nM and 2nM but our patient samples were not killed by these concentrations (Zarrinkar, *et al* 2009). Pauwels *et al.* and Smith *et al.* found that mutations in the kinase domain of FLT3 (F691, Y842, G697R, and N676D) can cause a resistance to AC220 (Pauwels, *et al* 2012, Smith, *et al* 2012). However, these mutations have been identified at relapse which means that resistance to FLT3 inhibitors are developed

after treatment with this inhibitors (Smith, *et al* 2012). Moreover, Pratz *et al.* found that some FLT3-ITD AML samples showed no cytotoxic effect from AC220 because AC220 is a highly selective FLT3 inhibitor, while the same samples were sensitive to CEP-701, which is a multi-targeted kinase inhibitor (Pratz, *et al* 2010). They reported that incubation of FLT3-ITD AML primary cells with IL-3 has decreased the cytotoxicity effect of AC220 to FLT3-ITD primary cells in vitro (Pratz, *et al* 2010). Thus, it is suggested that our FLT3-ITD sample has been affected by IL-3, which should not be incubated with AC220 in FLT3-ITD AML cells in vitro.

The effect of ATRA, in combination with AC220 on the cell lines and patient samples, did not enhance the reduction in BCL-2 and MCL-1 mRNA level significantly, but by adding AC220 alone a trend of decline in the level of BCL-2 and MCL-1 mRNA was seen in OCI-AML3, MV4-11, and MOLM-13 cell lines. At the protein level, the decrease in BCL-2 level in OCI-AML3 and homozygous FLT3-ITD cell lines followed the decrease in mRNA expression after adding ATRA and AC220. As results, the FLT3 inhibitor does not have a negative impact on ATRA in down-regulation of BCL-2 and MCL-1 mRNA in NPMc+AML cell lines.

Clinically, the administration of ATRA to NPMc+AML patients was investigated in combination with intensive chemotherapy. In the German group, ATRA was given after the induction therapy with idarubicin, cytarabine and etoposide on day 3 through to day 28. The complete remission rate in the NPMc+ patients was significantly improved after addition of ATRA. In addition, the relapse-free and overall-survival rates were better in those patients than in patients with other genetic markers (Schlenk, *et al* 2011, Schlenk, *et al* 2009). On the

other hand, the Medical Research Council UK trial data do not agree with the previous study and they found that the addition of ATRA to chemotherapy had no significant effect on the outcome of NPMc+AML patients (Burnett, *et al* 2010). In the MRC protocol, however, ATRA was given from the first day with the induction therapy, which consists of daunorubicin, Ara-C and thioguanine, while it was given on the third day of the therapy in the Schlenk protocol (Burnett, *et al* 2010, Schlenk, *et al* 2009). Moreover, there is evidence, which confirms that when ATRA was given after Ara-C, it showed a significant decline in BCL-2 protein and elevated apoptosis in AML patients (Andreeff, *et al* 1999). In APL cells, administration of ATRA before chemotherapy was shown to induce the trans-membrane drug transporter ABCB1 (MDR1) and lead to up-regulation doxorubicin resistance (Tabe, *et al* 2006). Therefore, it has been suggested that the effect of ATRA can be observed after the leukaemic cells are treated with cytotoxic agents (Schlenk, *et al* 2009).

In summary, the OCI-AML3 cells are more sensitive in response to ATRA at a lower concentration than the NPM1 wild-type cell lines that were tested in this work. In addition, the reduction of BCL-2 and MCL-1 levels was greater in NPMc+AML following ATRA than in the other cell lines. As a result, the percentage of apoptosis and the differentiation marker level both increased. However, further studies are required with more primary AML samples in order to confirm the effect of ATRA on BCL-2 and MCL-1 in NPMc+AML cells.

# **7. General Discussion**

## 7. General discussion:

NPM1 is an abundant phosphoprotein and is highly expressed in all tissues (reviewed in (Grisendi, *et al* 2006)). Although NPM1 is predominantly localised in the nucleolus, it shuttles continuously between the nucleus and cytoplasm and transports ribosomal components to the cytoplasm, participating in ribosomal assembly (reviewed in (Falini, *et al* 2007b)). NPM1 is involved in the cell proliferation process and acting as a molecular chaperone in protein synthesis, histone assembly, and nucleic acid interactions (reviewed in (Falini, *et al* 2007b, Grisendi, *et al* 2006)). In contrast, NPM1 is also considered as a tumour suppressor protein through the mediation of P53 activation by binding to the P53 negative regulator (HDM2), and ARF (Colombo, *et al* 2002, Kurki, *et al* 2004b).

NPM1 mutations are the most common mutation in AML with a normal karyotype. NPM1 mutations cause a frame-shift in the C-terminus which results in the deletion of two tryptophan residues, 288 and 290 (or at least 290 only) leading to the disruption of the nuclear localization signal (NLS) while, an additional leucine-rich nuclear export signal (NES) is generated causing delocalisation of NPM1 into the cytoplasm (Falini, *et al* 2006, Falini, *et al* 2007b). NPM1 mutations mainly occur in exon 12, but they can also be present in exons 9, 10 or 11 (Falini, *et al* 2005). The most common type is mutation A, which is a duplication of the TCTG tetra-nucleotide at positions 956 to 959 (Falini, *et al* 2005, Falini, *et al* 2007b). NPM1 mutations coincidence with other mutations and the presence of internal tandem duplication (ITD) mutations in the tyrosine kinase receptor FLT3 in NPMc+ AML accounts for around 40% of NPMc+ cases (Rau and Brown 2009, Verhaak,

*et al* 2005). In NPMc+AML, the prognosis is categorised as favourable with a complete remission rate around 80%, while in the presence of FLT3-ITD, the CR is reduced and considered as an intermediate prognosis (Dohner, *et al* 2005, Schnittger, *et al* 2005, Thiede, *et al* 2006).

In our experiments, five different leukaemic cell lines were used: OCI-AML3, M-07e, MOLM-13, MV4-11, and HL-60. OCI-AML3 is the only cell line known to harbour the NPMc+ mutation and so is widely used as a model of NPMc+AML in the literature (Quentmeier, *et al* 2005). M-07e, MV4-11, MOLM-13, and HL-60 cell lines were used as cell lines that express wild-type NPM1, whilst OCI-AML3, M-07e, MV4-11 and MOLM13 are P53 wild-type. HL-60 cells have a deletion in the P53 genes and were therefore only used in APE1 subcellular localisation experiments as a control for our results because the subcellular localisation of APE1 had been previously detected in the cytoplasm of HL-60 cells (Yoshida, *et al* 2003). MV4-11 and MOLM-13 cell lines were used in evaluating the effect of AC220 – FLT3 inhibitor - on BCL-2 and MCL-1 levels because they harbour FLT3-ITD mutations (Quentmeier, *et al* 2003). We would have used isogenetic cell lines expressing NPM1-wt/NPMc+ with or without FLT3-ITD, but these were unfortunately not available.

NPM1 is associated with the regulation of DNA repair and has been shown to induce proliferating cell nuclear antigen (PCNA), which acts as a platform for many enzymes in the response to DNA damage (Wu, *et al* 2002). In addition, ARF stability, which is a tumour suppressor protein, is achieved by its interaction with NPM1 via subsequent protection of ARF from degradation by blocking its ubiquitination (Khan, *et al* 2004, Korgaonkar, *et al* 2005, Kuo, *et al* 2004). ARF

translocates in the nucleoplasm and promotes P53 stabilisation by binding to HDM2, while the subcellular localisation of ARF in nucleoli is sequestered by NPM1 resulting in increased HDM2 binding to P53 and inactivation of P53 function (Korgaonkar, *et al* 2005). In NPMc+AML cells, ARF is delocalised into the cytoplasm by the mutant NPM1 leading to attenuation of ARF activity and hence P53 destabilisation and consequent reduction of activity (Colombo, *et al* 2006, den Besten, *et al* 2005). It has therefore been hypothesised that the favourable outcome in NPMc+AML cases could be a result of perturbation of DNA damage response.

In response to DNA damage agents, our assays showed that the DNA damage process was activated efficiently in NPMc+AML cells indicating that delocalisation of NPM1 into the cytoplasm has not impaired global repair of DNA. However, the protein level of NPM1 was elevated in NPMc+ cells in the nuclear and cytoplasmic fractions but relatively much more in the nucleus, whereas the NPM1 mRNA expression has not changed. The up-regulation in NPM1 protein level may contribute to the DNA damage response and the increase in NPM1 protein production and re-localisation of wild-type NPM1 into the nucleolus. The up-regulation in NPM1 protein level would appear that NPM1 expression is regulated at the level of translation. It has been found that NPM1 protein level depends on activation of mTOR signalling, which is a serine-threonine protein kinase that controls translation efficiency, cell cycle progression, and ribosomal biogenesis through its ability to integrate nutrient and mitogenic signals (Pelletier, *et al* 2007). TSC1 – an upstream inhibitor of mTOR – was found to repress NPM1 protein level, while deletion of TSC1 resulted in NPM1

protein induction through increased translation of existing nucleophosmin mRNAs (Pelletier, *et al* 2007).

As a result, It has been suggested that the subcellular localisation of wild-type NPM1 and mutant NPM1 should be identified using antibodies that only recognise wild-type NPM1 without interference with the mutant NPM1, in addition to using antibodies specifically against the mutant NPM1 after DNA damage response, in order to evaluate the subcellular localisation of wild-type and mutant NPM1 in response to DNA damage agent. Moreover, further studies are required to evaluate the mRNA and protein levels of NPM1 in response to stress at different time points. Previous data showed that NPM1 protein production is dependent on mTOR activation and rapamycin decreases NPM1 protein level without affecting NPM1 mRNA level (Pelletier, *et al* 2007). Thus, in order to evaluate the translational control of NPM1, we suggest treating NPMc+AML and wild-type NPM1 cell lines with rapamycin, which inhibits mTOR signalling pathway, and then the levels of NPM1 mRNA and protein are measured. Finally, with the aim of determine the important role of NPM1 in DNA repair function in NPMc+ cells, the mutant NPM1 and wild-type NPM1 or the mutant NPM1 only should be knocked-down in NPMc+AML cells, followed by exposure of the cells to DNA damage agents and evaluation of the repair activity in NPMc+ and wild-type NPM1 cells. We knocked-down NPM1 for only 48 hours, while about 96 hours of NPM1 down-regulation are required to study the repair assay after NPM1 siRNA nucleofection. Thus, it is recommended to use stable transfectants rather than transient ones to perform this experiment.

APE1 is an essential protein involved in the response to DNA damage. APE1 functions in the BER pathway and participate in the repair of certain DNA lesions and also acts as a redox co-activator of many transcription factors such as P53, and NF- $\kappa$ B by inducing their DNA binding (reviewed in (Fishel and Kelley 2007)). NPM1 is considered to fine-tune APE1 functions through binding to the N-terminal of APE1 and increasing its endonuclease activity (Vascotto, *et al* 2009). Recently, Vascotto *et al.* have demonstrated that NPM1 is essential for subcellular localisation of APE1 within nucleoli (Vascotto, *et al* 2013). In haematological cell lines, Vascotto *et al.* assessed the presence of APE1 in the cytoplasm of NPMc+AML cells by using OCI-AML3 cells and compared the results with OCI-AML2 cell line, which expresses wild-type NPM1 (Vascotto, *et al* 2013). They showed that the APE1 subcellular localisation is delocalised into the cytoplasm in OCI-AML3 cells due to the presence of NPMc+ compared with wild-type NPM1 cell line (Vascotto, *et al* 2013). However, we found that APE1 is localised in the cytoplasm of OCI-AML3, M-07e and HL-60 cell lines and because M-07e and HL-60 cells are NPM1 wild-type this suggests that cytoplasmic localisation is not independent of an NPMc+ mutation. The presence of APE1 in the cytoplasm has been seen in fibroblasts, lymphocytes, macrophages, and hepatocytes (Tell, *et al* 2009, Yoshida, *et al* 2003) and so is a common finding. In response to DNA damaging agents - etoposide and MMS, we showed that APE1 is translocated into the nucleus where it presumably participates in the DNA damage response.

A reduction in APE1 level or blocking of APE1 DNA repair function is associated with hypersensitivity of cells to alkylating agents (McNeill and Wilson 2007, Wang, *et al* 2004).

The sensitivity of NPM<sup>-/-</sup> mouse embryonic fibroblasts to a DNA damage inducer known to produce DNA lesions which are repaired by BER, is greater than NPM<sup>+/+</sup> cells (Vascotto, *et al* 2013). In addition, OCI-AML3 cells and bone marrow NPMc+AML patient cells were more sensitive than wild-type NPM1 cell lines and blast cells from healthy donor (Vascotto, *et al* 2013). Furthermore, the level of AP sites was higher in OCI-AML3 cell than in OCI-AML2 (Vascotto, *et al* 2013). In contrast, our work showed that MMS treatment of NPMc+AML cell line and other haematological cell lines with wild-type NPM1 showed no differences in sensitivity to the methylating agent. Vascotto *et al.* treated OCI-AML3 and OCI-AML2 cells with MMS at different concentrations for 8 hours and evaluated the cell viability without assessing the cells during the recovery (Vascotto, *et al* 2013). Whereas Our MMS sensitivity protocol was performed on three different leukaemic cell lines, which are OCI-AML3, MV4-11, and M-07e, and these cells were treated for 1 hour with MSS at different concentrations and then incubated for 3 days with free-drug medium to allow cell recovery in order to assess the ability of cells to survive after the DNA damage inducer. In addition, OCI-AML3 cells are the only cell line bearing NPMc+ mutations and the results were compared with no isogenetic control cells. Therefore, further work should be done on a large number of patient samples.

As a result, our work suggests that the repair of MMS in NPMc+AML cells when compared with the selected wild-type NPM1 cell lines has not been perturbed, this may either be due to a functional BER pathway or other DNA repair pathways which also act on this class of DNA damage. In BER, for example, inhibition of APE1, which is a protein involved in BER

process, leads to the formation and accumulation of DSB from unrepaired single strand breaks (Sultana, *et al* 2012). As a result, Homologous recombination pathway attempts to repair the DNA damage (Rehman, *et al* 2010, Sultana, *et al* 2012).

In western blot experiments, a lower band was detected by APE1 antibodies in the OCI-AML3 – NPM1 mutated cell line at 33kDa, in addition to the band at 37KDa which corresponds to the expected size of the APE1 protein. In wild-type NPM1 cell lines, only the expected APE1 band – 37KDa was observed. In the literature, a lower protein band, which was observed with APE1 antibody, has been identified as N $\Delta$ 33APE1 (Chattopadhyay, *et al* 2006, Yoshida, *et al* 2003). N $\Delta$ 33APE1 lacks the first 33 N-terminal residues and it is mainly located in the cytoplasm and mitochondria suggesting it may have a potential role in DNA repair activity in the mitochondria (Chattopadhyay, *et al* 2006, Yoshida, *et al* 2003). N $\Delta$ 33APE1 is characterised by higher endonuclease activity than the full-length APE1 and associated with an apoptotic phenotype (Vascotto, *et al* 2009, Yoshida, *et al* 2003). The generation of this product is by a proteolysis process at Lys31 through granzyme A protein, which cleavages APE1 and induces rapid cell death, leading to cleavage of the APE1 (Chattopadhyay, *et al* 2006, Guo, *et al* 2008). Therefore, an investigation of the potential N $\Delta$ 33APE1 product was undertaken by antibodies binding to the N-terminal domain of APE1. The N-terminal APE1 antibody reacts with the full-length APE1 at the N-terminal region, and therefore will not react with N $\Delta$ 33APE1 which lacks the N-terminal domain (Yoshida, *et al* 2003). The result shows that the lower band was still present on the western blot suggesting that it might not be N $\Delta$ 33APE1 but a different product containing the N-terminal domain.

Furthermore, APE1 mRNA was studied to see if alternative splice products could be seen but no such splicing was recognised. Whilst this thesis was being prepared Vascotto *et al.* published evidence that the cytoplasmic truncated APE1 in NPMc+AML cells is a result of a specific proteolytic activity independent of granzyme A protein, which is not expressed in OCI-AML3 cells (Guo, *et al* 2008, Vascotto, *et al* 2013).

Apoptosis is a major pathway in DDR which removes unwanted or damaged cells. Its deregulation may contribute to cancer development. BCL-2 family proteins are an integral part of the apoptotic process and either promote or prevent apoptosis. Anti-apoptotic BCL-2 expression has been shown to play a crucial role in the development of leukaemia and up-regulation of BCL-2 has been detected in the majority of patients with AML (Nagy, *et al* 2003). Moreover, MCL-1, which is another anti-apoptotic protein, has been shown to be essential for haematopoietic stem cell and early myeloid precursor cell survival and the expression of MCL-1 has been shown to be increased in FLT3-ITD AML cases (Yoshimoto, *et al* 2009).

The expression of BCL-2 and MCL-1 were evaluated in an NPMc+AML cell line and the results showed that the mRNA level of BCL-2 and MCL-1 were higher in the NPMc+AML compared to other cell lines with wild-type NPM1. However, when mutant NPM1, or total NPM1, was knocked-down by specific siRNAs, there was a reduction in the BCL-2 and MCL-1 mRNA level in NPMc+AML cells and the protein level of P53 was increased. Thus, these results revealed that NPM1 may participate in the abnormal over-expression of BCL-2 and MCL-1 in NPMc+AML. P53 negatively regulates BCL-2 expression through interaction with the BCL-2 promoter and in

NPMc+AML it is known that ARF, which binds to HDM2 and activates P53 function, is delocalised with the NPM1 into the cytoplasm (Colombo, *et al* 2006, Wu, *et al* 2001). Thus, we suggest two possible mechanisms that cause the up-regulation of BCL-2 and MCL-1 in NPMc+AML cells. Firstly, the delocalisation of NPM1 and ARF into the cytoplasm results in the inactivation of P53 function leading to activate the BCL-2 promoter and increase in BCL-2 level, and the second suggestion is that delocalisation of NPM1 into the cytoplasm causes NPM1 to interact with the pro-apoptotic BCL-2 family proteins and prevents activation of BAX and BAK leading to an increase in the level of BCL-2 and MCL-1. Moreover, in NPMc+AML, HEXIM1, which is an inhibitor of polymerase II transcription elongation, is delocalised in the cytoplasm by the mutant NPM1. As a result, the impairment of HEXIM1 function induces expression of genes that are associated with anti-apoptotic family proteins such as MCL-1 (Gurumurthy, *et al* 2008).

Further studies are needed to confirm the basal levels of BCL-2 and MCL-1 proteins by western blot and to compare these results with our flow cytometry measurements which would offer further validation of the method. In addition, our knock-down experiments were used to evaluate the mRNA level of BCL-2 and MCL-1, thus it is essential to verify the effect of down-regulation of BCL-2 and MCL-1 mRNA on its protein level. Thereafter, the impact of the mutant NPM1 on the expression of the anti-apoptotic proteins could be assessed by knock-down of the mutant NPM1 only in NPMc+AML, followed by evaluation of the levels of BCL-2, MCL-1 and P53. Moreover, the interaction of the mutant and wild-type NPM1 with other proteins in the cytoplasm should be studied,

particularly with those proteins involved in the modulation of apoptosis such as BH3-only proteins.

A reduction in the anti-apoptotic BCL-2 and MCL-1 levels in NPMc+AML cells after knock-down of NPM1 by siRNA led us to treat NPMc+AML with a drug that may target the anti-apoptotic BCL-2 proteins in NPMc+AML cells. Administration of ATRA causes an increase in cell differentiation and apoptosis which leads to increased sensitivity of AML blast cells to chemotherapy (Andreeff, *et al* 1999, Pisani, *et al* 1997). In clinical trials, non-APL AML patients have shown variable results in response to ATRA. UK-MRC trial failed to demonstrate a benefit of adding ATRA to standard chemotherapy (Burnett, *et al* 2010), whereas the Austrian-German AML study showed that the presence of NPMc+/FLT3-wt mutations resulted in high complete remission rate, and improved relapse-free and overall survival (Schlenk, *et al* 2011, Schlenk, *et al* 2009). Bradbury *et al.* have shown that the expression of BCL-2 is reduced to a greater extent in AML cells which are CD34 negative (Bradbury, *et al* 1996). Interestingly, this is a feature of NPMc+AML. Therefore, the NPMc+AML cells and wild-type NPM1 cells were treated with ATRA and the mRNA and protein expression of BCL-2 and MCL-1 were determined. Our results showed that ATRA decreased the level of BCL-2 and MCL-1 in all cell lines but a near total reduction was observed in NPMc+AML. In addition, the NPMc+AML cells were more sensitive to cell differentiation and apoptosis. Therefore, it seems that ATRA has a crucial impact on the NPMc+AML cells by down-regulation of BCL-2 and MCL-1 level. However, the exact mechanism has not been clarified but it has been noted that the mutant NPM1 in NPMc+AML cell line was decreased upon ATRA treatment

which is suggested to result in wild-type NPM1 being retained in the nucleus leading to induction of cell cycle arrest and apoptosis (Martelli, *et al* 2007).

Further experiments are needed to confirm the effect of ATRA on the anti-apoptotic proteins. Firstly, the levels of BCL-2 and MCL-1 proteins were detected by flow cytometry, which should be confirmed by western blot as a reference standard method. Moreover, we showed a down-regulation of BCL-2 in NPMc+AML upon ATRA treatment, thus it is important to confirm these results by up-regulating BCL-2 levels in these cells then treating the cells with ATRA and assessing the level of BCL-2 expression. With regard to the patient samples, the experiments were run on a small number of patient cells, therefore, to increase the power of the results more patient samples must be studied. In addition, the level of BCL-2 and MCL-1 mRNA level were detected in the patient samples, the protein levels of BCL-2 and MCL-1, and the expression of CD34 status should also be evaluated to establish the correlation of the mRNA with protein level, and the expression of CD34 with response to ATRA.

In NPMc+AML, 40% of the cases co-harbour FLT3-ITD mutations. It has been shown that FLT3-ITD play a major role to induce MCL-1 expression via activation of PI3K/Akt pathway (Yoshimoto, *et al* 2009). Therefore, we added AC220, which is a highly selective FLT3 tyrosine kinase inhibitor and induces differentiation of FLT3-ITD cells, to the ATRA-treated cells and evaluated BCL-2 and MCL-1 expression (Sexauer, *et al* 2012, Zarrinkar, *et al* 2009). BCL-2 and MCL-1 mRNA levels were decreased in NPMc+AML and FLT3-ITD cell lines upon treatment with AC220, while the protein levels did not change. In patient samples, the cell survival was not affected by the

addition of AC220. However, in combination with ATRA we showed the same impact as seen in cells treated with ATRA alone. However, more work is required to investigate the potential benefits of adding AC220 to ATRA in the treatment of NPMc+AML/FLT3-ITD patients by using patient samples harbouring both mutations and treating the cells with these drugs and evaluating the cell survival and anti-apoptotic levels.

The classic view of protein synthesis (the central dogma) states that DNA makes RNA makes protein. This view assumes that the production of protein is correlated to the mRNA level, but there are other biological factors that affect this relation (reviewed in (Maier, *et al* 2009)). In our results, the weak correlation between the mRNA and protein levels of NPM1, BCL-2 and MCL-1 could be a result of post-transcriptional processes, translational efficiency, the long half life of proteins, or other regulatory mechanisms such as miRNA which have been found to fine-regulate protein expression without causing change in gene expression (Maier, *et al* 2009, Vogel and Marcotte 2012).

In conclusion, although NPM1 subcellular localisation is perturbed in NPMc+AML leading to delocalisation of other proteins that are involved in DNA damage response, we have not demonstrated the impairment in DNA repair mechanisms in cells harbouring NPMc+ mutations. However, an increase in NPM1 levels in nuclear lysate has been observed to a similar level to that seen in wild-type NPM1 cells. Over-expression of anti-apoptotic proteins BCL-2 and MCL-1 in NPMc+AML was observed and these are suggested to play an essential role in leukaemogenesis development. ATRA has showed a significant effect on the level of anti-apoptotic BCL-2 and MCL-1 which

could be useful in combination with FLT3 inhibitors in NPMc+/FLT3-ITD AML cases. Furthermore, there are potential agents which could serve as good targets for leukaemia therapy, thus further research should be focused on the influence of adding the NPM oligomerization inhibitor, which disrupts NPM1 oligomer formation and inhibit aberrant NPM1 function in NPMc+AML cells, or the anti-apoptotic proteins inhibitors to the cytotoxic therapy for NPMc+AML patients.

**References:**

- Abdel-Fatah, T., Sultana, R., Abbotts, R., Hawkes, C., Seedhouse, C., Chan, S. & Madhusudan, S. (2013) Clinicopathological and functional significance of XRCC1 expression in ovarian cancer. *International Journal of Cancer*, **132**, 2778-2786.
- Adams, J.M. & Cory, S. (2007) The Bcl-2 apoptotic switch in cancer development and therapy. *Oncogene*, **26**, 1324-1337.
- Al-Attar, A., Gossage, L., Fareed, K.R., Shehata, M., Mohammed, M., Zaitoun, A.M., Soomro, I., Lobo, D.N., Abbotts, R., Chan, S. & Madhusudan, S. (2010) Human apurinic/aprimidinic endonuclease (APE1) is a prognostic factor in ovarian, gastro-oesophageal and pancreatico-biliary cancers. *British Journal of Cancer*, **102**, 704-709.
- Albiero, E., Madeo, D., Bolli, N., Giaretta, I., Di Bona, E., Martelli, M.F., Nicoletti, I., Rodeghiero, F. & Falini, B. (2007) Identification and functional characterization of a cytoplasmic nucleophosmin leukaemic mutant generated by a novel exon-11 NPM1 mutation. *Leukemia*, **21**, 1099-1103.
- Alcalay, M., Tiacci, E., Bergomas, R., Bigerna, B., Venturini, E., Minardi, S.P., Meani, N., Diverio, D., Bernard, L., Tizzoni, L., Volorio, S., Luzi, L., Colombo, E., Lo Coco, F., Mecucci, C., Falini, B., Pelicci, P.G. & Grp Italiano Malattie Ematol Maligne Adulto Acute Leukemia Working, P. (2005) Acute myeloid leukemia bearing cytoplasmic nucleophosmin (NPMc+) AML shows a distinct gene expression profile characterized by up-regulation of genes involved in stem-cell maintenance. *Blood*, **106**, 899-902.
- Andreeff, M., Jiang, S., Zhang, X., Konopleva, M., Estrov, Z., Snell, V.E., Xie, Z., Okcu, M.F., Sanchez-Williams, G., Dong, J., Estey, E.H., Champlin, R.C., Kornblau, S.M., Reed, J.C. & Zhao, S. (1999) Expression of Bcl-2-related genes in normal and AML progenitors: changes induced by chemotherapy and retinoic acid. *Leukemia*, **13**, 1881-1892.
- Andreeff, M., Ruvolo, V., Gadgil, S., Zeng, C., Coombes, K., Chen, W., Kornblau, S., Baron, A.E. & Drabkin, H.A. (2008) HOX expression patterns identify a common signature for favorable AML. *Leukemia*, **22**, 2041-2047.

- Andreeff, M., Zhao, S., Konopleva, M., Xie, Z., Zhang, X., Snell, V., McQueen, T., Jiang, S., Weidner, D., Estey, E., Thall, P., Sanchez-Williams, G., Kornblau, S.M. & Reed, J.C. (1998) The role of BCL-2 family genes in acute myeloid leukemia (AML): Therapeutic implications. *Proceedings of the American Association for Cancer Research Annual Meeting*, **39**, 572-572.
- Bacher, U., Kohlmann, A., Haferlach, C. & Haferlach, T. (2009) Gene expression profiling in acute myeloid leukaemia (AML). *Best Practice & Research Clinical Haematology*, **22**, 169-180.
- Balusu, R., Fiskus, W., Rao, R., Chong, D.G., Nalluri, S., Mudunuru, U., Ma, H., Chen, L., Venkannagari, S., Ha, K., Abhyankar, S., Williams, C., McGuirk, J., Khoury, H.J., Ustun, C. & Bhalla, K.N. (2011) Targeting levels or oligomerization of nucleophosmin 1 induces differentiation and loss of survival of human AML cells with mutant NPM1. *Blood*, **118**, 3096-3106.
- Balusu, R., Fiskus, W.C., Rao, R., Buckley, K.M., Wang, Y., Joshi, A., Koul, S., Jillella, A., Ustun, C., Sunay, S., Khoury, H.J. & Bhalla, K.N. (2009) Targeting Levels, Aberrant Localization or Oligomerization of Mutant Nucleophosmin Induces Differentiation and Loss of Survival of Human AML Cells with Mutant NPM1. *Blood*, **114**, 1041-1042.
- Boissel, N., Renneville, A., Biggio, V., Philippe, N., Thomas, X., Cayuela, J.M., Terre, C., Tigaud, I., Castaigne, S., Raffoux, E., De Botton, S., Fenaux, P., Dombret, H., Preudhomme, C. & Alfa (2005) Prevalence, clinical profile, and prognosis of NPM mutations in AML with normal karyotype. *Blood*, **106**, 3618-3620.
- Bolli, N., Nicoletti, I., De Marco, M.F., Bigerna, B., Pucciarini, A., Mannucci, R., Martelli, M.P., Liso, A., Mecucci, C., Fabbiano, F., Martelli, M.F., Henderson, B.R. & Falini, B. (2007) Born to be exported: COOH-terminal nuclear export signals of different strength ensure cytoplasmic accumulation of nucleophosmin leukemic mutants. *Cancer Research*, **67**, 6230-6237.
- Bolli, N., Payne, E.M., Grabher, C., Lee, J.-S., Johnston, A.B., Falini, B., Kanki, J.P. & Look, A.T. (2010) Expression of the cytoplasmic NPM1 mutant (NPMc plus ) causes the expansion of hematopoietic cells in zebrafish. *Blood*, **115**, 3329-3340.
- Bonetti, P., Davoli, T., Sironi, C., Amati, B., Pelicci, P.G. & Colombo, E. (2008) Nucleophosmin and its AML-associated mutant regulate c-Myc turnover through Fbw7 gamma. *Journal of Cell Biology*, **182**, 19-26.

- Boon, K., Caron, H.N., van Asperen, R., Valentijn, L., Hermus, M.C., van Sluis, P., Roobeek, I., Weis, I., Voute, P.A., Schwab, M. & Versteeg, R. (2001) N-myc enhances the expression of a large set of genes functioning in ribosome biogenesis and protein synthesis. *Embo Journal*, **20**, 1383-1393.
- Bradbury, D.A., Aldington, S., Zhu, Y.M. & Russell, N.H. (1996) Down-regulation of bcl-2 in AML blasts by all-trans retinoic acid and its relationship to CD34 antigen expression. *British Journal of Haematology*, **94**, 671-675.
- Brandts, C.H., Sargin, B., Rode, M., Biermann, C., Lindtner, B., Schwable, J., Buerger, H., Muller-Tidow, C., Choudhary, C., McMahon, M., Berdel, W.E. & Serve, H. (2005) Constitutive activation of Akt by Flt3 internal tandem duplications is necessary for increased survival, proliferation, and myeloid transformation. *Cancer Research*, **65**, 9643-9650.
- Burma, S., Chen, B.P., Murphy, M., Kurimasa, A. & Chen, D.J. (2001) ATM phosphorylates histone H2AX in response to DNA double-strand breaks. *Journal of Biological Chemistry*, **276**, 42462-42467.
- Burnett, A.K., Hills, R.K., Green, C., Jenkinson, S., Koo, K., Patel, Y., Guy, C., Gilkes, A., Milligan, D.W., Goldstone, A.H., Prentice, A.G., Wheatley, K., Linch, D.C. & Gale, R.E. (2010) The impact on outcome of the addition of all-trans retinoic acid to intensive chemotherapy in younger patients with nonacute promyelocytic acute myeloid leukemia: overall results and results in genotypic subgroups defined by mutations in NPM1, FLT3, and CEBPA. *Blood*, **115**, 948-956.
- Chan, P.K. & Chan, F.Y. (1995) NUCLEOPHOSMIN/B23 (NPM) OLIGOMER IS A MAJOR AND STABLE ENTITY IN HELA-CELLS. *Biochimica Et Biophysica Acta-Gene Structure and Expression*, **1262**, 37-42.
- Chattopadhyay, R., Wiederhold, L., Szczesny, B., Boldogh, I., Hazra, T.K., Izumi, T. & Mitra, S. (2006) Identification and characterization of mitochondrial abasic (AP)-endonuclease in mammalian cells. *Nucleic Acids Research*, **34**, 2067-2076.
- Chen, W.N., Rassidakis, G.Z. & Medeiros, L.J. (2006) Nucleophosmin gene mutations in acute myeloid leukemia. *Archives of Pathology & Laboratory Medicine*, **130**, 1687-1692.
- Cheng, K., Sportoletti, P., Ito, K., Clohessy, J.G., Teruya-Feldstein, J., Kutok, J.L. & Pandolfi, P.P. (2010) The cytoplasmic NPM mutant induces myeloproliferation in a transgenic mouse model. *Blood*, **115**, 3341-3345.

- Chou, W.C., Tang, J.L., Lin, L.I., Yao, M., Tsay, W., Chen, C.Y., Wu, S.J., Huang, C.F., Chiou, R.J., Tseng, M.H., Lin, D.T., Lin, K.H., Chen, Y.C. & Tien, H.F. (2006) Nucleophosmin mutations in De novo acute myeloid leukemia: The age-dependent incidences and the stability during disease. *Cancer Research*, **66**, 3310-3316.
- Collins, A.R. (2004) The comet assay for DNA damage and repair - Principles, applications, and limitations. *Molecular Biotechnology*, **26**, 249-261.
- Colombo, E., Bonetti, P., Denchi, E.L., Martinelli, P., Zamponi, R., Marine, J.C., Helin, K., Falini, B. & Pelicci, P.G. (2005) Nucleophosmin is required for DNA integrity and p19(Arf) protein stability. *Molecular and Cellular Biology*, **25**, 8874-8886.
- Colombo, E., Marine, J.C., Danovi, D., Falini, B. & Pelicci, P.G. (2002) Nucleophosmin regulates the stability and transcriptional activity of p53. *Nature Cell Biology*, **4**, 529-533.
- Colombo, E., Martinelli, P., Zamponi, R., Shing, D.C., Bonetti, P., Luzi, L., Volorio, S., Bernard, L., Pruneri, G., Alcalay, M. & Pelicci, P.G. (2006) Delocalization and destabilization of the Arf tumor suppressor by the leukemia-associated NPM mutant. *Cancer Research*, **66**, 3044-3050.
- Cordell, J.L., Pulford, K.A.F., Bigerna, B., Roncador, G., Banham, A., Colombo, E., Pelicci, P.G., Mason, D.Y. & Falini, B. (1999) Detection of normal and chimeric nucleophosmin in human cells. *Blood*, **93**, 632-642.
- Costa, R.M.A., Chigancas, V., Galhardo, R.D., Carvalho, H. & Menck, C.F.M. (2003) The eukaryotic nucleotide excision repair pathway. *Biochimie*, **85**, 1083-1099.
- Dalenc, F., Drouet, J., Ader, I., Delmas, C., Rochaix, P., Favre, G., Cohen-Jonathan, E. & Toulas, C. (2002) Increased expression of a COOH-truncated nucleophosmin resulting from alternative splicing is associated with cellular resistance to ionizing radiation in HeLa cells. *International Journal of Cancer*, **100**, 662-668.
- den Besten, W., Kuo, M.L., Williams, R.T. & Sherr, C.J. (2005) Myeloid leukemia-associated nucleophosmin mutants perturb p53-dependent and independent activities of the Arf tumor suppressor protein. *Cell Cycle*, **4**, 1593-1598.

- Doehner, H., Estey, E.H., Amadori, S., Appelbaum, F.R., Buechner, T., Burnett, A.K., Dombret, H., Fenaux, P., Grimwade, D., Larson, R.A., Lo-Coco, F., Naoe, T., Niederwieser, D., Ossenkoppele, G.J., Sanz, M.A., Sierra, J., Tallman, M.S., Loewenberg, B. & Bloomfield, C.D. (2010) Diagnosis and management of acute myeloid leukemia in adults: recommendations from an international expert panel, on behalf of the European LeukemiaNet. *Blood*, **115**, 453-474.
- Dohner, K. & Dohner, H. (2008) Molecular characterization of acute myeloid leukemia. *Haematologica-the Hematology Journal*, **93**, 976-982.
- Dohner, K., Schlenk, R.F., Habdank, M., Scholl, C., Rucker, F.G., Corbacioglu, A., Bullinger, L., Frohling, S., Dohner, H. & Grp, A.M.L.S. (2005) Mutant nucleophosmin (NPM1) predicts favorable prognosis in younger adults with acute myeloid leukemia and normal cytogenetics: interaction with other gene mutations. *Blood*, **106**, 3740-3746.
- Du, W., Zhou, Y., Pike, S. & Pang, Q.S. (2010) NPM phosphorylation stimulates Cdk1, overrides G(2)/M checkpoint and increases leukemic blasts in mice. *Carcinogenesis*, **31**, 302-310.
- Duguid, J.R., Eble, J.N., Wilson, T.M. & Kelley, M.R. (1995) DIFFERENTIAL CELLULAR AND SUBCELLULAR EXPRESSION OF THE HUMAN MULTIFUNCTIONAL APURINIC/APYRIMIDINIC ENDONUCLEASE (APE/REF-1) DNA-REPAIR ENZYME. *Cancer Research*, **55**, 6097-6102.
- Estey, E. & Doehner, H. (2006) Acute myeloid leukaemia. *Lancet*, **368**, 1894-1907.
- Falini, B., Bolli, N., Shan, J., Martelli, M.P., Liso, A., Pucciarini, A., Bigerna, B., Pasqualucci, L., Mannucci, R., Rosati, R., Gorello, P., Diverio, D., Roti, G., Tiacci, E., Cazzanica, G., Biondi, A., Schnittger, S., Haferlach, T., Hiddemann, W., Martelli, M.F., Gu, W., Mecucci, C. & Nicoletti, I. (2006) Both carboxy-terminus NES motif and mutated tryptophan(s) are crucial for aberrant nuclear export of nucleophosmin leukemic mutants in NPMc(+) AML. *Blood*, **107**, 4514-4523.
- Falini, B., Martelli, M.P., Bolli, N., Sportoletti, P., Liso, A., Tiacci, E. & Haferlach, T. (2011) Acute myeloid leukemia with mutated nucleophosmin (NPM1): is it a distinct entity? *Blood*, **117**, 1109-1120.

- Falini, B., Mecucci, C., Tiacci, E., Alcalay, M., Rosati, R., Pasqualucci, L., La Starza, R., Diverio, D., Colombo, E., Santucci, A., Bigerna, B., Pacini, R., Pucciarini, A., Liso, A., Vignetti, M., Fazi, P., Meani, N., Pettirossi, V., Saglio, G., Mandelli, F., Lo-Coco, F., Pelicci, P., Martelli, M.F. & Working, G.A.L. (2005) Cytoplasmic nucleophosmin in acute myelogenous leukemia with a normal karyotype. *New England Journal of Medicine*, **352**, 254-266.
- Falini, B., Nicoletti, I., Bolli, N., Martelli, M.P., Liso, A., Gorello, P., Mandelli, F., Mecucci, C. & Martelli, M.F. (2007a) Translocations and mutations involving the nucleophosmin (NPM1) gene in lymphomas and leukemias. *Haematologica-the Hematology Journal*, **92**, 519-532.
- Falini, B., Nicoletti, I., Martelli, M.F. & Mecucci, C. (2007b) Acute myeloid leukemia carrying cytoplasmic/mutated nucleophosmin (NPMc(+)) AML: biologic and clinical features. *Blood*, **109**, 874-885.
- Fantini, D., Vascotto, C., Marasco, D., D'Ambrosio, C., Romanello, M., Vitagliano, L., Pedone, C., Poletto, M., Cesaratto, L., Quadrifoglio, F., Scaloni, A., Radicella, J.P. & Tell, G. (2010) Critical lysine residues within the overlooked N-terminal domain of human APE1 regulate its biological functions. *Nucleic Acids Research*, **38**, 8239-8256.
- Fishel, M.L. & Kelley, M.R. (2007) The DNA base excision repair protein Ape1/Ref-1 as a therapeutic and chemopreventive target. *Molecular Aspects of Medicine*, **28**, 375-395.
- Fortini, P. & Dogliotti, E. (2007) Base damage and single-strand break repair: Mechanisms and functional significance of short- and long-patch repair subpathways. *DNA Repair*, **6**, 398-409.
- Fortini, P., Pascucci, B., Parlanti, E., Sobol, R.W., Wilson, S.H. & Dogliotti, E. (1998) Different DNA polymerases are involved in the short- and long-patch base excision repair in mammalian cells. *Biochemistry*, **37**, 3575-3580.
- Fung, H., Bennett, R.A.O. & Demple, B. (2001) Key role of a downstream specificity protein 1 site in cell cycle-regulated transcription of the AP endonuclease gene APE1/APEX in NIH3T3 cells. *Journal of Biological Chemistry*, **276**, 42011-42017.

- Fyodorov, D.V. & Kadonaga, J.T. (2001) The many faces of chromatin remodeling: SWITCHING beyond transcription. *Cell*, **106**, 523-525.
- Gale, R.E., Green, C., Allen, C., Mead, A.J., Burnett, A.K., Hills, R.K., Linch, D.C. & Med Res Council Adult Leukaemia, W. (2008) The impact of FLT3 internal tandem duplication mutant level, number, size, and interaction with NPM1 mutations in a large cohort of young adult patients with acute myeloid leukemia. *Blood*, **111**, 2776-2784.
- Gao, G. & Dou, Q.P. (2000) G(1) phase-dependent expression of Bcl-2 mRNA and protein correlates with chemoresistance of human cancer cells. *Molecular Pharmacology*, **58**, 1001-1010.
- Gjerset, R.A. (2006) DNA damage, p14ARF, Nucleophosmin (NPM/B23), and cancer. *Journal of Molecular Histology*, **37**, 239-251.
- Glaser, S.P., Lee, E.F., Tronson, E., Bouillet, P., Wei, A., Fairlie, W.D., Izon, D.J., Zuber, J., Rappaport, A.R., Herold, M.J., Alexander, W.S., Lowe, S.W., Robb, L. & Strasser, A. (2012) Anti-apoptotic Mcl-1 is essential for the development and sustained growth of acute myeloid leukemia. *Genes & Development*, **26**, 120-125.
- Gorello, P., Cazzaniga, G., Alberti, F., Dell'Oro, M.G., Gottardi, E., Specchia, G., Roti, G., Rosati, R., Martelli, M.F., Diverio, D., Lo Coco, F., Biondi, A., Saglio, G., Mecucci, C. & Falini, B. (2006) Quantitative assessment of minimal residual disease in acute myeloid leukemia carrying nucleophosmin (NPM1) gene mutations. *Leukemia*, **20**, 1103-1108.
- Gores, G.J. & Kaufmann, S.H. (2012) Selectively targeting Mcl-1 for the treatment of acute myelogenous leukemia and solid tumors. *Genes & Development*, **26**, 305-311.
- Graninger, W.B., Seto, M., Boutain, B., Goldman, P. & Korsmeyer, S.J. (1987) EXPRESSION OF BCL-2 AND BCL-2-IG FUSION TRANSCRIPTS IN NORMAL AND NEOPLASTIC-CELLS. *Journal of Clinical Investigation*, **80**, 1512-1515.
- Grimwade, D., Hills, R.K., Moorman, A.V., Walker, H., Chatters, S., Goldstone, A.H., Wheatley, K., Harrison, C.J., Burnett, A.K. & Natl Canc Res Inst Adult, L. (2010) Refinement of cytogenetic classification in acute myeloid leukemia: determination of prognostic significance of rare recurring chromosomal abnormalities among 5876 younger adult patients treated in the United Kingdom Medical Research Council trials. *Blood*, **116**, 354-365.

- Grisendi, S., Bernardi, R., Rossi, M., Cheng, K., Khandker, L., Manova, K. & Pandolfi, P.P. (2005) Role of nucleophosmin in embryonic development and tumorigenesis. *Nature*, **437**, 147-153.
- Grisendi, S., Mecucci, C., Falini, B. & Pandolfi, P.P. (2006) Nucleophosmin and cancer. *Nature Reviews Cancer*, **6**, 493-505.
- Gruszka, A.M., Lavorgna, S., Consalvo, M.I., Ottone, T., Martinelli, C., Cinquanta, M., Ossolengo, G., Pruneri, G., Buccisano, F., Divona, M., Cedrone, M., Ammatuna, E., Venditti, A., de Marco, A., Lo-Coco, F. & Pelicci, P.G. (2010) A monoclonal antibody against mutated nucleophosmin 1 for the molecular diagnosis of acute myeloid leukemias. *Blood*, **116**, 2096-2102.
- Guo, Y., Chen, J., Zhao, T. & Fan, Z. (2008) Granzyme K degrades the redox/DNA repair enzyme Ape1 to trigger oxidative stress of target cells leading to cytotoxicity. *Molecular Immunology*, **45**, 2225-2235.
- Gurumurthy, M., Tan, C.H., Ng, R., Zeiger, L., Lau, J., Lee, J.L., Dey, A., Philp, R., Li, Q.T., Lim, T.M., Price, D.H., Lane, D.P. & Chao, S.H. (2008) Nucleophosmin interacts with HEXIM1 and regulates RNA polymerase II transcription. *Journal of Molecular Biology*, **378**, 302-317.
- Gustafsson, A.B. & Gottlieb, R.A. (2007) Bcl-2 family members and apoptosis, taken to heart. *American Journal of Physiology-Cell Physiology*, **292**, C45-C51.
- Helleday, T. (2010) Homologous recombination in cancer development, treatment and development of drug resistance. *Carcinogenesis*, **31**, 955-960.
- Helleday, T., Petermann, E., Lundin, C., Hodgson, B. & Sharma, R.A. (2008) DNA repair pathways as targets for cancer therapy. *Nature Reviews Cancer*, **8**, 193-204.
- Hingorani, K., Szebeni, A. & Olson, M.O.J. (2000) Mapping the functional domains of nucleolar protein B23. *Journal of Biological Chemistry*, **275**, 24451-24457.
- Hoeijmakers, J.H.J. (2001) Genome maintenance mechanisms for preventing cancer. *Nature*, **411**, 366-374.

- Huang, X., Okafuji, M., Traganos, F., Luther, E., Holden, E. & Darzynkiewicz, Z. (2004) Assessment of histone H2AX phosphorylation induced by DNA topoisomerase I and II inhibitors topotecan and mitoxantrone and by the DNA cross-linking agent cisplatin. *Cytometry Part A*, **58A**, 99-110.
- Itahana, K., Bhat, K.P., Jin, A.W., Itahana, Y., Hawke, D., Kobayashi, R. & Zhang, Y.P. (2003) Tumor suppressor ARF degrades B23, a nucleolar protein involved in ribosome biogenesis and cell proliferation. *Molecular Cell*, **12**, 1151-1164.
- Jackson, S.P. & Bartek, J. (2009) The DNA-damage response in human biology and disease. *Nature*, **461**, 1071-1078.
- Jenuwein, T. & Allis, C.D. (2001) Translating the histone code. *Science*, **293**, 1074-1080.
- Jian, P., Li, Z.W., Fang, T.Y., Jian, W., Zhuan, Z., Mei, L.X., Yan, W.S. & Jian, N. (2011) Retinoic acid induces HL-60 cell differentiation via the upregulation of miR-663. *Journal of Hematology & Oncology*, **4**.
- Jiricny, J. (2006) The multifaceted mismatch-repair system. *Nature Reviews Molecular Cell Biology*, **7**, 335-346.
- Kastan, M.B. (2008) DNA damage responses: Mechanisms and roles in human disease. *Molecular Cancer Research*, **6**, 517-524.
- Katz, R.L., Patel, S., Sneige, N., Fritsche, H.A., Hortobagyi, G.N., Ames, F.C., Brooks, T. & Ordonez, N.G. (1990) COMPARISON OF IMMUNOCYTOCHEMICAL AND BIOCHEMICAL ASSAYS FOR ESTROGEN-RECEPTOR IN FINE NEEDLE ASPIRATES AND HISTOLOGIC SECTIONS FROM BREAST CARCINOMAS. *Breast Cancer Research and Treatment*, **15**, 191-203.
- Kau, T.R., Way, J.C. & Silver, P.A. (2004) Nuclear transport and cancer: From mechanism to intervention. *Nature Reviews Cancer*, **4**, 106-117.
- Kaufmann, S.H., Karp, J.E., Svingen, P.A., Krajewski, S., Burke, P.J., Gore, S.D. & Reed, J.C. (1998) Elevated expression of the apoptotic regulator Mcl-1 at the time of leukemic relapse. *Blood*, **91**, 991-1000.
- Khan, S., Guevara, C., Fujii, G. & Parry, D. (2004) P14ARF is a component of the p53 response following ionizing irradiation of normal human fibroblasts. *Oncogene*, **23**, 6040-6046.

- Kikushige, Y., Yoshimoto, G., Miyamoto, T., Iino, T., Mori, Y., Iwasaki, H., Niino, H., Takenaka, K., Nagafuji, K., Harada, M., Ishikawa, F. & Akashi, K. (2008) Human Flt3 is expressed at the hematopoietic stem cell and the granulocyte/macrophage progenitor stages to maintain cell survival. *Journal of Immunology*, **180**, 7358-7367.
- Kindler, T., Lipka, D.B. & Fischer, T. (2010) FLT3 as a therapeutic target in AML: still challenging after all these years. *Blood*, **116**, 5089-5102.
- Kiyoi, H., Naoe, T., Nakano, Y., Yokota, S., Minami, S., Miyawaki, S., Asou, N., Kuriyama, K., Jinnai, I., Shimazaki, C., Akiyama, H., Saito, K., Oh, H., Motoji, T., Omoto, E., Saito, H., Ohno, R. & Ueda, R. (1999) Prognostic implication of FLT3 and N-RAS gene mutations in acute myeloid leukemia. *Blood*, **93**, 3074-3080.
- Koike, A., Nishikawa, H., Wu, W.W., Okada, Y., Venkitaraman, A.R. & Ohta, T. (2010) Recruitment of Phosphorylated NPM1 to Sites of DNA Damage through RNF8-Dependent Ubiquitin Conjugates. *Cancer Research*, **70**, 6746-6756.
- Kondo, E., Nakamura, S., Onoue, H., Matsuo, Y., Yoshino, T., Aoki, H., Hayashi, K., Takahashi, K., Minowada, J., Nomura, S. & Akagi, T. (1992) DETECTION OF BCL-2 PROTEIN AND BCL-2 MESSENGER-RNA IN NORMAL AND NEOPLASTIC LYMPHOID-TISSUES BY IMMUNOHISTOCHEMISTRY AND INSITU HYBRIDIZATION. *Blood*, **80**, 2044-2051.
- Konoplev, S. & Bueso-Ramos, C.E. (2006) Advances in the pathologic diagnosis and biology of acute myeloid leukemia. *Ann Diagn Pathol*, **10**, 39-65.
- Korgaonkar, C., Hagen, J., Tompkins, V., Frazier, A.A., Allamargot, C., Quelle, F.W. & Quelle, D.E. (2005) Nucleophosmin (B23) targets ARF to nucleoli and inhibits its function. *Molecular and Cellular Biology*, **25**, 1258-1271.
- Kottaridis, P.D., Gale, R.E., Frew, M.E., Harrison, G., Langabeer, S.E., Belton, A.A., Walker, H., Wheatley, K., Bowen, D.T., Burnett, A.K., Goldstone, A.H. & Linch, D.C. (2001) The presence of a FLT3 internal tandem duplication in patients with acute myeloid leukemia (AML) adds important prognostic information to cytogenetic risk group and response to the first cycle of chemotherapy: analysis of 854 patients from the United Kingdom Medical Research Council AML 10 and 12 trials. *Blood*, **98**, 1752-1759.

- Kumaravel, T.S., Vilhar, B., Faux, S.P. & Jha, A.N. (2009) Comet Assay measurements: a perspective. *Cell Biology and Toxicology*, **25**, 53-64.
- Kuo, M.L., den Besten, W., Bertwistle, D., Roussel, M.F. & Sherr, C.J. (2004) N-terminal polyubiquitination and degradation of the Arf tumor suppressor. *Genes & Development*, **18**, 1862-1874.
- Kurki, S., Peltonen, K. & Laiho, M. (2004a) Nucleophosmin, HDM2 and p53 - Players in UV damage incited nucleolar stress response. *Cell Cycle*, **3**, 976-979.
- Kurki, S., Peltonen, K., Latonen, L., Kiviharju, T.M., Ojala, P.M., Meek, D. & Laiho, M. (2004b) Nucleolar protein NPM interacts with HDM2 and protects tumor suppressor protein p53 from HDM2-mediated degradation. *Cancer Cell*, **5**, 465-475.
- Kusec, R., Jaksic, O., Ostojic, S., Kardum-Skelin, I., Vrhovac, R. & Jaksic, B. (2006) More on prognostic significance of FLT3/ITD size in acute myeloid leukemia (AML). *Blood*, **108**, 405-406.
- Kutny, M.A., Collins, S.J., Loeb, K., Walter, R.B. & Meshinchi, S. (2010) All-Trans-Retinoic Acid (ATRA) Causes Extensive Differentiation In the NPM Mutant, Non-APL Leukemic Cell Line OCI-AML3. *Blood*, **116**, 1354-1354.
- Lee, C., Smith, B.A., Bandyopadhyay, K. & Gjerset, R.A. (2005) DNA damage disrupts the p14ARF-B23(nucleophosmin) interaction and triggers a transient subnuclear redistribution of p14ARF. *Cancer Research*, **65**, 9834-9842.
- Leong, S.M., Tan, B.X., Ahmad, B.B., Yan, T., Chee, L.Y., Ang, S.T., Tay, K.G., Koh, L.P., Yeoh, A.E.J., Koay, E.S.C., Mok, Y.K. & Lim, T.M. (2010) Mutant nucleophosmin deregulates cell death and myeloid differentiation through excessive caspase-6 and-8 inhibition. *Blood*, **116**, 3286-3296.
- Letai, A.G. (2008) Diagnosing and exploiting cancer's addiction to blocks in apoptosis. *Nature Reviews Cancer*, **8**, 121-132.
- Levis, M., Allebach, J., Tse, K.F., Zheng, R., Baldwin, B.R., Smith, B.D., Jones-Bolin, S., Ruggeri, B., Dionne, C. & Small, D. (2002) A FLT3-targeted tyrosine kinase inhibitor is cytotoxic to leukemia cells in vitro and in vivo. *Blood*, **99**, 3885-3891.
- Li, J., Sejas, D.P., Rani, R., Koretsky, T., Bagby, G.C. & Pang, Q.S. (2006) Nucleophosmin regulates cell cycle progression and stress response in hematopoietic stem/progenitor cells. *Journal of Biological Chemistry*, **281**, 16536-16545.

- Li, J., Zhang, X.L., Sejas, D.P. & Pang, Q.S. (2005) Negative regulation of p53 by nucleophosmin antagonizes stress-induced apoptosis in human normal and malignant hematopoietic cells. *Leukemia Research*, **29**, 1415-1423.
- Li, Z. & Hann, S.R. (2013) Nucleophosmin is essential for c-Myc nucleolar localization and c-Myc-mediated rDNA transcription. *Oncogene*, **32**, 1988-1994.
- Li, Z.L., Boone, D. & Hann, S.R. (2008) Nucleophosmin interacts directly with c-Myc and controls c-Myc-induced hyperproliferation and transformation. *Proceedings of the National Academy of Sciences of the United States of America*, **105**, 18794-18799.
- Li, Z.L. & Hann, S.R. (2009) The Myc-nucleophosmin-ARF network A complex web unveiled. *Cell Cycle*, **8**, 2703-2707.
- Lin, L.I., Chen, C.Y., Lin, D.T., Tsay, W., Tang, J.L., Yeh, Y.C., Shen, H.L., Su, F.H., Yao, M., Huang, S.Y. & Tien, H.F. (2005) Characterization of CEBPA mutations in acute myeloid leukemia: Most patients with CEBPA mutations have biallelic mutations and show a distinct immunophenotype of the leukemic cells. *Clinical Cancer Research*, **11**, 1372-1379.
- Lyman, S.D., Brasel, K., Rousseau, A.M. & Williams, D.E. (1994) THE FLT3 LIGAND - A HEMATOPOIETIC STEM-CELL FACTOR WHOSE ACTIVITIES ARE DISTINCT FROM STEEL FACTOR. *Stem Cells*, **12**, 99-110.
- Madhusudan, S. & Middleton, M.R. (2005) The emerging role of DNA repair proteins as predictive, prognostic and therapeutic targets in cancer. *Cancer Treatment Reviews*, **31**, 603-617.
- Madhusudan, S., Smart, F., Shrimpton, P., Parsons, J.L., Gardiner, L., Houlbrook, S., Talbot, D.C., Hammonds, T., Freemont, P.A., Sternberg, M.J.E., Dianov, G.L. & Hickson, I.D. (2005) Isolation of a small molecule inhibitor of DNA base excision repair. *Nucleic Acids Research*, **33**, 4711-4724.
- Maier, T., Guell, M. & Serrano, L. (2009) Correlation of mRNA and protein in complex biological samples. *Febs Letters*, **583**, 3966-3973.
- Mariano, A.R., Colombo, E., Luzi, L., Martinelli, P., Volorio, S., Bernard, L., Meani, N., Bergomas, R., Alcalay, M. & Pelicci, P.G. (2006) Cytoplasmic localization of NPM in myeloid leukemias is dictated by gain-of-function mutations that create a functional nuclear export signal. *Oncogene*, **25**, 4376-4380.

- Martelli, M.P., Pettirossi, V., Manes, N., Liso, A., Cecchetti, F., De Marco, M.F., Bigerna, B., Pucciarini, A., Nicoletti, I., Martelli, M.F. & Falini, B. (2007) Selective silencing of the NPM1 mutant protein and apoptosis induction upon ATRA in vitro treatment of AML cells carrying NPM1 mutations. *Blood*, **110**, 266A-266A.
- Martelli, M.P., Pettirossi, V., Thiede, C., Bonifacio, E., Mezzasoma, F., Cecchini, D., Pacini, R., Tabarrini, A., Ciurnelli, R., Gionfriddo, I., Manes, N., Rossi, R., Giunchi, L., Oelschlaegel, U., Brunetti, L., Gemei, M., Delia, M., Specchia, G., Liso, A., Di Ianni, M., Di Raimondo, F., Falzetti, F., Del Vecchio, L., Martelli, M.F. & Falini, B. (2010) CD34(+) cells from AML with mutated NPM1 harbor cytoplasmic mutated nucleophosmin and generate leukemia in immunocompromised mice. *Blood*, **116**, 3907-3922.
- Mattsson, G., Turner, S.H., Cordell, J., Ferguson, D.J.P., Schuh, A., Grimwade, L.F., Bench, A.J., Weinberg, O.K., Marafioti, T., George, T.I., Arber, D.A., Erber, W.N. & Mason, D.Y. (2010) Can cytoplasmic nucleophosmin be detected by immunocytochemical staining of cell smears in acute myeloid leukemia? *Haematologica-the Hematology Journal*, **95**, 670-673.
- Mazon, G., Mimitou, E.P. & Symington, L.S. (2010) SnapShot: Homologous recombination in DNA double-strand break repair. *Cell*, **142**, 646.e641-646, 646.e641.
- McNeill, D.R. & Wilson, D.M. (2007) A dominant-negative form of the major human abasic endonuclease enhances cellular sensitivity to laboratory and clinical DNA-damaging agents. *Molecular Cancer Research*, **5**, 61-70.
- Milligan, D.W., Wheatley, K., Littlewood, T., Craig, J.I.O., Burnett, A.K. & Clin, N.H.O. (2006) Fludarabine and cytosine are less effective than standard ADE chemotherapy in high-risk acute myeloid leukemia, and addition of G-CSF and ATRA are not beneficial: results of the MRC AML-HR randomized trial. *Blood*, **107**, 4614-4622.
- Mizuki, M., Fenski, R., Halfter, H., Matsumura, I., Schmidt, R., Muller, C., Gruning, R., Kratz-Abers, K., Serve, S., Steur, C., Buchner, T., Kienast, J., Kanakura, Y., Berdel, W.E. & Serve, H. (2000) Flt3 mutations from patients with acute myeloid leukemia induce transformation of 32D cells mediated by the Ras and STAT5 pathways. *Blood*, **96**, 3907-3914.
- Mollgard, L., Deneberg, S., Nahi, H., Bengtzen, S., Jonsson-Videsater, K., Fioretos, T., Andersson, A., Paul, C. & Lehmann, S. (2008) The FLT3 inhibitor PKC412 in combination with cytostatic drugs in vitro in acute myeloid

- leukemia. *Cancer Chemotherapy and Pharmacology*, **62**, 439-448.
- Mrozek, K., Heerema, N.A. & Bloomfield, C.D. (2004) Cytogenetics in acute leukemia. *Blood Reviews*, **18**, 115-136.
- Nagy, B., Lundan, T., Larramendy, M.L., Aalto, Y., Zhu, Y., Niini, T., Edgren, H., Ferrer, A., Vilpo, J., Elonen, E., Vettenranta, K., Franssila, K. & Knuutila, S. (2003) Abnormal expression of apoptosis-related genes in haematological malignancies: overexpression of MYC is poor prognostic sign in mantle cell lymphoma. *British Journal of Haematology*, **120**, 434-441.
- Naoe, T., Suzuki, T., Kiyoi, H. & Urano, T. (2006) Nucleophosmin: A versatile molecule associated with hematological malignancies. *Cancer Science*, **97**, 963-969.
- Neubauer, A., Dodge, R.K., George, S.L., Davey, F.R., Silver, R.T., Schiffer, C.A., Mayor, R.J., Ball, E.D., Wursterhill, D., Bloomfield, C.D. & Liu, E.T. (1994) PROGNOSTIC IMPORTANCE OF MUTATIONS IN THE RAS PROTOONCOGENES IN DE-NOVO ACUTE MYELOID-LEUKEMIA. *Blood*, **83**, 1603-1611.
- Nishimura, Y., Ohkubo, T., Furuichi, Y. & Umekawa, H. (2002) Tryptophans 286 and 288 in the C-terminal region of protein B23.1 are important for its nucleolar localization. *Bioscience Biotechnology and Biochemistry*, **66**, 2239-2242.
- Nomdedeu, J., Bussaglia, E., Villamor, N., Martinez, C., Esteve, J., Tormo, M., Estivill, C., Queipo, M.P., Guardia, R., Carricondo, M., Hoyos, M., Llorente, A., Junca, J., Gallart, M., Domingo, A., Bargay, J., Mascaro, M., Moraleda, J.M., Florensa, L., Ribera, J.M., Gallardo, D., Brunet, S., Aventin, A., Sierra, J. & Spanish, C. (2011) Immunophenotype of acute myeloid leukemia with NPM mutations: Prognostic impact of the leukemic compartment size. *Leukemia Research*, **35**, 163-168.
- Okuda, M., Horn, H.F., Tarapore, P., Tokuyama, Y., Smulian, A.G., Chan, P.K., Knudsen, E.S., Hofmann, I.A., Snyder, J.D., Bove, K.E. & Fukasawa, K. (2000) Nucleophosmin/B23 is a target of CDK2/Cyclin E in centrosome duplication. *Cell*, **103**, 127-140.
- Pallis, M., Syan, J. & Russell, N.H. (1999) Flow cytometric chemosensitivity analysis of blasts from patients with acute myeloblastic leukemia and myelodysplastic syndromes: The use of 7AAD with antibodies to CD45 or CD34. *Cytometry*, **37**, 308-313.

- Pallisgaard, N., Clausen, N., Schroder, H. & Hokland, P. (1999) Rapid and sensitive minimal residual disease detection in acute leukemia by quantitative real-time RT-PCR exemplified by t(12;21) TEL-AML1 fusion transcript. *Genes Chromosomes & Cancer*, **26**, 355-365.
- Paquette, R.L., Landaw, E.M., Pierre, R.V., Kahan, J., Lubbert, M., Lazcano, O., Isaac, G., McCormick, F. & Koeffler, H.P. (1993) N-RAS MUTATIONS ARE ASSOCIATED WITH POOR-PROGNOSIS AND INCREASED RISK OF LEUKEMIA IN MYELODYSPLASTIC SYNDROME. *Blood*, **82**, 590-599.
- Pattyn, F., Speleman, F., De Paepe, A. & Vandesompele, J. (2003) RTPrimerDB: The Real-Time PCR primer and probe database. *Nucleic Acids Research*, **31**, 122-123.
- Pauwels, D., Sweron, B. & Cools, J. (2012) The N676D and G697R mutations in the kinase domain of FLT3 confer resistance to the inhibitor AC220. *Haematologica-the Hematology Journal*, **97**, 1773-1774.
- Pelletier, C.L., Maggi, L.B., Jr., Brady, S.N., Scheidenhelm, D.K., Gutmann, D.H. & Weber, J.D. (2007) TSC1 sets the rate of ribosome export and protein synthesis through nucleophosmin translation. *Cancer Research*, **67**, 1609-1617.
- Pisani, F., DelPoeta, G., Aronica, G., Venditti, A., Caravita, T. & Amadori, S. (1997) In vitro down-regulation of bcl-2 expression by all-trans retinoic acid in AML blasts. *Annals of Hematology*, **75**, 145-147.
- Polo, S.E. & Jackson, S.P. (2011) Dynamics of DNA damage response proteins at DNA breaks: a focus on protein modifications. *Genes & Development*, **25**, 409-433.
- Ponziani, V., Gianfaldoni, G., Mannelli, F., Leoni, F., Ciolli, S., Guglielmelli, P., Antonioli, E., Longo, G., Bosi, A. & Vannucchi, A.M. (2006) The size of duplication does not add to the prognostic significance of FLT3 internal tandem duplication in acute myeloid leukemia patients. *Leukemia*, **20**, 2074-2076.
- Pratz, K.W., Sato, T., Murphy, K.M., Stine, A., Rajkhowa, T. & Levis, M. (2010) FLT3-mutant allelic burden and clinical status are predictive of response to FLT3 inhibitors in AML. *Blood*, **115**, 1425-1432.

- Quentmeier, H., Martelli, M.P., Dirks, W.G., Bolli, N., Liso, A., Macleod, R.A.F., Nicoletti, I., Mannucci, R., Pucciarini, A., Bigerna, B., Martelli, M., Mecucci, C., Drexler, H.G. & Falini, B. (2005) Cell line OCI/AML3 bears exon-12 NPM gene mutation-A and cytoplasmic expression of nucleophosmin. *Leukemia*, **19**, 1760-1767.
- Quentmeier, H., Reinhardt, J., Zaborski, M. & Drexler, H.G. (2003) FLT3 mutations in acute myeloid leukemia cell lines. *Leukemia*, **17**, 120-124.
- Rastogi, R.P., Richa, Kumar, A., Tyagi, M.B. & Sinha, R.P. (2010) Molecular mechanisms of ultraviolet radiation-induced DNA damage and repair. *Journal of nucleic acids*, **2010**, 592980-592980.
- Rau, R. & Brown, P. (2009) Nucleophosmin (NPM1) mutations in adult and childhood acute myeloid leukaemia: towards definition of a new leukaemia entity. *Hematological Oncology*, **27**, 171-181.
- Redner, R.L., Rush, E.A., Faas, S., Rudert, W.A. & Corey, S.J. (1996) The t(5;17) variant of acute promyelocytic leukemia expresses a nucleophosmin retinoic acid receptor fusion. *Blood*, **87**, 882-886.
- Rehman, F.L., Lord, C.J. & Ashworth, A. (2010) Synthetic lethal approaches to breast cancer therapy. *Nature Reviews Clinical Oncology*, **7**, 718-724.
- Reindl, C., Bagrintseva, K., Vempati, S., Schnittger, S., Ellwart, J.W., Wenig, K., Hopfner, K.P., Hiddemann, W. & Spiekermann, K. (2006) Point mutations in the juxtamembrane domain of FLT3 define a new class of activating mutations in AML. *Blood*, **107**, 3700-3707.
- Rothkamm, K., Kruger, I., Thompson, L.H. & Lobrich, M. (2003) Pathways of DNA double-strand break repair during the mammalian cell cycle. *Molecular and Cellular Biology*, **23**, 5706-5715.
- Rozen, S. & Skaletsky, H. (2000) Primer3 on the WWW for general users and for biologist programmers. *Methods in molecular biology (Clifton, N.J.)*, **132**, 365-386.
- Schittenhelm, M.M., Kampa, K.M., Yee, K.W.H. & Heinrich, M.C. (2009) The FLT3 inhibitor tandutinib (formerly MLN518) has sequence-independent synergistic effects with cytarabine and daunorubicin. *Cell Cycle*, **8**, 2621-2630.

- Schlenk, R.F., Doehner, K., Krauter, J., Gaidzik, V.I., Paschka, P., Heuser, M., Kindler, T., Luebbert, M., Martin, H., Salih, H.R., Kuendgen, A., Horst, H.A., von Lilienfeld-Toal, M., Goetze, K., Nachbaur, D., Wattad, M., Koehne, C.-H., Fiedler, W., Bentz, M., Wulf, G., Held, G., Hertenstein, B., Mergenthaler, H.-G., Salwender, H., Rummel, M.J., Raghavachar, A., Benner, A., Schlegelberger, B., Ganser, A. & Doehner, H. (2011) All-Trans Retinoic Acid Improves Outcome in Younger Adult Patients with Nucleophosmin-1 Mutated Acute Myeloid Leukemia - Results of the AMLSG 07-04 Randomized Treatment Trial. *Blood*, **118**, 38-39.
- Schlenk, R.F., Dohner, K., Kneba, M., Gotze, K., Hartmann, F., del Valle, F., Kirchen, H., Koller, E., Fischer, J.T., Bullinger, L., Habdank, M., Spath, D., Groner, S., Krebs, B., Kayser, S., Corbacioglu, A., Anhalt, A., Benner, A., Frohling, S., Dohner, H. & German-Austrian, A.M.L.S.G. (2009) Gene mutations and response to treatment with all-trans retinoic acid in elderly patients with acute myeloid leukemia. Results from the AMLSG Trial AML HD98B. *Haematologica-the Hematology Journal*, **94**, 54-60.
- Schneider, C.A., Rasband, W.S. & Eliceiri, K.W. (2012) NIH Image to ImageJ: 25 years of image analysis. *Nature Methods*, **9**, 671-675.
- Schnittger, S., Schoch, C., Kern, W., Mecucci, C., Tschulik, C., Martelli, M.F., Haferlach, T., Hiddemann, W. & Falini, B. (2005) Nucleophosmin gene mutations are predictors of favorable prognosis in acute myelogenous leukemia with a normal karyotype. *Blood*, **106**, 3733-3739.
- Schwickart, M., Huang, X., Lill, J.R., Liu, J., Ferrando, R., French, D.M., Maecker, H., O'Rourke, K., Bazan, F., Eastham-Anderson, J., Yue, P., Dornan, D., Huang, D.C.S. & Dixit, V.M. (2010) Deubiquitinase USP9X stabilizes MCL1 and promotes tumour cell survival. *Nature*, **463**, 103-U114.
- Seedhouse, C., Grundy, M., Shang, S.L., Ronan, J., Pimblett, H., Russell, N. & Pallis, M. (2009a) Impaired S-Phase Arrest in Acute Myeloid Leukemia Cells with a FLT3 Internal Tandem Duplication Treated with Clofarabine. *Clinical Cancer Research*, **15**, 7291-7298.
- Seedhouse, C. & Russell, N. (2007) Advances in the understanding of susceptibility to treatment-related acute myeloid leukaemia. *British Journal of Haematology*, **137**, 513-529.

- Seedhouse, C.H., Hunter, H.M., Lloyd-Lewis, B., Massip, A.M., Pallis, M., Carter, G.I., Grundy, M., Shang, S. & Russell, N.H. (2006) DNA repair contributes to the drug-resistant phenotype of primary acute myeloid leukaemia cells with FLT3 internal tandem duplications and is reversed by the FLT3 inhibitor PKC412. *Leukemia*, **20**, 2130-2136.
- Seedhouse, C.H., Pallis, M., Grundy, M., Shang, S.L. & Russell, N.H. (2009b) FLT3-ITD expression levels and their effect on STAT5 in AML with and without NPM mutations. *British Journal of Haematology*, **147**, 653-661.
- Seiter, K., Feldman, E.J., Halicka, H.D., Deptala, A., Traganos, F., Burke, H.B., Hoang, A., Goff, H., Pozzuoli, M., Kancherla, R., Darzynkiewicz, Z. & Ahmed, T. (2000) Clinical and laboratory evaluation of all-trans retinoic acid modulation of chemotherapy in patients with acute myelogenous leukaemia. *British Journal of Haematology*, **108**, 40-47.
- Sexauer, A., Perl, A., Yang, X., Borowitz, M., Gocke, C., Rajkhowa, T., Thiede, C., Frattini, M., Nybakken, G.E., Pratz, K., Karp, J., Smith, B.D. & Levis, M. (2012) Terminal myeloid differentiation in vivo is induced by FLT3 inhibition in FLT3/ITDAML. *Blood*, **120**, 4205-4214.
- Shimada, A., Taki, T., Kubota, C., Tawa, A., Horibe, K., Tsuchida, M., Hanada, R., Tsukimoto, I. & Hayashi, Y. (2007) No nucleophosmin mutations in pediatric acute myeloid leukemia with normal karyotype: a study of the Japanese Childhood AML Cooperative Study Group. *Leukemia*, **21**, 1307-1307.
- Shimada, M. & Nakanishi, M. (2006) DNA damage checkpoints and cancer. *Journal of Molecular Histology*, **37**, 253-260.
- Shipley, J.L. & Butera, J.N. (2009) Acute myelogenous leukemia. *Experimental Hematology*, **37**, 649-658.
- Shore, G.C. & Viallet, J. (2005) Modulating the bcl-2 family of apoptosis suppressors for potential therapeutic benefit in cancer. *Hematology / the Education Program of the American Society of Hematology. American Society of Hematology. Education Program*, 226-230.
- Sigurdson, A.J., Hauptmann, M., Alexander, B.H., Doody, M.M., Thomas, C.B., Struewing, J.P. & Jones, I.M. (2005) DNA damage among thyroid cancer and multiple cancer cases, controls, and long-lived individuals. *Mutation Research-Genetic Toxicology and Environmental Mutagenesis*, **586**, 173-188.

- Smith, C.C., Wang, Q., Chin, C.-S., Salerno, S., Damon, L.E., Levis, M.J., Perl, A.E., Travers, K.J., Wang, S., Hunt, J.P., Zarrinkar, P.P., Schadt, E.E., Kasarskis, A., Kuriyan, J. & Shah, N.P. (2012) Validation of ITD mutations in FLT3 as a therapeutic target in human acute myeloid leukaemia. *Nature*, **485**, 260-U153.
- Sonoda, E., Zhao, G.Y., Kohzaki, M., Dhar, P.K., Kikuchi, K., Redon, C., Pilch, D.R., Bonner, W.M., Nakano, A., Watanabe, M., Nakayama, T., Takeda, S. & Takami, Y. (2007) Collaborative roles of gamma H2AX and the Rad51 paralog Xrcc3 in homologous recombinational repair. *DNA Repair*, **6**, 280-292.
- Sportoletti, P., Varasano, E., Rossi, R., Bereshchenko, O., Cecchini, D., Gionfriddo, I., Bolli, N., Tiacci, E., Intermesoli, T., Zanghi, P., Masciulli, A., Martelli, M.P., Falzetti, F., Martelli, M.F. & Falini, B. (2013) The human NPM1 mutation A perturbs megakaryopoiesis in a conditional mouse model. *Blood*, **121**, 3447-3458.
- Sultana, R., McNeill, D.R., Abbotts, R., Mohammed, M.Z., Zdzienicka, M.Z., Qutob, H., Seedhouse, C., Laughton, C.A., Fischer, P.M., Patel, P.M., Wilson, D.M., III & Madhusudan, S. (2012) Synthetic lethal targeting of DNA double-strand break repair deficient cells by human apurinic/aprimidinic endonuclease inhibitors. *International Journal of Cancer*, **131**, 2433-2444.
- Tabe, Y., Konopleva, M., Contractor, R., Munsell, M., Schober, W.D., Jin, L.H., Tsutsumi-Ishii, Y., Nagaoka, I., Igari, J. & Andreeff, M. (2006) Up-regulation of MDR1 and induction of doxorubicin resistance by histone deacetylase inhibitor depsipeptide (FK228) and ATRA in acute promyelocytic leukemia cells. *Blood*, **107**, 1546-1554.
- Taussig, D.C., Vargaftig, J., Miraki-Moud, F., Griessinger, E., Sharrock, K., Luke, T., Lillington, D., Oakervee, H., Cavenagh, J., Agrawal, S.G., Lister, T.A., Gribben, J.G. & Bonnet, D. (2010) Leukemia-initiating cells from some acute myeloid leukemia patients with mutated nucleophosmin reside in the CD34(-) fraction. *Blood*, **115**, 1976-1984.
- Tell, G., Damante, G., Caldwell, D. & Kelley, M.R. (2005) The intracellular localization of APE1/Ref-1: More than a passive phenomenon? *Antioxidants & Redox Signaling*, **7**, 367-384.
- Tell, G., Quadrifoglio, F., Tiribelli, C. & Kelley, M.R. (2009) The Many Functions of APE1/Ref-1: Not Only a DNA Repair Enzyme. *Antioxidants & Redox Signaling*, **11**, 601-619.

- Thiede, C., Koch, S., Creutzig, E., Steudel, C., Illmer, T., Schaich, M., Ehninger, G. & Deutsche Studieninitiative, L. (2006) Prevalence and prognostic impact of NPM1 mutations in 1485 adult patients with acute myeloid leukemia (AML). *Blood*, **107**, 4011-4020.
- Tickenbrock, L., Schwable, J., Wiedehage, M., Steffen, B., Sargin, B., Choudhary, C., Brandts, C., Berdel, W.E., Muller-Tidow, C. & Serve, H. (2005) Flt3 tandem duplication mutations cooperate with Wnt signaling in leukemic signal transduction. *Blood*, **105**, 3699-3706.
- Tothova, E., Fricova, M., Stecova, N., Kafkova, A. & Elbertova, A. (2002) High expression of Bcl-2 protein in acute myeloid leukemia cells is associated with poor response to chemotherapy. *Neoplasma*, **49**, 141-144.
- Tzifi, F., Economopoulou, C., Gourgiotis, D., Ardavanis, A., Papageorgiou, S. & Scorilas, A. (2012) The Role of BCL2 Family of Apoptosis Regulator Proteins in Acute and Chronic Leukemias. *Advances in hematology*, **2012**, 524308-524308.
- Vardiman, J.W., Thiele, J., Arber, D.A., Brunning, R.D., Borowitz, M.J., Porwit, A., Harris, N.L., Le Beau, M.M., Hellstrom-Lindberg, E., Tefferi, A. & Bloomfield, C.D. (2009) The 2008 revision of the World Health Organization (WHO) classification of myeloid neoplasms and acute leukemia: rationale and important changes. *Blood*, **114**, 937-951.
- Vascotto, C., Fantini, D., Romanello, M., Cesaratto, L., Deganuto, M., Leonardi, A., Radicella, J.P., Kelley, M.R., D'Ambrosio, C., Scaloni, A., Quadrioglio, F. & Tell, G. (2009) APE1/Ref-1 Interacts with NPM1 within Nucleoli and Plays a Role in the rRNA Quality Control Process. *Molecular and Cellular Biology*, **29**, 1834-1854.
- Vascotto, C., Lirussi, L., Poletto, M., Tiribelli, M., Damiani, D., Fabbro, D., Damante, G., Demple, B., Colombo, E. & Tell, G. (2013) Functional regulation of the apurinic/aprimidinic endonuclease 1 by nucleophosmin: impact on tumor biology. *Oncogene*.
- Vassiliou, G.S., Cooper, J.L., Rad, R., Li, J., Rice, S., Uren, A., Rad, L., Ellis, P., Andrews, R., Banerjee, R., Grove, C., Wang, W., Liu, P., Wright, P., Arends, M. & Bradley, A. (2011) Mutant nucleophosmin and cooperating pathways drive leukemia initiation and progression in mice. *Nature Genetics*, **43**, 470-+.

- Verhaak, R.G.W., Goudswaard, C.S., van Putten, W., Bijl, M.A., Sanders, M.A., Hagens, W., Uitterlinden, A.G., Erpelinck, C.A.J., Delwel, R., Lowenberg, B. & Valk, P.J.M. (2005) Mutations in nucleophosmin (NPM1) in acute myeloid leukemia (AML): association with other gene abnormalities and previously established gene expression signatures and their favorable prognostic significance. *Blood*, **106**, 3747-3754.
- Vogel, C. & Marcotte, E.M. (2012) Insights into the regulation of protein abundance from proteomic and transcriptomic analyses. *Nature Reviews Genetics*, **13**, 227-232.
- Wakui, M., Kuriyama, K., Miyazaki, Y., Hata, T., Taniwaki, M., Ohtake, S., Sakamaki, H., Miyawaki, S., Naoe, T., Ohno, R. & Tomonaga, M. (2008) Diagnosis of acute myeloid leukemia according to the WHO classification in the Japan Adult Leukemia Study Group AML-97 protocol. *International Journal of Hematology*, **87**, 144-151.
- Wang, D., Luo, M.H. & Kelley, M.R. (2004) Human apurinic endonuclease 1 (APE1) expression and prognostic significance in osteosarcoma: Enhanced sensitivity of osteosarcoma to DNA damaging agents using silencing RNA APE1 expression inhibition. *Molecular Cancer Therapeutics*, **3**, 679-686.
- Wang, H.-F., Takenaka, K., Nakanishi, A. & Miki, Y. (2011) BRCA2 and Nucleophosmin Coregulate Centrosome Amplification and Form a Complex with the Rho Effector Kinase ROCK2. *Cancer Research*, **71**, 68-77.
- Wang, J., Fong, C.-C., Tzang, C.-H., Xiao, P., Han, R. & Yang, M. (2009) Gene expression analysis of human promyelocytic leukemia HL-60 cell differentiation and cytotoxicity induced by natural and synthetic retinoids. *Life Sciences*, **84**, 576-583.
- Wang, W., Budhu, A., Forgues, M. & Wang, X.W. (2005) Temporal and spatial control of nucleophosmin by the Ran-Crm1 complex in centrosome duplication. *Nature Cell Biology*, **7**, 823-830.
- Ward, I.M. & Chen, J.J. (2001) Histone H2AX is phosphorylated in an ATR-dependent manner in response to replicational stress. *Journal of Biological Chemistry*, **276**, 47759-47762.
- Wertz, I.E., Kusam, S., Lam, C., Okamoto, T., Sandoval, W., Anderson, D.J., Helgason, E., Ernst, J.A., Eby, M., Liu, J., Belmont, L.D., Kaminker, J.S., O'Rourke, K.M., Pujara, K., Kohli, P.B., Johnson, A.R., Chiu, M.L., Lill, J.R., Jackson, P.K., Fairbrother, W.J., Seshagiri, S., Ludlam, M.J.C., Leong, K.G., Dueber, E.C., Maecker, H., Huang, D.C.S. & Dixit, V.M. (2011)

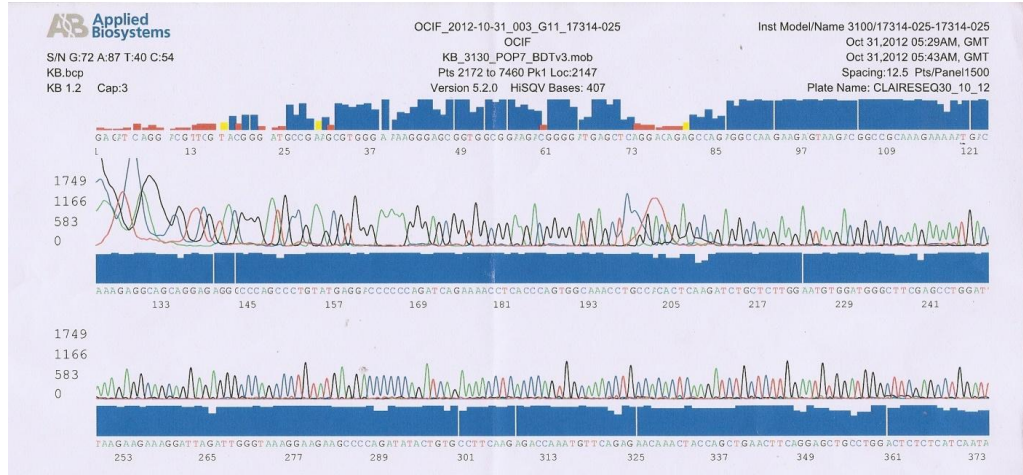
- Sensitivity to antitubulin chemotherapeutics is regulated by MCL1 and FBW7 (vol 471, pg 110, 2011). *Nature*, **475**, 122-122.
- Whitman, S.P., Liu, S.J., Vukosavljevic, T., Rush, L.J., Yu, L., Liu, C.H., Klisovic, M.I., Maharry, K., Guimond, M., Strout, M.P., Becknell, B., Dorrance, A., Klisovic, R.B., Plass, C., Bloomfield, C.D., Marcucci, G. & Caligiuri, M.A. (2005) The MLL partial tandem duplication: evidence for recessive gain-of-function in acute myeloid leukemia identifies a novel patient subgroup for molecular-targeted therapy. *Blood*, **106**, 345-352.
- Wolner, B., van Komen, S., Sung, P. & Peterson, C.L. (2003) Recruitment of the recombinational repair machinery to a DNA double-strand break in yeast. *Molecular Cell*, **12**, 221-232.
- Wong, L.Y., Recht, J. & Laurent, B.C. (2006) Chromatin remodeling and repair of DNA double-strand breaks. *Journal of Molecular Histology*, **37**, 261-269.
- Wu, M.H., Chang, J.H. & Yung, B.Y.M. (2002) Resistance to UV-induced cell-killing in nucleophosmin/B23 over-expressed NIH 3T3 fibroblasts: enhancement of DNA repair and up-regulation of PCNA in association with nucleophosmin/B23 over-expression. *Carcinogenesis*, **23**, 93-100.
- Wu, Y.L., Mehew, J.W., Heckman, C.A., Arcinas, M. & Boxer, L.M. (2001) Negative regulation of bcl-2 expression by p53 in hematopoietic cells. *Oncogene*, **20**, 240-251.
- Xanthoudakis, S., Miao, G.G. & Curran, T. (1994) THE REDOX AND DNA-REPAIR ACTIVITIES OF REF-1 ARE ENCODED BY NONOVERLAPPING DOMAINS. *Proceedings of the National Academy of Sciences of the United States of America*, **91**, 23-27.
- Yang, J., Yu, Y.N., Hamrick, H.E. & Duerksen-Hughes, P.J. (2003a) ATM, ATR and DNA-PK: initiators of the cellular genotoxic stress responses. *Carcinogenesis*, **24**, 1571-1580.
- Yang, L.J., Zhao, H.S., Li, S.W., Ahrens, K., Collins, C., Eckenrode, S., Ruan, Q.G., McIndoe, R.A. & She, J.X. (2003b) Gene expression profiling during all-trans retinoic acid-induced cell differentiation of acute promyelocytic leukemia cells. *Journal of Molecular Diagnostics*, **5**, 212-221.
- Yoshida, A. & Ueda, T. (2003) Human AP endonuclease possesses a significant activity as major 3'→5' exonuclease in human

- leukemia cells. *Biochemical and Biophysical Research Communications*, **310**, 522-528.
- Yoshida, A., Urasaki, Y., Waltham, M., Bergman, A.C., Pourquier, P., Rothwell, D.G., Inuzuka, M., Weinstein, J.N., Ueda, T., Appella, E., Hickson, I.D. & Pommier, Y. (2003) Human apurinic/aprimidinic endonuclease (Ape1) and its N-terminal truncated form (AN34) are involved in DNA fragmentation during apoptosis. *Journal of Biological Chemistry*, **278**, 37768-37776.
- Yoshimoto, G., Miyamoto, T., Jabbarzadeh-Tabrizi, S., Iino, T., Rocnik, J.L., Kikushige, Y., Mori, Y., Shima, T., Iwasaki, H., Takenaka, K., Nagafuji, K., Mizuno, S.-i., Niino, H., Gilliland, G.D. & Akashi, K. (2009) FLT3-ITD up-regulates MCL-1 to promote survival of stem cells in acute myeloid leukemia via FLT3-ITD-specific STAT5 activation. *Blood*, **114**, 5034-5043.
- Yu, Y., Maggi, L.B., Jr., Brady, S.N., Apicelli, A.J., Dai, M.-S., Lu, H. & Weber, J.D. (2006) Nucleophosmin is essential for ribosomal protein L5 nuclear export. *Molecular and Cellular Biology*, **26**, 3798-3809.
- Zarrinkar, P.P., Gunawardane, R.N., Cramer, M.D., Gardner, M.F., Brigham, D., Belli, B., Karaman, M.W., Pratz, K.W., Pallares, G., Chao, Q., Sprankle, K.G., Patel, H.K., Levis, M., Armstrong, R.C., James, J. & Bhagwat, S.S. (2009) AC220 is a uniquely potent and selective inhibitor of FLT3 for the treatment of acute myeloid leukemia (AML). *Blood*, **114**, 2984-2992.
- Zhang, J.W., Gu, J., Wang, Z.Y., Chen, S.J. & Chen, Z. (2000) Mechanisms of all-trans retinoic acid-induced differentiation of acute promyelocytic leukemia cells. *Journal of Biosciences*, **25**, 275-284.
- Zhang, Y., Wang, J., Xiang, D., Wang, D. & Xin, X. (2009) Alterations in the expression of the apurinic/aprimidinic endonuclease-1/redox factor-1 (APE1/Ref-1) in human ovarian cancer and identification of the therapeutic potential of APE1/Ref-1 inhibitor. *International Journal of Oncology*, **35**, 1069-1079.
- Zorko, N.A., Bernot, K.M., Whitman, S.P., Siebenaler, R.F., Ahmed, E.H., Marcucci, G.G., Yanes, D.A., McConnell, K.K., Mao, C., Kalu, C., Zhang, X., Jarjoura, D., Dorrance, A.M., Heerema, N.A., Lee, B.H., Huang, G., Marcucci, G. & Caligiuri, M.A. (2012) Mll partial tandem duplication and Flt3 internal tandem duplication in a double knock-in mouse recapitulates features of counterpart human acute myeloid leukemias. *Blood*, **120**, 1130-1136.

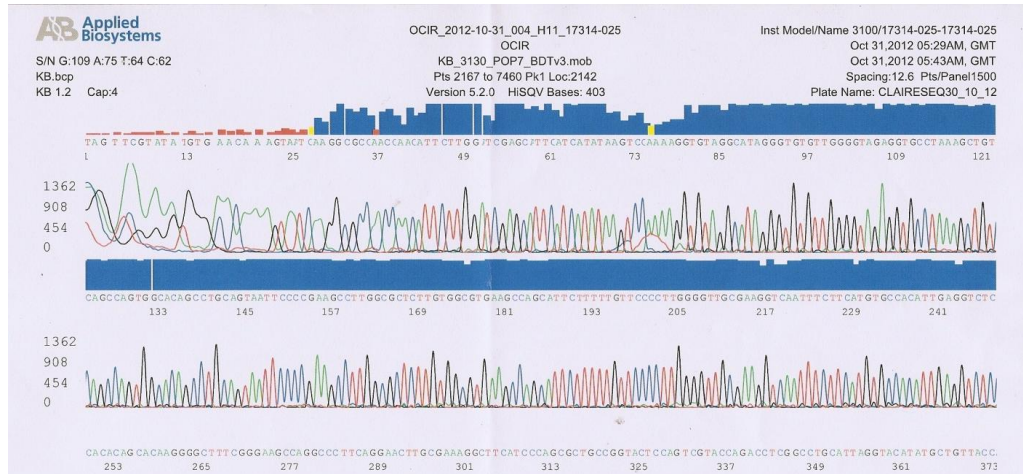
### Appendix:

## 4.1 APE1 mRNA sequencing results in the leukaemic cell lines:

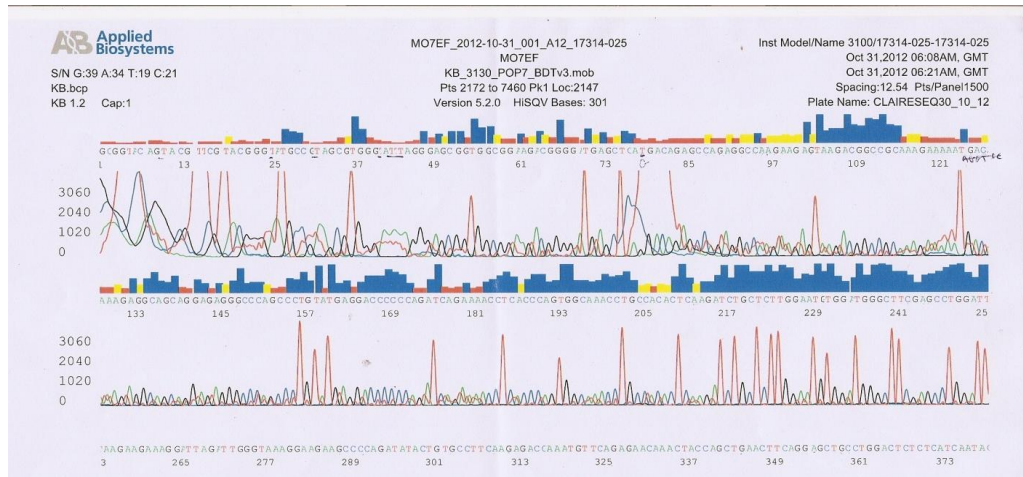
### (A) 1- OCI-AML3 Forward:



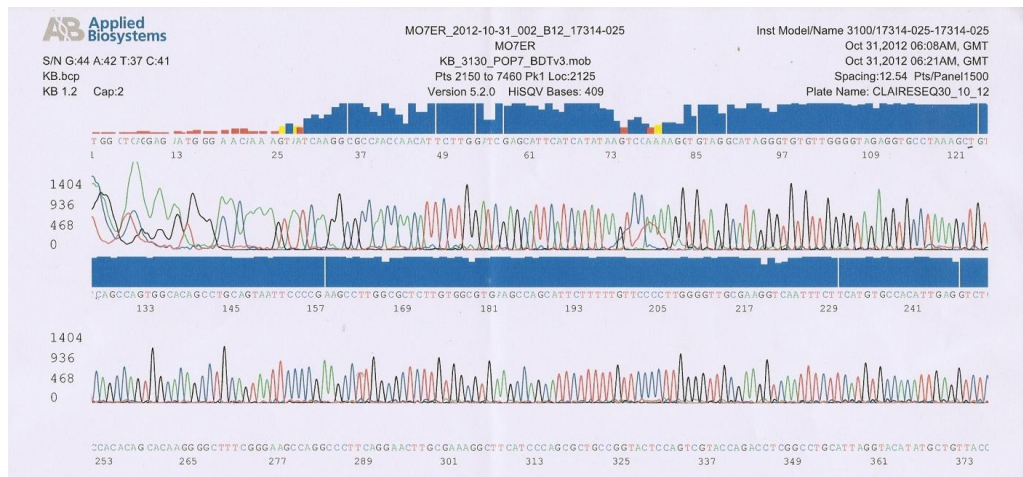
### 2- OCI-AML3 Reverse:



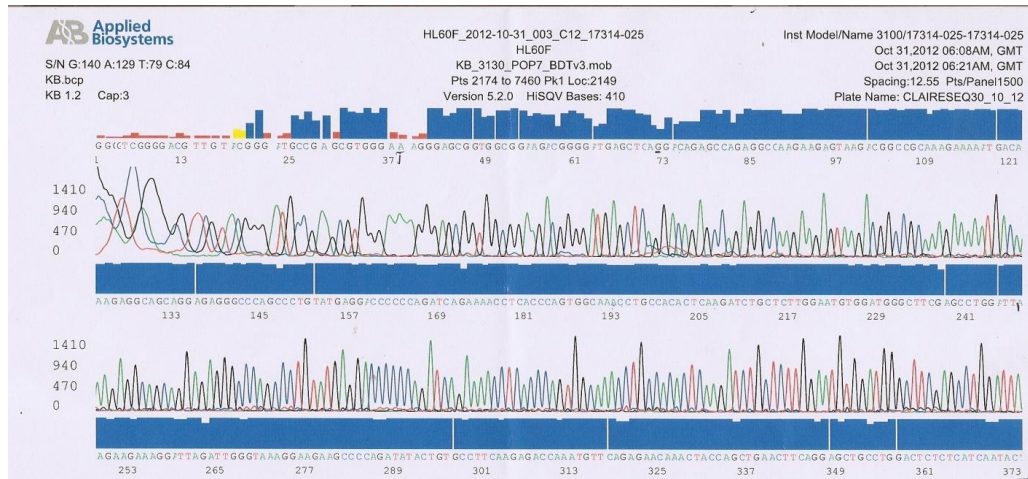
**(B) 1- M-07e Forward:**



**2- M-07e Reverse:**



**(C) 1- HL-60 Forward:**



**2- HL-60 Reverse:**

